TNF-related apoptosis-inducing ligand in abdominal aortic aneurysms

Liu, Xun

Award date:
2006

Awarding institution:
University of Bath

TNF-related apoptosis-inducing ligand in abdominal aortic aneurysms

Submitted by
Xun Liu
For the degree of Doctor of Philosophy
The University of Bath
School for Health
2002-2006

ProQuest LLC
789 East Eisenhower Parkway
P.O. Box 1346
Ann Arbor, MI 48106-1346

I Acknowledgments

I would like to express my gratitude to all those who have aided me in completing this thesis. I want to thank Professor Michael Horrocks for giving me the opportunity to commence this research and providing abdominal aortic aneurysm samples. I also want to thank Dr. David Mitchell for normal aortic samples supply. My colleagues Dr. Vivienne Winrow, Dr. Tulin Bodamyali and everyone in Medical Science in the University of Bath gave me continued support, and valuable insights which helped to further my research.

I am deeply indebted to Dr. Cliff Stevens whose help and encouragement helped me throughout the research for and writing of this thesis, and in overcoming all problems I met in my oversea life.

I have furthermore to thank Ms. Rebecca Hurwitz, Dr. Katherine Webster and Mr Benjamin Weekes who looked closely at the first version of the thesis for English style and grammar, offering suggestions for improvement. Miss Saffron who is a lovely dog and looks like a panda always reminds me my home country and makes me laugh when I am tired of writing up.

Finally, I would like to dedicate this thesis to my parents who love me unconditionally and my cat.

II Abstract

Abdominal aortic aneurysm (AAA) is a progressive weakening of the aortic wall commonly associated with vascular calcification. Human AAA tissue displays cells undergoing all stages of apoptosis. It is known that aortic medial layer thinning, leads to aneurysmal formation through loss of aortic wall tone and increased wall stresses. Medial layer thinning is also associated with a decrease in smooth muscle cell (SMC) numbers. The cause of this loss of SMCs is attributed to apoptosis. Tumour necrosis factor (TNF)-related apoptosis-inducing ligand (TRAIL) is capable of inducing apoptosis in transgenic cells from various disease states but not in normal cells. An inhibitor of TRAIL, osteoprotegerin (OPG), is involved in osteoporosis and vascular calcification. We wished to investigate this link between vascular calcification and apoptosis by examining TRAIL and its receptors in AAA.

Both qualitative and quantitative analysis of calcification in AAA walls was determined using Von Kossa staining and pre-operation computer tomography (CT) scans. Apoptosis in human AAA sections was confirmed by TUNEL assay and detection of apoptosis cellular marker by histology staining. Protein blots and RT-PCR were carried out to investigate the expression of TRAIL and its receptors in AAA walls. Comparative analysis was performed between normal aortae and AAA. A significant difference was observed between normal aortae and AAA for death receptor TRAIL-R2 mRNA (decreasing in AAA, $p<0.01$) and OPG protein (decreasing in AAA, $p<0.01$). Significant differences were also observed between tissues displaying different extents of calcification for TRAIL mRNA (increases while the calcification level increseas; $p<0.05$). To mimic the AAA development models, AAA specimens were dissected into three different areas according to the anatomy structure. This separation is also confirmed by CT scan and supported by blood flow diametric theory.

III Abbreviations and acronyms

3-OH= 3'-hydroxyl

5-FU=5-fluorouracil

aa= amino acid

AAA= abdominal aortic aneurysm

AB= apoptosis body

ABC= avidin-biotin complex

AC= aortic calcification

ALPSII= acute lymphoproliferative sydome type II

Apaf-1= apoptotic protease-activating factor-1

AMPS = ammonium persulphate

AI= apoptotic index

AIDS= acquired immune deficiency syndrome

AIF= apoptosis-inducing factor

ATP= adenosine triphosphate

dATP= deoxyadenosine triphosphate

Bcl-2= B-cell leukaemia/ lymphoma 2

BMP= bone morphogentic

BIR= baculoviaus IAP repeat

BSA= bovine serum albumin

CABG= coronary artery bypass graph

CAS= carotid artery stenosis

Ca^{2+} = calcium

CBBG= Coomassie Brilliant Blue G-250

CVC= calcifying vascular cells

cDNA =complementary DNA

CHX= cycloheximide

CO_2 = carbon dioxide

CT = computer tomography

cFLIP= cellular FLICE-like inhibitory protein

DAB= 3,3'-diaminobenzidine tetrahydrochloride

DAPI= 4´,6-diamidino-2-phenylindole

DC= dentritic cells

DEPC = diethyl pyrocarbonate

DPX= DePeX

DMEM = dulbeccos's modified eagle medium

DNA= deoxyribonucleic acid

DISC= death inducing signalling complex

DTT= dithiothreitol

RNA= ribonucleic acid

EDTA = ethylenediamine tetraacetic acid

ESRD= end stage renal disease

EVAR= endovascular abdominal aortic aneurysm repair

FASL= FAS ligand

FADD= FAS associated death domain

FADD-DN= negative version of FADD

FCS = fetal calf serum

FLICE= FADD-like apoptotic cystein protease

FLIP= FLICE-inhibitory proteins

FLIPL= long term of FLIP

FLIPS= short term of FLIP

FITC-dUTP= fluoresecent-deoxyuridine triphosphate nucleotides

FTIR= transformed infrared spectroscopes

GAPDH= hlyceraldehyde-3-phosphate dehydrogenase

GLA= glutamate

GM-CSF= granulocyte/Macrophage colony stimulating factors

H&E= haematoxylin and Eosin

H_2O = water

HBSS = Hank's balanced salt solution

HCC= hepatocellular carcinoma

HCl = hydrochloric acid

HDL= high density lipoprotein

H_2O_2 = hydrogen peroxide

Hp= haptoglobin phenotype

HRP= houseradish peroxidase

IAP= inhibitor of apoptosis protein

IFN= interferon

IL= interleukin

IMS = industrial methylated spirits

Kb=kilobase

kD = kilodalton

LDL= low density lipoproteins

LM= light microscope

M. = molarity

Mg^{2+}= Magnesium

mg/dL = milligrams per decilitre

mRNA= messenger ribonucleic acid

MRI= magnetic resonance imaging

MGP= matrix glutamate protein

MMP = matrix metalloproteinase

N_2= liquid nitrogen

NaCL= sodium chloride

NF-κB = nuclear factor kappa B

NK= natural killer

NO = nitric oxide

NO_3-= nitrate

NO_2^- = nitrite

$O_2^-\cdot$ = superoxide

OPG = osteoprotegerin

PAD= peripheral arterial disease

PAGE = polyacrylamide gel electrophoresis

PAP= peroxidase anti-peroxidase

PBS = phosphate buffered saline

PrEC= prostate epithelial cells

PrSC= prostate stromal cells

PT= permeability transition

pmoles = Pico(x10-2).moles

RANK = receptor activator of nuclear factor-κB

RANKL = receptor activator of nuclear factor-κB ligand (TRANCE, OPGL, ODF)

rRNA= ribosomal RNA

RNAse= ribonuclease

RT-PCR= reverse transcription-polymerase chain reaction

SMAD6= similar to Mothers against decapentaplegic homolog 6

SDS = sodium dodecylsulphate (lauryl sulphate)

Smac= second mitochondrial activator of caspase

SMCs= smooth muscle cells

SMHC= smooth muscle heavy chain

SIG= small inducible gene

std = standard deviation

TDT= terminal deoxynucleotidyl transferase

TEMED = N,N,N',N'-Tetramethylethylene diamine

TNF = tumour necrosis factor

TRADD = Tumour necrosis factor receptor-associated death domain

TRANCE = TNF (tumour necrosis factor).activation-induced cytokine

TRAIL= TNF-related apoptosis-inducing ligand

TRAIL-R1= TRAIL receptor 1 (CD4)

TRAIL-R2= TRAIL receptor 2 (CD5)

TRAIL-R3= TRAIL receptor 3 (DcR1)

TRAIL-R4= TRAIL receptor 4 (DcR2)

TRAIL-rTRAIL= TRAIL and its receptors

tRNA =transfer RNA

Tris-HCl = Tris [hydroxymethyl] amino methane hydrochloride

TRIR= total RNA isolation reagen

TIA= transient ischaemic attack

TUNEL= terminal deoxynucleotidyl transfrase biotin-dUTP nick end labelling

Tween 20 = poloxethylene sorbitan monolaurate

XIAP= X-linked inhibitor of apoptosis

VC= vascular calcification

VEGF= vascular endothelia growth factor

IV Table of contents

V List of Figures

VI List of tables

SECTION I

INTRODUCTION

1.

Chapter 1 General Introduction

1.1 Overview

At autopsy, 75-95% of men and women have coronary artery calcification regardless of the cause of their death (Chirgwin *et al.*, 1979). Aortic calcification has been found in two 3000 year-old mummies by x-ray analysis, first described by Czernak in 1852 (Reginald Magee, 1998). For over a hundred years, scientists have tried to find the mechanism of vascular calcification (VC). Recent studies have begun to shed light on some aspects of the mechanisms of VC. Nowadays it is well established that an unhealthy lifestyle contributes to VC; however there are also genetic factors predisposing the disease. Up until about 20 years ago, the mechanism of VC was thought to be a passive process in which calcium deposits on the vessel wall. Somewhat controversially, it has now been suggested that calcification is regulated by biological processes similar to those in developing bones. Additionally, VC has been found to occur when there is either histological or pathological evidence of cell death and a failure of clearance of the resulting apoptotic bodies. This might indicate that VC involves both positive and negative modulators (Giachelli *et al.*, 2005; Sambrook and Fritsch, 1989; Schreurs O. *et al.*, 1997).

Vascular calcification is characteristic of most vascular diseases. Peripheral arterial disease (PAD), aneurysm, hypertension, diabetes mellitus, chronic renal failure, aortic stenosis and Monckeberg's sclerosis are detailed in brief in the following section.

Tumour necrosis factor (TNF) -related apoptosis-inducing ligand (TRAIL) is a member of the TNF family which was first found in 1995. It is attracting increasing interest from many different scientific fields because it mostly induces apoptosis in tumour cells and not in normal cells, giving it great clinical potential. Recent studies by Proudfoot *et al.* (2000-2001) have shown that apoptotic bodies (AB) can calcify in the same way as matrix vesicles (often found in bone), and that human cultured vascular smooth muscles cells (SMCs) were able to undergo apoptosis *in vitro*. Additionally, osteoprotegerin (OPG) as a decoy receptor of TRAIL is also an inhibitor in osteoporosis. TRAIL and its receptors appear to be a strong link between apoptosis and the bone related protein OPG.

The possibility led us to conduct a study of the role of TRAIL and its receptors (TRAIL-rTRAIL system) in VC.

1.2 Vascular calcification-related diseases

1.2.1 Peripheral arterial disease

Peripheral arterial disease (PAD) is a narrowing of the arteries that supply the legs with blood. The plaque contains calcium and other substances inside the arteries will narrow the arteries in the legs. This narrowing of the arteries in the legs, leads to inadequate blood flow inducing walking impairment such as claudication (Hiatt *et al.*, 2005).

1.2.2 Aneurysm

An aneurysm is defined as a permanent localised dilatation of an artery, with an increase in diameter of greater than 1.5 times its normal diameter (Kiernan, 2001). Abdominal aortic aneurysms may be manifested by catastrophic rupture, signs of pressure on other viscera or an embolism originating in the aneurismal wall, but most cases are asymptomatic (Crawford *et al.*, 2003). Smaller abdominal aortic aneurysms can be detected by regular ultrasound measurements or computer tomography (CT) scans.

1.2.3 Hypertension

Hypertension is a common complication in which blood pressure is abnormally high, occurring when the blood flows through the vessels at a greater than normal force (systolic pressure ≥140 mmHg, diastolic pressure ≥90mmHg). The most common cause is increased peripheral vascular resistance, although it can be caused by prolonged periods of elevated cardiac output (Paul and Smith, 2005).

Hypertension is commonly associated with VC. It strains the heart, harms the arteries causing arteriolosclerosis, and increases the risk of a heart attack, stroke, kidney and eye problems, inducing ischaemia or infarction.

1.2.4 Diabetes mellitus

Diabetes mellitus is a metabolic disorder characterised by a congenital or acquired inability to transport sugar from the bloodstream into cells. Patients with diabetes mellitus may exhibit arterial calcifications, particularly involving the aortae, internal carotid artery, renal artery and the arteries of the pelvis and lower extremities. Clinically unsuspected diabetes mellitus may be discovered when radiographs reveal calcification of the interdigital arteries of the feet. Subclinical atherosclerosis is considered to be one of strongest predictors of this disease (Proudfoot *et al.*, 2001).

1.2.5 Chronic renal failure

Chronic renal failure is the progressive loss of kidney function. The kidneys attempt to compensate for renal damage by hyperfiltration (excessive straining of the blood) within the remaining functional nephrons (filtering units that consist of a glomerulus and corresponding tubule). Over time, hyperfiltration causes further loss of function. Of deaths in patients with end stage renal disease (ESRD) 40-50% are caused by vascular calcification. Arterial calcification presents a high risk factor for cardiovascular morbidity and mortality in this population (Raggi, 2005). Medial calcification of conduit arteries and coronary calcification are very common in ESRD. Also, the vascular SMCs of ESRD patients have been shown to express osteopontin messenger ribonucleic acid (mRNA) that would normally be found in osteoblasts in addition to showing the formation of hydroxyapatite (Raggi, 2005).

1.2.6 Aortic stenosis

Stenosis means narrowing. Aortic stenosis is then a narrowing of the aortic valve or a narrowing of the aorta directly above (supravalvar) or below (subvalvar) the aortic valve. A normal tricuspid aortic valve will undergo calcification, this is termed senile calcific aortic stenosis (Otto *et al.*, 1991).

1.2.7 Monckeberg's sclerosis

Monckeberg's sclerosis is a disease of unknown aetiology characterised by dystrophic calcification of the media of arteries. This condition is usually seen in the major lower limb arteries of elderly patients, and may also be seen in the head, neck and pelvis, especially the uterine arteries. It progresses with age and is common in patients with diabetes mellitus and chronic renal failure and it is strongly associated with osteoporosis (Schoppet *et al.*, 2004).

1.2.8 Idiopathic infantile arterial calcification

Idiopathic infantile arterial calcification is a rare disease that is characterised by calcification in the media and fibroproliferative changes in the intima of larger arteries. The vascular elasticity and blood flow is sometimes reduced (Whitehall *et al.*, 2003). It is not associated with atherosclerosis.

1.3 Summary

Vascular calcification occurs at two distinct sites in the vessel wall: the intimal and medial layers. Intimal calcification is associated with atherosclerosis and can be seen at the early second decade of life as well as in elderly patients. Medial calcification is completely independent of intimal calcification and atherosclerosis and is commonly found in the patients with Monckeberg's sclerosis (Proudfoot and Shanahan, 2001). Atherosclerosis is a common disease which can lead to other vascular diseases. It affects arteries in two opposing ways; stenosis (a narrowing of an artery) or aneurysm (a dilation of an artery). A population-based study of asymptomatic patients was performed in which a whole-body CT gave access to the carotid, coronary, proximal and distal aortae and iliac vessels. Earliest calcification tends to happen in the coronary arteries for those below 50 years, and the distal aortae for those aged 50 to 60. Additionally, the same study identified a significant correlation between the risk factors of age and hypertension, and calcified atherosclerosis in different vascular beds (Allison *et al.*, 2004).

The death caused by abdominal aortic aneurysms (AAA) rupture is the 13th leading cause of death in the USA (www.vascularweb.org, 2006). The mortality

for AAA ruptures in the United Kingdom peaks amongst 65 to 75 year-olds; rupture accounts for 1.7% of all deaths in men in this age group. A progressive and continuing increase death rate from AAA over the 30-year period to 1988 was shown in England and Wales. The increased prevalence of aneurysm has paralleled the pattern of smoking addiction, which rose during the period 1916 to 1948; a cohort effect with a 40-year time lag has been suggested to explain this observation (Crawford *et al.*, 2003). Taking this information and operable accessibility of aneurysm into account, AAA was chosen as a model to study VC.

2.

Chapter 2 Abdominal aortic aneurysm and vascular calcification

2.1 Overview

Vascular calcification is highly associated with patient morbidity and mortality (Raggi, 2005). Wang *et al.* found a positive correlation between valve calcification and cardiovascular disease as well as all-cause mortality in a cohort of 192 patients. Cardiovascular mortality was 7 times higher in patients with vascular calcification than in those without it. In another study of a cohort of 202 patients, it was demonstrated that vascular calcification was a predictor of all-cause as well as cardiovascular mortality regardless of classical risk factor for atherosclerosis (Wang *et al.*, 2003). Blacher *et al.* discovered the presence and extent of vascular calcification were strongly associated with an adverse outcome in a study of 110 patients (Blacher *et al.*, 2001).

2.2 The anatomy of normal arteries

There are three kinds of vascular structures in the human body; veins, (carrying blood into the heart), arteries (carrying blood away from the heart) and capillaries (embedded in the tissue connecting arteries and veins (Frederic H.Martini, 2005; Kiernan, 2001; Luiz Carlos Junqueira *et al.*, 1998; Shire D. *et al.*, 2003).

In the vast majority of cases, vascular calcification occurs in human arteries and rarely in veins (Chirgwin *et al.*, 1979; Demer and Tintut, 2003). The arterial system is ramified like a tree; the aorta acts like the trunk, extending to the peripheral parts of the body and then to the organs (Gray H., 1918). Most of the time, human arteries carry blood rich in oxygen to the organs, the exception being the pulmonary artery which carries venous blood from the right ventricle of the heart to the lungs. The normal aorta is the main trunk of the series of arteries and its maximum diameter is approximately 3cm. It is divided into the right and left common iliac arteries which provide blood to the pelvis and legs. The carotid artery is the main artery which supplies the blood to the neck and brain. It is divided into external and internal carotid arteries (see Figure 2.1). When an atherosclerotic plaque forms on the carotid artery wall, it will completely or partly block the blood flow to the brain, inducing a transient ischaemic attack (TIA) or stroke. The abdominal aorta locates anteriorly in the midline between a point 2.5cm above the transpyloric plane and a point slightly inferior and a little to the

left of the umbilicus. The transpyloric plane is an imaginary horizontal plane located midway between the xiphisternal joint and the umbilicus. The aortic bifurcation into the common iliac arteries occurs just to the left of the midpoint of the line joining the highest points of the iliac crests (intercristal line) (Gray H., 1918).

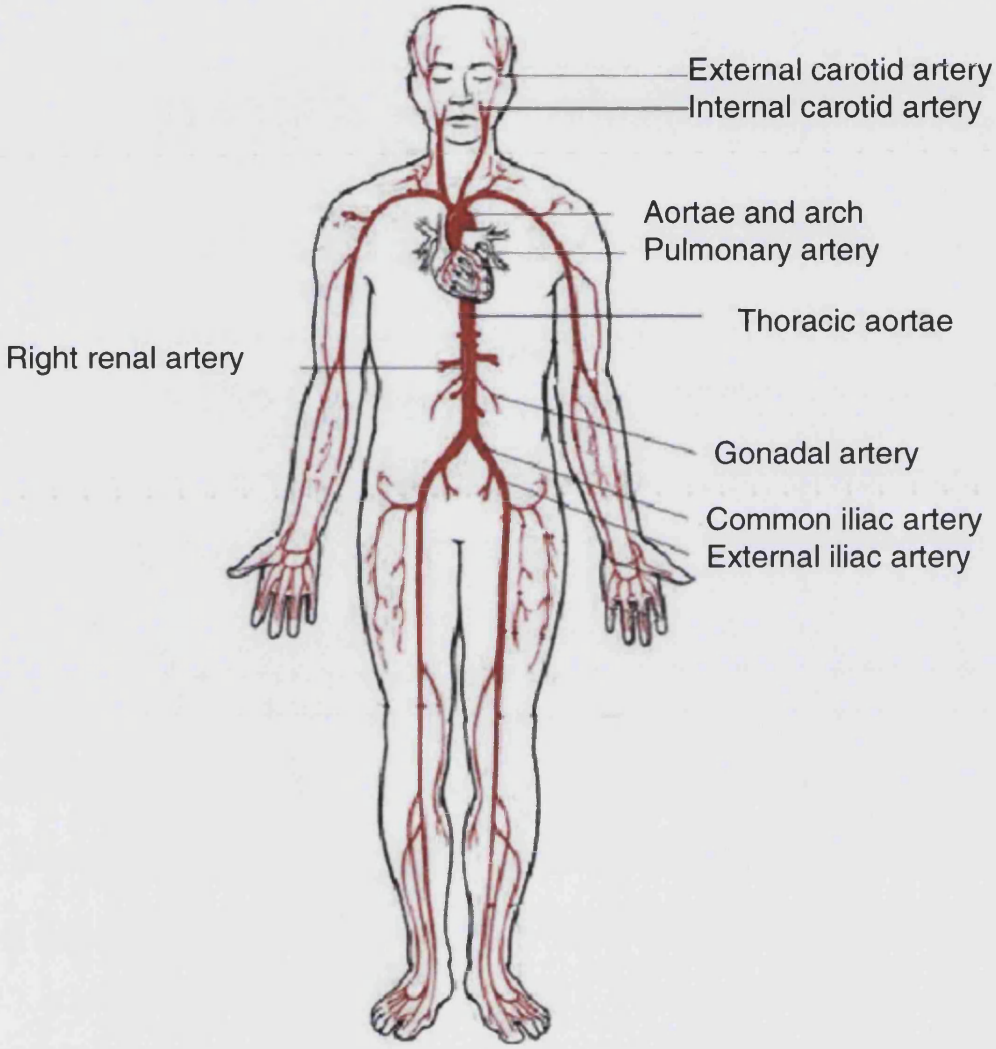

Figure 2.1 A diagrammatical representation of the human vascular tree

Under the light microscope (LM), it can be clearly seen that artery walls are composed of three layers, *tunica adventitia*, *tunica media*, and *tunica intima* (from the outer layer to the inner layer, see Figure 2.2). The *tunica adventitia* includes connective tissue, elastic and collagenous fibres. It mainly attaches the arteries to the neighbouring tissues. The *tunica media* consists of smooth muscle tissue and elastic connective tissue. Changes in blood vessel diameter depend

on the encircling smooth muscle tissue. The *tunica intima* is made of mainly endothelium, which effects nutritional absorption and prevents platelet aggregation (Frederic H.Martini, 2005; Kiernan, 2001; Luiz Carlos Junqueira *et al.*, 1998; Shire D. *et al.*, 2003).

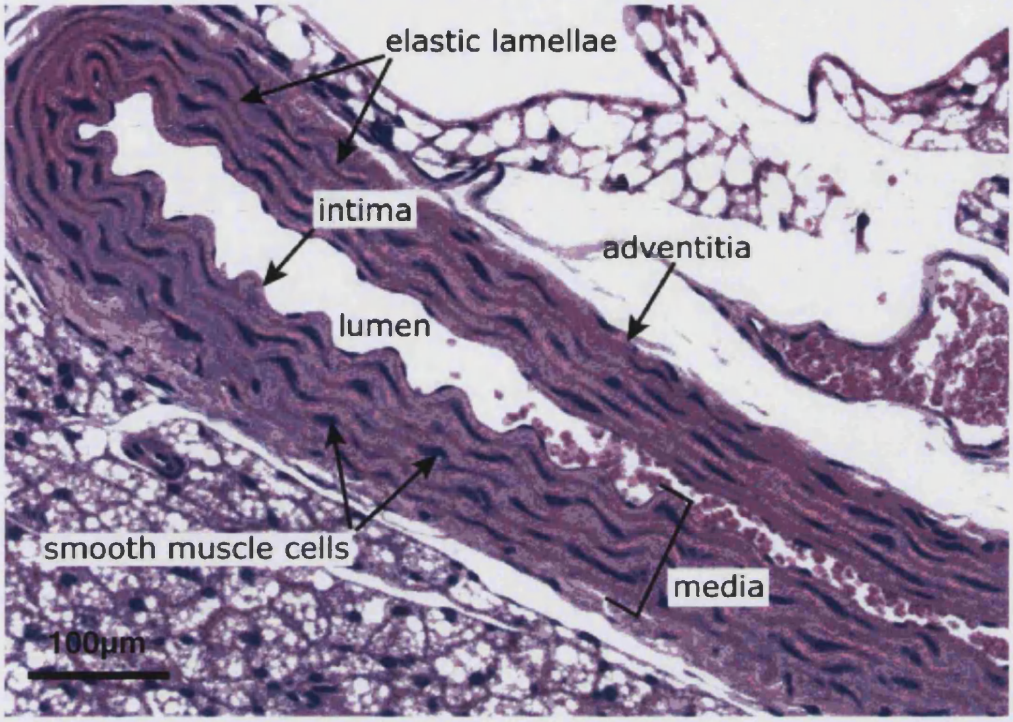

Figure 2.2 The three layers of normal artery stained by Haematoxylin and Eosin (H&E) under the LM.

2.3 The anatomical changes in calcified arteries

Vascular calcification is not only an end-stage disease but also evident in early stage vascular diseases or asymptomatic events which can be detected by clinical assessments. It can be observed by CT scan and ultrasound scan, etc (Demer and Tintut, 2003). Through the LM the arterioles in the stenosis artery are observably thicker than normal lumen and in section exhibit layering like an onion-skin (see Figure 2.3 from www.healcenter.org). The word atherosclerosis comes from two main components of calcified plaque in the arterial wall which are hard collagenous (sclerosis) and soft lipid-rich components (atherosis). Collagenous plaques make up the majority of the calcified plaque volume. The soft components make up a small part of the volume and are prone to rupture

(Dixon.K.J. *et al.*, 1997). Under the LM, the hard plaque (fibrous plaque) is covered by a cap of multiple layers of SMCs densely packed in the surrounding connective tissue. Beneath the cap is a body of SMCs, macrophages and occasional lymphocytes. In the centre of the core of plaque there may be areas of necrotic debris and cholesterol crystals. The soft plaques (ulcerated plaques) may have a disrupted surface with thrombus on top. These atherosclerotic plaques may result in the reduction of the vessel lumen when is large enough to give rise to clinical signs of ischaemia (Gronholdt, 1999).

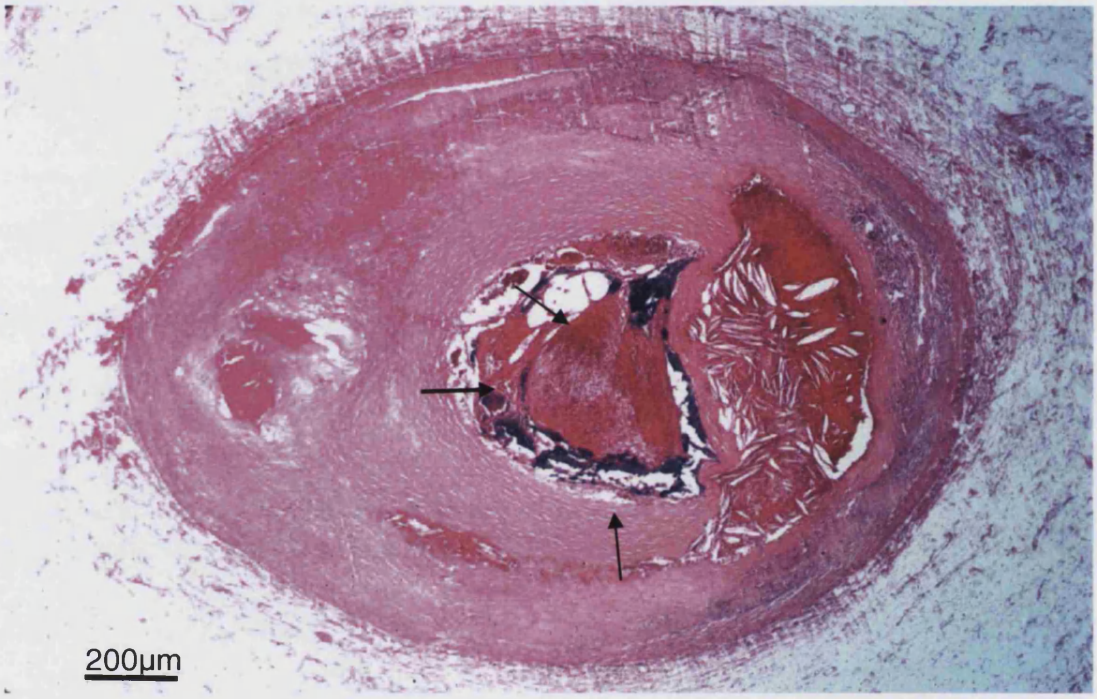

Figure 2.3 A coronary artery with atherosclerosis showing build-up of waxy deposits inside the vessel. The artery wall is thicker and irregular looking. The arrows indicate rupture plaque. (From heal resource, www.healcenter.org)

In the arteriograph, the surface of the artery wall is smooth and continuous under normal conditions. The surface becomes tortuous and broken in calcified arteries as shown in the pictures below (www.bocaradiology.com).

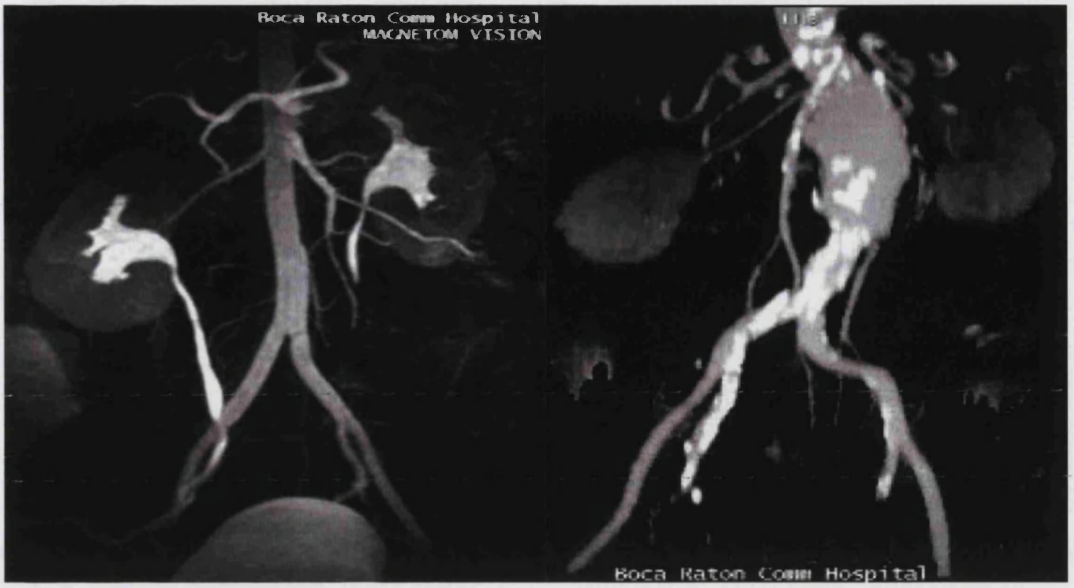

Figure 2.4 Computer tomography scans demonstrating normal aorta and normal bilateral kidney excretion (left) and abnormal aortic aneurysm (right).

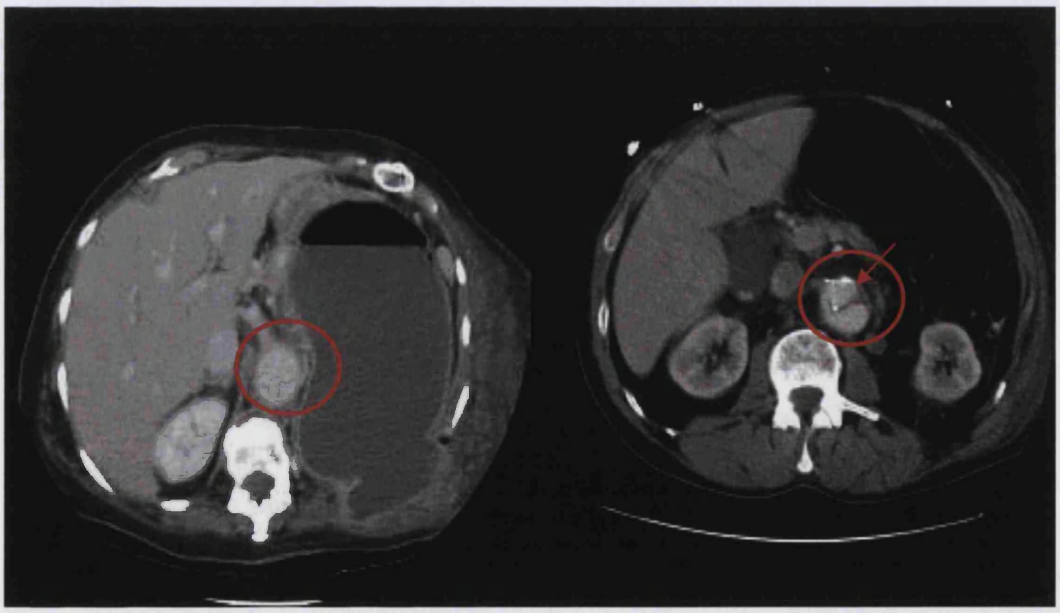

Figure 2.5 Computer tomography scans of a normal aorta (left) and calcified aorta (right). The left red circle indicates normal aorta without calcification. The right red circle and the arrow indicate calcified aorta. (From heal resource, www.healcenter.org)

2.3.1 The anatomical changes in AAA

Abdominal aortic aneurysm is caused by a progressive weakening of the aortic wall that causes dilation, or "ballooning" of the vessel (see Figure 2.6). The aneurysm will grow larger and eventually rupture if it is not diagnosed and treated (Bostrom, 2001; Sambrook and Fritsch, 1989).

Atherosclerosis is associated strongly with the phenomena of stenosis and aneurysm. Stenosis occurs most commonly in the coronary arteries and aneurysm occurs in the infrarenal abdominal aortae. In typical coronary atherosclerosis, expansion of the intimal lesion produces stenosis. The *tunica media* underlying the intima is thinned, but the general structure is preserved relatively well. In contrast, laminar structure of normal *tunica media* disappears with loss of elastic laminae in aneurysm. Smooth muscle cells in the media layer disappear although those in stenosis remain (Crawford *et al.*, 2003; Ernst, 1993).

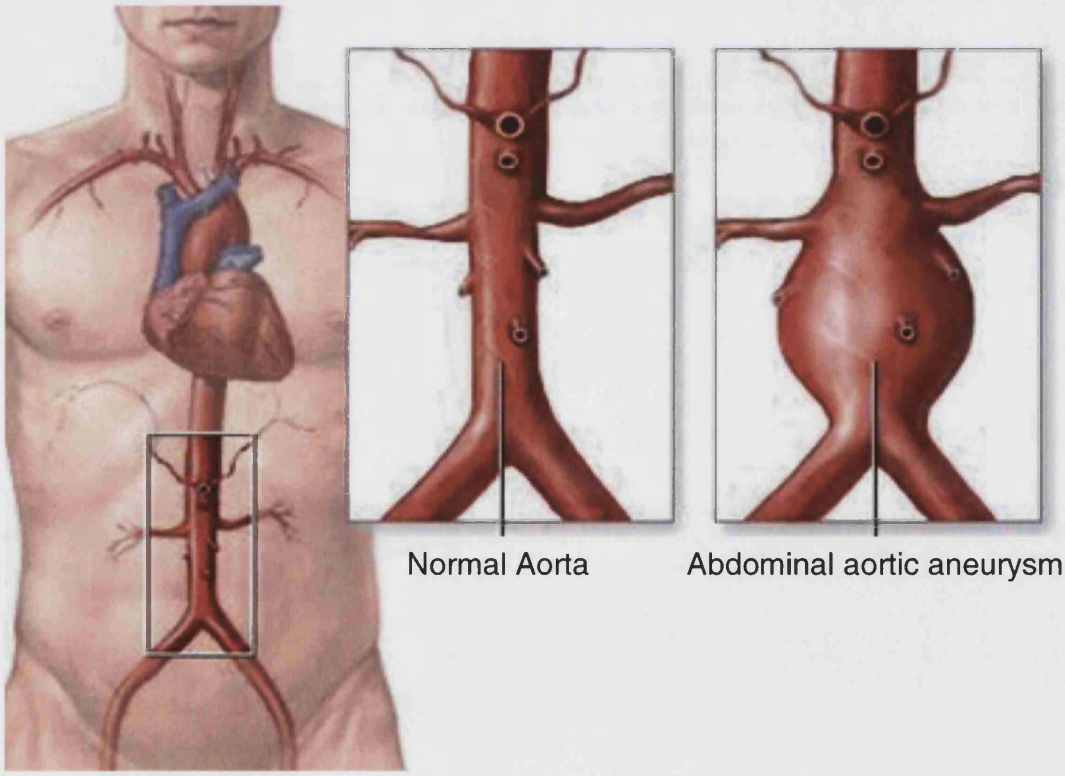

Figure 2.6 Aorta in normal and AAA conditions (from www.nlm.gov)

2.4 The histology change of vascular cells

Smooth muscle cells, macrophages and mast cells are believed to be the primary cells involved in vascular calcification (Chirgwin *et al.*, 1979). Firstly, Schor *et al.* (1990) showed microvascular pericytes produced vascular calcification in nodules *in vitro.* Since then, Giachelli *et al.* (1991) found expression of osteopontin (bone related protein, always found in calcified bones and produced by osteoblasts) in immature SMCs. Bostrom *et al.* (1999) showed a subpopulation of aortic SMCs is responsible for mineralisation by dilutional cloning. These findings support the theory that vascular cells are at least partly regulated by osteoblastic differentiation (Demer and Tintut, 2003).

However, recent evidence has indicated that all the component cells of the atherosclerotic plaque can, at least in culture, undergo apoptosis. Cell death occurs after the removal of serum survival factors, with deregulated expression of specific gene products, or after exposure to oxidised lipids or drug therapy (Proudfoot *et al.*, 2000).

2.4.1 Vascular SMCs

Smooth muscle cells are fusiform. Each cell has a single nuclear located in the centre of the broadest part of the cell. They are normally located in the *tunica media* of the artery wall and engaged in regulation of artery wall tension (Luiz Carlos Junqueira *et al.*, 1998). Smooth muscle cells become engaged in the formation of atherosclerotic lesions. They transform into 'synthetic' cells with morphology similar to that of the SMCs characteristic of prenatal developing arteries. Smooth muscle cells also express a number of bone matrix proteins BMP-2 and MGPthat regulate or facilitate the vascular calcification process (Chen and Moe, 2003; Speer *et al.*, 2002). In the early stages of the atherosclerosis process, medial SMCs are miragrated into the intima. In the intima SMCs participate in the formation of raised lesions not only by active proliferation but also by secreting large amounts of connective tissue matrix. Tumour necrosis factor-α treatment of vascular SMCs results in a partial differentiation to an osteoblast-like phenotype with alkaline phosphatase expression and mineralization (Chirgwin *et al.*, 1979; Thorne *et al.*, 1996). Furthermore, in mice that had matrix r-carboxylated glutamate (GLA) protein

eliminated (MGP knockout), it was observed that there was a loss of SMCs characteristics and that cartilage molecules started to appear in the vessels after 2 weeks (Speer *et al.*, 2002). Matrix r-carboxylated glutamate is a vitamin K-dependent circulating and bone-associated protein that can bind calcium in soft tissues.

Calcifying vascular cells (CVC) are a subpopulation of SMCs from cell culture medium that exhibit osteoblastic characteristics and form calcified nodules *in vitro.* Calcifying vascular cells have features in common with pericytes including a stellate shape and positive staining sharing similarities to osteoblasts (Shin *et al.*, 2004).

2.4.2 Macropages

Macropages are amoeboid-like cells. When a foreign body invades, it is ingested by the macrophage and destroyed by the action of lysosomal enzymes (Luiz Carlos Junqueira *et al.*, 1998). During atherosclerosis, macrophages express a variety of bone-related proteins including MGP, osteopontin, alkaline phosphatase and bone sialoprotein which are believed to be involved in calcification (Chirgwin *et al.*, 1979).

2.4.3 Mast cells

Mast cells contain metachromatic granules which store inflammatory mediators (Luiz Carlos Junqueira *et al.*, 1998). When vascular calcification occurs, extracelluar mast cells containing tryptase are often seen at sites of early calcification and around small calcium deposits, but seldom seen around larger, more solid calcifications. This finding suggests that mast cells may have a role in the initiation of calcification by an unknown mechanism (Chirgwin *et al.*, 1979).

2.5 The histology changes of AAA

As mentioned before, AAA is comprised of medial and adventitial structure degeneration. The most important histological changes of AAA are extensive disruption and degeneration of the medial elastic lamellae and accelerated

turnover of collagen. These two changes are responsible for the decrease in tensile strength of the arterial wall, resulting in AAA rupture. Other changes include chronic immune and inflammatory cell transmural infiltration, immunoglobulin deposition and the decrease in number of medial SMCs (Thompson *et al.*, 1997).

Figure 2.7 Aneurysm stained by van Gieson staining. Red staining shows collagen, yellow staining shows cytoplasm and black staining shows nuclear. It shows the portion of *tunica media* of aneurysm with thickened and disrupted collagen.

2.6 The mechanism of vascular calcification and AAA

2.6.1 Passive mechanism of vascular calcification

Up to about 20 years ago vascular calcification was considered to be a passive process that occurred as a non-specific response to tissue injury or necrosis (Bostrom, 2001; Sambrook and Fritsch, 1989). There have been many popular

explanations for the hardening of the arterial wall. One of these explanations was that lipid deposition resulted as a secondary response to the infection process. This was thought to be a protective physical change (Demer and Tintut, 2003). Recently, there has been increasingly strong evidence that the phenomenon could be biologically controlled, in a similar way to that of bone formation (Bostrom, 2001).

2.6.2 Possible active mechanism of vascular calcification

Arterial calcification is considered to be an active, cell controlled event, which is supported by the expression of mineralisation inhibiting and initiating protein (Tintut and Demer, 2006).

2.6.2.1 Similarities between bone formation and vascular calcification

The clinical coincidence of osteoporosis (low bone mineral density) and vascular disease has been realised (Pennisi *et al.*, 2004; Sattler *et al.*, 2004; Schulz *et al.*, 2004). Both diseases were thought to be passive, degenerative and inevitable as the end-stage processes of ageing, but are now recognised as active, regulated, treatable and preventable disorders. Bone tissue forming within the atherosclerotic artery wall has been known since at least the 1800s and it was reported that red marrow elements were found in bone tissue within atherosclerotic plaque in 1908 (Demer, 2002). Epidemiologically, lipid-lowering treatments seemed to be inhibiting VC in humans as well as reducing fractures in osteoporosis patients in retrospective studies but not confirmed in prospective ovariectomy-induced bone loss (Hofbauer and Heufelder, 2001). Severe osteoporosis in the hip may indicate advanced atherosclerosis and therefore convey an increased risk for not only hip fractures but also for coronary heart disease (Tanko *et al.*, 2003). Clinically, in bone-loss studies (Demer and Tintut, 2003), OPG treatment has been found to increase high mineral density in the hip and to decrease VC mortality among the elderly (Schulz *et al.*, 2004). Serum osteocalcin (inhibitor of calcification) is used as an early marker of bone turn over and is increased in women with aortic atherosclerosis (Dhore *et al.*, 2001). The

evidence has shown an extremely strong link between cardiovascular calcification and bone disease in ESRD patients (Raggi, 2005). It has been found that both diseases were caused by at least three different conditions: deficiency of OPG, deficiency of essential fatty acids and hyperlipidaemia (Demer, 2002). All above findings may suggest that VC has certain unknown genetic links with bone formation in humans.

At the cellular level, vascular SMCs and bone cells share similar phenomena especially in the atherosclerotic plaque. They both differentiate from the same embryonic layer. Vascular calcification has many similarities to embryonic bone formation and bone repair (Bostrom, 2001; Speer *et al.*, 2002). Bone formation proteins such as osteopontin, osteonectin and osteocalcin (Speer *et al.*, 2002) and bone morphogenetic protein 2 (BMP-2) were found in calcified plaques (Bostrom, 2001). The major bone components, BMP-2, osteopontin, collagen I, MGP, osteonectin, biglycan, osteocalcin, and matrix vesicles, have been found not only in calcified bones (Tyson *et al.*, 2003) but also in calcified vascular lesions, which means instrumentally these components may contribute to the composition of atherosclerotic plaques (Bostrom, 2001). In ESRD patients, several mediators of bone mineralisation are believed to contribute to VC though an unidentified mechanism (Raggi, 2005). Osteoclast cells were present in the artery wall in calcified human atherosclerotic lesions (Demer and Tintut, 2003). Interestingly, the calcium deposits in some of the arteries did not only contain complete bone tissue but also bone marrow and fat tissue in autopsy tissue (Demer and Tintut, 2003). This strongly supports that VC is not a simple calcium depositing process, but that it is actually an active process like bone formation (Chen and Moe, 2003; Fitzpatrick *et al.*, 2003; Raggi, 2005).

Vascular calcification also has been seen in animal models where bone related proteins had been knocked out. Medial calcification occurred in a number of mice which were deficient in MGP, similar to Mothers against decapentaplegic homolog 6 (SMAD6, an intracellular mediator of bone morphogenetic protein signalling) and Klotho (a gene associated with aging) (Schoppet *et al.*, 2004). It also occurred in mice treated with supraphysiological doses of vitamin D or warfarin. Additionally, medial calcification in the treated mice can be prevented by inhibitors of osteoclasts, including OPG, bisphosphonates, and a selective

inhibitor of the osteoclastic V-H^+-adenosine triphosphatase, providing further evidence for a mechanistic link between vascular calcification and bone metabolism (Schoppet *et al.*, 2004).

2.6.2.1.1 OPG-RANK-RANKL system in VC

Osteoprotegerin, a receptor activator of nuclear factor- κB ligand (RANKL) and a receptor activator of nuclear factor-κB (RANK) system is produced by and targets vascular cells (endothelial cells and vascular SMCs) *in vivo.* Osteoprotegerin is a neutralising soluble decoy receptor for RANKL and TRAIL (Hofbauer and Heufelder, 2001; Sattler *et al.*, 2004). It has been found in bone related cells, such as bone marrow stromal cells, osteoblast-like cells, osteosarcoma cells and pulp cells in teeth as well as in endothelial cells (Dhore *et al.*, 2001). Osteoblastic cells, T cells and tumour cells produce RANKL, and *in vitro* studies have identified that RANKL is expressed in endothelial and SMCs. The receptor RANK is stimulated by its RANKL and is expressed on the surface of osteoclasts. Ligation of the receptor stimulates all aspects of osteoclast function, such as differentiation, maturation, fusion, survival, and activity (Van *et al.*, 2006).

The RANKL-OPG system has been shown to be involved in the progress of VC. Firstly, RANKL and OPG were localised in normal and atherosclerotic human vessels by immunohistochemical analyses, and were found in normal vascular walls and early atherosclerotic lesions by immunoreactivty. In particular, OPG was found in the borders of calcified structures and was expressed most abundantly in the media of large arteries among the tissue, where RANKL was found adjacent to calcium deposits (Sattler *et al.*, 2004). In addition, the vascular phenotype of OPG-/- mice can be completely rescued by prenatal activation of an OPG transgene. Targeted deletion of OPG has been shown to result in both osteoporosis and calcifications of the medial layers of the aortae and renal arteries, affecting two thirds of OPG-/- mice (Collin-Osdoby, 2004). Of note, dexamethasone enhances differentiation of vascular SMCs toward an osteoblastic phenotype *in vitro* and concurrently inhibits OPG expression by osteoblasts (Schoppet *et al.*, 2004). Above all, OPG might be a protective factor to inhibit the vascular calcification in mice.

However, the use of OPG in vascular disease is controversial. Serum OPG levels were independently associated with vascular calcification by aortic calcification index research in Tokyo. The serum levels of OPG and RANKL were also measured in patients with PAD indicating that OPG and RANKL serum levels are similar in patients and controls (Pennisi *et al.*, 2004). Hence, there is insufficient evidence to support that the RANKL-OPG system was activated in PAD. Nevertheless, Nitta *et al.* documented that rapid progression of vascular calcification was associated with serum OPG concentration on long-term haemodialysis (Nitta *et al.*, 2003). Increased OPG serum levels also have been found to be associated with the presence and severity of coronary artery disease, which may indicate an insufficient regulatory mechanism in the protective role of OPG in the vascular system (Jono *et al.*, 2002). The elevated levels of serum OPG have been found to be associated with intima-medial thickness of carotid artery and may play a role in the pathogenesis of atherosclerotic disease (Erdogan *et al.*, 2004). Finally, single nucleotide polymorphisms in the OPG gene were found associated with cardiovascular morphology and function (Brandstrom *et al.*, 2004).

2.6.2.2 Intimal Calcification

Intimal calcification only occurs within atherosclerotic plaques and can be seen in the second decade of life. It can be used as a surrogate marker for atherosclerosis because calcium mineral deposits are frequently found in the atherosclerotic plaque (Proudfoot and Shanahan, 2001). Atherosclerosis can severely narrow and block arteries. This deposition which is comprised of fatty substances, cholesterol, cellular waste products, calcium and other substances, is called plaque. It has a diffuse, punctate morphology and appears as aggregates of calcium crystals. These deposits can coalesce to form large solid crystals, occasionally with the characteristics of true bone (Frederic H.Martini, 2005; Raggi, 2005). Atherosclerosis usually affects large and medium-sized arteries. The atherosclerotic plaques that rupture cause blood clots to form that can block blood flow or break off and travel to another part of the body. If either happens and blocks a blood vessel that feeds the heart, it causes a myocardial infarction; if it blocks a blood vessel that feeds the brain, it causes a stroke; if blood supply to the arms or legs is reduced, it can cause claudication and

eventually gangrene. Therefore atherosclerosis can induce ischaemia and infarction in end stage of organs (Doherty *et al.*, 2004).

In summary, it is believed that atherosclerosis begins with damage to the innermost layer of the artery, the endothelium. The damage to the endothelium causes deposition of fats, cholesterol, platelets, cellular waste products, calcium and other substances in the artery wall. These may stimulate artery wall cells to produce other substances that result in further build-up of cells. These cells and surrounding material thicken the endothelium significantly. The artery's diameter shrinks and blood flow decreases, reducing the oxygen supply. Often a blood clot forms near this plaque and blocks the artery, stopping the blood flow (Schinke and Karsenty, 2000). However, numerous studies demonstrated that intimal calcification is not a passive progress requiring active inhibitors, but is more like biological net with active initiating and inhibiting components. Taken together, the mechanism responsible for this has not yet been illustrated (Demer and Tintut, 2003).

2.6.2.2.1 Potential mechanisms of intimal calcification

In a review by Proudfoot and Shanahan in 2001, it is suggested that there are four possible classes of mechanisms of intimal calcification. These are involving apoptotic bodies/ matrix vesicles, bone-associated proteins, lipids and calcium and phosphate ions.

2.6.2.2.1.1 Apoptotic bodies (AB)/ matrix vesicles

It has been found through electron microscopic and histological studies that calcification occurs in association with matrix vesicles which are most commonly found in cartilage, bone and organelle-remnants which are shed from intima vascular SMCs (Upchurch, Jr. and Schaub, 2006). Chondrocyte ABs, like matrix vesicles can act as a nidus for calcium crystal formation *in vitro*. In addition, ABs derived from human vascular SMCs can also undergo calcification *in vitro* (Upchurch, Jr. and Schaub, 2006). This suggested that AB is crucial in initiating VC. Matrix vesicles or AB should be cleared by phagocytic macrophages rapidly, but the presence of either of them suggests a deficiency of phagocytes. This

might be due to the competing presence of oxidised lipids (Proudfoot and Shanahan, 2001).

2.6.2.2.1.2 Bone-associated proteins

Human SMCs express many bone calcifying regulation proteins such as osteopontin, BMP-2 and MGP which were found accumulated in the area of calcification. However, the function of these proteins in vascular walls is not clear. This could be due to phenotypic change in SMCs leading to VC, or could be only secondary to calcification (Proudfoot and Shanahan, 2001).

2.6.2.2.1.3 Lipids, calcium and phosphate ions

It is well known that a diet high in lipids and cholesterol carries with it a high risk of atherosclerosis. Lipids and cholesterol were also found in the atherotic plaques. Lipid filled SMCs were found in human carotid atherosclerotic plaques. Of interest, spontaneous lipid accumulation was found in cultured human SMCs before calcification. It could be a potential nidus for calcification. Also oxidised lipids were shown to induce osteoblastic differentiation in CVCs and to compete with macrophages in clearing ABs. Another possible mechanism is an increase of calcium and phosphate ion concentration will attract calcium deposition. Smooth muscle cells respond by increasing calcium uptake, and a higher concentration of phosphate ions was found to be able to induce osteogenic differentiation in human SMCs, resulting in calcification (Proudfoot and Shanahan, 2001).

2.6.2.3 Medial Calcification

Medial calcification occurs independently of intimal calcification and atherosclerosis. It commonly occurs in the peripheral arteries of the lower limbs in otherwise healthy elderly patients (Monckeberg's sclerosis) or ESRD patients. It also occurs in younger patients with diabetes and chronic renal failure (Labat-Moleur *et al.*, 1998). Severe medial calcification is also seen in calcific uremic arteriolopathy (calciphylaxis), a relatively rare and often fatal syndrome of ischaemic necrosis of skin, muscles, and subcutaneous fat occurring almost exclusively in uremic patients. Finally, there are a number of genetic disorders

with unknown aetiology which result in medial calcification. These include idiopathic calcification of infancy and Singleton-Merton syndrome (Schreurs O. *et al.*, 1997). The arteries of both diabetic and non-diabetic patients were free of atherosclerosis, and no difference was observed between two groups of intimal thickness and intima-to-media thickness ratio. It was noticed that calcification was found in *tunica media*, but not in *tunica intima*, obviously greater in diabetic than in non-diabetic patients, and independent of known risk factors such as hypertension, hyperlipidemia, obesity and history of old myocardial infarction (Sakata *et al.*, 2003).

Medial calcification morphology differs from intimal calcification, appearing in its earliest form as linear deposits along elastic lamellae. It is responsible for arterial stiffening and a decrease in arterial compliance, leading to systolic hypertension, left ventricular hypertrophy and ultimately left ventricular failure (Labat-Moleur *et al.*, 1998; Proudfoot and Shanahan, 2001; Raggi, 2005). Medial calcification progresses with age and at its most severe, it forms a dense circumferential sheet of calcium crystals in the centre of the media, bounded on both sides by vascular SMCs and often contains bone trabeculae and osteocytes (Labat-Moleur *et al.*, 1998).

2.6.2.3.1 Potential mechanisms of medial calcification

In the review by Proudfoot and Shanahan in 2001, it is suggested that there are two possible classes of mechanisms of intimal calcification. These are involving apoptosis/elastin and bone-associated genes.

2.6.2.3.1.1 Apoptosis/ elastin

Medial calcification is absent of lipid and inflammatory cells and occurs along the elastic lamellae between layers of vascular SMCs and elastin (Schreurs O. *et al.*, 1997). Apoptotic bodies have been shown to be calcified in a similar way to matrix vesicles. This is possibly because when medial vascular SMCs undergo apoptosis, ABs are released and are not efficiently cleared. When crystals are formed on these matrix vesicles in the media of artery wall, it is likely that crystal growth occurs along elastin fibres due to its suitability as a substrate. It is also possible that elastic lamellae create a physical barrier between vascular SMCs,

preventing ABs of vascular SMCs to be phagocytosed, which could explain the location of calcification in the vessel media (Schreurs O. *et al.*, 1997). In addition, apoptosis has not been found in medial calcification but if it does occur within the media, lack of clearance of apoptotic cells would cause higher extracellular concentrations of calcium and phosphate ions. This could lead to deposition of calcium crystals (Proudfoot and Shanahan, 2001).

2.6.2.3.1.2 Bone-associated genes

Mice lacking MGP developed extensive medial calcification. When medial calcification occurs, MGP decreased, and there was an increase in some bone-related proteins secreted by SMCs which act as nucleators of calcium. This could result in VC by absence or inactivity of calcification inhibitor proteins (Proudfoot and Shanahan, 2001).

2.6.2.3.1.3 Summary

Intimal calcification and medial calcification both are strongly associated with high morbidity and mortality. Increasing amounts of evidence suggest that a regulating process of calcification, including initiating and inhibiting proteins is involved. Taken together, the above conditions all have potential to induce VC. The failure of clearance of AB, the lack of bone-related calcification inhibitors and the expression of the initiating proteins for calcification all provide a favourable environment for the generation of VC.

2.6.2.4 The possible mechanism of AAA formation

Atherosclerosis produces both stenosis (narrowing) and aneurysms (dilation) which are directly opposite in nature (see picture below for the concept of stenosis and aneurysm). Also atherosclerosis and AAA frequently coexist (Jorgensen *et al.*, 2004). A strong association exists between cardiovascular risk factors and measures of clinical and subclinical atherosclerosis, cardiovascular disease, and prevalence of aneurysms (Crawford *et al.*, 2003).

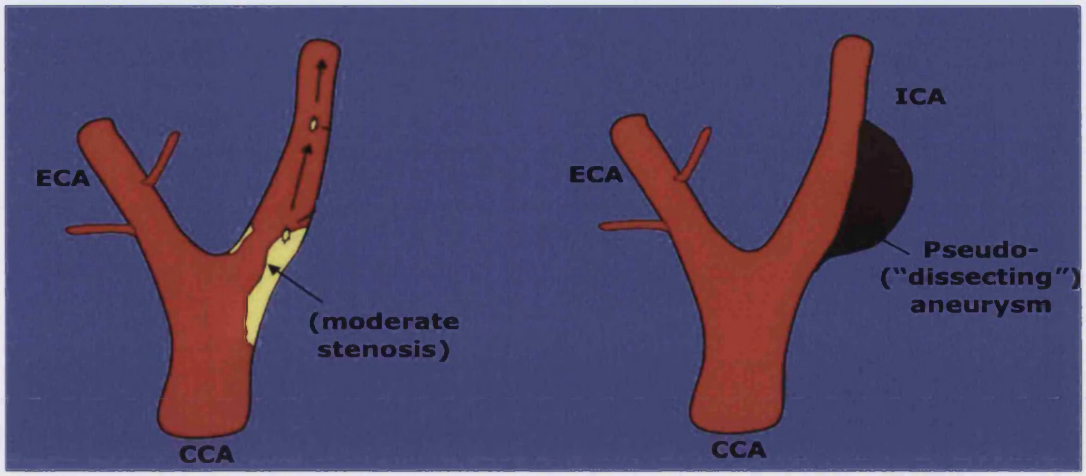

Figure 2.8 Diagram of carotid aneurysm (right) and stenosis (left).

Abdominal aortic aneurysms are characterised by destruction of elastin and collagen in the media and adventitia, loss of medial SMCs with thinning of the vessel wall, and transmural infiltration of lymphocytes and macrophages (Crawford *et al.*, 2003; Ernst, 1993).

Like stenosis, aneurysm formation is not well understood. The National Heart, Lung, and Blood Institute has described aneurysm formation in 4 different ways, a combination of these 4 multiple factors is more likely to reflect the truth (Crawford *et al.*, 2003).

2.6.2.4.1 Potential mechanisms of AAA

- Proteolytic degradation of aortic wall connective tissue
- Inflammation and immune responses
- Biomechanical wall stress
- Molecular genetics

Aneurysm formation involves a complex process of destruction of the aortic media and supporting lamina through degradation of elastin and collagen. The degradation of elastin, collagen, and other constituents might be a reason for the widespread destruction of elastic laminae. Matrix metalloproteinases (MMPs) and their inhibitors have been found to be expressed in vessel walls favouring elastin and collagen degradation, which has attracted a lot of interest in AAA

studies. However, the biological mechanism for initiation of AAAs is still uncertain (Crawford *et al.*, 2003).

The *tunica media* of abdominal aorta is lacking of vasa vasorum (the vessel of the blood vessel wall) causes relative less blood supply in this particular portion than the rest of arteries (Libby Peter, 2002). This could explain that aneurysm often occur in the abdominal aorta. Additionally, ß-blockers which could reduce wall stress have been suggested to be used as protection against continued aneurysm dilation and rupture in animal models. Also, once AAA has developed, the increased vessel wall stress affects the dilation of the aneurysm and the outcome of AAA such as AAA rupture. Increased shear and tension on the aortic wall results in collagen remodelling; furthermore, a decrease in the elastin to collagen ratio from the proximal to the distal aortae may be clinically relevant (Upchurch, Jr. and Schaub, 2006). In addition, AAA was shown to be affected by inflammation. Smooth muscle cell destruction might be due to apoptosis triggered by inflammatory mediators and induce AAA formation (Plutzky, 2003).

Currently, no single genetic polymorphism or defect has been identified as a common denominator for AAAs. Some phenotypes have been found to be associated with AAAs, such as the haptoglobin phenotype (Hp)-21 and deficiencies in α1-antitrypsin. Additionally, there is a decreased frequency of AAAs in patients with a Rh-negative blood group, and an increased frequency in patients with MN (in humans, the MN blood group is characterised by the presence of molecules called glycoproteins on the surface of red blood cells) or Kell-positive blood groups (a family of antigens found in erythrocytes and designated K, k, Kp^a, Kp^b, and Ku; antibodies to the K antigen, which occurs in about 10% of the population of England, have been associated with haemolytic transfusion reactions and with haemolytic disease) (Upchurch, Jr. and Schaub, 2006).

2.6.2.5 Animal models

The clinical significance of arterial calcification is continually growing with population age. Study of human samples is very frustrating because only established-stage samples can be obtained. Thus, appropriate animal models to

imitate VC *in vitro* will lead to new insights into the pathogenesis of arterial calcification.

The mouse models lack specific calcification inhibitors which has been demonstrated by developing a complex regulation of the calcification process (Chirgwin *et al.*, 1979). Osteocalcin-deficient mice developed increased bone formation, but retained normal blood vessel formation (Dhore *et al.*, 2001). Matrix GLA protein knockout mice have been found to develop vascular calcification *in vivo* (Dhore *et al.*, 2001). Osteoprotegerin knockout mice develop medial and subintimal calcification apparent at 2 weeks and marked by 2 months. These animals also develop severe osteoporosis, and exhibit the same relationship between VC and osteoporosis as that shown in humans (Collin-Osdoby, 2004; Kiernan, 2001). Therefore, MGP is considered as an inhibitor of mineralisation in arteries and cartilages in mice. Of note, patients with Keutel syndrome (a disease caused by functional MGP absence) showed calcification of cartilage but not in the arteries. This finding shows human arterial calcification does not depend on MGP, but may rely on some other proteins acting in a similar fashion participate in the inhibition of mineralisation (Schinke and Karsenty, 2000). Dystrophic calcification is not observed in smaller arteries, capillaries or veins, suggesting that these vessels express additional unknown inhibitors of calcification (Demer and Tintut, 2003).

A rat model of aortic allografts was built up to analyse the arteriosclerotic progress. Endothelial cells were reported firstly to gradually disappear at the graft lumen. Subsequently, SMCs, lymphocyte and macrophages proliferated in the *tunica intima* of the vascular wall. After 4-8 weeks, progressive apoptosis was found in the media. Finally, accumulation of macrophages and calcification were observed in the media and endothelial cells reappeared at the graft surface (Religa *et al.*, 2003). These findings show that proliferation and apoptosis of SMCs is a major change.

2.6.2.5.1 Animal models with OPG

The arteries of the OPG knockout mice that exhibited calcification are also sites of endogenous OPG expression, suggesting that OPG may have a specific role in protecting these arteries from calcification. The OPG knockout mice also

developed partial aortic dissection and SMC proliferation in the intima and media suggesting additional regulatory roles for OPG (Dhore *et al.*, 2001; Jono *et al.*, 2002; Kiernan, 2001). In addition, OPG injection in OPG knockout mice cannot reduce the calcification but can reverse bone loss in OPG knockout mice. This implied that OPG cannot reverse the calcification once it has occurred (Collin-Osdoby, 2004). Thus, administration of OPG in arterial calcification might be associated with some other molecules. Interestingly, OPG administration can prevent arterial calcification caused by warfarin or high vitamin D in rats (Collin-Osdoby, 2004). In some animal models, cell death appears to be the principal stimulus for calcification. Arterial calcification in the balloon-injured rabbit aorta occurred early (at 2-4 days) in areas of the media where cells had been killed by necrosis or apoptosis. Calcification occurred before the matrix protein osteocalcin was detected, indicating that the early calcification process in this model was more closely associated with cell death than to the expression or deposition of bone- associated proteins (Luiz Carlos Junqueira *et al.*, 1998).

Hence, a question needs to be addressed. Do vascular calcification animal models reflect the truth of VC in humans? Further effort is required to answer this question.

3.

Chapter 3 APOPTOSIS

3.1 Cell death

Cell death occurs in two main ways: necrosis and apoptosis. Necrosis is usually referred to as traumatic cell death caused by overheating, toxin or hypoxia. When damaged cells undergo necrotic cell death, they swell and the membranes spilt resulting in the intrinsic chemical substances exuding and infecting the cells around them. Briefly, apoptosis is described as a cell suicide or programmed cell death. It does not affect the surrounding cells, and is characterised by various biological and morphological changes of affected cells. The biological changes include an alteration of mitochondrial membrane potential, activation of caspases, DNA fragmentation and formation of apoptotic bodies (AB). The morphological changes include loss of cell surface structures, cell shrinkage and shape modification, condensation of cytoplasm and nuclei, nuclear envelope alterations, nuclear fragmentation and membrane blebbing. The blebbing phenomenon of apoptotic cells lasts for only few minutes and is impossible to detect by light microscopy, but the formation of AB remains visible for 1 to 2 hours and can be observed if the size is over 0.5μm (Anna-Kaisa Eerola, 2000). Differences between necrosis and apoptosis are detailed in appendix B.

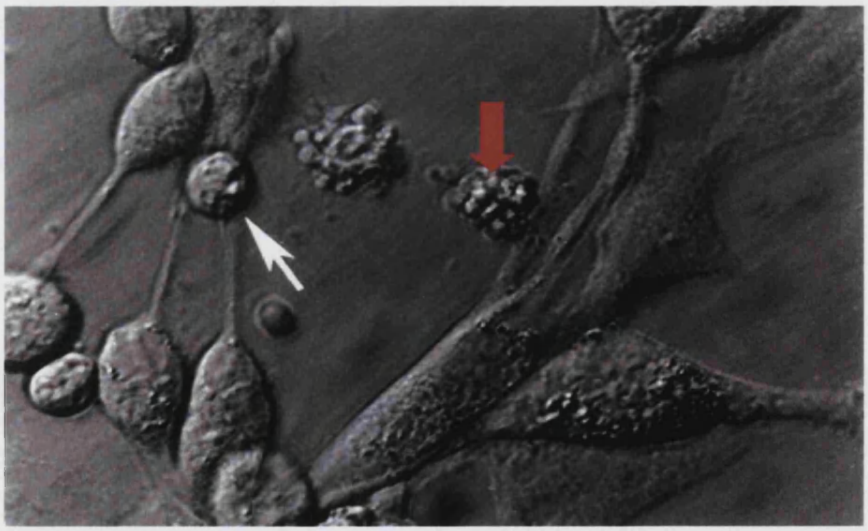

Figure 3.1 Apoptotic vascular SMCs were photographed by videomicrograph. The white arrow indicates an apoptotic body. It appears as round masses and the red arrow indicates membrane blebbing (Bennett *et al.*, 1995).

3.2 Apoptosis

3.2.1 Overview

The Nobel Prize in physiology or medicine in 2002 was awarded for fundamental discoveries concerning the genetic regulation of organ development and programmed cell death in the model organism (Fadeel and Orrenius, 2005). Apoptosis is defined as a type of programmed cell death which plays an important role in many physiological and pathological conditions. Approximately 5% of the cells of an organism undergo apoptosis each day.

Originally, the word apoptosis comes from the Greek, meaning 'falling off' (Michael Quinion, 1996). The principles of apoptosis were first described by Carl Vogt in 1842. It has become a hot topic since 1972, when an Australian scientist, John Kerr, published his finding "Apoptosis; a basic biological phenomenon with wide ranging implication in tissue kinetics" in the British Journal of Cancer (Kerr *et al.*, 1972). The cellular mechanisms that regulate and initiate apoptosis were first elucidated by genetic studies of the roundworm, *Caenorhabditis elegans* (Ellis and Horvitz, 1986).

3.2.2 Apoptosis related disorders

Many of the proteins that control apoptosis that were initially identified in the study of *Caenorhabditis elegans* have also been found in mammals. These include proteins such as ced-3, ced-4, ced-9 and egl-1 in *Caenorhabditis elegans.* The protein of ced-3 encodes a protease of the caspase family in mammals. The protein of ced-4 is an adaptor protein that is similar to apoptotic protease-activating factor-1. Both of them oligomerize to form an apoptosome like complex to induce apoptosis. Proteins of ced-9 and egl-1 encode members of the Bcl family: ced-9 is an anti-apoptotic protein with four Bcl-2 homology domains, whereas egl-1 is a pro-apoptotic BH3-only-domain protein. Molecular model of apoptosis activation (Caspase family and Bcl family are detailed in the next section) (Lettre and Hengartner, 2006). Subsequently, these genes were found to be mutated in tumours of cancer patients. Many other mutated genes found in tumours are associated with cell cycle regulation. These findings appear

to indicate the uncontrolled cell proliferation of cancer results from either excess cell division or insufficient apoptosis (Finley, 2003; Sedghizadeh *et al.*, 2004).

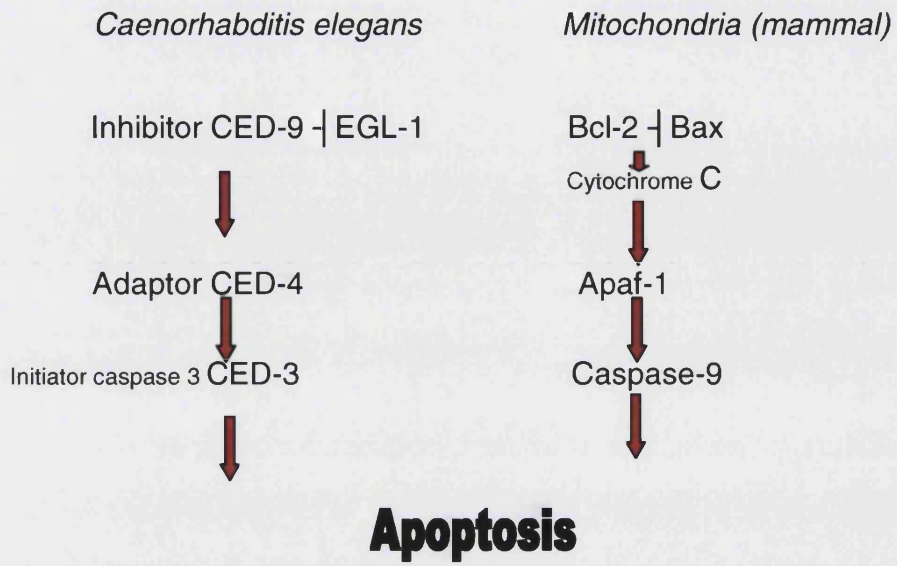

Figure 3.2 Proteins in the *Caenorhabditis elegans* encodes the proteins in mammal.

Derangement of apoptosis contributes to many human diseases directly or indirectly, resulting in either cell accumulation or cell loss (Fadeel and Orrenius, 2005). Apoptosis deficiency is suggested to be associated with cancer. Conversely, excess apoptosis is associated with numerous diseases, such as acquired immune deficiency syndrome (AIDS), neurodegenerative disorders (Alzheimer's Disease, Parkinson's Disease), blood diseases (aplastic anaemia), low-oxygen injury (heart attacks or stroke), or even toxin-induced liver disease (such as that caused by alcohol) (Fadeel and Orrenius, 2005).

3.2.3 Apoptosis pathways

There are two main pathways initiating apoptosis in cells: one is through the cellular death receptor-mediated activation i.e. Fas and TNFR's; the other is mediated by changes in the mitochondrial permeability. Simply, they were described as the extrinsic pathway and the intrinsic pathway respectively. These two pathways have different mechanisms, but both of them result in the cellular

morphological and biochemical alterations that are characteristic of apoptosis (Lesauskaite *et al.*, 2003).

3.2.3.1 Extrinsic pathway

The extrinsic pathway is important in the maintenance of tissue homeostasis, (Ballou *et al.*, 1996). External signals activate the Fas ligand (FasL or CD95L) which then binds to the Fas receptor (CD95). This allows the assembly of a death-inducing signalling complex (DISC); active Fas-associated death domain protein (FADD). This complex then recruits pro-caspase 8. Pro-caspase 8 can autocatalyse releasing the active enzyme which then cleaves the inhibitory pro-section of caspase 3. The active caspase 3 is an effector caspase of apoptosis, resulting in the eventual death of the cell. The TNF family of proteins, including TRAIL, follow a similar method of inducing apoptosis. The TNF ligands bind to their receptors; triggering the assembly of the TNF receptor associated death domain (TRADD). The initiator caspases (8 etc) activate the effector caspapse (3, 7 etc) to induce apoptosis (Fadeel and Orrenius, 2005). Caspases are subject to inhibitions by a family of inhibitor of apoptosis proteins (IAPs) and FLIP (FLICE (FADD-like apoptotic cysteine protease)-inhibitory proteins). This inhibitor, IAP, binds to the substrate groove of caspase 3 and 7, thus blocking access of protein substrate to the active caspase (Chai *et al.*, 2001; Huang *et al.*, 2001; Riedl *et al.*, 2001; Shi, 2004). This inhibitory protein, FLIP, shares significant homology with caspase-8 (also called FLICE) with an additional death effector domain, but lacks the catalytic active site of the caspases and has no protease activity (Boatright *et al.*, 2004; Peter, 2004).

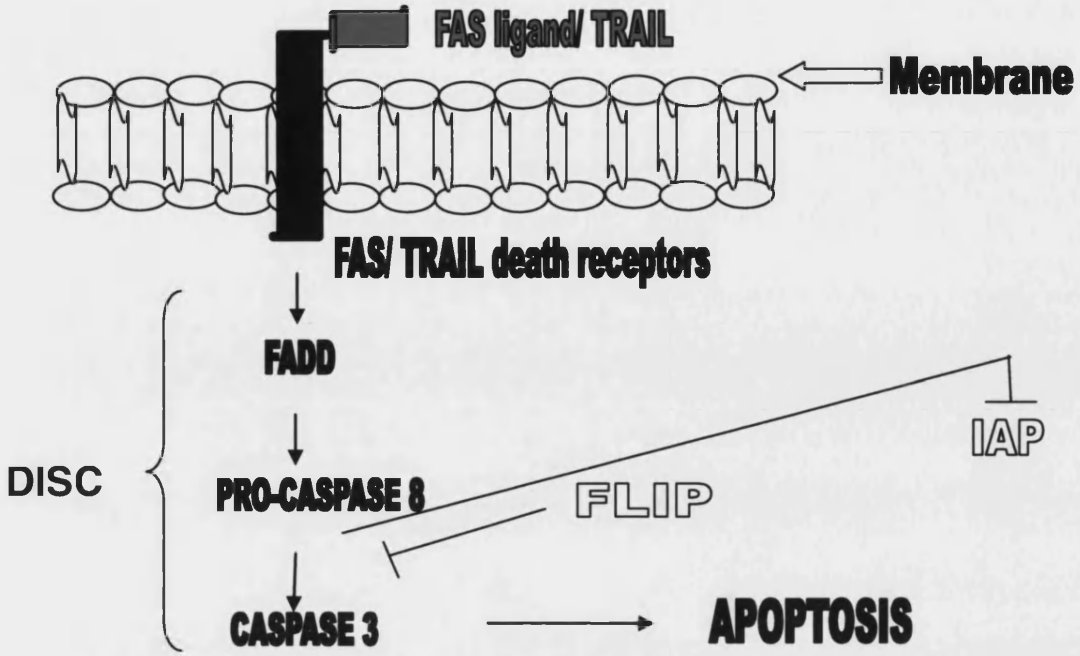

Figure 3.3 Extrinsic apoptosis pathway. FAS ligand and TRAIL bind to their death receptors and results in the activation of effector caspases within cell. Affected cell finally undergoes apoptosis. FLIP and IAP are inhibitors of apoptosis.

3.2.3.2 Intrinsic pathway

The intrinsic pathway is also called mitochondrial pathway. This is because mitochondria are crucial for the execution of cell death during this pathway, although the endoplasmic reticulum has been implicated (Parone *et al.*, 2002). The intrinsic pathway plays an essential role in response to foreign body invasion or internal insults such as desoxyribonucleic acid (DNA) damage (Fadeel and Orrenius, 2005;Hay and Kannourakis, 2002). This pathway in instigated by pro-apoptotic signals which are suicide signal originating from inside the cell. Pro-apoptotic signals activate the mitochondria. Apoptotic proteins are compartmentalised within and are release from functional mitochondria. They have been placed in close proximity to their apoptotic sites of action, and consequently apoptosis occurs.

Cytochrome c is normally localised in the intermembrane space of the mitochondria. It interacts with apoptotic protease-activating factor-1 (Apaf-1), adenosine triphosphate (ATP)/ deoxyadenosine triphosphate (dATP), and caspase 9 to form the apoptosome. Cytochrome c and ATP/dATP, Apaf-1 undergoes a conformational change permitting self-aggregation. Caspase 9 binds to Apaf-1 forming a complex while cytochrome C and dATP are present. This complex leads to cleavage of caspase-9, converting it to effector caspase 9. Caspase 9 can then directly activate the effector caspases 3 and 7, which results in the orderly death of the cell through controlled proteolytic processing of various downstream targets. Cytochrome C, Apaf-1, ATP/dATP and caspase are all essential in activation of caspase 3 and 7 (Anna-Kaisa Eerola, 2000; Li *et al.*, 1997).

The second mitochondria-derived activator of caspase (Smac) is also located in the mitochondria and released into the cytosol in response to apoptotic stimuli. Smac removes IAPs inhibitory effect on caspase activity by binding to baculovirus IAP repeat (BIR) domains to promote procaspase-9 activation (Du *et al.*, 2000).

The apoptosis-inducing factor (AIF) is a mitochondrial flavoprotein that translocates to the nucleus following apoptotic stimulation. Desoxyribonucleic acid (DNA) fragmentation was triggered by AIF and chromatin condensation in the nucleus-independent from caspases. However it promotes apoptosis cooperating with other factors such as endonuclease G (Cregan *et al.*, 2004).

The p53 tumour suppressor gene is a 53kDa phosphoprotein. This gene arrests cells in the G0/G1 phase whenever DNA is damaged in order to allow the cell's DNA repair mechanism to function. If DNA repair is unsuccessful, p53 induces apoptosis by upregulating the apoptosis-inducer bax and down-regulating the anti-apoptotic bcl-2, leading cells to apoptotic death. It resides primarily in the nucleus and functions as a transcriptional regulator. The gene p53 promotes apoptosis when cells become hypoxic or are exposed to UV irradiation. It also triggers apoptosis when DNA damage occurs, growth factors are withdrawn or in the presence of mitogenic oncogene expression in cells (Semenza, 2006).

Human bcl-2 family is very important in the initiation and the inhibition of apoptosis. Members of the inhibitory bcl family of proteins include bcl-2, bcl-xL, mcl-1, bcl-w, A1 and Boo; members of initiatory family of bcl proteins include bax, bak, bok/mtd, bcl-xS, bik/nbk, hrk/dp5, bim/bod, blk, bad, bid. Inhibitory group (the Bcl-2 proteins) proteins reside on the outer mitochondrial membrane while initiatory group proteins (the bax proteins) reside in the cytosol. High expression of the bcl-2 proteins inhibits apoptosis and high expression of the bax proteins induces apoptosis. The ratio of bcl-2 to bax determines the susceptibility of a cell to apoptosis and p53 probably regulates this ratio. When overexpressed, bax forms homodimers, thereby accelerating apoptosis. In contrast, when bcl-2 is expressed in excess, it heterodimerises with bax and apoptosis is suppressed (Israels and Israels, 1999).

The bax proteins receive apoptotic signals and then migrate and bind to the mitochondrial membrane inducing membrane changes. These changes result in cytochrome c and AIF being released from mitochondria to induce apoptosis (Israels and Israels, 1999).

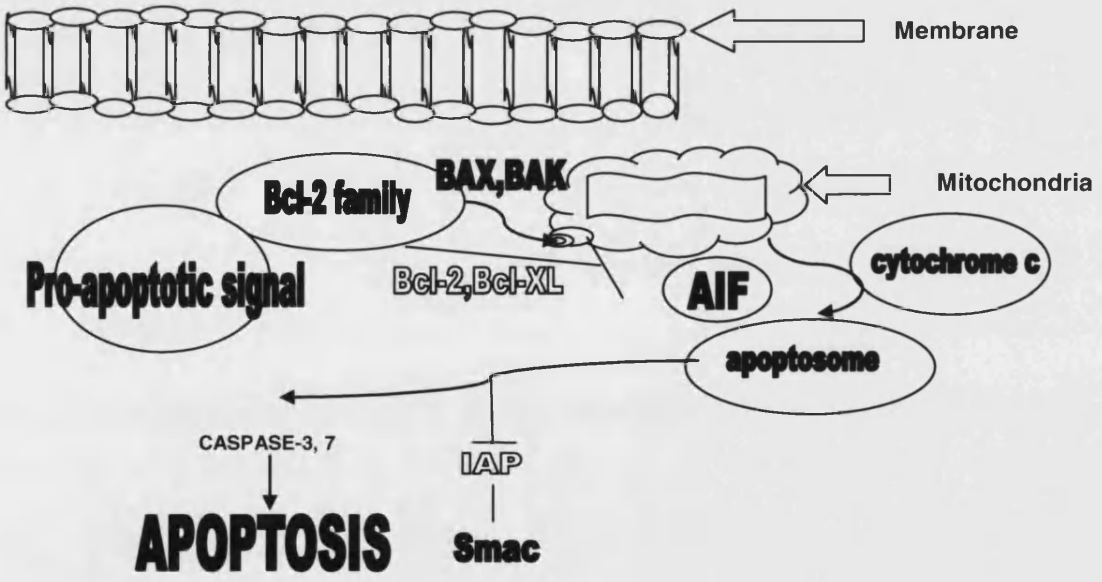

Figure 3.4 Intrinsic apoptosis pathway. Pro-apoptotic signals actives caspase 3 by a number of different proteins released from mitochondria, resulting in apoptosis.

3.2.3.3 Other apoptosis pathways

There are other apoptosis pathways excluding the intrinsic and the extrinsic pathways described. For example, cytotoxic T cells and natural killer cells trigger apoptosis either by FAS ligand pathway or perforin/ granzyme B-dependent pathway. Perforin/ granzyme B-dependent pathway involves a pore-forming protein, perforin and a serine protease, granzyme B. Granzyme B can directly cleave and activate pro-caspase 3 to initiate apoptosis. This pathway mainly operates in viral defence and immune surveillance against cancer. It also works to protect immune homeostasis. In addition, granzymes A and C also play roles in the apoptosis pathway (Israels and Israels, 1999). Granzyme A is independent from granzyme B but still synergistically induce apoptosis in a perforin-dependent manner (Israels and Israels, 1999; Lieberman, 2003). Whereas granzyme C acts through another independent apoptotic pathway from perforin-dependent manner (Anna-Kaisa Eerola, 2000; Lieberman, 2003).

3.3 Apoptosis correlated with vascular calcification

The link between cell death and VC has been noted in pathological studies. Vascular cells that undergo apoptosis or necrosis may provide membrane fragments that play a role in initiating calcification. Apoptosis has been shown to precede calcification *in vitro*, and has been identified in normal cultured animal and human vascular SMCs and in the remodelling of new born animal's arterial walls. The formation of ABs may act as a nucleation site for calcium crystal formation in the vessel wall (Proudfoot and Shanahan, 2001). Lynch *et al.* have shown that apoptosis is an integral part of osteoblast differentiation and calcification in foetal rat calvarial osteoblast cultures (Lynch *et al.*, 1992). Proudfoot *et al.* provided experimental evidence of a role for apoptosis in the initiation of VC (Proudfoot *et al.*, 2000). Under the electron microscope, the ABs have a similar structure to the matrix vesicle, membrane-bound vesicles that are produced by osteoblasts, chondrocytes and odontoblasts, containing the necessary calcium-binding proteins and phosphatases for nucleation of hydroxyapatite (Proudfoot *et al.*, 2001). These proteins were found in forming

bones and mineralising cartilages as well as calcified arteries and heart valves. Furthermore, bax proteins were found in SMCs which were derived from advanced carotid atherosclerotic plaques. It is a sign of remnants of apoptotic cells. Cytoplasmic vesiculation is a recognised feature here, and the formation of matrix vesicles may therefore represent a manifestation of programmed cell death. It backs up the evidence of apoptosis in VC occurring via an extracellular pathway (Proudfoot *et al.*, 2000).

Although calcification in atherosclerosis has been detected mainly in association with extracellular structures, intracellular calcification has also been detected, such as calcified cell organelles or calcified structures that have been engulfed by SMCs. Consequently, apoptosis appears to be a relatively common event in atherosclerotic arteries and after arterial injury.

3.4 The events of apoptosis in the formation of vascular calcification

Women tend to have more calcified vascular diseases after menopause. It is known that oestrogen deficiency occurs after menopause and it also results in osteoporosis in humans. Additionally, it has been proven that oestrogen prevents glucocorticoid-induced apoptosis in osteoblasts (Gohel *et al.*, 1999). Proudfoot *et al.* (2000) found apoptosis occurred in the early stages of VC before calcium crystal deposition in the SMC nodules. Kondo *et al.* found the frequency of apoptosis was significantly higher in the earlier stage of VC. In progressive saccular aneurysms, medial SMCs had almost disappeared at the dome; apoptosis of SMCs took place in the neck portion. Thus, the aneurysmal wall expands and the aneurysm becomes larger (Kondo *et al.*, 1998). These observations showed that apoptosis precedes the onset of VC. However, the mechanism of regulation the VC by apoptosis remains unknown.

Studies have been carried out to investigate whether inhibitors of apoptosis also inhibit VC and conversely if initiators of apoptosis initiate VC (Jian *et al.*, 2003; Proudfoot *et al.*, 2000). However, there are few studies that focus on whether inhibiting VC will inhibit apoptosis and *vice versa*. To test whether apoptosis was actually required for calcification to occur, apoptosis was inhibited in nodules by

the caspase inhibitor ZVAD.fmk. A decrease in calcification was found after the treatment. Conversely, when apoptosis was initiated by anti-Fas IgM and cyclohexamide in the SMC nodules this resulted in a 10-fold increase in calcification (Proudfoot *et al.*, 2000). In addition, when cultured SMCs underwent TNF-initiated apoptosis they presented with calcific aortic stenosis cusps (Jian *et al.*, 2003). Taken together, all the evidence strongly supports the role of apoptosis in calcification.

Another possibility is that ABs are the initiators of calcification. This concept was tested experimentally in rat aortic segments by Religa *et al.* (Religa *et al.*, 2003). Calcification was minimal when the segments were grafted and contained inflammatory cells and then placed in Millipore chambers in the peritoneal cavity. As phagocytes are the professional scavengers in the human body, they should recognise and phagocytose ABs in the early stages of apoptosis. However, ABs were still capable of stimulating calcium crystal growth because phagocytes become less efficient which might due to the presence of oxidised lipids. Oxidised lipids are known to compete with ABs for phagocytes binding. Therefore, a potential mechanism of induction of calcification was assumed as the absence of efficient phagocytic cells in atherosclerotic lesions or a lack of clearance of ABs (Proudfoot *et al.*, 2000).

Smooth muscle cell AB and chondrocyte matrix vesicles both initiate VC but in a different manner. Apoptotic bodies could induce VC independent of ATP while matrix vesicles only induce VC in the presence of ATP. As a matter of fact, ATP was not necessary for matrix vesicle calcification according to different studies (Hashimoto *et al.*, 1998). When SMC-derived AB were permeabilised with NP-40, no calcium accumulation was observed indicating that calcium accumulation occurs via a mechanism requiring an intact AB membrane (Proudfoot *et al.*, 2000). Proudfoot *et al.* suggested that calcium is taken up into SMC AB by an ion channel or calcium-binding protein that does not require ATP for its activity. This suggests that AB may contain sufficient ATP to accumulate calcium. Furthermore, when adding exogenous ATP to vascular SMCs, there is no additive effect in VC. This implies that vascular SMC AB may not contain the necessary enzymes for ATP hydrolysis, which is present in matrix vesicles (Proudfoot *et al.*, 2000).

Confocal imaging revealed that calcium was concentrated in calcein-loaded AB. Calcium was seen throughout the AB, rather than being localised at the membrane. This was supported by elemental analysis of the ABs in calcifying solutions containing abundant calcium but very low phosphate. Additionally, AB contain calcium carbonate as the preferred form of calcium. These observations implied that SMC-derived ABs can concentrate and crystallise calcium in a form that is found *in vivo* (Proudfoot *et al.*, 2000).

Apoptotic bodies derived from SMC in atherosclerotic plaques are similar to matrix vesicles derived from chondrocytes (Proudfoot *et al.*, 2001). It seems that these two components may share the same pathways to initiate calcification. However, it appears that SMC AB and chondrocyte-derived matrix vesicles produce a different type of calcium crystal *in vitro* and use a different method to accumulate calcium. This may be attributable to differences in *in vitro* culture conditions or perhaps to intrinsic differences in protein expression (Proudfoot *et al.*, 2000). It is also worthy of note that not all chondrocyte matrix vesicles calcify, this only occurs at specific sites in the cartilage matrix. Only tissues normally engaged in mineralisation produce mineralisation-competent vesicles. Matrix vesicles only calcify *in vitro* if they are preincubated in ascorbate- and phosphate-rich medium, which generates matrix vesicles enriched with annexin V (which can act as a Ca^{2+} channel) and alkaline phosphatase. Above all, it suggests that not all matrix vesicles encourage VC. However, it is also possible that non-mineralising tissues produce inhibitors of matrix vesicle function to block mineralisation. Therefore, a lack of production of inhibitors of matrix vesicle calcification may lead to the development of pathological calcification (Proudfoot *et al.*, 2001).

Apoptosis occurs not only in SMCs but also in other vascular cells such as endothelial cells and macrophages. Endothelial cells that are undergoing apoptosis have exposed phosphatidylserine on their cell membrane increasing the likelihood of arterial thrombosis. Macrophages that are undergoing apoptosis contribute to the formation and progression of the lipid core and promote thrombosis of atherosclerosis in disordered arteries (Lesauskaite *et al.*, 2003). Additionally, TRAIL, which is a member of TNF family, is expressed by vascular SMCs and may promote cell death in an autocrine or paracrine fashion when

induced in conditions such as diabetes, hyperlipidemia, chronic renal failure, or atherosclerosis (Wang and El-Deiry, 2003). Nevertheless, no evidence shows that apoptosis is the only mechanism of VC.

3.4.1 Apoptosis in AAA

Smooth muscle cells in the medial layer of AAA have been proven to contribute to the formation of AAA. Some researchers found that the number of SMCs in the medial layer of AAA decreases (He and Roach, 1994; Lopez-Candales *et al.*, 1997). Furthermore, SMCs in the medial layer of AAA appear intact and are thinner than is usually seen, lying between the layers of the degraded lamellae (Lopez-Candales *et al.*, 1997). Medial layer SMCs have been observed to display characteristic apoptotic morphological and biological changes at the ultrastructural level in addition to DNA fragmentation being detected by agarose gel electrophoresis (Thompson *et al.*, 1997).

Further investigations have been performed to test AAA apoptosis *in vivo.* Apoptotic cells were observed in intimal and medial layers of AAA vessel walls and the majority of apoptotic cells in the media were SMCs. The tumour suppressor gene p53 was also found in AAA *in vivo.* It has been shown that p53 protein expression was much higher in the AAA than in normal aorta and atherosclerotic occlusive disease. Another important finding was that the p53 accumulated in the medial of AAA but not in the medial of normal aorta and atherosclerotic occlusive disease. Additionally, p53 positive cells co-expressed α-actin which is a typical stain for vascular SMCs. It is worthy of note that FAS was also detected in medial SMCs in human AAA tissues (Thompson *et al.*, 1997).

All the above evidence implicates apoptosis to be involved in AAA but it is still unclear whether apoptosis is a key mechanism of AAA. Three suggestions have been taken together to discuss the potential impact of apoptosis in the mechanism of AAA formation. Firstly, high local concentrations of oxidants produced in atherosclerotic tissue including nitric oxide, oxygen free radicals and oxidised low-density lipoproteins (LDL) induce apoptosis in the medial SMCs in AAA. Secondly, apoptosis in AAA medial SMCs might be subject to ischaemic

injury of the arterial wall. Finally, extensive matrix degradation might be responsible for apoptosis in AAA (Thompson *et al.*, 1997).

4.

Chapter 4 Tumour Necrosis Factor (TNF). - Related Apoptosis- Inducing Ligand (TRAIL).

4.1 The TRAIL Apoptosis System

Tumour necrosis factor-related apoptosis-inducing ligand (TRAIL) is a type II transmembrane protein with a trimeric structure (Hymowitz *et al.*, 2000). It is an important apoptosis-inducing member of the TNF family whose main role is to induce programmed cell death in tumour cells from various tissue origins (Griffith and Lynch, 1998). It was firstly cloned from human heart and lymphocyte DNA libraries initially with 32 kDa molecular weight in 1995 (Wiley *et al.*, 1995) then discovered by an independent lab in 1996 (Pitti *et al.*, 1996). Human TRAIL is 281 amino acid (aa) residues long, with 17aa residue cytoplasmic tail, a 21 aa residue transmembrane segment, and 243 aa residue extracelluar region. It shares highest sequence homology with FASL which is also a member of TNF family (Gruss, 1996). Like the other members of the TNF family, TRAIL is capable of inducing apoptosis in many tumour cells, but, interestingly, not in normal cells. TRAIL and its five receptors are expressed in the almost all normal and abnormal human tissues. They are predominantly localised in germ cells (Grataroli *et al.*, 2004) and cells of the immune system (Wang and El-Deiry, 2003). The system plays a role in both T-cell- and natural killer cell-mediated tumour surveillance and the suppression of tumour metastasis (Wang and El-Deiry, 2003).

TRAIL's 5 receptors are divided into two groups: death receptors and decoy receptors. Death receptors include TRAIL receptor 1 (TRAIL-R1, CD4) and TRAIL receptor 2 (TRAIL-R2, CD5, killer) which both initiate apoptosis (Schneider and Tschopp, 2000). Decoy receptors include TRAIL receptor 3 (TRAIL-R3, DcR1), TRAIL receptor 4 (TRAIL-R4, DcR2) and OPG which are all inhibiting receptors (LeBlanc and Ashkenazi, 2003). Additionally, it has been reported that two novels splice variants of human TRAIL, TRAIL-beta and TRAIL-gamma exist that do not show apoptotic potential (Krieg *et al.*, 2003).

The receptor 1 of TRAIL (TRAIL-R1) is 468 aa residues long, with 220 aa residue cytoplasmic domain, a 19 aa residue transmembrane segment, and 226 aa residue extracelluar region. It is a type I transmembrane protein with extracelluar N-terminus and intracellular C-terminus death domain (Schneider and Tschopp, 2000). The receptor 2 of TRAIL (TRAIL-R2) is 411 aa residues long, with 206 aa

residue cytoplasmic domain, a 22 aa residue transmembrane segment, 132 aa residue extracelluar region and 51 aa residue signal sequence (LeBlanc and Ashkenazi, 2003). Both death receptors contain 2 cysteine-rich motifs in extracelluar region and C- terminus death domains which are independent of FADD.

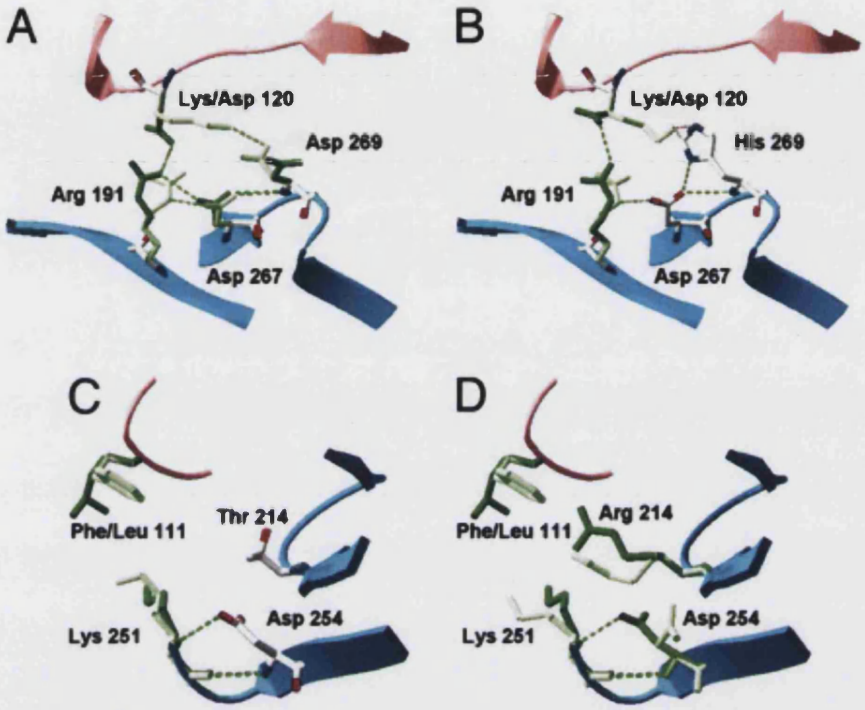

Figure 4.1 The molecular structure of TRAIL and interaction of TRAIL with its death receptors (TRAIL-R1 and TRAII-R2). Red ribbons indicate the receptors, and blue ribbons indicate TRAIL. Residues in DR5 complexes are in dark green, and residues in DR4 complexes are in light green. (Hymowitz *et al.*, 2000)

In contrast to these death-inducing receptors, TRAIL-R3, which shares homology with TRAIL death receptors, is devoid of a cytoplasmic domain and exists as a glycophospholipid-anchored protein on the cell surface. It is 259 aa residues long, with a 19 aa residue transmembrane segment, 217 aa residue extracelluar region and 23 aa residue signal sequence (Schneider *et al.*, 1997a). Since TRAIL-R3 mRNA was preferentially found in normal cells but not in transformed cells, it is thought that TRAIL-R3 might be responsible for the cellular resistance of some normal cells to TRAIL-mediated cytotoxicity (gli-Esposti *et al.*, 1997). It has been suggested that TRAIL-R3 can protect cells from TRAIL-induced

apoptosis by competing with the death-inducing TRAIL receptors for TRAIL binding. The receptor 4 of TRAIL (TRAIL-R4) is 386 aa residues long, with 154 aa residue cytoplasmic domain, a 21 aa residue transmembrane segment, 125 aa residue extracelluar region and 31 aa residue signal sequence. The cytoplasmic domain containing a truncated death domain lacking 4 out 6 aa essential for recruiting adapter proteins that cannot transmit a death signal but can weakly activate necrosis factor (NF)-κB. It has been shown that NF-κB activation may increase the anti-apoptotic threshold of cells and tissues exposed to cytotoxic cytokines such the TNF family to inhibit TRAIL-induced apoptosis. Also TRAIL-R4 may protect the cells from apoptosis by competing with TRAIL death receptors using a similar inhibiting mechanism as TRAIL-R3 (gli-Esposti *et al.*, 1997; Marsters *et al.*, 1997). Osteoprotegerin is the last decoy receptor, but is unlike the other two decoy receptors. It is a soluble receptor. It is a secretory glycoprotein consisting of 401 aa residues with a molecular weight of 60 kDa as a monomer and 120 kDa (Blair *et al.*, 2006) as a disulfide-linked dimer which is produced in different tissues including the cardiovascular system e.g. heart, arteries and veins and is found in particularly high levels in aortic and renal arteries (Collin-Osdoby, 2004; Miyashita *et al.*, 2004). In addition, OPG inhibits the binding of RANK to RANKL (TRANCE, osteoprotegerin ligand, OPGL, osteoclast differentiation factor, ODF) and thus inhibits the recruitment, proliferation and activation of osteoclasts (bone cells associated with bone removal and absorption). Since OPG exhibits an inhibitory effect on osteoclasts, it acts as a soluble factor in the regulation of bone mass. Osteoclast formation activity may be monitored principally by determination of concentration ratio of RANKL /OPG. Alteration of this ratio may be the cause of bone loss in many imbalances in bone metabolism such as osteoporosis (bone mass decrease), osteopetrosis (bone mass increase), hypercalcemia (high level of calcium in the blood), metastatic osteolytic lesions and rheumatic bone degradation. The protein RANKL is expressed by osteoblastic lineage cells and T lymphocytes and acts by binding to its physiological receptor RANK, which is expressed on osteoclasts. As mentioned in chapter 2, ligation of RANK stimulates all aspects of osteoclast function including differentiation, maturation, fusion, survival, and activity (Blair *et al.*, 2006). By contrast, OPG is produced by a variety of tissues, including the cardiovascular system, and acts as a soluble decoy receptor by neutralising RANKL (Schoppet *et al.*, 2004). In summary, OPG is a decoy

receptor of TRAIL and RANKL. For the above reasons, it appears to be a genetic factor that has influence in both arterial and bone systems.

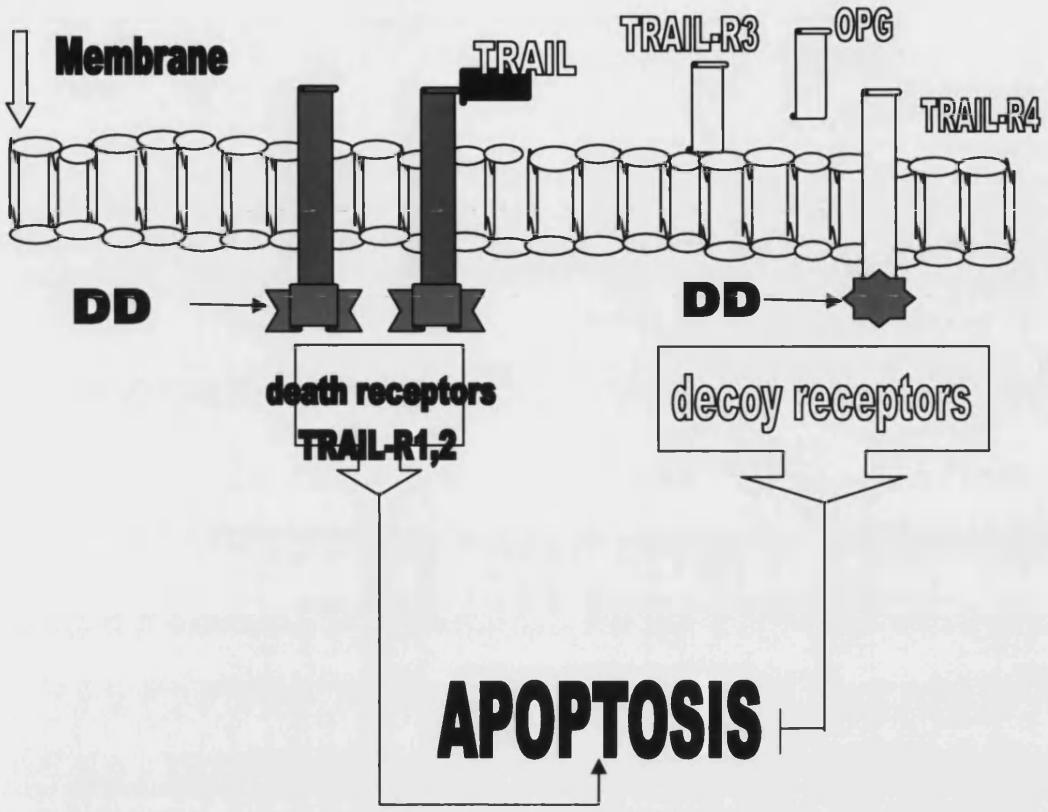

Figure 4.2 Representative diagram represents TRAIL and its five receptors. Transmembrane protein TRAIL-R1 and TRAIL-R2 bind to TRAIL to induce apoptosis. Transmembrane receptor TRAIL-R4 and non-transmembrane receptors TRAIL-R3 and soluble receptor OPG bind to TRAIL to inhibit apoptosis. DD represents death domain.

4.2 Biochemistry of TRAIL-induced Apoptosis

The fact that TRAIL has five receptors, all slightly differing in their mode of action with TRAIL, indicates that a complex regulation of cellular susceptibility to TRAIL-mediated apoptosis exists at the level of receptor expression.

The roles of TRAIL in health and disease have not been identified since it was first discovered in 1995 (Song *et al.*, 2000). Recently, increasing evidence suggests that TRAIL not only is a potential anticancer therapeutic agent both *in*

vitro and *in vivo*, but also, because of its ubiquitous expression in many normal tissues may also have other important physiological and biochemical roles. Song *et al* suggested that TRAIL is a potent inhibitor of autoimmune arthritis. The inhibitory effect of TRAIL on arthritis may be a result of inhibition of cell cycle progression and/or cytokine production (Song *et al.*, 2000). Lee *et al* showed TRAIL may specifically protect the visual axis from tumour growth and metastasis. This is consistent with the fact that tumours rarely occur in the eye compared with other organs. Both TRAIL and FASL have been found to be expressed in the eye and are capable of inducing apoptosis of tumour cells *in vivo*. However, it has been indicated that the mechanism of TRAIL action is different from that of FASL. Whereas FASL induces apoptosis of activated T cells, TRAIL appears to inhibit their proliferation without eliminating them through apoptosis (Lee *et al.*, 2002). This finding is consistent with the unique trait of TRAIL in inducing apoptosis of tumour cells but not normal cells.

Although very little is known about possible non-apoptotic functions induced by TRAIL, it has been shown that endothelial cells express the mRNA for all TRAIL receptors and that TRAIL protein is expressed by the medial smooth cell layer of aortae and pulmonary artery (Gochuico *et al.*, 2000). It is also noteworthy that cleavage of membrane TRAIL from the cell surface requires the action of cysteine proteases (Muzio, 1998), which are abundantly present in the vessel wall (Garcia-Touchard *et al.*, 2005). The magnitude of the TRAIL-induced proliferative response is similar to that of more thoroughly characterised angiogenic factors, such as vascular endothelial growth factor (VEGF). An interesting parallel between VEGF and TRAIL is that both are produced by the vascular SMCs of the human vascular wall and most likely modulate endothelial cell functions in a paracrine pathway (Mitsiades *et al.*, 2002). Thus, TRAIL may also be implicated in the homeostatic control of endothelial biology and possibly in angiogenesis. These data demonstrated that TRAIL has a direct effect on endothelial cell survival and proliferation without inducing inflammatory markers and proposes its potential role in SMCs (Secchiero *et al.*, 2003).

The mechanism of TRAIL triggering apoptosis *in vivo* is unclear. Similar to the other TNF members, TRAIL induces apoptosis by both the intrinsic pathway and the extrinsic pathway (Qian and Chen, 2002). The intrinsic pathways of TRAIL

involve late dissipation of the mitochondrial membrane potential and cytochrome c release that follows activation of caspase-8 and caspase-3 and inducing DNA fragmentation. However, inhibition of caspase-8 but not caspase-3 can prevent mitochondrial permeability transition (PT) and apoptosis. Various cells that are overexpressing the anti-apoptotic proteins bcl-2 or bcl-XL are not or are only marginally protected against TRAIL-induced apoptosis. In contrast, apoptosis induced by the chemotherapeutic drug etoposide was severely impaired in these cells. In addition, in other cell types this invokes a different phenomenon e.g. pancreatic tumour cell lines which are primarily TRAIL-resistant can be rendered TRAIL-sensitive by bcl-xL antisense treatment (Thomas *et al.*, 2000). Additionally, high levels of cellular FLIP (c-FLIP) often correlated with resistance of cells to TRAIL-induced apoptosis (Sayers and Murphy, 2006). The external apoptosis pathway of TRAIL is similar to the extrinsic apoptosis pathway of FASL. It is to be noted that NF-κB activation occurs in collagen-induced arthritis, and that inhibition of NF-κB activation in T cells prevents this disease. This indicates that TRAIL also induces apoptosis by activating NF-κB. Different use of FADD or TRADD as the molecular switch might contribute to whether proximal caspase or NF-κB be activated (Sayers and Murphy, 2006). The connection and crosslink between two main pathways (will be detailed in 4.3) might contribute into TRAIL systems behaviour such as it inducing apoptosis in tumour cells but not in normal cells. However, various signal transduction pathways of TRAIL receptors are yet to be defined. Unidentified pathways may be responsible for the inhibitory effect of TRAIL in inflammation and cell cycle progression (Song *et al.*, 2000). Therefore, it is necessary to determine whether these pathways also occur in normal cells, and if so, whether this is responsible for the cell cycle–arresting effect.

4.3 Analysis of TRAIL apoptosis pathways

Under native conditions, which molecules transmit the TRAIL death signal has not been fully determined. Further studies of the cloned TRAIL-rTRAIL system were carried out to illustrate this remaining question.

As detailed in chapter 3, a great number of proteins known to be involved in various aspects of apoptosis signalling have been suggested to also play a role

in TRAIL-induced apoptosis. It has been documented that TRAIL receptors can activate both caspase (through FADD/ TRADD) and NF-κB pathways in tumour cells (Song *et al.*, 2000).

Firstly, FADD as a death domain for TRAIL death receptors and caspase-8 are revealed. The death-inducing signalling complex (DISC) of TRAIL and FASL is quite similar. FADD and caspase-8 recruited to the TRAIL DISC have been identified in cell lines, such as hepatocellular carcinoma (HCC) cell lines that exhibit differential sensitivity to TRAIL. Pre-treatment with chemotherapeutic drugs, e.g. 5-fluorouracil (5-FU) rendered the TRAIL-resistant HCC cell lines sensitive to TRAIL-induced apoptosis. Analysis of the TRAIL DISC revealed substantially increased caspase-8 recruitment and activation after sensitisation with unchanged FADD. At the same time marked downregulation of c-FLIPL and c-FLIPS or upregulation of TRAIL-R1 and -R2 was noted after 5-FU treatment. In summary, the results suggest that TRAIL-mediated apoptosis in this cell line is controlled at the DISC level through the ratio of caspase 8 and cFLIP (Ganten *et al.*, 2004).

The role of FADD in TRAIL mediating apoptosis pathway is controversial. When cells express FADD-DN (negative version of FADD, lacking of death receptor domain), these cells showed an insensitivity to both TRAIL and FASL mediated killing (Ou *et al.*, 2005). It also has been implicated in TRAIL death receptors. However, it is reported that cells were still capable of undergoing apoptosis upon stimulation of TRAIL death receptors in mice lacking of FADD by Yeh *et al (Yeh Wen-Chen et al., 1998)*. It indicated that there was some adapter protein like FADD involved. However, most researchers concluded that FADD is required for TRAIL death receptors to mediate apoptosis (Berger and Kretzler, 2002).

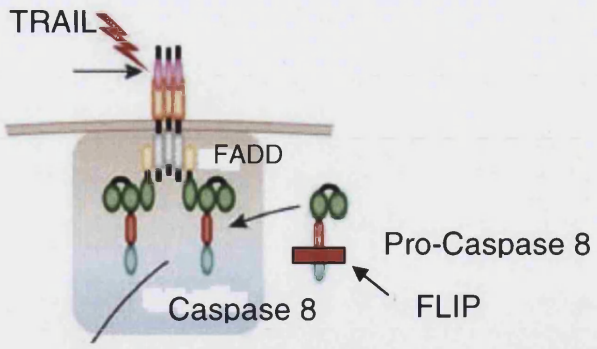

Figure 4.3 Linking TRAIL and its death receptors through the the DISC of FADD, caspase 8. FLIP inhibits the process pro-caspase 8 activation.

Secondly, the involvement of another protein, namely caspase-10, in DISC formation and apoptosis induction by death receptors has been controversial. Caspase-10 is the only other caspase besides caspase-8 that contains a death effector domain, the domain necessary to dock to adaptor proteins like FADD (Cohen, 1997). Interestingly, mutations in caspase-10 have been identified in patients with autoimmune lymphoproliferative syndrome type II (ALPS II). Resulting defects in TRAIL-induced apoptosis were suggested to be causative for ALPS II. Caspase-10 is found further to be cleaved during FASL-induced apoptosis of activated T cells. These two findings suggested that the observed caspase-10 mutations in ALPS II patients may be causative for this disease by inhibiting proper DISC formation and caspase activation not only at the TRAIL DISC, but also at the FASL DISC (Jackson and Puck, 1999; Wang *et al.*, 1999). However, as it has been controversial whether caspase-10 is a constituent of the apoptosis initiating DISC protein complex it was tested whether or not this caspase forms part of the native TRAIL and/or the native FASL DISC. It has been shown that caspase-10 is recruited to both, the native TRAIL DISC and the native FASL DISC (Choi and Benveniste, 2004). It has also been shown that FADD is necessary for recruitment of caspase-10 and its activation at these two protein complexes (MacFarlane, 2003).

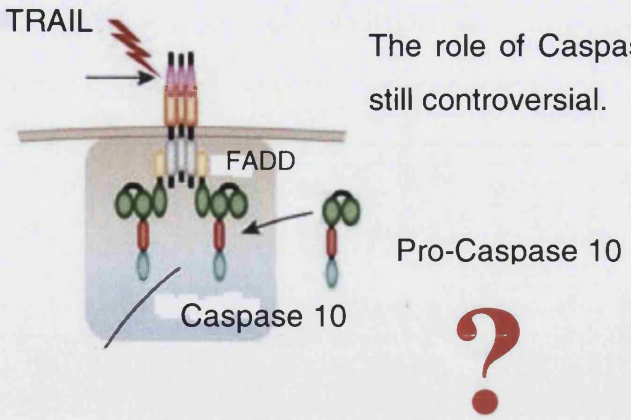

Figure 4.4 Linking TRAIL and its death receptors through the the DISC of FADD, caspase-10. The role of caspase 10 activation in the DISC is still controversial.

Binding of TRAIL to its receptors TRAIL-R1 or TRAIL-R2 triggers rapid apoptosis in many cells, however unlike FASL; its expression has been shown to be constitutive in many tissues (Wang and El-Deiry, 2003). No essential adapter molecule has been identified that associates with the TRAIL death receptors to initiate apoptosis. A study in FADD- deficient mice has indicated that FADD is not necessary for triggering apoptosis via these receptors. FADD and caspase-8 constitute integral components of the TRAIL-R2-DISC. FADD and caspase-8 are necessary for the TRAIL-R2 DISC to be functional in Jurkat cells that lack either FADD or caspase-8 and that are completely resistant to apoptosis induced either by TRAIL-R2-specific agonistic antibodies or by TRAIL itself (Jin *et al.*, 2004; Marini *et al.*, 2003). One question that remains to be solved is whether TRAIL-R1 or heteromeric TRAIL-R1/R2-DISCs also uses these signalling molecules or whether the various possible complexes use different pathways to signal cell death (Schneider *et al.*, 1997).

TRAIL has been shown to induce a rapid activation of NF-κB. TRAIL was shown to exert potent cytotoxic activity against transformed keratinocytes, whereas primary cells are relatively resistant against TRAIL. Moreover, upon inhibition of TRAIL-induced NF-κB activation, primary keratinocytes were dramatically sensitised to TRAIL-induced apoptosis. At the molecular level, sensitisation to TRAIL-induced apoptosis was independent of the activation of caspase 8 or its receptors, but correlated with full caspase 3 maturation and the release of

cytochrome c and Smac from the mitochondrion. These data suggest that modulation of proteasomal function sensitises keratinocytes to TRAIL-induced apoptosis at or upstream of the mitochondrion, but downstream of caspase 8 activation at the DISC, leading to cytochrome c and Smac release from the mitochondrion and concomitant full caspase 3 maturation (Leverkus *et al.*, 2003).

It has been reported that TRAIL-R1 acts as an essential receptor in apoptosis in some cells. Normal prostate epithelial cell (PrEC) and prostate stromal cells (PrSC) were compared to test the cytotoxicity of the combination of doxorubicin and TRAIL. Although PrSC were more resistant than PrEC, all cells undergo apoptosis by this combination. There was no correlation between TRAIL phenotype and expression of c-FLIP, caspases or TRAIL decoy receptors, but PrSC failed to express TRAIL-R1. Additionally, a TRAIL-R1-specific antibody, which behaved as an agonist in combination with doxorubicin, was also used in this comparison, and found to selectively induce cell death in malignant but not normal prostate cells. Although normal PrEC expressed TRAIL-R1 protein as determined by western blot, flow cytometry revealed that only malignant prostate cancer cells and not PrECs exhibited TRAIL-R1 surface expression. Therefore, effective TRAIL-R1 seems crucial to inducing apoptosis in malignant prostate cells (Voelkel-Johnson, 2003).

It was also reported that TRAIL-R2 plays an important role in transducing apoptosis signals. TRAIL-R2 was internalised into the cytoplasm where it recruits FADD under TRAIL stimulation in both sensitive and resistant cells. TRAIL-induced apoptosis through TRAIL-R2 and was mediated by caspase-8-initiated extrinsic and intrinsic mitochondrial pathways in sensitive glioma cell lines. In addition, TRAIL also triggered apoptosis in resistant glioma cell lines through the same pathways, but only if the cells were pretreated with chemotherapeutic agents, such as cisplatin, camptothecin and etoposide. A more general effect of these agents is to downregulate caspase-8 inhibitor, c-FLIP and up-regulate Bak. However, the active form of caspase-8 was recruited to FADD and only sensitive cells showed increased caspase-8 activity upon TRAIL stimulation. The caspase-8 specific inhibitor, Z-IETD, impaired caspase-8 activation and completely abrogated TRAIL-induced apoptosis. TRAIL resistant cells are due to negative regulation at the level of caspase-8 activation and that caspase-8 activation is an

indispensable process in TRAIL-induced apoptosis (Song *et al.*, 2000). Interestingly, in some cell lines, TRAIL sensitivity and caspase-8 activity was enhanced or restored with the treatment of cycloheximide (CHX). In addition, X-linked inhibitor of apoptosis (XIAP) levels decreased significantly and rapidly following treatment with CHX. Down-regulation of XIAP may be responsible for enhancement or restoration of TRAIL sensitivity after CHX treatment in B-lymphocytic leukaemia cells (Kang *et al.*, 2003).

In summary these studies show TRAIL-induced apoptosis can be regulated at several steps in the signalling cascade. Further studies will be aimed at defining the nature of the molecules involved and their mechanisms of regulation.

4.4 Physiological Role of the TRAIL Apoptosis System

The physiological function of TRAIL and its receptors remains unknown (Wang and El-Deiry, 2003). A number of studies has been carried out focusing on the functional expression of TRAIL-rTRAIL system to discover its expression on different cell surfaces. Amongst them are type II interferon (IFN-)-stimulated monocytes (Nakayama *et al.*, 2000), type I IFN (Chou *et al.*, 2001) or T cells (Kayagaki *et al.*, 1999), non-stimulated TRAIL-R1 positive T cells (Kayagaki *et al.*, 1999), IFN stimulated as well measles virus-infected dendritic cells (DC) (Fanger *et al.*, 1999), and natural killer cells (Ochi *et al.*, 2004). Interestingly, functional surface expression of TRAIL was often associated with stimulation by interferon in these studies. Therefore, it is likely that the anti-tumour effect of IFN may at least be partially mediated by TRAIL-induced direct killing of TRAIL-sensitive tumour cells. Yet, the main physiological function attributed to IFN resides in their anti-viral activity.

In fact, it has been shown that TRAIL induced apoptosis specifically in virally-infected cells while sparing non-infected normal cells. Thus, the TRAIL system might have evolved in order to control viral transformation (Matsuda *et al.*, 2005). The fact that many oncogenically transformed cells are also sensitive to TRAIL might be a beneficial side effect of the function of TRAIL to kill virally transformed cells. On the other hand, death receptors for TRAIL have to be involved on the

target side of the newly discovered physiological activities of TRAIL. However, it is still unknown which one of the two death receptors or combination is a crucial transducer of the apoptotic signal in different physiological and pathophysiological situations either. As detailed in 4.3, TRAIL-R1 or TRAIL-R2 tends to works differently in individual types of cells. In addition, the desired experiments with mice deficient for one or a combination of the TRAIL death receptors will be crucial in the determination of the function of each individual receptor.

It is still unclear which decoy receptors or the combination thereof serves as inhibitors of apoptosis induced by TRAIL. Moreover, there may be other mechanisms that reduce TRAIL-induced apoptosis (Gochuico *et al.*, 2000). Since TRAIL induces apoptosis mostly in transformed cells not in normal cells, it seemed as if the existence of these functional decoy receptors might provide an answer to the differential sensitivity to TRAIL observed between normal and transformed cells. In addition, it has recently been shown for various cellular systems that TRAIL resistance is controlled intracellularly rather than at the simple level of TRAIL-R3 and/or TRAIL-R4, the putative "decoy receptors" by using monoclonal antibodies specific for each one of the individual surface-bound TRAIL receptors (Leverkus *et al.*, 2000). Expression of TRAIL-R3 and R4 was more prevalent in normal tissue than in most cancer cells. Nevertheless, no good correlations were found between these two decoy receptors and TRAIL sensitivity (Sayers and Murphy, 2006). As a hypothesis, the difference of TRAIL death receptors and decoy receptors and the ratio of receptors/TRAIL might be more interesting to examine in apoptosis associated vascular calcification.

Some studies in different cell lines showed that the TRAIL system has various roles in inducing or inhibiting apoptosis. In melanoma cells rTRAIL expression levels did not significantly correlate with sensitivity towards all TRAIL receptors. The cell death is determined by the level of surface expression of TRAIL death receptors especially TRAIL-R2 (Chawla-Sarkar *et al.*, 2002). TRAIL-R2 is also markedly increased in bile-ligated mouse atherefore inducing apoptosis resulting in liver hepatotoxicity (Higuchi *et al.*, 2002). TRAIL and TRAIL-R2 are expressed in megakaryocytes and platelets and regulate megakaryocytopoiesis whereas the other receptors are rarely seen (Crist *et al.*, 2004; Melloni *et al.*, 2005).

Decoy receptors appear to play a very minor role in determining cells susceptibility to TRAIL. In endothelial cells, decoy receptors appear to play an important role in protection against TRAIL-induced apoptosis (Zhang *et al.*, 2000). Conversely, they were not correlated with the sensitivity to TRAIL. In the Primary versus transformed keratinocytes the levels of cFLIP are inversely correlated with sensitivity to TRAIL and TRAIL-R1/R2-specific antibodies whereas TRAIL-R3 and -R4 were not involved. When human blood-derived DC were examined, immature DC was susceptible to TRAIL whereas mature DC was not. Also, while the TRAIL-R surface expression pattern did not change upon DC maturation cFLIP levels increased over time in DC. The increase in cFLIP expression may, thus, be responsible for TRAIL resistance of fully mature DC. Human peripheral blood T cells were not efficiently killed by TRAIL (always less than 5%) when stimulated by conventional means. In conclusion, the decoy concept awaits confirmation in non-overexpression systems and the biochemical function of the non-apoptosis-inducing receptors, TRAIL-R3, TRAIL-R4, and OPG, remains unsolved. Taken together, cFLIP seems to be one of the prime candidates as an intracellular regulator of TRAIL sensitivity versus resistance in a number of different cell types. Yet, other intracellular inhibitors of apoptosis are likely to be involved in resistance to TRAIL. TRAIL-induced apoptosis is enhanced by the level of HBV replication in human hepatocytes, in part, by HBxAg-dependent upregulation of TRAIL-R1/DR4 (Janssen *et al.*, 2003; Krieg *et al.*, 2003). TRAIL treatment in combination with chemo- or radiotherapy enhances TRAIL sensitivity or reverses TRAIL resistance by regulating the downstream effectors. Efforts to identify agents that activate death receptors or block specific effectors may improve therapeutic design (Wang and El-Deiry, 2003). Finally, in support of the role of apoptosis in calcification *in vivo*, mice lacking matrix Gla protein or osteoprotegerin develop medial vascular calcification and both proteins have potential roles in apoptosis (Proudfoot *et al.*, 2000). However, there is no sufficient evidence in the study of the role of TRAIL-rTRAIL system in arterial systems.

4.5 Treatment Potential of TRAIL

The property of TRAIL to kill tumour cells more efficiently than normal cells implies a clinical treatment potential of TRAIL *in vivo*. TRAIL treatment might be combined with chemo- or radio-therapy, improving TRAIL efficacy (Wu *et al.*, 2004). Because recombinant forms of TRAIL can successfully eradicate human tumours in mice, without unwanted toxicity (Wu *et al.*, 2004), TRAIL has been hypothesised to be a key component of anti-tumour immunity *in vivo*. For example, in the study of prostate cancer, combination of doxorubicin and an antibody to TRAIL-R1 were found to have therapeutic potential for the treatment of prostate cancer by selectively targeting malignant prostate cells (Voelkel-Johnson, 2003). TRAIL was also found to be capable of inhibiting tumour growth in the absence of any overt toxicity in mice. These suggest TRAIL anti-tumour potential.

Most chemotherapeutic drugs and radiation therapy used in the treatment of malignancies lead to apoptosis primarily by engagement of the mitochondrial pro-apoptotic machinery (Russo *et al.*, 2006). Since TRAIL leading apoptosis by both pathways, it combined with different chemotherapeutic drugs have been seen synergistic induction of apoptosis. Systemic administration of recombinant TRAIL, but not FASL, selectively kills tumour cells while sparing normal host cells. Additionally, it is supported by a observation that TRAIL can inhibit DNA synthesis and provides direct evidence that TRAIL can prevent G1 to S phase progression of lymphocytes (Song *et al.*, 2000). Also in many cases Bcl-2 or Bcl-xL overexpression is the reason for therapy resistance. TRAIL can bypass the anti-apoptotic effect of Bcl-2 or Bcl-xL overexpression in some tumour systems (Sinicrope and Penington, 2005). Thus, it could be an alternative therapy for tumour treatment.

Two major biochemical pathways lead to the induction of apoptosis under physiological conditions: the death receptor pathway and the mitochondrial pathway as mentioned in the last section. In many cancer cells one of these pathways or both pathways are blocked due to mutations in genes encoding proteins that are part of the apoptotic cascade or due to over expression of genes that code for anti-apoptotic proteins (Wajant, 2006). This results in the incapability of the cancer cell to die when triggered by physiological means.

Consequently, the equilibrium between cell growth and cell death is unbalanced. In recent years the most currently used post-operative cancer therapies - i.e. radiation and chemotherapy - achieved therapeutic effect by killing tumour cells via induction of apoptosis (Toloza *et al.*, 2006). Both chemotherapy and radiation mainly trigger the mitochondrial apoptotic machinery of cancer cells (Watson and Fitzpatrick, 2005). These therapeutic measurements often fail in the long run because the tumour develops therapy-resistance by generating variants of the original tumour cell which are resistant to apoptosis induction via the mitochondrial pathway.

4.6 Summary and Formulation of hypothesis

Abdominal aortic aneurysm (AAA) rupture accounts for 10,000 death annually in UK (Dawson *et al.*, 2006). It is possible to detect AAA occurrence at a very early stage by the modern diagnosis methods including X-ray, CT scan and ultrasound (Cates, 1997). However, surgical repair is the only treatment to reduce the chance of AAA rupture (Dawson *et al.*, 2006). The *Nature Medicine* of 11th, December, 2005 issued a new possibility in medical treatment of AAA regression (Yoshimura *et al.*, 2005). This inspires the other potential of pharmacotherapy studies.

Abdominal aortic aneurysm is associated with Atherosclerosis (Prisant and Mondy, III, 2004). It has been suggested that atherosclerosis or VC are events which are similar to osteogenesis. Osteogenesis involves four possible phenomena: activation of osteogenesis, loss of inhibitory factors, enhanced bone turnover and abnormalities in mineral metabolism. A number of proteins have also been suggested to be concerned. They are OPG, RANKL and RANK (Dellegrottaglie *et al.*, 2006).

Apoptosis was found in human and animal AAA (Thompson *et al.*, 1997). A role for apoptotic bodies has also been implicated in AAA. Apoptosis might result in the SMC layer of AAA becoming thinner (Dellegrottaglie *et al.*, 2006), resulting in AAA dilation or rupture (Prisant and Mondy, III, 2004). TRAIL is a member of TNF family which has five known receptors. Osteoprotegerin is one of its decoy receptors to inhibit the apoptosis induced by TRAIL. Hence, TRAIL and its

receptors appear to be a strong link between apoptosis and osteogensis. The possibility shed a light for us to study of the role of TRAIL and its receptors (TRAIL-rTRAIL system) in the AAA.

Human lung cancer cells (immortal in normal medium) were observed to die in half an hour when human breastmilk was included in the medium. The same study also showed that breastmilk can kill immature cancer cells but not mature ones by the very common milk protein called alphalactalbumin through apoptosis (Hakansson *et al.*, 1995). Osteoprotegerin has been found to be in the human breast milk (Vidalk *et al.,* 2004). Also OPG has been used in the clinical trials for bone disease treatment. Thus, it is great potential to use OPG as a medical treatment.

It is hypothesised whether TRAIL can be a novel treatment for vascular calcification cause of TRAIL inducing apoptosis by both apoptotic pathways but mainly by direct caspase pathway, also of TRAIL having two different types of receptors while decoy receptors to be induced into human to prevent the apoptosis. However, the physiological role of the TRAIL system is still unclear. Above all, every single clinical treatment about TRAIL should all base on the truth which is vascular calcification is initiated by apoptosis induced by TRAIL at least taking apart. Therefore, it is necessary to illustrate TRAIL function in vessel wall.

SECTION II

METHODOLOGY AND RESULTS

5.

Chapter 5 TRAIL and receptors gene expression in human normal and calcified aortic samples

5.1 Introduction

5.1.1 TRAIL-rTRAIL system expression in calcified vessels

Increased aortic calcification has been shown to be associated with bone density loss in humans (Schulz *et al.*, 2004). As OPG deficiency is known to result in human osteoporosis, it is important to investigate OPG in VC. Firstly, serum OPG levels were reported to be associated with human vascular diseases (Brandstrom *et al.*, 2002) and are positively correlated with the progression of coronary artery disease (Jono *et al.*, 2002). Secondly, OPG can be produced by various tissues, including the cardiovascular system where it is released by vascular endothelial cells. In addition, mice lacking OPG developed not only bone density loss (osteoporosis) but also showed extensive calcification in the medial and subintimal regions of the ascending aorta, and intimal calcification in the renal arteries (Bucay *et al.*, 1998). Furthermore, both of these clinical manifestations in OPG-treated mice are completely prevented by the restoration of OPG (Min *et al.*, 2000). Taken together, it has been proven that OPG is involved in osteoporosis and VC. However, the mechanism of the OPG effect in VC is still uncertain.

Osteoprotegerin is a decoy receptor of TRAIL which acts as an inhibitor of apoptosis induced by the latter. TRAIL induces apoptosis in vascular SMCs and endothelial cells in culture and increases TRAIL decoy receptors *in vivo* and *in vitro* (Gochuico *et al.*, 2000). Smooth muscle cells and endothelial cells have been found in atherosclerotic plaques and express calcification-related proteins that are commonly found in bones, e.g. MGP, osteocalcin (often acts in the bone formation), osteonectin (may acts in the tissue mineralisation) (Giachelli *et al.*, 2005). As discussed in chapter 2, these proteins contain calcium and apatite properties and accumulate in the areas of calcification (Geng *et al.*, 1996). Additionally, the number of SMCs in the intimal layer increases during atherogenesis, and apoptotic SMC and endothelial cells have been discovered in vascular injuries and areas of inflammation (Gochuico *et al.*, 2000). A soluble form of TRAIL is required in cells in these processes. The generation of TRAIL involves the action of cysteine protease (Mariani and Krammer, 1998) which is

enriched in the human vessel wall (Chapman *et al.*, 1997). Thus, there is a strong possibility that TRAIL-induced apoptosis participates in VC.

5.1.2 Abdominal aortic aneurysm, osteoporosis and vascular calcification

Atherosclerosis and abdominal aortic aneurysms (AAA) have been found to be positively correlated (Matsushita *et al.*, 2000) and calcified plaques are often found in the walls of aneurysms (Jorgensen *et al.*, 2004). Predisposing risk factors for AAA and atherosclerosis are similar to those for osteoporosis, such as smoking, low serum levels of high density lipoprotein (HDL), cholesterol, high serum levels of low density lipoprotein (LDL), and hypertension (Blanchard, 1999; Singh *et al.*, 2001). These all suggest that there might be some link between the three clinical manifestations. Atherosclerosis has been proven to be associated with osteoporosis (Schulz *et al.*, 2004). However, bone mineral density has not been found to have any relation to the prevalence of AAA in a majority of elderly men and women. There may be a possible association in younger men and women, but this needs further confirmation (Jorgensen *et al.*, 2004).

All this strongly suggests that the interaction of TRAIL and its receptors, including OPG, might play a role in the calcifying process during the formation of AAA.

5.1.3 Computer tomography (CT) scan

A number of non-invasive imagining techniques are available for assessing the presence of vascular calcification. Plain X-ray, echocardiography and ultrasound can be used to identify the presence of vascular calcification but not to quantify its extent. In contrast, CT scan can be used to quantify calcification as well as being a highly effective way of detecting and accurately localising plaques anywhere in the body. This is due to its ability to differentiate calcium from adjacent soft tissues (Stanford and Thompson, 1999).

5.1.4 Reverse transcription-polymerase chain reaction (RT-PCR)

Numerous procedures have been used for detecting and determining the abundance of a particular mRNA in a total RNA sample. The most popular methods are: Northern blot analysis, Nuclease Protection Assays, *in situ* hybridisation, and reverse transcription-polymerase chain reaction (RT-PCR). Among those techniques, RT-PCR is a very sensitive method for qualifying and quantifying of mRNA from very small amounts of tissue and cells. The AAA samples obtained from elective surgeries were largely calcified tissue and of small amounts. Since RT-PCR is inexpensive, rapid, simple and sensitive for small amount samples, it was used for mRNA analysis in this project.

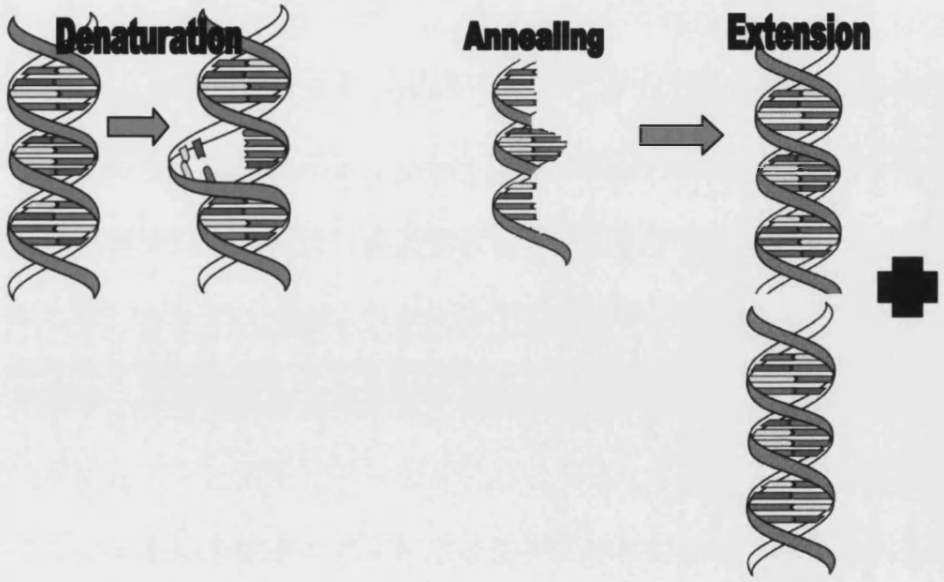

Figure 5.1 This diagrammatic picture mimics that the process in the PCR tube. DNA double helix is separated in the denaturation step. Then primers bind to single DNA strand which is called annealing. Finally, the process of DNA copy completes.

Specific sequence primers of TRAIL-rTRAIL system were applied (see Table 5.1 Sequence of primers used.). An internal control that was multiplexed in the same RT-PCR reaction with the gene specific primers was used. The human house-keeping gene, glyceraldehyde-3-phosphate dehydrogenase (GAPDH), and β-actin were used as internal positive controls and placenta was used as an external positive control. The signal from the internal positive controls was used

to normalise sample data to account for tube-to-tube differences caused by variable RNA quality or RT efficiency, inaccurate quantitation or pipetting. For RT-PCR data to be meaningful, the PCR reaction was terminated when the products from both the internal control and the gene of TRAIL-rTRAIL system are detectable. Because housekeeping genes are highly abundant, their amplification only needs very few PCR cycles.

The same PCR program works slightly different on different thermocyclers (PCR machine) because the temperature and time profiles vary depending on the manufacture construction, therefore it is necessary to test the best PCR programme for each primer pairs for optimal results. The same volumes of cDNA from same sample were tested by using different annealing temperature. The PCR products were then tested for the band density. Eventually, the most suitable PCR programme was decided.

5.2 Aims and Objective

- To determine whether TRAIL and its receptors are expressed in normal control tissues
- To determine whether TRAIL and its receptors are expressed in calcified AAA tissues
- To determine whether there are gene expression differences of TRAIL and its receptors' expression between normal control samples and AAA samples
- To determine whether there are variations among TRAIL and its receptors in tissues with different level of calcification

5.3 Materials and methods

5.3.1 Computer tomography (CT) scan material and methods

5.3.1.1 Samples

The CT Scans used in this analysis were from patients who had undergone AAA repair and had supplied samples for the other parts of this study. This study group included 5 females and 20 males with an age range from 59 to 96 years (mean age 76±7 years). More than half of the patients (55%) had hypertension, 17% had hypercholesterolemia, and 78% were ex-smokers or current smokers. None of them had diabetes mellitus, hypocalcaemia or chronic renal failure. Most patients (78%) had various other vascular diseases. The maximum diameters of these 25 patients AAA were from 5cm to 8.3cm (mean diameter 6.5 ±1 cm).

5.3.1.2 Methods

A CT scanner is a special type of X-ray machine that is used to produce images of the inside of the body. Images can be produced through many different levels (termed slices) of the area of interest. The image slices are black, white and grey providing detailed information and can be built up by computer software to give a three dimensional view. Patients are scanned while awake and without the need for any anaesthetic. They simply lie on a table which slides through the scanning machine. The table is positioned to make sure the part of the body being examined within the machine. Also it moves backwards or forwards when each new image slices were taken. The scanner can rotate around the target body parts. Each image was obtained with 100-millisecond scan time and 10-20 mm slice thickness. Twenty slices were required to include the entire abdominal aorta area (Raggi, 2005; Stanford and Thompson, 1999).

Professional radiologists use an aortic calcification score (AC score), which is calculated as the product of calcified area by its density, to reflect the amount of calcium deposition of the calcified plaque. In this study the AC score was semi-quantitatively derived by averaging the scores of 2 individual experienced investigators. In the AC score scoring system used here, 0 represents no

calcification; 1 represents speckled calcification (figure 5.3-1a); 2 represents plaques of calcification (figure 5.3-1b) and 3 represents continuous calcification (figure 5.3-1c). Therefore the larger the score refers the more severe the calcification.

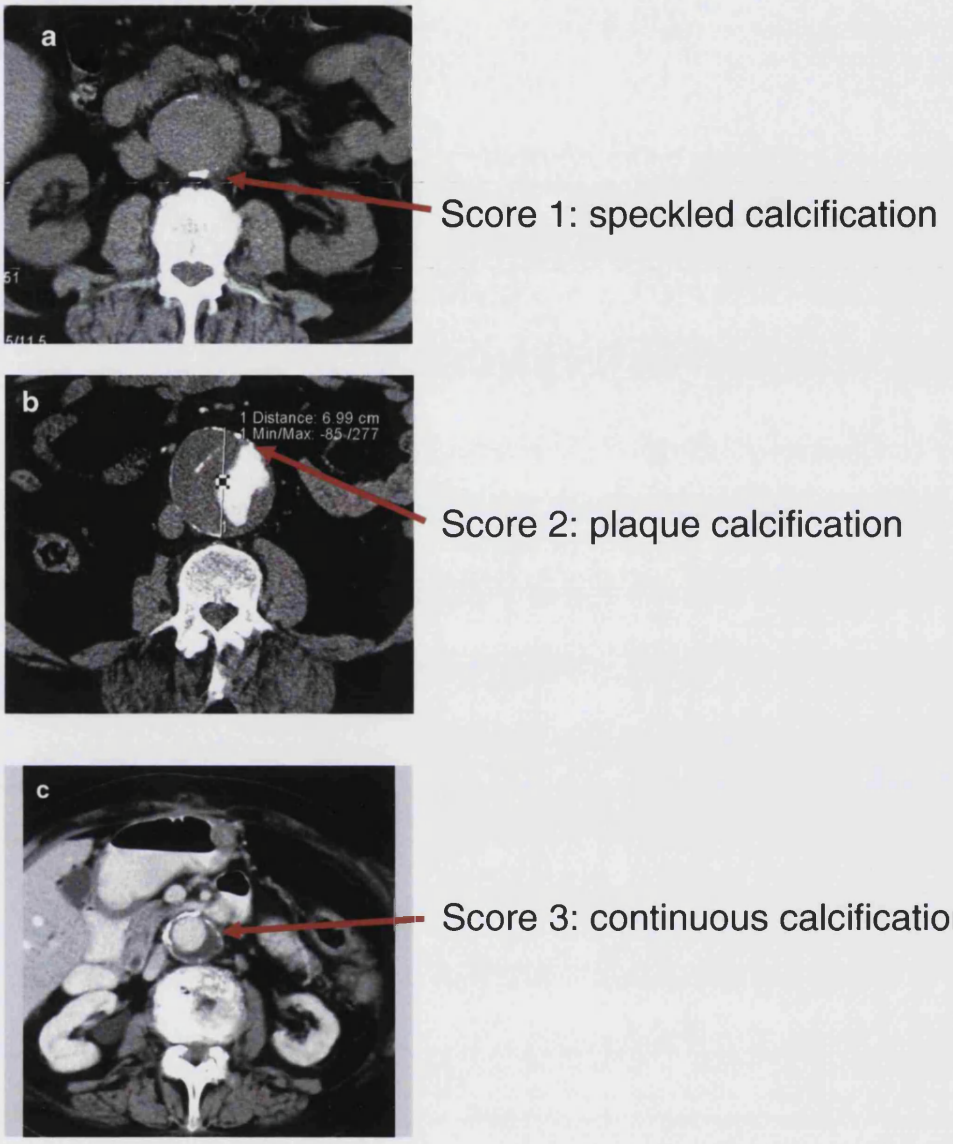

Figure 5.2 Representative CT scans of AC scores. Calcified tissue (normally appearing in bone or teeth in human), is depicted as bright areas on a CT scan. The representative CT scans shown are of AAA demonstrating enlarged aortic artery and thinned aortic wall. The white condensed area, indicated by the red arrows, on the aortic wall are considered as calcium deposition on a standard CT scan. Panel a shows speckled calcification (Score 1). Panel b shows plaqued calcification (score 2) and panel c shows continuous calcification (score 3), note this scan was done with an intravenous contrast medium to also highlight blood filled organs.

Calcification scores were obtained form the proximal outer layer, proximal inner layer, body outer layer, body inner layer, distal out layer and distal inner layer of each AAA examined. Proximal AAA represents the nearest point of the AAA to the heart. Body AAA represents the centre of the enlarged or swollen aorta at the point of the aneurysm. Distal AAA represents the farthest point of AAA from the heart close to the iliac artery. Inner layer stands for intimal and medial layer of vascular wall and the outer layer stand for adventitial layer of vascular wall.

5.3.1.3 Statistical analysis

The AC scores of all the areas examined were analysed by ANOVA for multiple comparisons. Paired analysis between two groups (e.g., between proximal and body AAA) was performed by paired t test when ANOVA indicated significance for the multiple comparison.

All analyses were performed using the GraphPad Prism Instat package, Version 3.02, GraphPad Software Inc., San Diego USA. Differences were considered at *P <0.05 levels and confidence >95%. All error bars are ± standard error of the mean (SEM). One star refers to *P< 0.05 and two stars refers to **P< 0.01. Three stars refers to ***P< 0.001.

5.3.2 Gene expression

5.3.2.1 Samples

Vascular calcification occurs frequently in advanced atherosclerotic lesions. However it has been documented that there are different genetic mechanisms involved in the pathology of VC and atherosclerosis(Schinke and Karsenty, 2000). All samples used were obtained from AAA repair surgery from end-stage disease and most were atherosclerotic. Normal aorta was used as normal control.

5.3.2.2 Normal controls

As described in section 2.2, the abdominal aorta begins at the aortic hiatus of the diaphragm, in front of the lower border of the body of the last thoracic vertebra, and, descending in front of the vertebral column. It ends at the body of the fourth lumbar vertebra, commonly a little to the left of the middle line, by dividing into the two common iliac arteries (Gray H., 1918). It carries the blood and oxygen from the heart to the lower portion of the body. Surplus aorta tissue distal to the infra-renal artery on donor kidneys was considered as normal controls for AAA. Because most of the samples were frozen for transport and storage they are the best to be used for extracting mRNA and protein and not for histological analysis. Paraffin embedding for histology and cell culturing were performed occasionally when fresh normal aorta was obtained.

Umbilical artery obtained from donated umbilical cords was also used as normal control in early studies for this project. The umbilical arteries follow the hypogastric arteries where are along side the bladder and embed in the umbilical cord to the placenta. They transfer the blood to the placenta (Gray H., 1918).

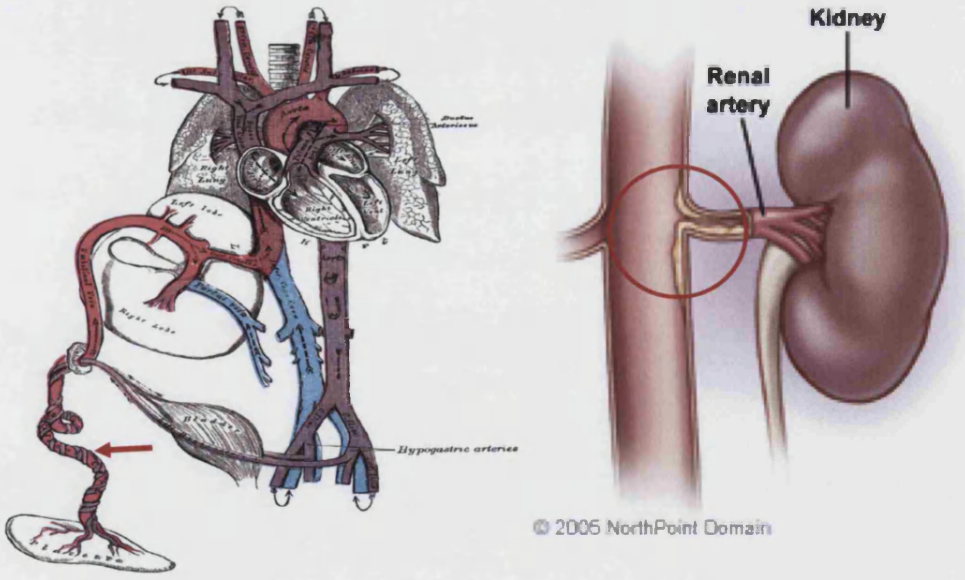

Figure 5.3 Anatomic structures of umbilical arteries and normal aorta. Umbilical arteries as red arrow indicated in the left picture. (from Henry

Gray on-line resource). Normal aorta sample as red circle indicated in the right picture. (from www.wiheart.cardiolohydomain.com)

5.3.2.3 Abdominal aortic aneurysms

Abdominal aortic aneurysm is defined as a focal dilation of the aorta which is 1.5 times greater than normal aorta diameter. It appears a bulging or ballooning out in the arterial wall which is characterised as atherosclerosis (Upchurch, Jr. and Schaub, 2006). Smoking, hypertension or family history (especially in male (Salo *et al.*, 1999)) are the risk factors for AAA (Alcorn *et al.*, 1996). A Swedish study conducted from 1958-1986 documented AAA rising rapidly in men from the age of 55 and in woman from the age of 70 (Ernst, 1993). The mechanism responsible for AAA still needs to be elucidated.

Normally, AAA has no obvious clinical symptoms. It can be detected by X-ray or by imaging techniques such as echocardiography, magnetic resonance imaging (MRI) and CT scan. When AAAs rupture, massive internal bleeding will occur that is fatal without immediate intervention (Upchurch, Jr. and Schaub, 2006).

To date, surgery is the only effective treatment for AAA (www.surgical-tutor.org.uk, 2006). An artificial piece of blood vessel is used to replace the diseased tissue in the open aneurysm repair. Aneurysms for this project were taken from elective open surgeries (n=25) or emergency aneurysm rupture repair (n=6) as calcified samples. The fresh samples were dissected into the proximal (2cm from aneurysm body and close to the heart, referred to as the neck of AAA), the body (the biggest dilation in the AAA) and the distal regions (2cm from aneurysm body and away from the heart, often this was iliac artery). The aneurysm sample was also separated into outer (*tunica adventitia* and outer *tunica media* of aortae) and inner (*tunica intima* and tunica neointima of aortae). The intimal layer is thicker which is called tunica neointima and the *tunica media* is thinner in the AAA (Crawford *et al.*, 2003; Ernst, 1993).

The aneurysms are divided into two classed based on their shape: fusiform and saccular aneurysm. Fusiform aneurysm is enlarged evenly in all directions and

saccular aneurysm only occurred in one side of aortic wall. Among all samples obtained, there are 29 fusiform aneurysms and 2 saccular aneurysms.

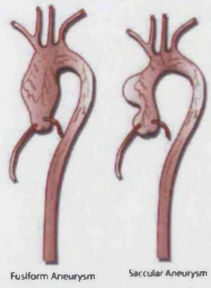

Figure 5.4 The diagrams of fusiform aneurysm (left) and saccular aneurysm (from www.csmc.edu)

Samples were snap frozen in liquid nitrogen (N2) for total RNA and total protein isolation, or stored in specimen pots with 10% formol saline for paraffin bedding. Cultured SMCs were extracted from the medial layer of the aneurysms.

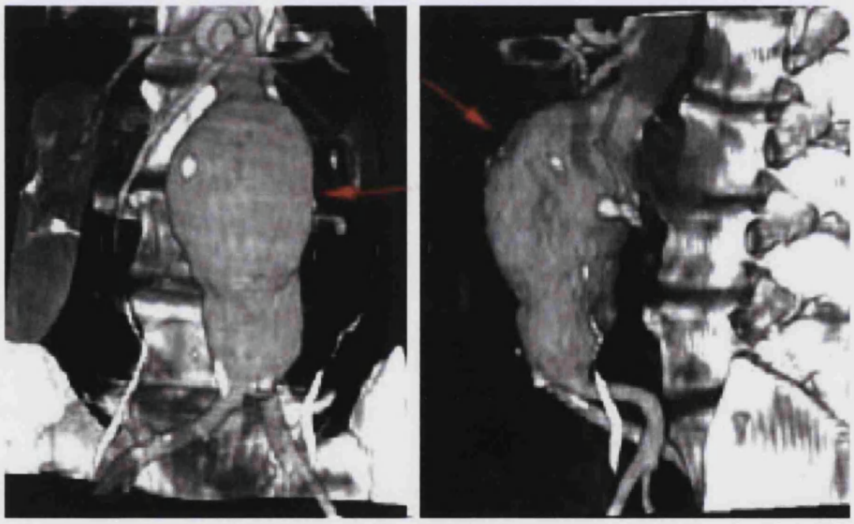

Figure 5.5 Computer tomography scans of AAA. The diameter of the aorta is 1.5 times greater than normal aorta as red arrows indicate.

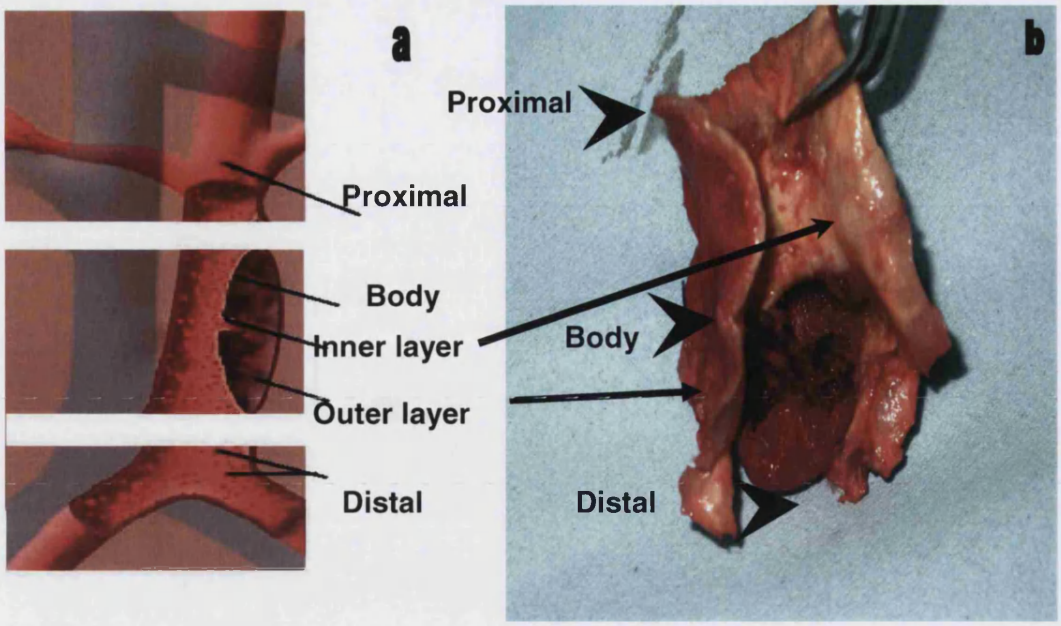

Figure 5.6 A diagramtic picture and a photo of AAA speciment. Panel a shows a diagrammatic picture shows that dissection of AAA as performed in this project. (From www.stanfordhospital.com) Panel b shows a representative photo of the AAA specimens. Black arrow indicates the inner later of the AAA displaying yellow atherosclerosis plaque. The black arrow heads indicate the proximal, body and distal region of the AAA in the order from top to bottom.

5.3.2.4 Gene expression materials and methods

5.3.2.4.1 Total RNA extraction

- Chloroform, Sigma-Aldrich Co Ltd, Poole, UK
- Diethyl pyrocarbonate (DEPC), Sigma-Aldrich Co Ltd, Poole, UK
- Ethanol, Sigma-Aldrich Co Ltd, Poole, UK
- RNAse free tubes, Abgene Inc., Rochester, NY
- RNAse free water, Gibco, Life Tech, Paisley, UK
- Isopropanol, Sigma-Aldrich Co Ltd, Poole, UK
- Total RNA isolation reagent, Abgene Inc., Rochester, NY

Freshly obtained AAA specimens were stored in sterile tubes at 4°C before homogenisation. Two methods for RNA extraction were evaluated because the

method of mRNA extraction affects the outcome of PCR (Boom *et al.*, 1990;Villahermosa *et al.*, 2000). These methods were the liquid nitrogen method and the homogeniser machine (Ultr-Turrax T25 Homogeniser, IKA, Germany) methods prior to RT. Results obtained by the both methods or their combination were compared in three aspects: the proportion of amplified samples, RNA purity, and band intensity.

When the tissue is removed from the human body, the rapid onset of action of degradative enzymes occurs which starts the process of autolysis. Thus, fresh samples were fast frozen in the liquid nitrogen and cut into small pieces in order to extract RNA. Then these samples were ground thoroughly at cryogenic temperature prior to homogenisation in the total RNA isolation reagent (TRIR). The first method is based on a lysis-centrifugation process followed by a column filtration through a silica membrane in an RNase-free glass tube starting with 50 µl of TRIR. In detail, tiny specimens were ground with mortar and pestle into fine power and then transferred into the glass tube with 50 µl TRIR. Press the handle of the glass tube to squeeze the solution. Gradually add 50 µl TRIR each time until samples were entirely homogenised. The second method is based on the manual instruction of STAT-60. The TRIR solution was added into the samples before machine homogenisation on ice. RNA extracts obtained by these two methods were tested in parallel for RNA purity and RNA band intensity after RT.

In conclusion, the second method is more reliable. It could be because its high efficiency to breakdown the cells and homogenise samples more quickly. In summary, total RNA was extracted from freshly frozen sample in DEPC treated tubes (see appendix A). Samples were added about 1ml total RNA isolation reagent/ 0.1g sample. The mixture was then homogenised thoroughly and transferred to Eppendorf tubes (about 1.0ml/ per tube). These Eppendorf tubes were incubated on ice for 5 minutes followed by addition of 0.2ml chloroform / 1ml RNA Isolation reagent, shaking well for 15 seconds by hand. They were returned to ice for 5 minutes and then centrifuged at 12,000 rpm for 15 minutes at 4°C. The aqueous phase was transferred to fresh tubes (approximately 1ml each). Isopropanol (0.5ml) was added to each sample then samples were stored on ice for 10 minutes. They were centrifuged at 12,000 rpm for 10 minutes at 4°C. Supernatant was removed and 1ml 75% ethanol was added to each tube,

shaking well by hand. These tubes were centrifuged at 7,500 for 5 minutes at 4°C. Repeat above two steps. The tubes were air-dried for approximately 10 minutes. Eventually, RNA were added with 10-20µl RNase free water and stored in -80°C freezer for future study.

5.3.2.4.2 RT-PCR materials and methods

- Agarose, Fisher Scientific UK Ltd
- Ethidium bromide, Fisher Scientific UK Ltd
- RNAse free PCR tube, Abgene Inc., Rochester, NY
- RNAse free water, Gibco, Life Tech, Paisley, UK
- RT-PCR reaction kits, including oligo-dT, 5X strand synthesis buffer, MgCl2, RNAse inhibitor, dNTP-mixer, RT, RCR mixer, Promega, UK
- Human β-actin primes, R&D system, UK
- Human GAPDH, TRAIL, TRAIL-R1, TRAIL-R2, TRAIL-R3, TRAIL-R4 , OPG, RANK, RANKL primers, Invitrogen, UK

Total RNA was quantified by using spectrophotometric absorption at 260nm (UV1101 Biotech Photometer). Total RNA sample (2µl) was mixed with 198 µl RNAse-free water. The reading of photometric absorption at 260nm (A260), 280 nm (A280) and the ratio of A260/A280 were recorded. The concentration of RNA was calculated according to the equations below. The purity of RNA was assessed by the ratio of A260/ A280. A high purity of RNA has the ratio of 1.8-2.0 (Wilfinger *et al.*, 1997).

$RNA_{concentration}$ = 40µg/ml x A260 X dilution factor (2µl RNA in 200 µl liquid).
Total RNA µg/ml = concentration x volume of sample (ml).

RNA was reverse transcribed to cDNA by RT according to the Promega kit instruction manual. Total RNA (1µg) was added with 1µl oligo-dT with enough RNase free water to make up the total volume to 5µl. The mixture was heated briefly at 70°C for 5 minutes for denaturation. Then 4µl 5X strand synthesis buffer, 2 µl MgCl2, 1µl RNase inhibitor, 1µl dNTP-mixer and 0.5µl RT and 6.5µl RNase-free water were added to the mixture. The tubes were incubated at 25°C

for 5 minutes then 42°C for 1 hour, final extension were processed at 75°C for 10 minutes in the thermal cycler (Peltier Thermal Cycler PTC-200). Final products were stored at -80°C for future use or in ice for subsequent PCR.

PCR was carried out to elucidate the clear picture of mRNA expression. GAPDH or ß-actin was used as internal positive control. The primer pairs used for PCR amplification of the cloned sequence that were eventually used for cDNA probe preparation are shown in Table 3. PCR was performed in a final volume of 50 µl containing 1µl cDNA of a defined specimen, 1µl of each primer for housekeeping gene and OPG, RANK, RANKL or 5µl of each primers for TRAIL and its other four receptors, 25µl PCR mixer and RNase water. Individual PCR programme were employed for every PCR target (see table 3). PCR products were loaded, 10µl per well, alongside a 100bp DNA ladder and electrophoresed in 1.2% agarose gels (see appendix A for recipe for gel). Specific products were identified after ethidium bromide staining under UV light (Syngene, Cambridge, UK).

Target gene	Primers	
TRAIL	Sense	CACATTGTCTTCTCCAAACTC
	anti-sense	GTCCATGTCTATCAAGTGCTC
TRAIL-R1	Sense	ACTCGCTGTCCACTTTCGTCTCTGA
	anti-sense	AGGCATCCCCTGGGCCTGCTGTA
TRAIL-R2	Sense	GGGAGCCGCTCATGAGGAAGTT
	anti-sense	CTGGGTGATGTTGGATGGGAGAGT
TRAIL-R3	Sense	GAAGAATTTGGTGCCAATGCCACT
	anti-sense	CTCTTGGACTTGGCTGGGAGATGT
TRAIL-R4	Sense	CAACTGGTGGGCTCCGAAAAG
	anti-sense	ACCGCATGTGGCCTAAAACGAC
GAPDH	Sense	AAAGGGTCATCATCTCTGCC
	anti-sense	TGACAAAGTGGTCGTTGAGG
RANK	Sense	TTAAGCCAGTGCTTCACGGG
	anti-sense	ACGTAGACCACGATGATGTCGC
ß-actin	Sense	TCACCCACACTGTGCCCATCTACGA
	anti-sense	CAGCGGAACCGCTCATTGCCAATGG

Table 5.1 Sequence of primers used.

Target gene	Denaturation	Annealing	Extension	cycles
TRAIL	95°C for 45 Sec	55°C45Sec	72°C60Sec	35
TRAIL-R1	95°C for 45Sec	60°C45Sec	72°C60Sec	35
TRAIL-R2	95°C for 45Sec	60°C45Sec	72°C60Sec	35
TRAIL-R3	95°C for 45Sec	58°C45Sec	72°C45Sec	35
TRAIL-R4	95°C for 45Sec	58°C45Sec	72°C60Sec	35
OPG	94°C for 45Sec	55°C45Sec	72°C45Sec	35
GAPDH	94°C for 45Sec	55°C45Sec	72°C45Sec	35
RANK	94°C for 45Sec	65°C45Sec	72°C45Sec	30
RANKL	94°C for 45Sec	55°C45Sec	72°C45Sec	35
ß-actin	94°C for 45Sec	55°C45Sec	72°C45Sec	35

Table 5.2 PCR programs for target gene.

5.3.2.4.2 Optimisation and semi-quantitation

Final PCR gel image was exposed to UV light and then captured by digital camera within the Syngene machine. The equipment allows for adjustment of exposure time to produce an optimal best image on the screen.

The images then saved as .TFT file for digital analysis by an image densitometry system (Scion image software, http://www.scioncorp.com accessed, see appendix A for more details). The image was first inverted and then a measurement area mask was selected of sufficient size to include the largest band to be analysed. The mask was applied to all the bands and the software gave a calculation of the band density. The software gives final results according to the volume (density x area). The amount of cDNA was normalised to the internal positive control (GAPDH).

5.3.2.4.3 Statistical analysis

All mRNA data were presented normalised to GAPDH mRNA. The analyses were carried out in duplicate. Comparisons between groups for study variables were made using the unpaired t test for normal distributions and Mann-Whitney u-test for non-normal distributions. The differences of mRNA expressions were analysed by ANOVA for multiple comparisons. Paired analysis between two

groups (e.g., between proximal and body AAA mRNA expression) was performed by paired t test when ANOVA indicated significance for the multiple comparison. The linear regression test (Pearson test) was used to determine the correlation between mRNA expression in the TRAIL-rTRAIL system. Differences were considered at *P <0.05 levels and confidence >95%. All error bars are ± standard error of the mean (SEM). One star refers to *P< 0.05 and two stars refers to **P< 0.01. Three stars refers to ***P< 0.001.

All analyses were performed using the GraphPad Prism Instat package, Version 3.02, GraphPad Software Inc., San Diego USA.

5.4 Results

5.4.1 Calcification level of CT Scan

The calcification level by preoperational CT scan was quantified by two independent consultant vascular surgeons. Out of 31 AAA donors, 27 CT scans were examined the remaining 3 patients, who underwent emergency repair after rupture did not have a preoperational CT scan. Proximal, body and distal regions of each AAA were given AC score respectively.

Proximal	Body	Distal	Proximal	Body	Distal
1	1	1	2	2	3
0	1	0	1	2	3
1	1	1	1	2	3
0	1	0	0	1	2
0	1	1	1	1	2
1	1	0	1	1	2
1	2	1	1	1	2
1	2	1	1	1	3
1	2	1	1	2	2
0	1	0	2	1	3
1	2	1	1	2	1
0	1	0	0	2	1
0	1	1	1	1	2
			2	1	2

Table 5.3 shows the semi-quantitative AC scores of all examined AAA areas of 27 patients. As discussed in the methods, O is equal to non-calcification. 1 is equal to speckled calcification. 2 is equal to plaqued calcification. 3 is equal to continuous calcification.

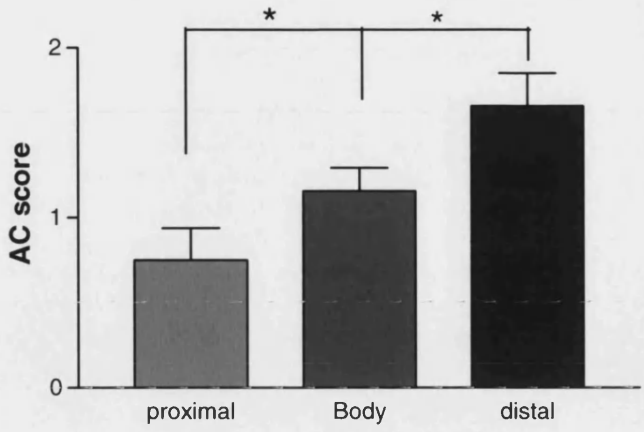

Figure 5.7 AC score of proximal, body and distal lesions of AAAs. Distal is the most calcified areas and proximal is the least calcified areas according to CT scan. Proximal calcification level is significantly less than distal area (*p< 0.05, one way ANOVA test, confidence > 95%); so does body area (*p< 0.05, one way ANOVA test, confidence > 95%).

5.4.2 Assay development

Following representative pictures are RNA isolated by different isolation methods running on the 1.2% argarose gel as described in the methods.

An efficient and accurate method for isolation of RNA from AAA tissue is very important. It is the first step for the entire RT-PCR procedure and the good quality mRNA is necessary for PCR results.

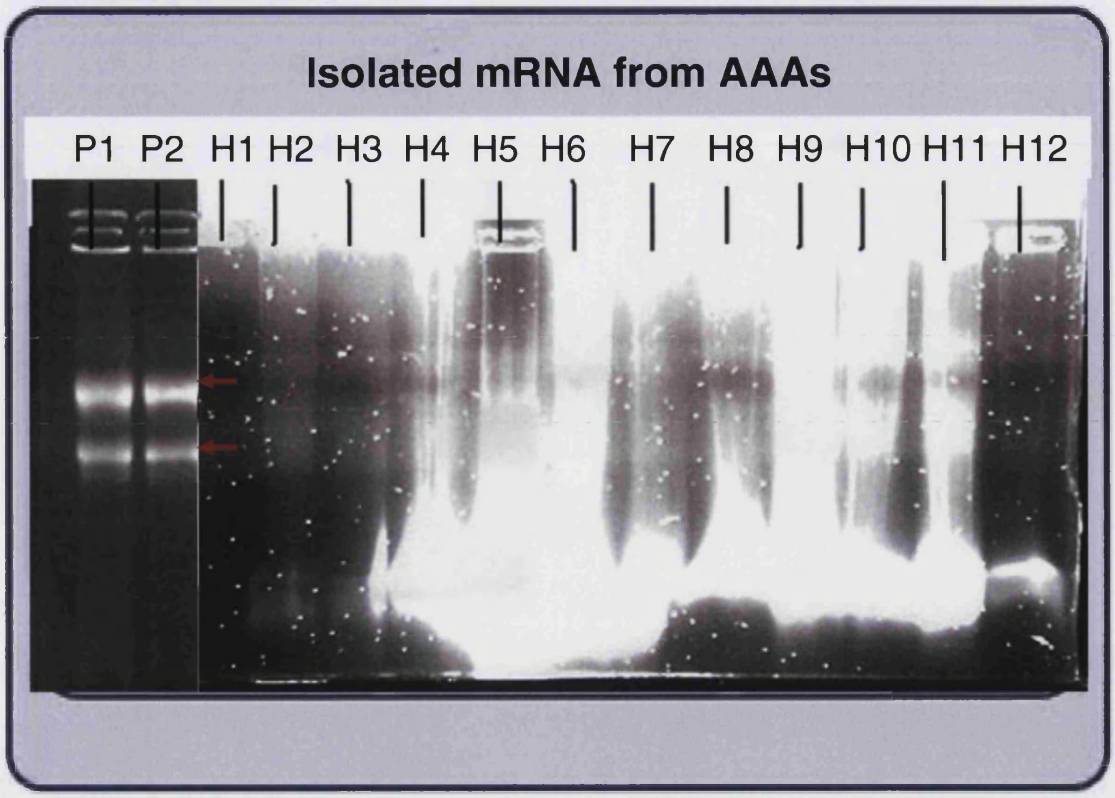

Figure 5.8 Comparsion of isolated RNA from AAA by two isolation methods. They were run on the 1.2% agarose gel. Total RNA was isolated by two methods as described in the methods section. P1 and P2 represent good quality RNA which was isolated by homogeniser on ice. H1 to H12 represent bad quality RNA which was isolated by unsuccessful extraction methods. The RNA has broken down and shows a much lower band density than that of P1 and P2 because the original gel has been exposed maximally. The red arrows indicate that 18sRNA (top arrow) and 28sRNA (bottom arrow) running in the gel.

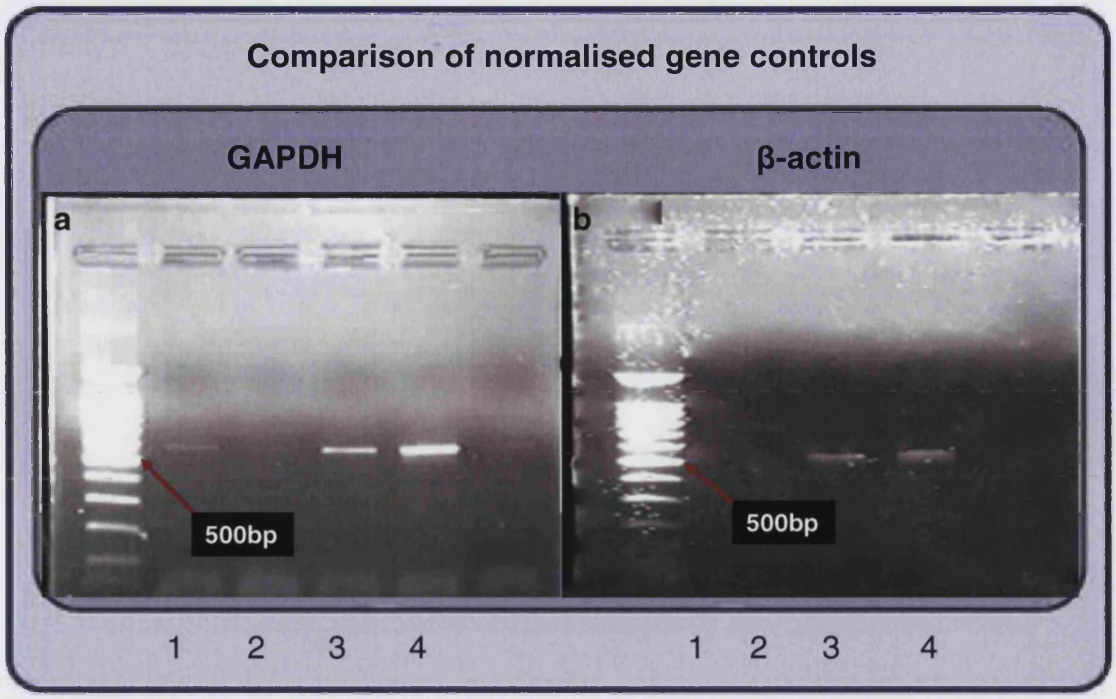

Figure 5.9 The comparison of GAPDH (600bp) and ß-actin (500bp) expression. Two 1.2% electrophoretic gels of cDNA isolated from AAA. Four PCR amplified cDNA were shown in each gel. GAPDH was used as primers in the gel a, and ß-actin was used as primers in the gel b. Red arrows indicated the size of PCR products. It is clearly shown that gene expression for GAPDH in all four AAA samples and two of samples expressions for ß-actin were absent. Thus, GAPDH is better to be used in the AAA studies.

5.4.3 Messenger RNA expression in normal controls

The abdominal aorta is that part of aorta that passes from the diaphragm and continues down the abdomen. It ends where it divides to form the two iliac arteries that go to the legs (Gray H., 1918). Normal aorta samples obtained from kidney donors are mainly iliac lesions of the aorta. Thus, they are a most suitable normal control sample for the study of AAA.

The umbilical artery is comparatively much easier to access than the normal aorta. For that reason, the mRNA expression for TRAIL and its receptors were compared in an umbilical artery and a normal aorta. The placenta was regarded as an external positive control and GAPDH was applied as the internal positive

control. GAPDH was expressed in all three samples, confirming the presence of cDNA. TRAIL and all its five receptors were expressed in the placenta and umbilical artery, but in contrast, TRAIL and TRAIL-R1 were not detected in the normal aorta. Thus, the umbilical artery is not the best normal control sample for the study of the TRAIL-rTRAIL system in AAA samples. The normal aortic samples as positive controls are better than umbilical arteries. Consequently normal aortae were used as a normal control.

It is well known that the placental circulation is cut off immediately at birth and umbilical arteries actually carry venous blood. These two facts could be reasons of the mRNA differences between normal aorta and umbilical artery but there is no evidence.

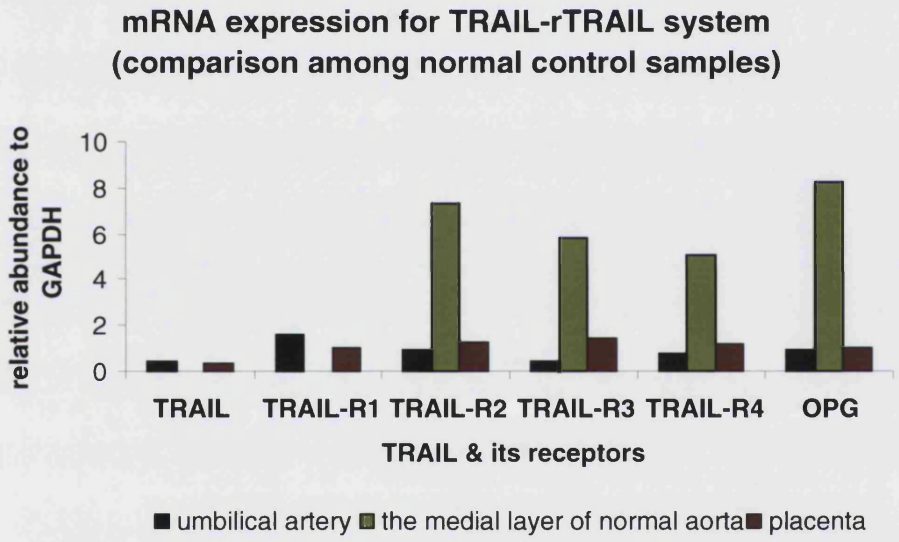

Figure 5.10 The relative abundance of mRNA expression (normalised to the level of GAPDH mRNA expression, semi-quantitative) in the umbilical artery, placenta and normal aorta. It shows clearly that this normal aorta lacks TRAIL and TRAIL-R1 mRNA, and there is a visible difference between the umbilical artery and the normal aorta.

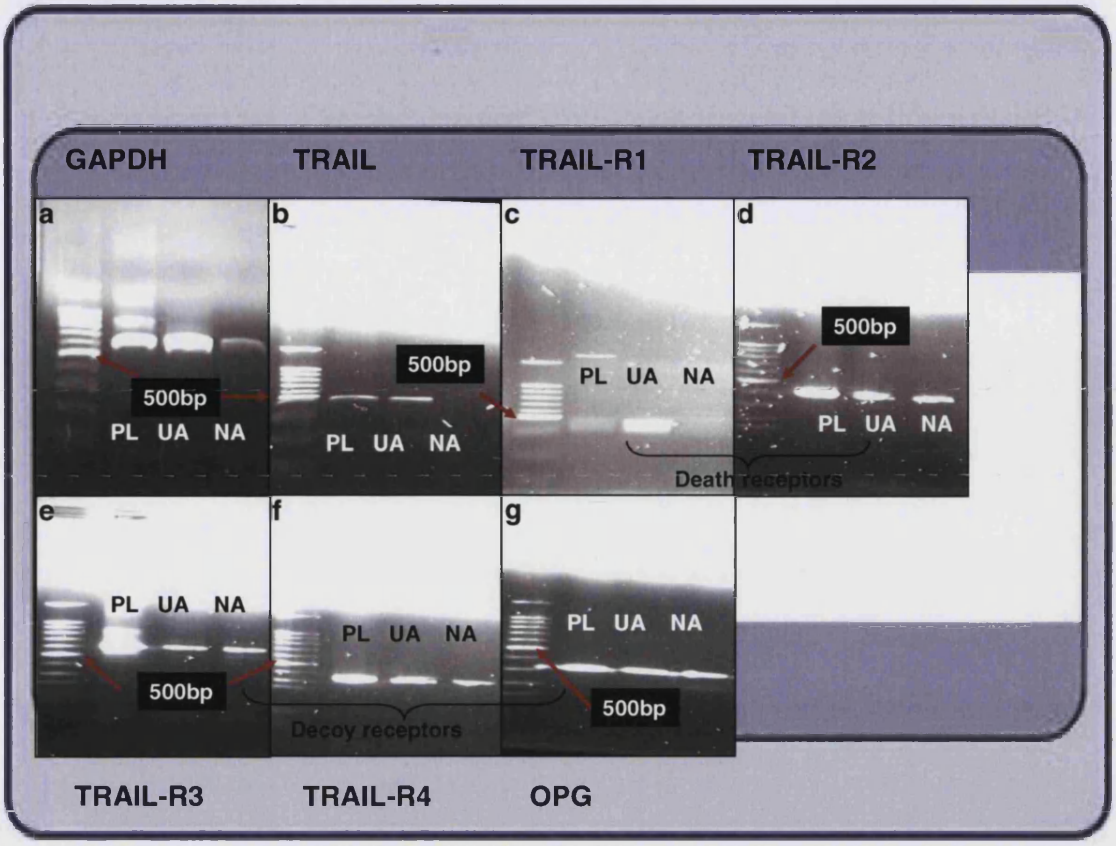

Figure 5.11 These gel images demonstrate the mRNA expression of umbilical artery and normal aorta. UA represents umbilical artery; PL represents placenta and NA represents medial normal aorta. These PCR products were loaded and run on 1.2% agarose/TBE analytical gels and stained with ethidium bromide. The PCR products were then compared with the standard, loaded in the same gel. The red arrows indicate the size of the samples on the DNA ladder. Panel a indicates the PCR products for GAPDH (600bp); the normal aorta showed a lower expression level than the other two products. Panel b indicates the PCR products for TRAIL (443 bp) and there was a missing band for the normal aorta. Panel c indicates the PCR products for TRAIL-R1 (506 bp); panel d indicates the PCR products for TRAIL-R2 (502 bp); panel e indicates PCR products for TRAIL-R3 (512bp); panel f indicates PCR products for TRAIL-R4 (453 bp); and panel g indicates PCR products for OPG (371 bp).

5.4.4 Messenger RNA expression for TRAIL-rTRAIL system in normal aortae

Messenger RNA expressions for TRAIL-rTRAIL system by RT-PCR were carried out in eight normal aortic vessel walls. According to the level of their TRAIL mRNA expression, they were separated into two groups for analysis. Group 1 includes five normal aortic samples whose GAPDH mRNA was expressed at a lower level than that of the placenta samples. Group 2 includes three normal aortae whose GAPDH mRNA was expressed at a similar level to that of the placenta.

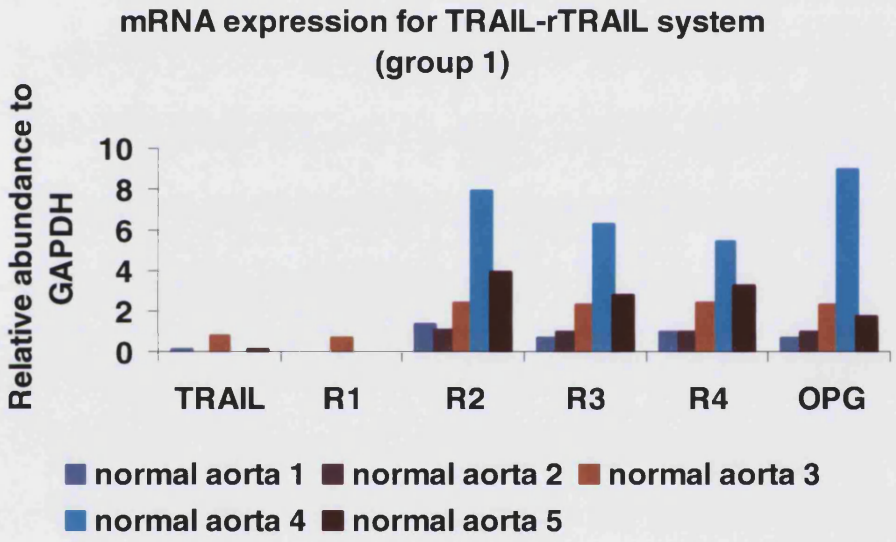

Figure 5.12 This graph illustrates the mRNA expression of TRAIL (normalised to GAPDH) and its receptors in group 1 normal aortae. A similar trend is found in individual normal aorta in the group 1 although big differences were observed between one and another. The highest bar of each sample symbolises the mRNA expression of TRAIL-R2 and the lowest point of each one symbolises the mRNA expression of TRAIL-R1. Decoy receptors are expressed higher than death receptors and TRAIL.

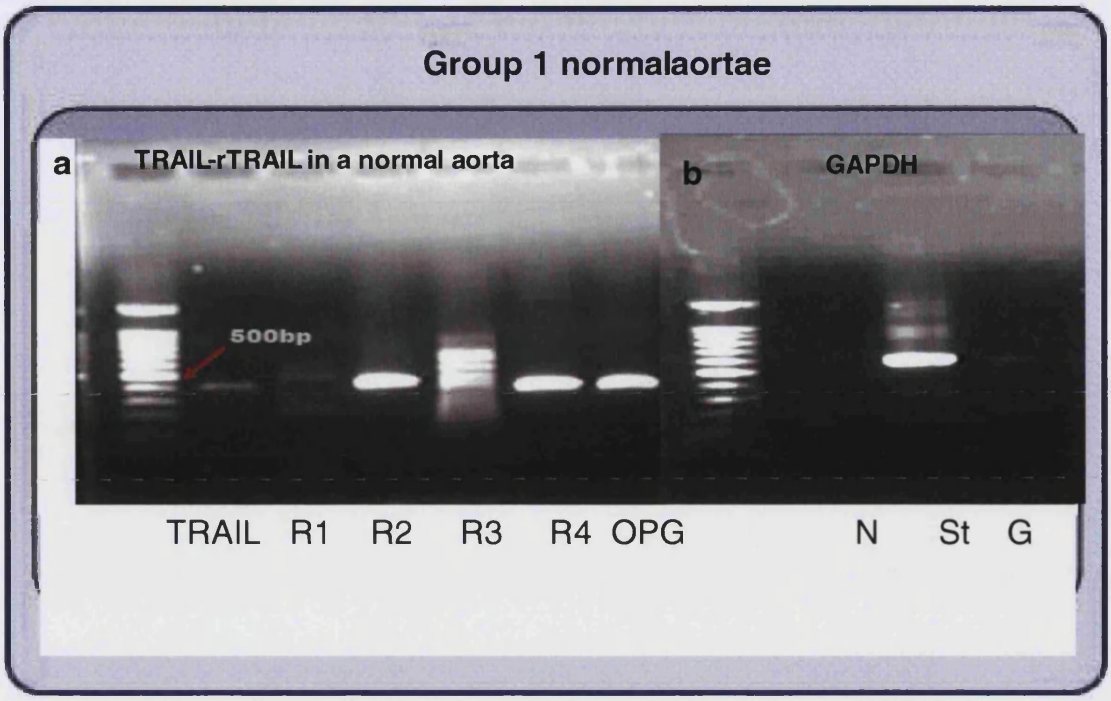

Figure 5.13 This representative gel image shows eight PCR reactions for group 1 normal aortae. The reactions amplified TRAIL, TRAIL-R1, TRAIL-R2, TRAIL-R3, TRAIL-R4 and OPG gene as shown in graph a. An aliquot of each product was loaded and run in the same 1.2% agarose/ TBE gel and stained with ethidium bromide. The PCR products were then compared with the standard and loaded in the same gel. The normal aortic sample's GAPDH (G) was compared to normal standard GAPDH (st) as shown in panel b. Negative control (N) of GAPDH (RNase free water) was loaded in the lane 1. Positive control of GAPDH was loaded in the lane 2 and normal aortic sample was loaded in the lane 3. The normal aortic GAPDH is barely observable. The red arrows indicate the size of the samples on the DNA ladder. This represents a very low level of expression for TRAIL mRNA, whereas TRAIL decoy receptors had much higher expressions which were found consistently in group 1 normal aortae.

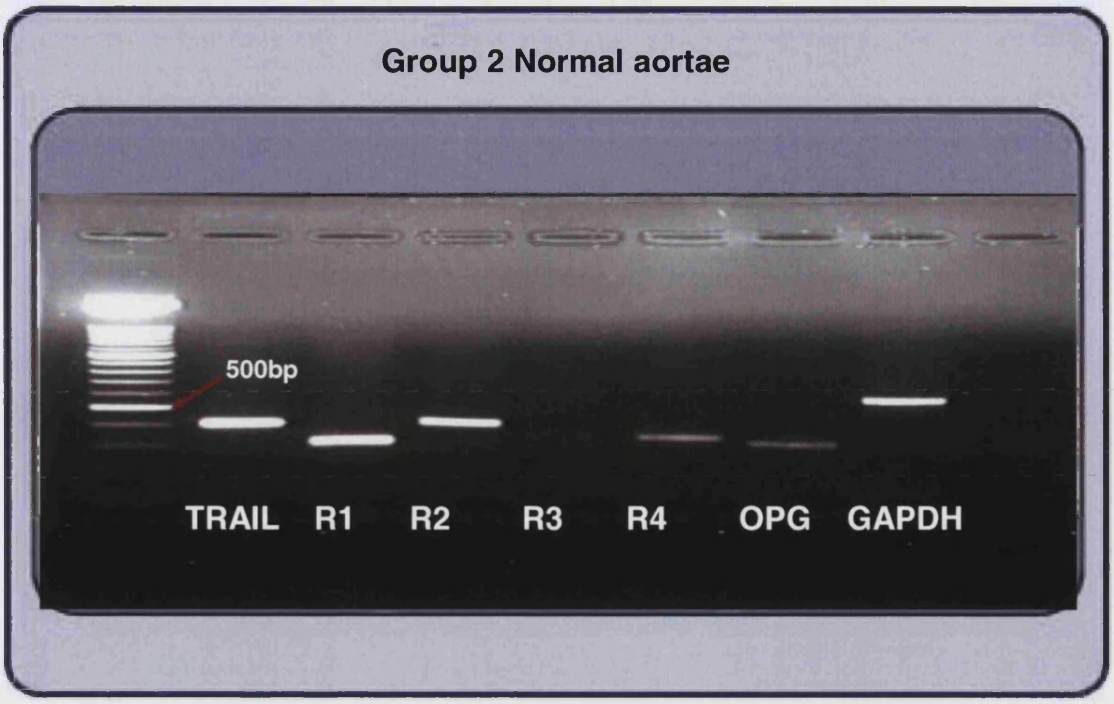

Figure 5.14 This representative gel image shows seven PCR reactions that were set up on the isolated RNA in group 2 normal aortae. One PCR reaction was GAPDH-controlled PCR on the same normal aortic sample. The rest of the reactions amplified TRAIL, TRAIL-R1, TRAIL-R2, TRAIL-R3, TRAIL-R4, OPG gene as shown here. An aliquot of each product was loaded and run in the same 1.2% agarose/ TBE gel and stained with ethidium bromide. The PCR products were then compared with the DNA ladder and loaded in the same gel. The red arrows indicate the size of the samples. This represents a higher TRAIL mRNA expression than in group 1. TRAIL-R3 was expressed at a very low level that was only detectable on the original image. The level of the mRNA expression of TRAIL decoy receptors was lower than in group 1 (shown in Figure 5.13).

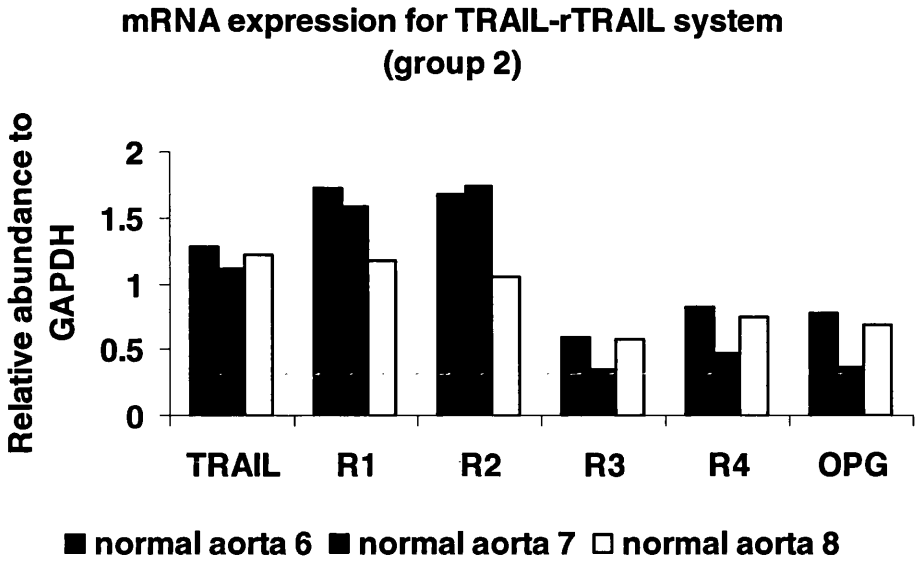

Figure 5.15 This graph shows that a different trend is found in group 2 to that found in group 1 (shown in Figure 5.12). The values of mRNA expression are normalised to GAPDH. The highest point of each sample symbolises the mRNA expression for TRAIL-R2 and the lowest point of each symbolises the mRNA expression for TRAIL-R3. The death receptors and TRAIL are expressed higher than decoy receptors.

Two completely different trends in mRNA expression in normal aortae were found (see Figure 5.12 and Figure 5.15). Among group 1 normal aortae, TRAIL-R1 tends to express in a similar way to TRAIL, and the decoy receptors appeared highly expressed. In contrast, the decoy receptors in group 2 normal aortae showed relatively lower expression than TRAIL and TRAIL-R1. Interestingly, TRAIL-R2 retains the highest level of expression among eight normal aortae.

5.4.5 Messenger RNA expression for TRAIL-rTRAIL system in AAA

Expression of TRAIL and its receptors at mRNA levels was examined by RT-PCR in 33 freshly-isolated human AAA specimens. Messenger RNA expressions for TRAIL-rTRAIL systems were found in the normal aortae constantly, though TRAIL and TRAIL-R1 showed slightly variable expression, as shown in section 5.4.4.

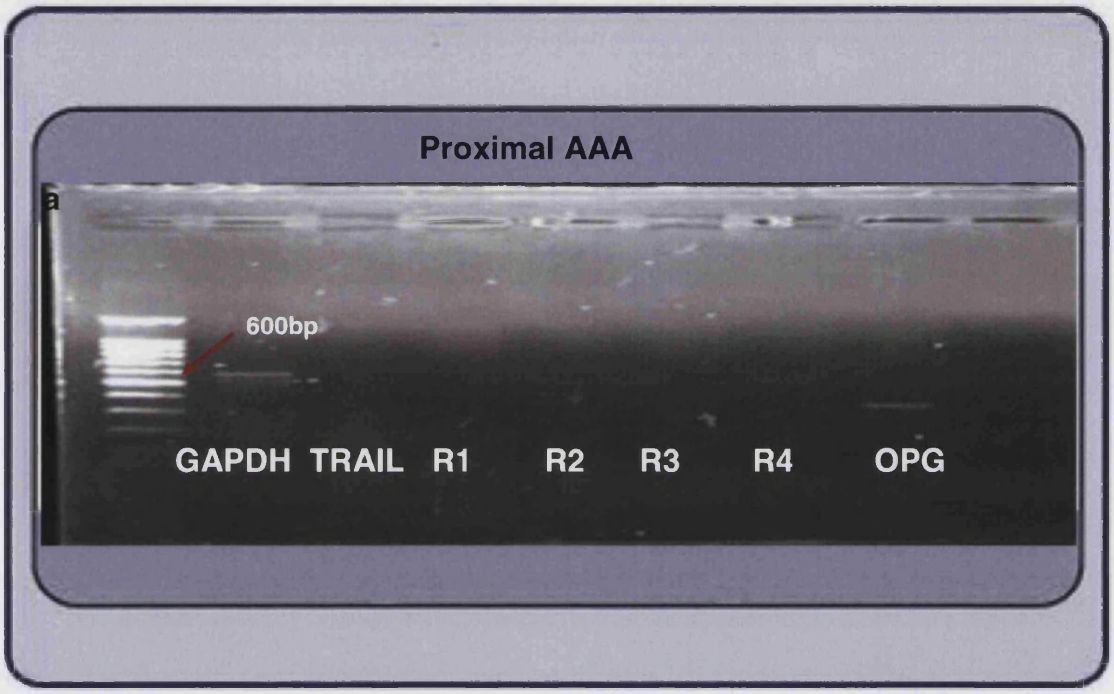

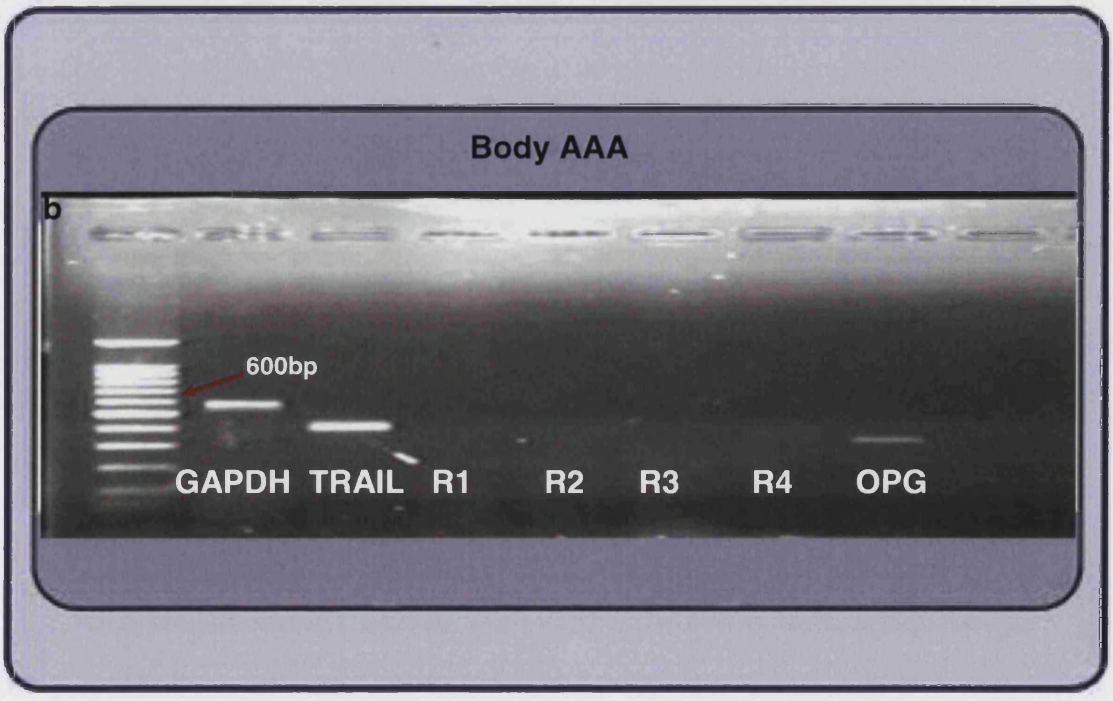

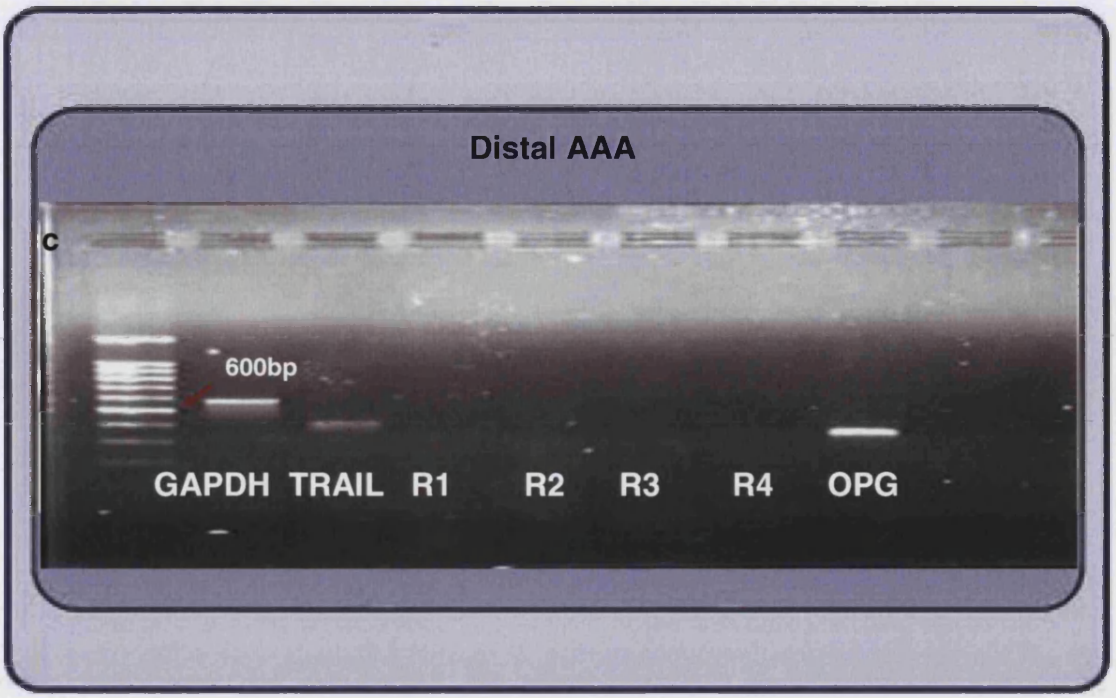

Figure 5.16 The representative gel image here shows seven PCR reactions that were set up on the isolated RNA for proximal, body and distal AAAs as described in methods. One PCR reaction was GAPDH-controlled PCR on each AAA sample. The rest of the reactions amplified TRAIL, TRAIL-R1, TRAIL-R2, TRAIL-R3, TRAIL-R4 and the OPG gene, as shown here. A 10µl aliquot of each product was loaded and run in the same 1.2% agarose/ TBE gel and stained with ethidium bromide. The PCR products were then compared with the standard, loaded in the same gel. The red arrows indicate the size of the samples on the DNA ladder. Panel a indicates gene expression on proximal AAA; panel b indicates gene expression on body AAA; and panel c indicates gene expression on distal AAA. These three gel images show clearly the variable pattern of the mRNA expression for TRAIL-rTRAIL systems.

The messenger RNA of TRAIL (76%) was widely expressed on AAA vessel walls and the mRNA for decoy receptors was also extensively expressed (OPG 82%, TRAIL-R4 75% and TRAIL-R3 70%). Surprisingly, TRAIL death receptors were expressed much less frequently on the AAA wall than were decoy receptors. Both were expressed on 42% of AAA vessel walls.

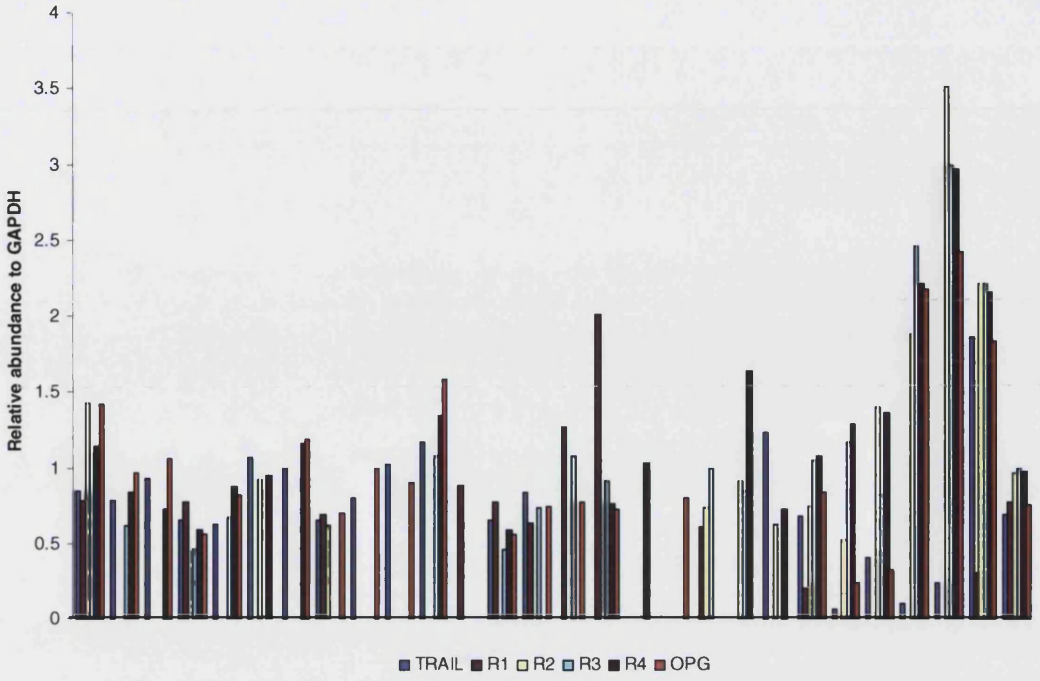

Figure 5.17 The summary graph of TRAIL and its receptors in AAA. It clearly shows the variable expression in each AAA wall.

5.4.5.1 Correlation of TRAIL and its all receptors in AAA

To explore the relationship between TRAIL and its receptor, correlation tests were carried out. In the correlation, the value r represents correlation coefficient and r^2 represents correlation r squared. A correlation coefficient is a number between -1 and +1 which measures the degree to which two variables are linearly related. When a positively perfect linear relationship exists between two variables, r equals 1. If there is a positive correlation (both variations increase and decrease together), then r is greater than 0. Correspondingly, r equals -1 when a negatively perfect linear relationship between two variables exists. If there is a negative correlation (whenever one variation increases another one decreases), then r is less than 0 and greater than -1. Value r equals 0, which means there is no linear relationship between the variables.

	TRAIL R2-R3	TRAIL R2-R4	TRAIL R3-R4	TRAIL R3-OPG	TRAIL R4-OPG	TRAIL R2-OPG	TRAIL-OPG	TRAIL-R4
r	0.79	0.78	0.75	0.67	0.55	0.52	0.28	0.10
r^2	0.63	0.61	0.57	0.45	0.31	0.27	0.08	0.01

Table 5.4 This table shows positive correlations among TRAIL and TRAIL receptors. All decoy receptors share positive correlations. TRAIL-R2 positively correlates with all decoy receptors. TRAIL positively correlates with OPG and TRAIL-R4. (Statistical correlation, n=33).

	TRAIL R1-OPG	TRAIL R1-R2	TRAIL – TRAILR1	TRAIL R1-R4
r	-0.10	-0.20	-0.24	-0.33
r^2	0.01	0.04	0.06	0.11

Table 5.5 Negative correlations among TRAIL and its receptors. TRAIL-R1 has negative correlation with TRAIL and all the receptors apart from TRAIL-R3. (n=33)

a

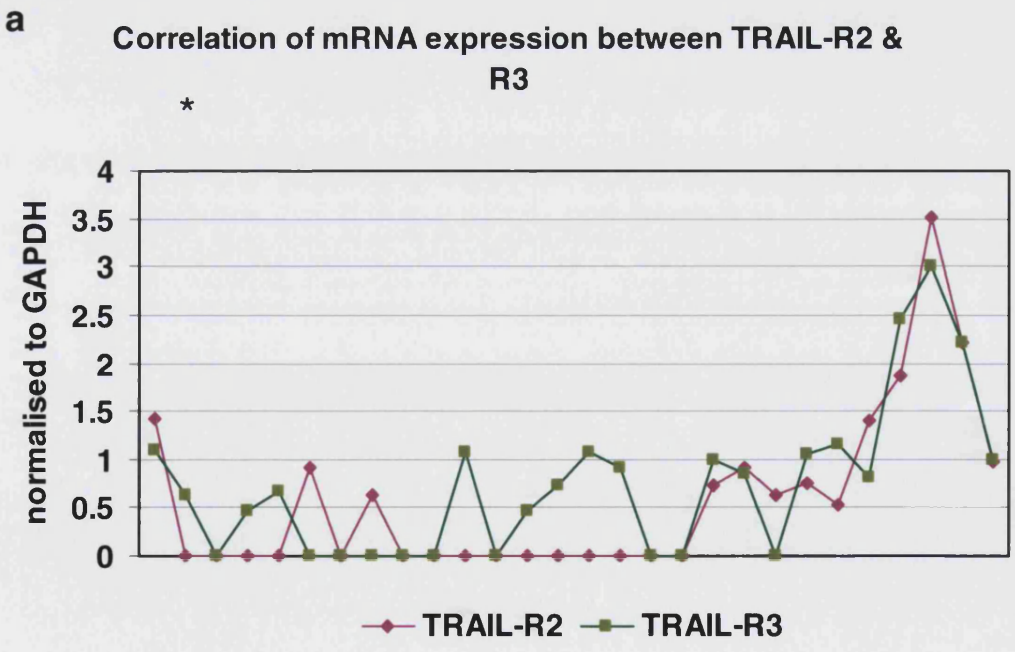

Coefficients	Standard Error	t Stat	P-value
0.31	0.11	2.75	0.01

b

Correlation of mRNA expression between TRAIL-R2 & R4

*

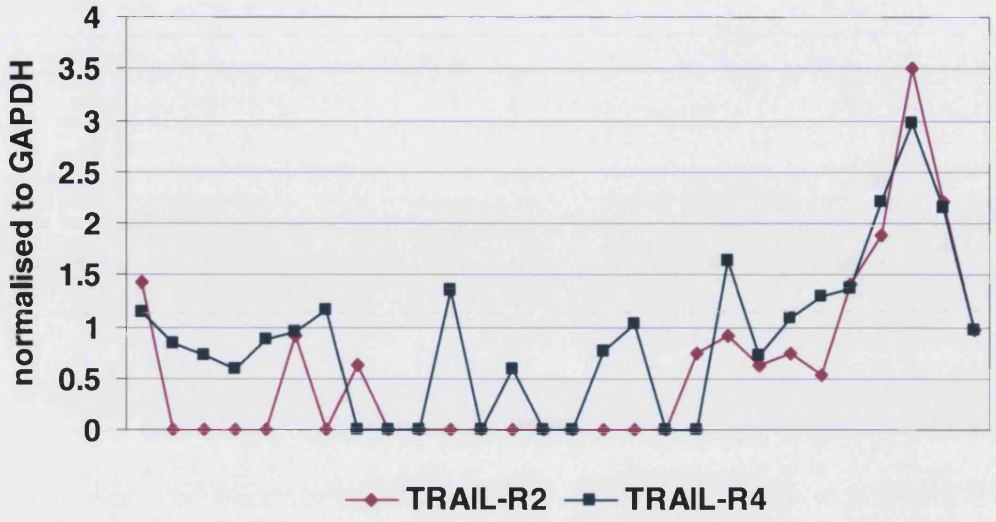

Coefficients	Standard Error	t Stat	P-value
0.46	0.11	4.17	0.003

c

Correlation of mRNA expression between TRAIL-R2 & OPG

*

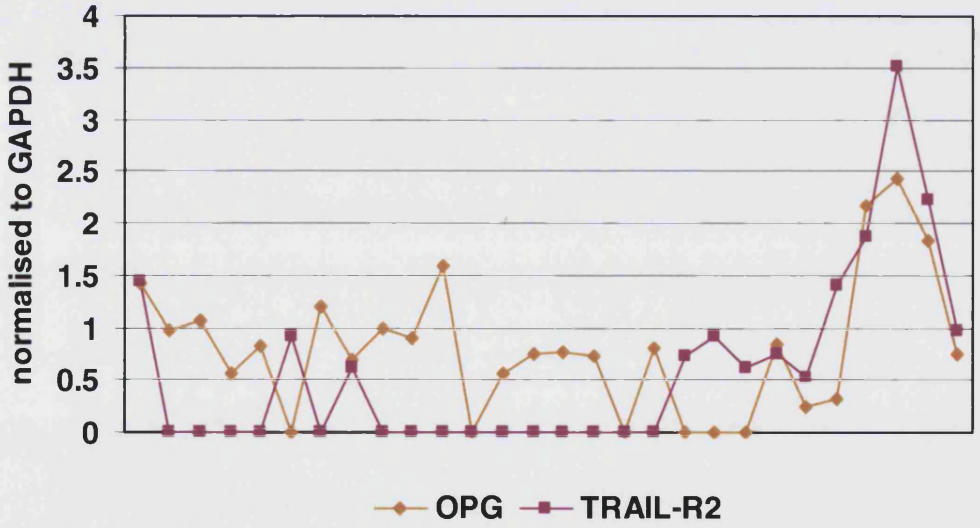

Coefficients	Standard Error	t Stat	P-value
0.56	0.13	4.34	0.0001

d

Correlation of mRNA expression between TRAIL & TRAIL-R2

**

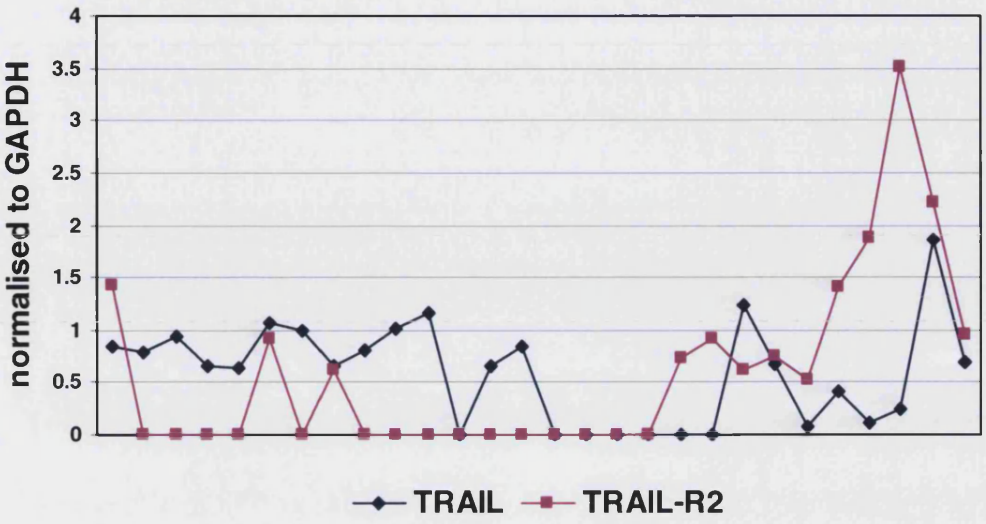

Coefficients	Standard Error	t Stat	P-value
0.56	0.11	4.91	4.17

e

Correlation of mRNA expression between TRAIL & OPG

**

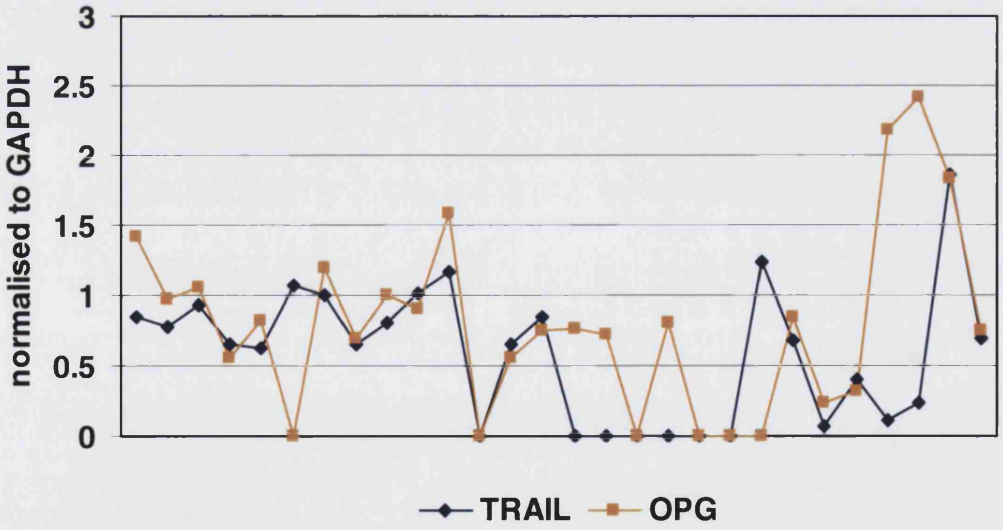

Coefficients	Standard Error	t Stat	P-value
0.57	0.18	3.05	0.005

f correlation of mRNA expression between TRAIL & TRAIL-R1

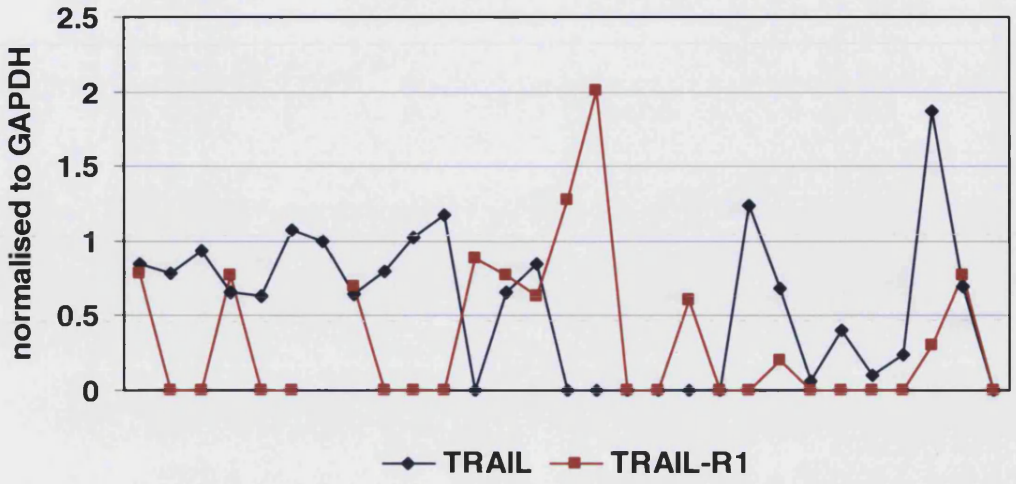

g Correlation of mRNA expression between TRAIL-R1 & OPG

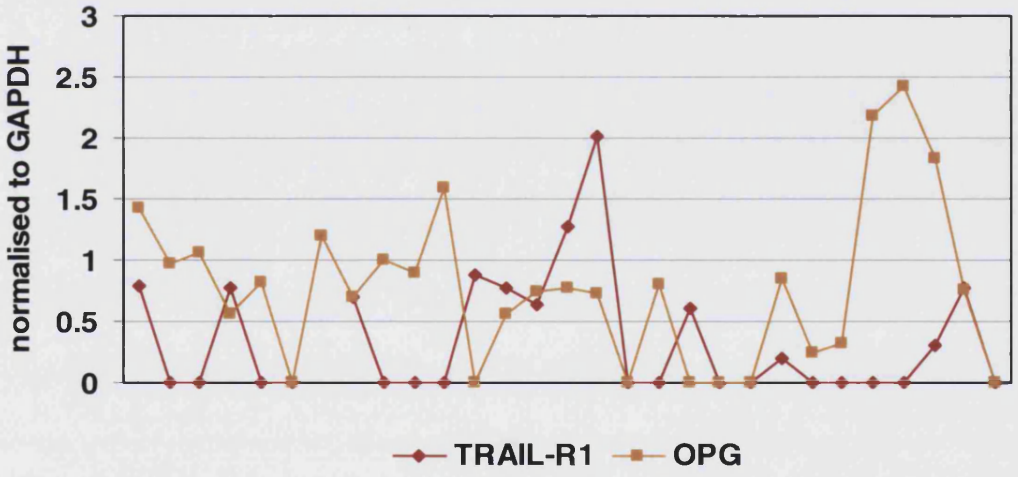

Figure 5.18 These graphs show correlations of mRNA expression among TRAIL, TRAIL-R2 and decoy receptors in the AAAs (n=28). Each pair of different colour dots on the same X axis refers to the mRNA expression of different genes but from the same AAA sample. Panel a represents a positive correlation of mRNA expression between TRAIL-R2 and TRAIL-R3 (significant difference, *P< 0.05). Panel b represents a positive correlation of mRNA expression between TRAIL-R2 and TRAIL-R4 (significant difference, *P< 0.05). Panel c represents a positive correlation of mRNA expression between TRAIL-R2 and OPG (significant difference, *P< 0.05).

Panel d represents a positive correlation of mRNA expression between TRAIL-R2 and TRAIL (significant difference, *P< 0.01). Panel e represents a positive correlation of mRNA expression between TRAIL and OPG (significant difference, *P< 0.01). All results were tested by linear regression (confidence > 95%). Panel f represents a negative correlation of mRNA expression between TRAIL and TRAIL-R1. Panel g represents a negative correlation of mRNA expression between TRAIL-R1 and OPG.

5.4.6 Comparison between normal aortae mRNA and AAA mRNA

5.4.6.1 Frequency of TRAIL-rTRAIL mRNA existence

In comparison, there is no certain pattern of mRNA expression in individual AAA samples (see Figure 5.19). TRAIL and its receptors were missing from AAA vessel walls. However, mRNA fragments of appropriate size were detected in the placenta, which was an external control. Compared with the frequency of mRNA expression in normal aortae, TRAIL death receptors were significantly lower in AAA. This indicates that TRAIL death receptors might be involved in AAA formation.

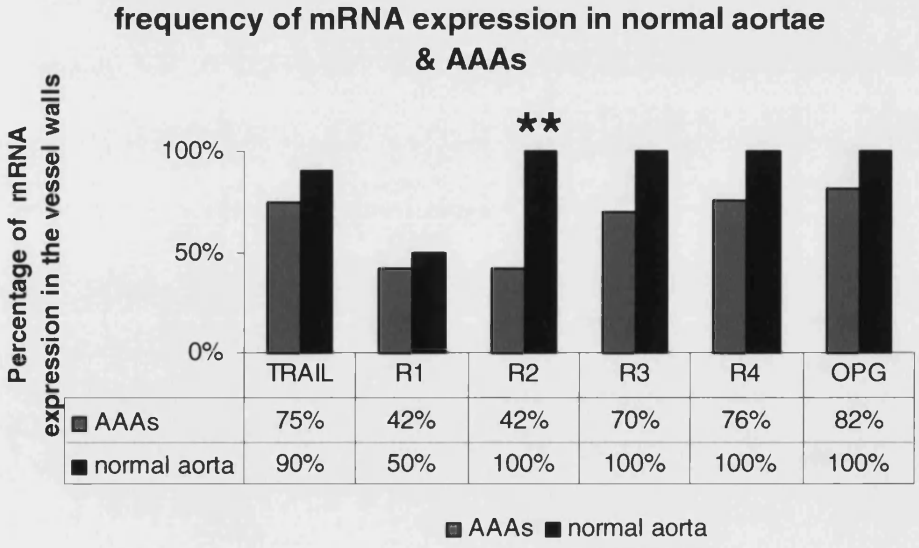

Figure 5.19 The graph illustrates the frequency of mRNA expression in 8 normal aortae and in 33 AAA vessel walls. There is a significant difference

between the frequency of mRNA TRAIL-R2 & R3 expression in normal aortae and in AAAs (P<0.01, t test, two tails, confidence > 95%).**

5.4.6.2 Relative abundance of mRNA for TRAIL-rTRAIL system expression

There are big differences in the percentage of vessel walls expressing mRNA between normal aorta and AAA. This indicates that TRAIL and its receptors are expressed in the normal and abnormal aortae. To compare the mRNA level in the normal aortae and AAA, semi-quantitative PCR results were shown.

Since TRAIL was expressed similarly in human normal aortae and AAAs (Figure 5.20a) and the ratio of TRAIL to death receptors is higher in AAA than normal aortae it follows that death receptors are higher in normal aortae. Similarly, because the ratio of TRAIL to decoy receptors is higher in AAA compared to normal aortae it follows that decoy receptors are expressed higher in normal aorta (Figure 5.20b).

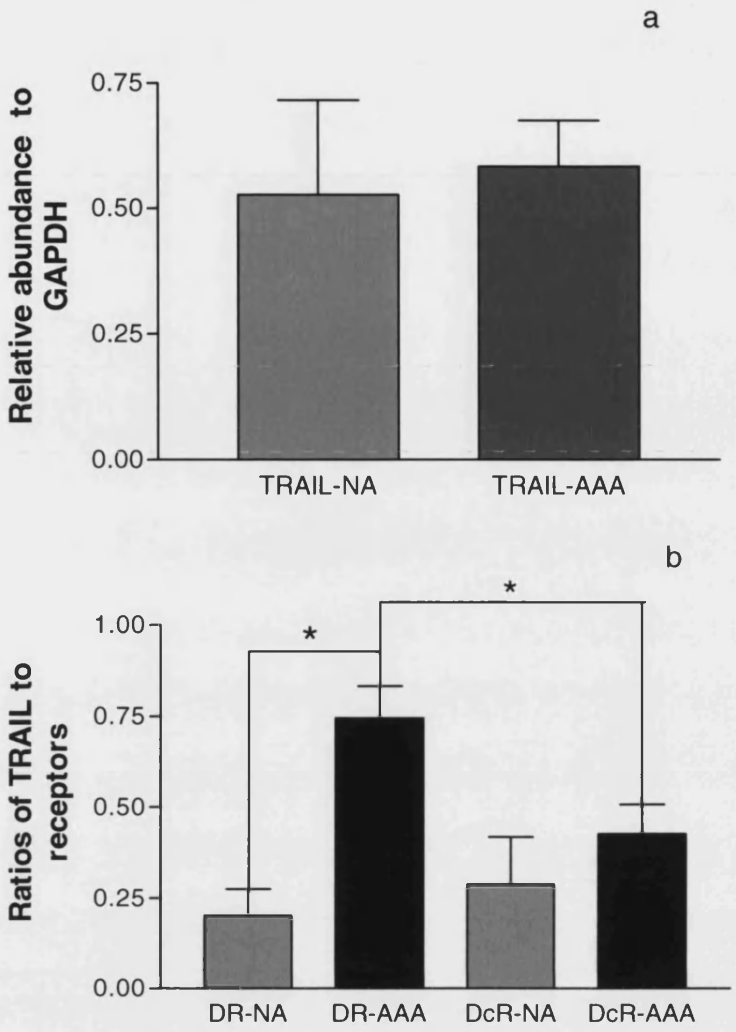

Figure 5.20 The comparison of TRAIL-rTRAIL mRNA expression in normal aortae and AAAs. Panel a shows mRNA expression for TRAIL in normal aortae and AAAs. TRAIL is expressed at similar levels on both tissues. Figure b shows the ratios of TRAIL to death receptors and TRAIL to decoy receptors in normal aortae and AAAs. DR-NA indicates that the ratios of TRAIL to death receptors in normal aorta. DcR-NA indicates that the ratios of TRAIL to decoy receptors in AAAs. DR-AAA indicates that the ratios of TRAIL to death receptors in AAAs. DcR-AAA indicates that the ratios of TRAIL/decoy receptors in AAAs. DR-AAA is significantly increased (* $p<0.5$) in AAAs. DcR-AAA was expressed significantly lower than DR-AAA(* $p<0.5$). No other significant difference was observed. The top of the bar represents standard error.

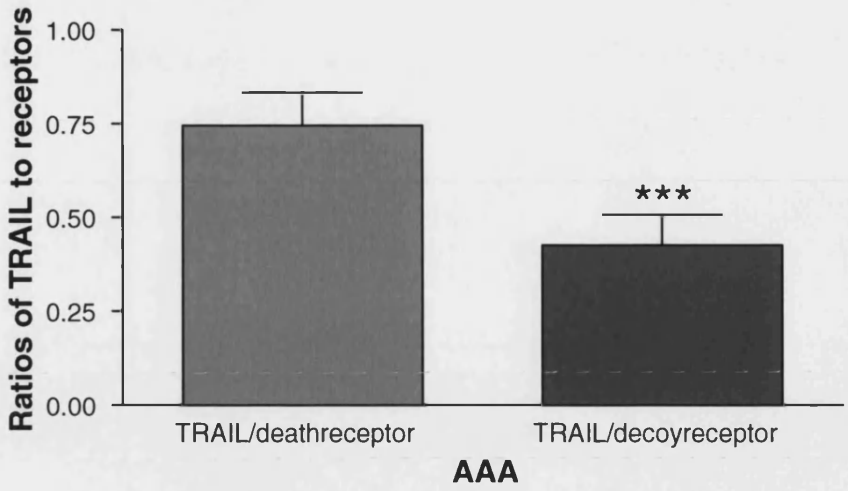

Figure 5.21 This figure shows the ratios of the mRNA expressions of TRAIL/death receptors and TRAIL/decoy receptors in AAAs (normalised to GAPDH). There is a significant difference between the ratio of TRAIL/death receptors and TRAIL/decoy receptors (*p<0.0001, paired t test, two tailed, confidence > 95%). Where TRAIL was expressed more often than death receptors, the value is greater than 1. Where the ratio is less than 1, it means that TRAIL was expressed less often than death receptors. Where the ratio equal to 1, it means that TRAIL and death receptors were absent in AAA walls (n=3). In conclusion, in the AAAs, more decoy receptors were expressed than TRAIL, and fewer death receptors were expressed than TRAIL. The top of the bar represents standard error.**

When no good correlation was found, one-way ANOVA was the best statistical method for further tests to test whether there is significant difference. In addition, more analysis was carried out on different areas of AAAs according to the level of their calcification.

5.4.7 The correlation of CT scan results and mRNA expression results

5.4.7.1 Frequency of mRNA expression in different areas of AAA

In an attempt to determine the involvement of the TRAIL system in the progression of aneurysmal disease, we used a model of aneurysm stages (early stage, developing stage and late stage) that involved taking samples from three different areas of the aneurysm wall to correlate with these stages (proximal, body and distal respectively). This approach was taken because most aneurysms available to us from surgery were of medium size developing stage (> 50mm and smaller than 69mm); early and late stage availability was extremely limited.

Calcification levels of different AAA lesions were determined by CT scan. Clearly, proximal area is the least calcified area and distal is the most calcified area (Figure 5.7, *$p<0.05$).

These data are compatible with previous findings of mRNA levels in normal aortae and AAAs.

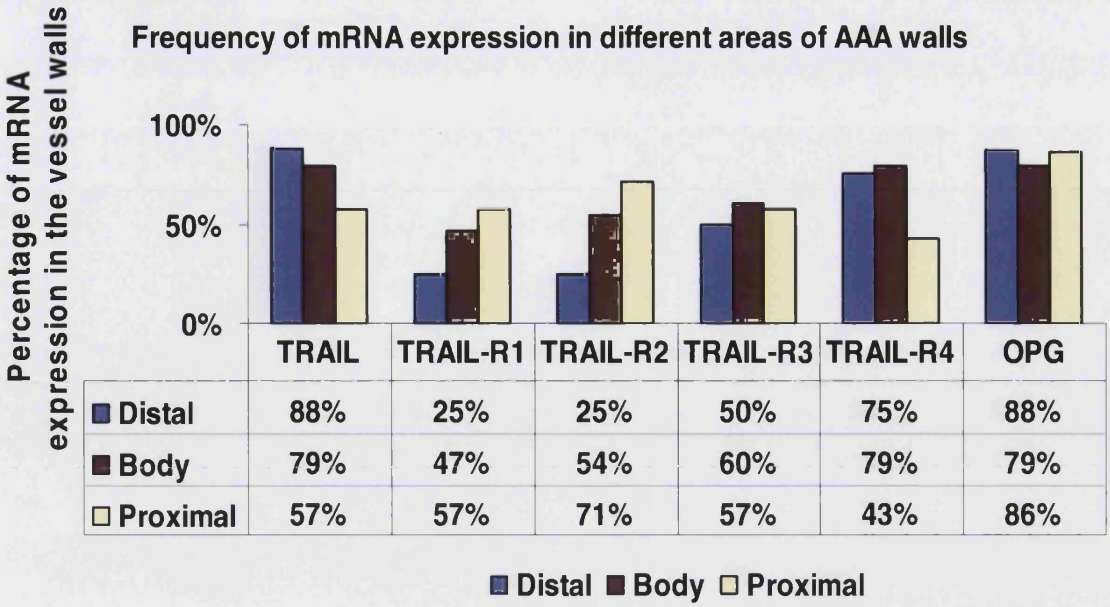

	TRAIL	TRAIL-R1	TRAIL-R2	TRAIL-R3	TRAIL-R4	OPG
Distal	88%	25%	25%	50%	75%	88%
Body	79%	47%	54%	60%	79%	79%
Proximal	57%	57%	71%	57%	43%	86%

Figure 5.22 This graph shows that TRAIL and all its five receptors were expressed widely in different areas of AAA vessel walls. Each bar represents the frequency of mRNA expression for TRAIL or its receptors in proximal, body and distal AAAs (proximal, n=8; body n=15; distal n=7). There is no significant differences among TRAIL and its receptors in these three areas of vessel wall (one-way ANOVA test, confidence>95%). According to results from CT scan, body AAA refers to severe calcification, proximal AAA refers to calcification in progress and distal AAA refers to end-stage calcification. In the distal area where calcification level increased, more vessels express TRAIL. In contrast, while calcification level increase; less vessels express TRAIL death receptors (TRAIL-R1 and TRAIL-R2). Regardless the calcification level, all areas of aorta express similar level of TRAIL decoy receptors with the one exception being a low expression rate of TRAIL-R4 (43%) in the proximal region.

5.4.7.2 Relative abundance of mRNA expression in different areas of AAA

The previous results show that more calcified vessels express more TRAIL and less TRAIL-death receptors, while the decoy receptors stay relatively level in all AAA areas. To express the results in a different way, comparisons were made between the expressions of TRAIL system components (TRAIL, death receptors and decoy receptors) by semi-quantitative PCR.

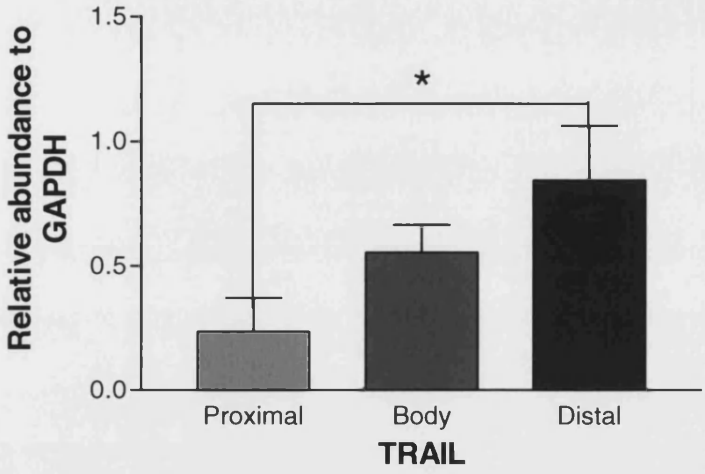

Figure 5.23 The graph shows the mRNA expression for TRAIL in proximal, body and distal AAA (normalised to GAPDH). Proximal, n=8; body n=15; distal n=7. TRAIL increased while calcification level increased. Significant difference was found between proximal and distal AAA (*p<0.05). This is compatible with the findings in the frequency comparison. More vessels expressed TRAIL in the more calcified region. The top of the bar represents standard error.

Since TRAIL is not expressed constantly in these three AAA regions, the ratios of TRAIL to its receptors are not meaningful as mentioned in the chapter 4. The graphs below show the mRNA expression for TRAIL death receptors (TRAIL-R1 and TRAIL-R2) and TRAIL decoy receptors (TRAIL-R3, TRAIL-R4 and OPG). As it is shown in the frequency results, decoy receptors were expressed similar in all three regions. Interestingly, TRAIL death receptors were expressed the most in

the body AAA while only half of vessels express them. This shows that TRAIL death receptors expression is upregulated in the body area of the AAA.

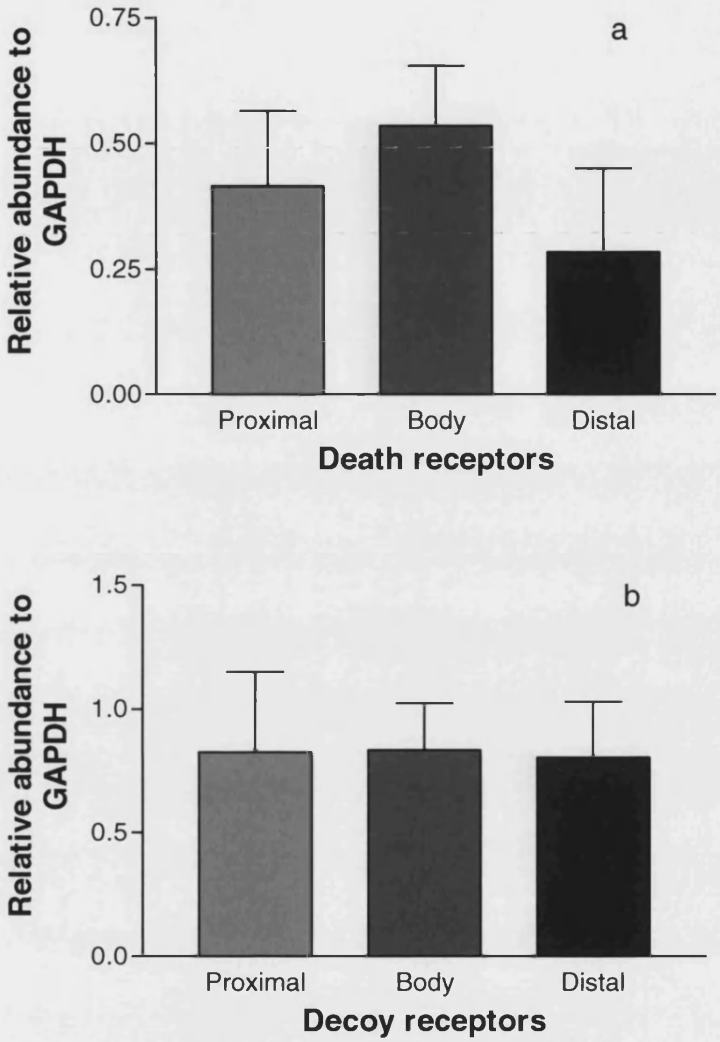

Figure 5.24 These graphs show the TRAIL decoy receptors (TRAIL-R3, TRAIL-R4 and OPG) and TRAIL death receptors (TRAIL-R1 and TRAIL-R2) in proximal, body and distal AAA. Panel a illustrates the mRNA expression for TRAIL death receptors and panel b illustrates the mRNA expression for TRAIL decoy receptors. TRAIL decoy receptors were expressed consistently in all three regions and death receptors were expressed variably from one region to the other. Their expression was expressed mostly in the body AAA and the least in the distal AAA. However, this is only a tendency, with no significant difference observed (by ANOVA test, confidence > 95%). The top of the bar represents standard error.

Figure 5.24b demonstrates TRAIL decoy receptors are expressed similar from one region to another in the AAA. Thus, the ratio of TRAIL death receptors to TRAIL decoy receptors is comparative.

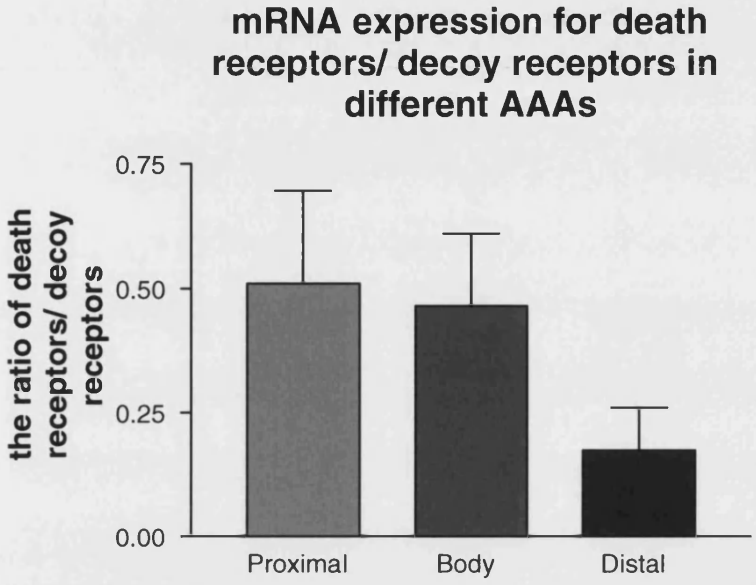

Figure 5.25 The graph shows the ratios of the mRNA expression for death receptors / decoy receptors in proximal, body and distal AAAs (normalised to GAPDH). Overall, the ratios are less than 1, which means that decoy receptors were expressed more often than death receptors in all three types of AAA (proximal n=8; body n=15; distal n=7). The ratios decreased while calcification level increased. However, this is only a tendency, with no significant difference observed (by ANOVA test, confidence > 95%). The top of the bar represents standard error.

5.4.7.3 The correlations of TRAIL and its receptors in different areas of AAA

As mentioned before, the correlation test for TRAIL and its receptors is also carried out in three AAA regions. Some almost perfect positive correlations were

observed in mRNA expression among TRAIL, TRAIL-R1, TRAIL-R2 and OPG in the different types of AAAs (see Table 5.4-5.6).

proximal				
	TRAIL	TRAILR1	TRAIL-R2	OPG
TRAIL	1	0.99	-0.22	0.99
TRAIL-R1		1	-0.23	0.99
TRAIL-R2			1	-0.22
OPG				1
Body	TRAIL	TRAILR1	TRAIL-R2	OPG
TRAIL	1	-0.46	-0.25	0.10
TRAIL-R1		1	-0.35	-0.20
TRAIL-R2			1	-0.20
OPG				1
distal	TRAIL	TRAILR1	TRAIL-R2	OPG
TRAIL	1	-0.23	-0.20	0.99
TRAIL-R1		1	0.14	-0.20
TRAIL-R2			1	-0.20
OPG				1

Table 5.6 This table shows correlations value r (correlation co-efficient, see 5.4.5.1 for details) among TRAIL, TRAIL-R1, TRAIL-R2 and OPG in the proximal, body and distal AAA (proximal n=8; body n=15; distal n=7). The red highlights clearly indicate an almost perfect correlation between TRAIL and TRAIL-R1, TRAIL and OPG, and TRAIL R1 & OPG in proximal AAA. TRAIL and OPG are also perfectly correlated in the distal AAA. TRAIL, TRAIL-R1 and OPG were expressed least often in proximal AAA (less calcified). TRAIL and OPG were expressed most often in distal AAA (most calcified).

The positive correlations between TRAIL and OPG may imply that OPG is compensated for TRAIL activation in AAA formation. Of note, the entire three decoy receptors were expressed similarly irrespective of AAA area. This may indicate that OPG plays a central role in protection against TRAIL activation in the developing AAA.

5.5 Discussion

5.5.1 Messenger RNA expression for TRAIL and its receptors in normal aortae

All normal aortic specimens were obtained with informed consent from pulseless kidney donors from Bristol Southmead Hospital; unfortunately complete information on these specimens is missing. Firstly, two different trends of mRNA expression in normal aortae were found. This could be explained by the age difference of the specimen donors. Osteoprotegerin is known to be expressed more in the old than in the young because OPG functions as an inhibitor of bone loss *in vivo* and osteoporosis occurs more frequently in the old than in the young ones (Hak *et al.*, 2000;Jono *et al.*, 2002). Since OPG appeared to be expressed more in group 1 normal aortae than group 2, it suggests that group 1 normal aortae might be obtained from an older age group.

Secondly, GAPDH in normal aortae was shown to have inconsistent expression. As mentioned in the methodology section, hypoxia and post-mortem delay could affect GAPDH expression severely (Zhong and Simons, 1999). All normal aorta specimens were obtained from open surgeries in normoxic conditions thus post-mortem delay would be an explanation for inconsistent GAPDH expression. Taken together, normal aortae were divided into 2 groups according to the mRNA level of TRAIL expression for accurate analysis.

Additionally, RANK mRNA was not detected while RANKL was detected consistently in the normal aortae and AAA (n=5, data not shown), which is different from the finding of Min at al., (2000) and (Hofbauer *et al.*, 2001). It might suggest that RANK and RANKL are not involved in AAA formation.

5.5.2 The correlation of the TRAIL-rTRAIL system mRNA expression in AAA

The physiological function of TRAIL and its receptors in different cell types is still not certain (Wang and El-Deiry, 2003). As detailed in 4.3, another question that has not been addressed is whether TRAIL-R1 or TRAIL-R2 is dominant in the initiation of apoptosis in certain cell types or whether the possible complexes of these two work together to signal cell death (Schneider *et al.*, 1997). To investigate this, analysis was carried out in pairs of TRAIL and its receptors. TRAIL-R2 positively correlated with TRAIL, TRAIL-R3, TRAIL-R4 and OPG. TRAIL-R1 negatively correlated with TRAIL, TRAIL-R2, TRAIL-R4 and OPG (refer to table 5.4-5.5). These results combined with the findings of a decrease in the compensatory responses of decoy receptors to death receptors suggest that TRAIL-R1 might have the dominant influence in the AAA.

5.5.3 TRAIL and its receptors mRNA expression in normal aortae and AAAs

5.5.3.1 The frequency of mRNA expression

TRAIL and its receptors are expressed extensively in miscellaneous tissues such as brain, heart and lung in human (Spierings *et al.*, 2004). For example, TRAIL-R1, TRAIL-R2 and TRAIL-R3 but not TRAIL are expressed in the human brain. TRAIL and all its receptors are expressed in the human heart and in this study TRAIL and its receptors were found in human normal aortae and AAA tissue. This is a novel finding since, to date, no other report of the TRAIL-rTRAIL system in aorta or AAA has been published.

Significant differences between normal aortae and AAA of TRAIL death receptors' frequency were found (see Figure 5.19). This strongly suggests the participation of TRAIL death receptors in the AAA formation. It is interesting to note that significantly fewer AAAs express death receptors than normal aortae. This suggests that the TRAIL-rTRAIL system may be involved in the initiation of abdominal aneurysm formation. There is considerable variability in TRAIL receptor expression in human AAA tissues. This could be because of two factors.

The first factor is the loss of gene coding for the receptors. Significantly, there are only 42% of AAA vessel walls expressing TRAIL-R2 mRNA but 100% normal aortae expressing TRAIL-R2 mRNA. The AAA vessel walls expressed less TRAIL and the other receptors than normal aortae. The possibility is that more diseased cells in the AAA samples explain the lower level of gene expression encoding the subunits of TRAIL and it receptors. Of note, greater differences were found for TRAIL death receptors than decoy receptors between human normal and abnormal aortic samples. This would support the association of dead cells with loss of encoding genes. Also, the significant difference between TRAIL death receptors and decoy receptors in AAA may indicate an imbalance between these receptors with respect to the normal situation. The second reason could be that death receptor mRNA was possibly lost from the AAA because the of the survival pressure exerted by TRAIL.

5.5.3.2 Relative abundance of mRNA expression

Messenger RNA for death receptors was expressed much more abundantly than the decoy receptors but on fewer normal aortic vessel walls. However, the opposite pattern of expression was seen in the AAA. Decoy receptors were expressed much more abundantly than death receptors (statistically significant difference) in AAA, and this is consistent with their protein expression (see next chapter). This might suggest that decoy receptors mRNA are raised in response to the disease state, and may act as protective agents against AAA progression. The increased decoy receptors in AAA might be a compensatory response to the change of death receptors.

TRAIL was expressed similarly in the normal aortae and AAA. Thus, any difference between the ratio of TRAIL to death receptors and the ratio of TRAIL to decoy receptors might suggest how the balance is tipped with respect to TRAIL in its capacity to induce or inhibit apoptosis. The former ratio is significantly greater than the latter in AAA (see Figure 5.20). This indicates that TRAIL death receptor expression is less than that of decoy receptors in AAA. This finding is consistent with the results of the expression frequency. In summary, the loss of encoding gene might be associated with the disease cells in the AAA samples and the survival pressure exerted by TRAIL.

5.5.4 The TRAIL and rTRAIL system mRNA expression in different areas of AAA

5.5.4.1 The frequency of the TRAIL-rTRAIL system expression in the different areas of AAA

The criteria attached to elective AAA open repair surgery restricted the size of AAA specimens that could be obtained from selective surgeries (occasionally obtained from emergency AAA rupture repair). The size and calcification level of AAA specimens are quite similar and at the end stage of disease (all diameters of AAA >50mm). For a better understanding of the contribution of TRAIL and its receptors to AAA formation, AAA specimens were separated into three groups according to different calcification levels to imitate the developing progression of AAA. The expression of TRAIL mRNA increased while calcification levels increased. The mRNA of TRAIL death receptors was significantly decreased as the calcification level increased. TRAIL decoy receptors maintained a similar expression in all stages of AAA (see **Figure 5.24**). This might suggest a continuous inhibition of calcification by decoy receptors and TRAIL death receptors initiation at an earlier stage of calcification.

5.5.4.2 The relative abundance of the mRNA expression for TRAIL-rTRAIL system in the different areas of AAA

TRAIL was expressed more abundantly in the more calcified area. This supports the proposition that TRAIL capacity for triggering apoptosis increases and prevention of apoptosis diminishes in the more calcified AAA regions. TRAIL decoy receptors were expressed similarly in the three AAA regions examined. This is consistent with the findings of bone calcification-inhibiting proteins (MGP, osteocalcin and bone sialoprotien) being found to be expressed at all stages of human atherosclerosis (Dhore *et al.*, 2001). This correlation may imply a functional association between TRAIL decoy receptors and bone calcification-inhibiting proteins.

Interestingly, the fact that TRAIL death receptors were expressed highest in the AAA body suggests that the general situation of a developing aneurysm (body area) is where apoptosis might be upregulated. The lowest level of death receptors were found in the distal region that would consist of damaged apoptotic cells incapable of expressing mRNA or new protein. This is also coherent with previously published results of bone related activators of calcification (BMP-2, BMP-4, osteopontin and osteonectin) which were restricted to advanced, calcified lesions (Dhore *et al.*, 2001). All these findings suggest that AAA formation similar to the vascular calcification process is the result of time and plaque-stage-restricted activation and continuous inhibition. The TRAIL-rTRAIL system may play a role in this developing process.

5.5.4.3 The correlation of mRNA expression for the TRAIL-rTRAIL system in the different areas of AAAs

TRAIL and OPG are positively associated in the proximal and distal AAA. Thus, OPG was increasingly expressed while calcification level increased. This feature might be representative of a counter-regulatory mechanism of OPG limiting apoptosis in the less calcified areas and therefore the restricting the initiation of calcification. Since OPG has been found to play a role in the process of vascular calcification in an animal model, there is a strong implication that OPG also plays a role in AAA pathogenesis.

Atherosclerosis is associated with the AAA. It is possible that the different calcification level of aneurysm could be a result of unsteady three-dimensional blood flow that might also simulate atherosclerosis in abdominal aortic aneurysm. A Japanese research group successfully produced a model of such three dimensional blood flow using a graphics workstation (Taylor and Yamaguchi, 1994). This aneurysm flow stimulation model predicts that a single asymmetric blood flow occurs in the proximal (neck) region of the AAA which coincides with the area of least calcification found in this study. In the aneurysm body, two symmetric vortices were formed which might lead to more calcification than found in the proximal area. In a similar way, the model proposes that as the

blood passes through the wide body of the AAA into the narrower distal region, a greatly increased stress is exerted on the vessel wall. This correlates with the region identified here as being the most calcified and may indicate that this distal region of the AAA is where rupture is most likely to occur.

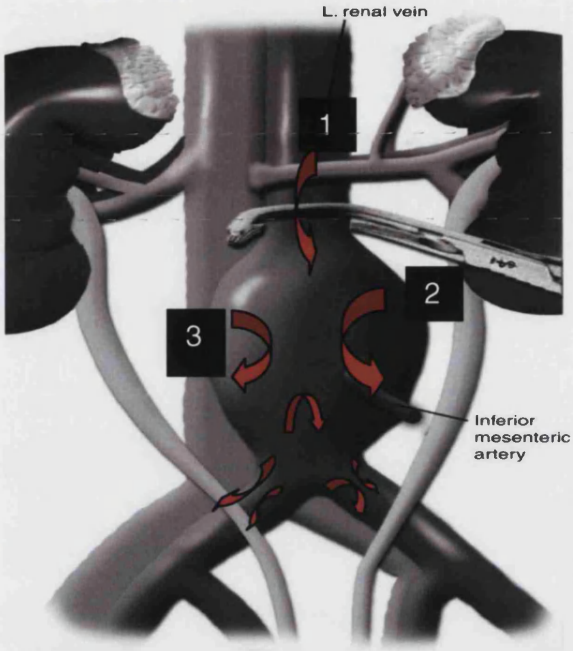

Figure 5.26 Blood flows in the calcified AAA as red arrows indicated. The no.1 vortices where is proximal AAA becomes no.2 vortices where is body AAA. The no.2 blood flow forms a small circulation inside the enlargement of AAA increasing the burden of the vessel wall then causing the more sever calcification. While no.2 blood flow stream arrives at narrow distal area, the extra stress of the vessel wall suddenly increases. This could be a reason of distal area is the most calcified region. (The graph is from Heal, national video library)

6.

Chapter 6 TRAIL, TRAIL-R1 and OPG protein expression in human normal and calcified aortic samples

6.1 Introduction

6.1.1 The role of OPG in vascular calcification

The role of OPG in vascular calcification is still uncertain. Osteoprotegerin is present in heart, arteries, and veins of the cardiovascular system, where it is particularly high in the aorta and the renal arteries (Collin-Osdoby, 2004). The protein OPG was found in the borders of calcified structures and areas surrounding calcified regions in arterial medial calcification (Collin-Osdoby, 2004).

Osteoprotegerin was found in human aortic fibrocalcific plaque without immunoactivity (Dhore *et al.*, 2001). It was also found in the calcified aorta and renal arteries in mice (Min *et al.*, 2000). Injection of OPG can prevent the onset of vascular calcification in these mice but cannot change the incidence of VC in adult mice even on high dose (Min *et al.*, 2000). Additionally, it has been demonstrated that serum OPG levels are often associated in vascular calcification diseases, such as carotid stenosis in postmenopausal woman, coronary artery disease and vascular calcification in patients with long term haemodialysis (Erdogan *et al.*, 2004; Jono *et al.*, 2002; Nitta *et al.*, 2003). The role of the circulating levels of OPG still needs further investigation. It may reflect the correction of over-mineralisation processes and possibly demonstrates a protective role at the biological level. It is believed to inhibit directly vascular calcification and provides an indicator of vascular pathology (Collin-Osdoby, 2004).

The physiological roles of OPG that may influence vascular SMC and endothelial cells are also not certain, especially in the SMC (Collin-Osdoby, 2004). In the rat endothelial cells undergoing apoptosis, OPG binds to TRAIL and prevents TRAIL interaction with its receptors (Malyankar *et al.*, 2000). Rats treated with warfarin or Vitamin D_3 develop vascular calcification which can be suppressed by OPG serving as a protective agent in the vasculature (Bucay *et al.*, 1998; Min *et al.*, 2000). Osteoprotegerin and TRAIL have been found to be expressed in human atherosclerotic or calcified vessels (Schoppet *et al.*, 2004). Also human OPG promotes polymorphisms that protective against coronary artery disease or atherosclerotic-like vascular changes (Brandstrom *et al.*, 2002). Osteoprotegerin

may be an important autocrine/ paracrine factor protecting against arterial calcification and the vascular-damaging effects of inflammatory cytokines through enhancing endothelial cell survival. This could be via two possible mechanisms; first by conveying NF-κB–induced survival signals and secondly by directly binding and neutralising the pro-apoptotic actions of TRAIL released from vascular SMCs (Collin-Osdoby, 2004; Pritzker *et al.*, 2004; Scatena and Giachelli, 2002; Schoppet *et al.*, 2004).

Consequently, further research is needed to learn if and how OPG might interface with TRAIL in regulating mineralisation within the vascular systems.

6.1.2 Western Blot introduction

Western blotting is a commonly used method for identifying a specific protein from a protein mixture. It detects the target protein by its specific reaction with an antibody and determination of its size relative to standard proteins of known size.

Total protein is separated on the gel that includes molecular weight markers. Molecules are separated on the gel according to their charge, size and shape. More highly charged species move more rapidly in an electric field; larger molecules, and those less spherical in shape, are retarded by the gel to a greater extent. Small polynucleotide fragments (up to 1 kilo base (Kb)) are separated on polyacrylamide gels; larger nucleic acids, such as restriction fragments are separated on agarose gel. Hence, the choice of gel and gel size is critical for optimal results.

When only the molecular size is relevant, the proteins are denatured with sodium dodecylsulphate (SDS). Sodium dodecylsulphate is an anionic detergent which denatures proteins by wrapping around the polypeptide backbone. In so doing, SDS confers a net negative charge to the polypeptide which is in proportion to its length. When treated with SDS and a reducing agent, the polypeptides become rods of negative charges with even "charge densities" or charge per unit length. Since the charge per unit length of the SDS-polypeptide complex is constant, the electrical force exerted on the complex per unit length is also constant. Thus the migration velocity is totally determined by the sieving effect of the acrylamide

matrix so that proteins are separated according to their molecular weight (Swank *et al.*, 2006). The proteins to be examined here are TRAIL, TRAIL-R1 and OPG which are 20 kDa, 55 kDa and 16kDa respectively, therefore SDS-PAGE gels were used for Western blot for separation of total protein in this project.

The upper layer, through which the sample passes first, is known as the "stacking gel". It is a large-pore gel, which is non-restrictive to the protein sample. The buffer in which the stacking gel is made contains an ion (usually an anion) whose electrophoretic mobility is greater than that of the protein, while the tank buffer, or electrode buffer, contains an ion whose mobility is less than that of the protein. As electrophoresis begins, the "leading ion" in the stacking gel moves faster than the protein and leaves behind it a zone of lower conductivity. The higher voltage gradient of this zone causes the protein to move faster and to "stack" at the boundary between the leading and trailing ions (Swank *et al.*, 2006).

Below the stacking gel is a deeper layer of gel with a smaller pore size, known as the resolving gel. This gel is prepared in a buffer of higher concentration and pH in an anionic system. In this environment, the mobility of the trailing ion increases so that its boundary moves ahead of the protein. The protein is resolved into individual bands according to size (Riederer and Goodman, 1987). For the purpose of this study, 12% resolving gel was used when OPG and TRAIL were the target protein and 9% resolving gel was used when TRAIL-R1 was the target protein. This is because the size difference. For good final detection results, target protein is ideally suited in the middle of the gel.

Antibodies react with specific protein which is based on enhanced chemiluminescence (Swank *et al.*, 2006). This is achieved by performing oxidation of luminol by the Horseradish peroxidase (HRP) in the presence of hydrogen peroxide (H_2O_2). The excited intermediate that is formed emits light which is detected by a photo-sensitive film. This light emission can be enhanced by chemical enhancers such as phenols. This increases the output of light by approximately 1000 fold. The detection is summarised in the diagram below:

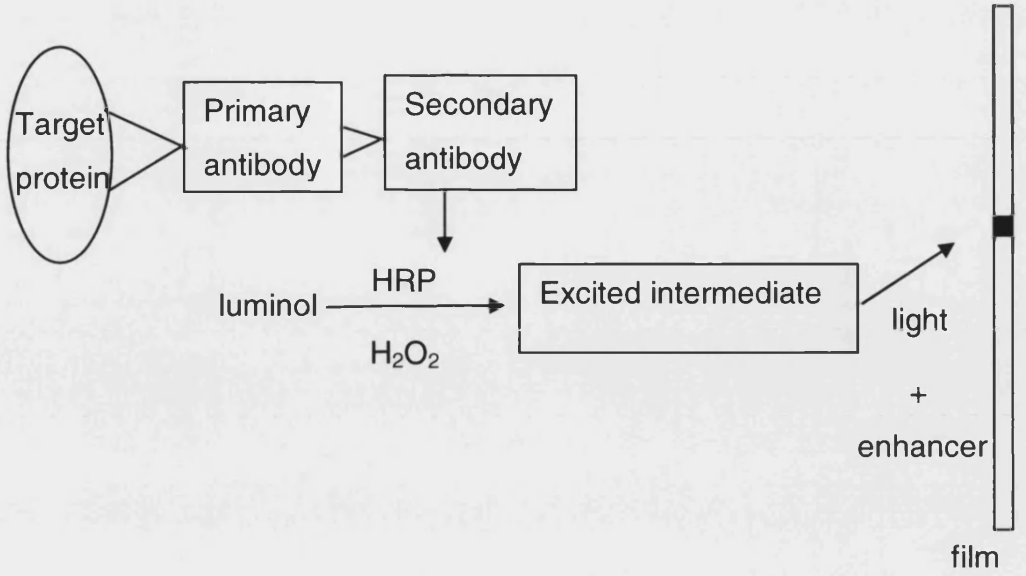

Figure 6.1 Principles of enhanced chemiluminescence detection method used for visualisation of Western blots.

6.1.3 Bradford assay introduction

The Bradford assay is one of the most commonly used protein assay methods. It works by the action of Coomassie Brilliant Blue G-250 (CBBG). This dye specifically binds to proteins at arginine, tryptophan, tyrosine, histidine and phenylalanine residues, especially at arginine (da Silva and Arruda, 2006). The assay is very sensitive and suitable for detecting protein isolated from vessel walls. The CBBG solution is mostly anionic and binds to those residues at absorbance maximum at 595 nm (blue). It also contains some free dye in the cationic form, which has an absorbance maximum at 470 nm (red). The assay is monitored at 595 nm in a spectrophotometer to measures the protein complexed with CBBG.

6.1.4 Dot blots introduction

Dot blotting is another technique similar to Western blot for detecting, analysing, and identifying proteins. The protein loaded on the nitrocellulose membrane are not separated electrophoretically but are only observed through circular

templates of the membrane. Dot blots can only be used when both the primary and secondary antibodies are specific for the antigen as can be assessed by Western blotting first.

Western blotting is a time-consuming technique and is restricted by a limited number of samples per gel (usually only 8). Comparatively, Dot blot has the advantages of being rapid and allowing large numbers of samples to be analysed simultaneously (maximum 96 protein samples can be loaded each time). This also gives the opportunity to automate or semi-automate analysis of multiple samples. Moreover, Dot blot has been documented to be approximately 10- to 1000-fold more sensitive than Western blot (Rapley R. and Walker J.M., 1998).

6.1.5 General Immunohistochemistry (IHC) introduction

There are two methods of antigen detection commonly used in tissue in IHC: direct and indirect. The direct way uses only one antibody which is quicker but not very sensitive. The indirect method involves two antibodies, primary and secondary antibodies, and results in an enhancement of the signal for antigen detection. Primary antibody reacts with the antigen in tissue and secondary antibody reacts with primary antibody. The secondary antibody is against the IgG of the animal species in which the primary antibody has been raised. It is also can be labelled with fluorescent dye which is called immunofluorescence method or be labelled with enzyme such as peroxidase, alkaline phosphatase or glucose oxidase which is called immunoenzyme method. A substrate is reacted with these enzymes and demonstrated presence of antigen in tissues.

Two of the commonly used indirect methods are:

- PAP Method (peroxidase anti-peroxidase method)
- Avidin-Biotin Complex (ABC) Method:

The PAP method amplifies the signal by using a complex composed of antibody to peroxidase coupled with peroxidase forming a very stable peroxidase anti-peroxidase system. The complex acts as a magnified layer antigen binding to the unconjugated secondary antibody.

The ABC method is a standard and widely used IHC method. The secondary antibody is biotinylated. Avidin which is a large glycopyrotein, has a very high affinity for biotin. It can be labelled with peroxidase or fluorescein. The amplified signal is a complex composed of avidin-biotin peroxidase. Biotin is a low molecular weight vitamin. Finally, the peroxidase is developed by substrates to produce colourimetric products.

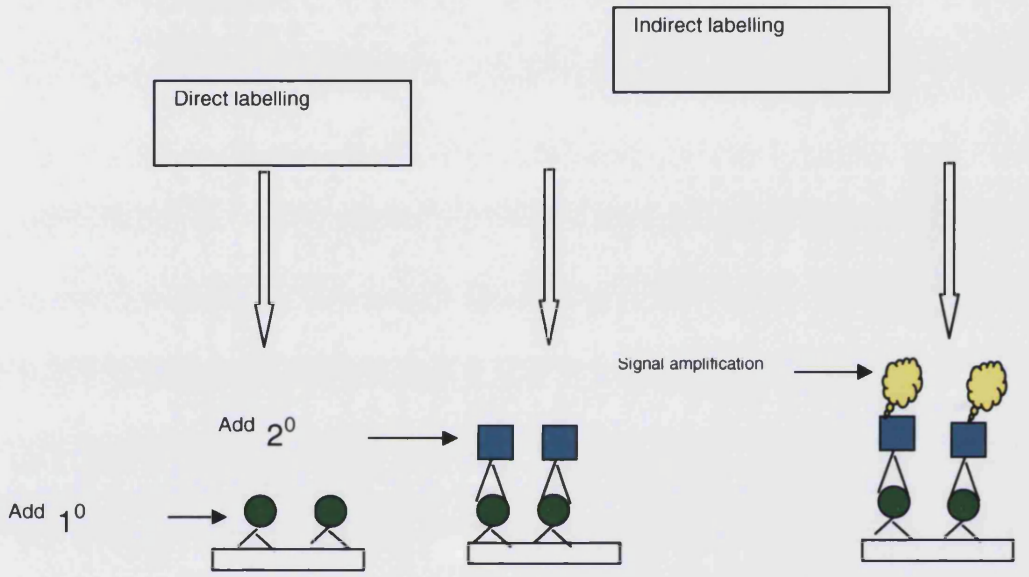

Figure6.2 Diagrammatic representation of general IHC. This includes direct labelling, indirect labelling with/without labelling with amplified signal. Direct labelling as shown on the left of the diagram, where the primary antibody (Add 1^0) is directly attached to the target protein. Indirect labelling without signal amplification is diagrammatically shown in the centre, depicting the target protein reacting with the primary antibody (Add 1^0) and then with the secondary antibody (Add 2^0). The final method involves three steps. Firstly, the primary antibody (Add 1^0) reacts with the target protein; secondly, it reacts with secondary antibody (Add 2^0, such as biotinylated antibody); lastly, this combination reacts with amplifying streptavidin to enhance the signal.

6.2 Aims and objectives

- To determine whether TRAIL, TRAIL-R1 and OPG are expressed in normal tissues
- To determine whether TRAIL, TRAIL-R1 and OPG are expressed in calcified AAA tissues
- To determine whether there are protein expression differences of TRAIL and its receptors' expression between normal control samples and AAA samples
- To determine whether there are variations among TRAIL, TRAIL-R1 and OPG in tissues with different level of calcification
- To determine where TRAIL, TRAIL-R1 and OPG localisation is consistent with the calcification deposition

6.3 Materials and methods

6.3.1 Protein expression materials and methods

6.3.1.1 Samples

Protein detection and determination was performed on normal aortae and AAA tissues that were sourced as described in chapter 5. The AAA samples were from the same 31 donors but 12 different normal aorta samples were analysed as there was insufficient sample remaining of the tissues used in gene expression study (chapter 5). The age range of normal aorta donors was from 15 to 57 (mean age 46± 13 year old). None of them had AAA but one sample had visible atherosclerosis on the aortic wall. The age of this donor is 57.

6.3.1.2 Protein isolation materials and methods

- NaCl (sodium chloride), Promega, UK
- Tris-HCL (Tris (hydroxymethyl) aminomethane) HCL (hydrochloric acid), Sigma-Aldrich Co Ltd, Poole, UK

- Triton X100, Promega, UK
- Ethylene diamine tetraacetic acid (EDTA), Promega, UK
- Leupeptin, Promega, UK
- Aprotinin, Promega, UK

Choosing the most suitable lysis buffer for AAA protein isolation is a very important step for good quality protein detection. A standard Triton X100 lysis buffer was used containing 0.15M NaCl, 10mM Tris-HCl (pH=4), 1% Triton X100, 5mM EDTA (pH=8) and the protease inhibitors, leupeptin and aprotinin. This buffer is less denaturing, but gives a higher background and less likely to inhibit kinase activity and disrupt protein complexes. Sodium fluoride is an inhibitor of serine/threonine protein phosphatases. Tris-HCL functions as an inhibitor of phosphatases. EDTA prevents phosphorylation in the lysate. The concentration of the detergent Triton X100 was varied to determine the optimal conditions for lysis of the samples. Concentrations of 0.1%, 1% and 10% were tested and 1% Triton X100 showed the best results by Bradford assay (detailed below).

Human AAA and normal aorta tissues were stored at -80°C for total protein isolation. Tissues were ground into powder by using liquid N_2 followed by adding the lysis buffer (see appendix A for recipe and chapter 5 methods for isolation details). The solution was transferred into new Eppendorf tubes and centrifuged at 13,000rpm at 4°C for 10 minutes. Final total protein samples were stored at -80°C for future study (Bollag *et al.*, 1996).

6.3.1.3 Bradford protein assay materials and methods

- Bovine Serum Albumin (BSA), Bio-Rad, Hertfordshire, UK
- Biorad Reagent, Bio-Rad, Hertfordshire, UK
- 96-well, flat-bottomed tissue culture test plates, Orange scientific, Belgium

For improved isolation of protein, 1% Triton X100 was used in the lysis buffer. The detergent in the lysis buffer concentration (1%Triton X100) is incompatible with Biorad reagent (Biorad being compatible with 0.1% Triton X100). This would interfere with the standard curve. Two completely different curves appeared

when BSA was run with water and with lysis buffer. The standard curve with lysis buffer was very flat. This is because the Triton X100 in lysis buffer interacts with Biorad reagent. Thus, the lysis buffer was diluted 100 times with Milli-Q water to correct the interference. The total protein samples were diluted 100 times in Milli-Q water in the Bradford assay for accurate results.

Bovine serum albumin was used as protein standard in the Bradford assay. It was diluted into different dilutions for the standard curve (see Table 6.1 and Figure 6.3 for individual concentration and standard curve).

cuvette	Buffer µl	BSA µl	Concentration (µg/ml).
0(Blank).	1000µl	0.0µl	0
1	996.5µl	3.5µl	5
2	992.5µl	7.5µl	10
3	989.0µl	11.0µl	15
4	985.2µl	14.8µl	20
5	982.0µl	18.0µl	25

Table 6.1 Dilution of BSA for standard curve.

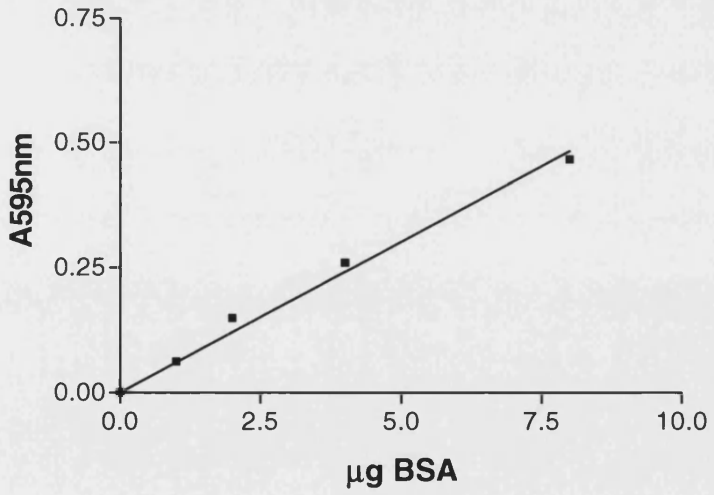

Figure 6.3 Typical standard curve for protein assay.

Diluted sample solution (800µl) was mixed with 200µl Biorad reagent. Each dilution (100µl) was then added to a 96-well plate in triplicate. The well plate was shaken vigorously to prevent bubbles from forming. The final solution was incubated at room temperature for 10 minutes to allow colour development (no more than 45 minutes to avoid the effects of Biorad reagent degradation). Absorbance at 595 nm was measured using a multi-well plate reader (Dynex Technologies, MRX TC II). The concentration of sample protein was determined from the standard protein curve using GraphPad Prism 3.2 data analysis software.

6.3.1.4 Polyacrylamide gel electrophoresis (SDS-PAGE) materials and methods

- Acrylamide 40% or 30%, Anachem Bioscience, UK
- Ammonium Persulphate (AMPS), Sigma-Aldrich Co Ltd, Poole, UK
- Bromophenol Blue, Promega, UK
- DTT, Sigma-Aldrich Co Ltd, Poole, UK
- Glycine, Sigma-Aldrich Co Ltd, Poole, UK
- Rainbow marker (molecular weights, 250-10KD), Amersham Life Sciences, UK
- SDS, Sigma-Aldrich Co Ltd, Poole, UK
- TEMED, Promega, UK
- Trizma base, Promega, UK

Acrylamide gel was prepared according to Laemmli (Laemmli, 1970) on a Hoefer Mighty Small Dual Gel Caster (Hoefer Pharmacia Biotech Inc. USA). Five percent stacking gel includes 1.3ml 30% acrylamide, 2ml 4X stacking gel buffer, 4.7ml H_2O, 21.6µl 20% AMPS and 8µl TEMED. This stacking gel buffer (100ml) includes 0.4g SDS, 0.05g Trizma base (pH=6.8). The composition of 12% resolving gel includes 9.6ml 30% acrylamide, 3ml 8X resolving gel buffer,11.4ml H_2O, 60µl AMPS and 12µl TEMED; the 9% resolving gel includes 7.2ml 30% acrylamide, 3ml 8X resolving gel buffer, 60µl 20% AMPS and 12µl TEMED. This resolving gel buffer (100ml) includes 0.8g SDS and 36.3g Trizma base (pH=8.8). As detailed in the introduction, stacking gel (the upper layer) is responsible for

sweeping up proteins in a sample between two moving boundaries so that they are compressed into micrometer thin layers when they reach the separating gel. The resolving gel (the lower layer) is designed to separate polypeptides by size. The gel includes SDS which is used to denature the proteins and acrylamide which is the material for preparing electrophoretic gels to separate proteins by size. A cross-linked polymer network forms when acrylamide is mixed with AMPS. Then AMPS produces free radicals faster in the presence of TEMED. The size of the pores created in the gel is inversely related to the amount of acrylamide used and often is used to resolve large proteins. Hence, lower % acrylamide gels will have larger pores. The gel limits larger molecules to slower migration than smaller molecules. Thus, protein can be separated by SDS-PAGE gel by estimating relative molecular mass.

An equal volume of reducing sample buffer was added to the protein samples which were prepared as detailed in 6.3.1.4. These were diluted to different concentrations in Eppendorf tubes and boiled for 5 minutes at 99°C, then cooled on ice for 5 minutes. This reducing sample buffer (pH=8) includes 130nM Tris-HCl, 20% (v/v) glycerol, 4.6% (w/v) SDS, 0.02% Bromophenyl Blue and 2% dithiothreitol (DTT). Glycerol is a stabilising factor and helps with protein sample loading in the well. Bromophenyl blue is a dye that is functional for visualising protein samples in the well and tracking the progress through the gel. DTT is used for protein denaturation. Tris-HCL is used for adjustment of pH value. Rainbow marker (10µl) was mixed with an equal volume of reducing sample buffer. It was then centrifuged at 10,000 rpm for 30 seconds and incubated on ice for 5 minutes.

The gel plates were placed in the electrophoresis equipment (Hoefer Pharmacia Biotech Inc. USA) which was then filled with running buffer. The running buffer (1L) included 3.03g Trizma base, 14g glycine and 10g SDS. An equal volume (10µl) mixture (protein sample mixed with sample buffer) was carefully loaded into the gel wells, in parallel with rainbow marker mixed with sample buffer. The gel was then subjected to electrophoresis at a constant voltage of 100V for approximately 1 hour, or until the dye reached the base of the gel. If the bands are not sharp on the developing film after ECL, the voltage could be reduced to solve the problem.

6.3.1.5 Protein blotting and immuno-detection materials and methods

- Blue reagent, Sigma-Aldrich Co Ltd, Poole, UK
- Enhanced chemiluminescence detection kit, Amersham Life Sciences, UK
- Chromatography paper 17 CHR, Whatman International Plc., UK
- Kodak X-OMAT AR auto rad film, Amersham Life Sciences, UK
- Methanol, Fisher Scientific UK Ltd.
- Nitrocellulose paper (hybond-C extra), Amersham Life Sciences, UK
- PBS, Oxoid Ltd., UK
- Ponceau S, Sigma-Aldrich Co Ltd, Poole, UK
- Primary antibody and secondary antibody (see table 6.3-2 for details)
- Tween 20, Sigma-Aldrich Co Ltd, Poole, UK
- Western blotting tank, Hoeffer Scientific, CA
- Non fat dried milk, Marvel©, UK

Following electrophoresis, the gel was carefully removed and incubated in blotting buffer. Add 3.3g Trizma base and 14g Glycine with 1L Milli Q water and this is called BLOT A. The blotting buffer (1L) includes 800ml BLOT A and 200ml methanol. Then at the same time Hybond-C extra nitrocellulose paper and chromatography paper (17 CHR - Whatman) were cut to the size of the gel and soaked in the blotting buffer in order to avoid fuzzy bands occurring. A Western blot cassette holder (see Figure 6.4) was used, into which 3 filter papers were placed on top of the sponges on one side of the holder. The nitrocellulose membrane and the gel were placed on one set of filter papers carefully removing all air bubbles. A further set of 3 filter papers was then placed on top of the gel and the cassette was closed. This was then transferred to a Western blotting tank making sure that the nitrocellulose paper was nearest to the positive electrode (anode). Blotting buffer was added to the tank and the proteins were blotted for 4-5 hours at a current depending on the area of the gel (normally 6X9 cm) determined by the equation;

$1mm^2$ gel= 1 mA.

Figure 6.4 A schematic diagram of the blotting apparatus used to transfer proteins onto nitrocellulose paper.

After this the cassette was removed from the tank and the gel was stained with blue reagent solution for analysis of complete transfer of protein to the nitrocellulose paper. The membrane was stained with 1% Ponceau S to detect protein expression. The positions of different molecular weight markers were marked on nitrocellulose paper with a pencil. The nitrocellulose was then incubated in blocking buffer (5% milk / PBS Tween) at 4 °C overnight or on the rocker at room temperature for an hour.

The nitrocellulose membrane blot was then transferred to 20 ml tube containing 5ml of the diluted primary antibody (and

Table **6.2** for details). This was incubated on a rocking plate for 2 hours at room temperature then thoroughly washed in 0.5% Tween 20/ PBS (see appendix A for making) 3 times, 15 minutes each. The blot was then incubated with the diluted secondary antibody (see

Table **6.2** for details) for 1 hour at room temperature. The blot was again washed in 0.5% Tween 20/ PBS 3 times, 15 minutes each. As controls the primary and secondary antibodies were adsorbed with the individual specific protein standards. Different primary antibodies were chosen and tested (see

Table **6.2** for details).

Equal volumes of solution A and solution B from the enhanced chemiluminescence detection kit (Amersham Life Sciences) were mixed and added to the membrane immediately making sure the whole of the membrane was covered. The membrane was incubated for 60 seconds and the excess drained off and covered in SaranWrap™ ensuring that all bubbles were smoothed out and placed in a film cassette, protein side up. In a dark room, a sheet of Kodak autoradiography film was carefully placed on top of the membrane and exposed initially for 5 minutes. Exposure time was adjusted for optimal results. This film was then developed using Fuji RG II X-ray film processor (Fuji Photo Film Company Ltd, Japan). Analysis of data was performed using Scion Imaging Software.

6.3.1.6 Optimisation of blotting procedures troubleshooting

Many problems occurred before a successful Western blot image was obtained. Low protein signal could be a result of ineffective blotting; therefore it is important to perform the pre-detection staining of the gel and membrane as described. Another reason for low signal could be that the concentration of target protein is too low in the total protein sample. This could be solved by concentrating the total protein in a High Performance Centrifugal Spin Concentrator (Orbital Biosciences). Low affinity of primary antibody is another possible reason for low signal that can be remedied by increasing the incubation times and/or temperature and increasing the concentration of primary antibody or by trying a primary from a different source. The right choice of secondary antibody is imperative too. To confirm that the ECL system works the detection reagent A and B were pre-mixed and added to 1µl HRP-labelled antibody in the dark room. Blue light is visible if the reagent is working. Finally, it is worth checking whether the X-ray detection procedure works and if so enhancement can be achieved by exposing the film for a longer time such as in the fridge overnight.

In contrast, excessive diffuse signal occurs sometimes. A simple first fix is to load less protein on the gel and also check the transfer from gel to membrane stage

were bubbles may interfere with the quality of the signal. Obviously, reducing the exposure time and/ or increasing washing time are potentially other solutions.

High background on the film could result from 3 main causes. These are: too high concentrations of primary antibody and/or secondary antibody; contaminated buffers or equipment; and insufficient blocking. Simply increasing the blocking time would be the first attempt to remedy high background and/ or increasing the blocking buffer from 5% milk to 10% milk in PBS Tween 20. Additionally, different dilution buffers could be tried for different proteins. Four dilution buffers for antibody were tested here, 10%, 5%, 1% and 0% milk powder in 0.05% PBS Tween 20. The detergent Tween 20 can reduce the background on the final film but high concentration of Tween 20 could reduce the affinity with primary antibody. Ultimately, 0.05% PBS Tween 20 was chosen. One percent milk / PBS Tween 20 buffer was used as dilution the buffer for primary antibodies and PBS Tween 20 without milk was used as the dilution buffer for secondary antibodies as the possibility of biotin in the milk may cause non-specific binding.

6.3.1.7 Stripping blot materials and methods

- 2-Mecaptoethanol, Sigma-Aldrich Co Ltd, Poole, UK
- Tris-HCL, Sigma-Aldrich Co Ltd, Poole, UK
- SDS, Sigma-Aldrich Co Ltd, Poole, UK

Sometimes it was necessary to strip the bound antibodies from the gels to troubleshoot and to save time and protein samples. Stripping methods for blots allow the first set of protein probes (the primary antibody and the secondary antibody) to be removed from the target protein on the membrane in Western blot. Thus, the different proteins on the membrane can be detected by a second set of protein probes. To do this the membrane was washed in PBS Tween 20 for 5 minutes followed by incubation in stripping buffer for 30 min at 50-60°C. Generally, stripping buffer is sufficiently harsh to dissociate the affinity interaction between protein probes and the target proteins. It is also an efficient way to remove protein probes without damaging the proteins on the membrane. The stripping buffer used comprises 62.5 mM Tris-HCl (pH 6.8), 2% SDS and a final

concentration of 0.1 M 2-Mecaptoethanol. The membrane was shaken by hand every 15 minutes and finally was washed in PBS Tween 20 for 5 minutes twice. Empirical testing by using Ponceau S to visualise the protein band to ensure the stripping process was effective and the protein was still present on the membrane. The membrane was then ready for re-blocking followed by normal Western blot protocol as described.

	TRAIL	TRAIL-R1	TRAIL-R2	OPG
Primary antibody	Mouse anti-human MNL AB (BD Pharmingen). 1:1000	Rabbit anti-human polyclonal AB (BD Pharmingen). 1:1000	Rabbit anti-human polyclonal AB (Chemicon). 1:500	Rabbit anti-OPG polyclonal AB (Santa Cruz). 1:500
	Rabbit anti-TRAIL polyclonal AB (Chemicon). 1:500	Rabbit anti-human polyclonal AB (Chemicon). 1:500		
	Mouse anti-TRAIL MNL AB (Santa Cruz). 1:500			
Dilution buffer for AB	1%milk/ PBS Tween 20	1%milk/ PBS Tween 20	1%milk/ PBS Tween 20	1%milk/ PBS Tween 20
Duration for AB	2 hours	2 hours	2 hours	2 hours
Secondary antibody	goat anti-mouse (DAKO).	swine anti-rabbit (DAKO).	swine anti-rabbit (DAKO).	swine anti-rabbit (DAKO).
Dilution buffer for AB	1:1000 in PBS Tween 20	1:1000 in PBS Tween 20	1:1000 in PBS Tween 20	1:1000 in PBS Tween 20
Duration for AB	1 hour	1 hour	1 hour	1 hour
Positive control	Recombinant human TRAIL (Peprotech EC).	Recombinant human TRAIL-R1 (Peprotech EC).	Recombinant human TRAIL-R2 (Peprotech EC).	Recombinant human OPG (Peprotech EC).

Table 6.2 Primary antibodies and secondary antibodies that were used in the Western blot.

6.3.1.8 Dot blots materials and methods

- Enhanced chemiluminescence detection kit, Amersham Life Sciences, UK
- Chromatography paper (17 CHR), Whatman International Plc., UK
- Kodak X-OMAT AR auto rad film, Amersham Life Sciences, UK
- Hybond-C Extra Nitrocellulose paper, Amersham Life Sciences, UK
- PBS, Oxoid Ltd., UK
- Ponceau S, Sigma-Aldrich Co Ltd, Poole, UK
- Primary antibody and secondary antibody (see table 6.2 for deatails)
- Tween 20, Sigma-Aldrich Co Ltd, Poole, UK

If primary antibodies specifically bind only the target protein, Dot blots provide a good alternative to the Western blot.

In a Dot blot, a nitrocellulose membrane is placed in a 96-well Dot blotter (DHM-96, Jencons Scientific Inc. PA) (see Figure 6.5 for details) into which the protein samples are applied. The sample is aspirated into the membrane which allows the protein to penetrate the membrane in good quantities. Dot blots allow comparisons of more samples at once and giving more accurate indication of level of expression.

Protein samples were prepared (detailed in 6.3.1.2) for loading on to the Dot blot according to their concentrations assessed by the Bradford assay. Two pieces of Whatman paper (17 CHR) were assembled underneath a piece of nitrocellulose membrane (Hybond-C extra) to make a Dot blot "sandwich" and then soaked in the running buffer. Positive control, protein samples and pure H_2O which was used as a negative control were loaded into each well of the Dot blot apparatus. The suction power was kept on for 30 seconds after loading to drain excess blot buffer. The nitrocellulose blotting membrane was blocked in the blocking buffer and incubated in the primary and secondary antibody as previously described in section 6.3.1.5.

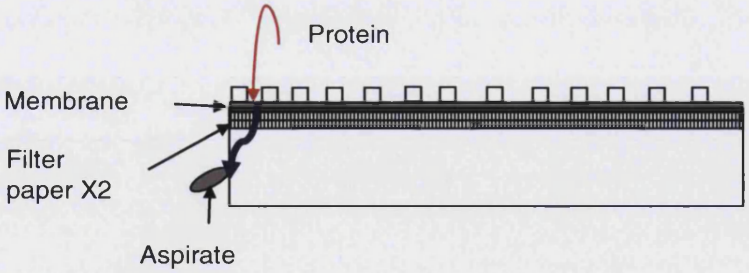

Figure 6.5 A schematic diagram of the Dot blot apparatus. Protein is loaded into the well as the red arrow indicates. Membrane and filter paper were assembled as shown. The blue arrow indicates the flow direction.

6.3.1.9 Statistical analysis

As discussed in the introduction, a standard curve was constructed using the results of blotting pure protein controls (10 µg, 20 µg and 30 µg) on membrane at the same time as the test samples. Test protein concentrations were measured by reading off the standard curve after densitometric scanning. The analyses were carried out in duplicate. All extracted proteins were finally subjected to Dot blots simultaneously for more accurate results. Paired analysis between two groups was performed by paired t test. The linear regression test (Pearson test) was used to determine the correlation between protein expressions in the TRAIL-rTRAIL system. Significant differences were considered at *P <0.05 levels and confidence >95%. All error bars are ± standard error of the mean (SEM). One star refers to *P< 0.05 and two stars refers to **P< 0.01. Three stars refers to ***P< 0.001.

All analyses were performed using the GraphPad Prism Instat package, Version 3.02, GraphPad Software Inc., San Diego USA.

6.3.2 Immunohistochemistry material and methods

6.3.2.1 Fixation and Sectioning materials and methods

Fixation is usually performed to preserve tissue architecture and cell morphology prior to staining. It acts to crosslink and stabilise proteins in the tissue. The choice of fixation, dehydration and clearing methods can impact the final result depending on the antigen to be detected and also the antibodies used. Inappropriate or prolonged fixation may dramatically reduce the target antigen lability. Neutral buffered formalin is a commonly used standard fixation method which preserves tissue structure well.

- Formol saline, BDH laboratory supplies, Poole, UK
- Xylene, Fisher Scientific UK Ltd.

Dissected tissues were fixed in 10% formalin for at least 24 hours prior to dehydration in a graded series of alcohol solutions and embedding in paraffin wax using a Shandon Hypercentre 2 automated tissue processor (programmed for use as follow). In brief, specimens were incubated in a series of diluted (70%, 80%, 90%, 100%) alcohol to dehydrate tissue followed by incubation in xylene, then wax.

The tissue blocks were sectioned (to 4-6 µm) using a sledge microtome and placed on glass slides, then oven dried at 60°C overnight.

Substance	Time(hour)	Wash time(minutes)
IMS 70%	01:00	15
IMS 80%	01:00	15
IMS 90%	01:00	15
IMS 95%	01:00	15
IMS 100%	01:30	15
IMS 100%	01:30	15
IMS 100%	01:30	15
Xylene	01:30	15
Xylene	01:30	15
Wax	02:00	15
Wax	08:00	15

Table 6.3 Embedding process procedure

6.3.2.2 Deparaffinisation and tissue rehydration materials and methods

- Xylene, Fisher Scientific UK Ltd.
- IMS, Sigma-Aldrich Co Ltd, Poole, UK

Deparaffinisation and rehydration is essentially the reverse process of embedding process. Generally, tissue blocks were deparaffinised in xylene, rehydrated in alcohol, and finally soaked in water. In detail, slides were incubated twice in xylene for 5 minutes each. The slides were then placed twice in IMS for 5 minutes each to hydrate samples. Slides were lastly incubated in water for 5 minutes.

6.3.2.3 Avidin-Biotin complex- Alkaline Phosphatase (ABC-AP)

- Aquamount, VWR International, Poole, UK
- Fast red, Sigma-Aldrich Co Ltd, Poole, UK
- Horse serum, (65mg/ml) Sigma-Aldrich Co Ltd, Poole, UK
- PBS (10X), VWR International, Poole, UK
- Mayer's Haematoxylin, Sigma-Aldrich Co Ltd, Poole, UK
- Negative control Mouse IgG1, DakoCytomation Ltd, Ely, UK
- VECTA STAIN ABC Kit, Vector Laboratories Ltd, Orton Southgate, Peterborough, UK

The ABC-AP technique was superior to PAP method for staining tissues rich in endogenous peroxidase (Cordell *et al.*, 1984) such as arterial wall.

The following protocol was applied to sample slides and positive control slides (placenta) with the appropriate staining controls. Following the antigen retrieval process the slides were incubated with normal horse serum solution (65mg/ml * 10µl per slide) for 20 minutes to block non-specific binding of immunoglobulin and followed by rinsing twice in PBS for 5 minutes each. Blocking solution was

then removed and slides were incubated in diluted primary antibody in a humid box overnight at room temperature. Slides were then incubated with secondary antibody diluted in buffer (50µl biotinylated antibody in 10ml PBS) for 30 minutes at room temperature. At the same time, enzyme solution AB (100µl solution A in 10ml PBS, then add 100 µl solution B, mix well) was prepared and was left for 30 minutes at room temperature. Slides were washed twice in PBS for 5minutes each. Enzyme solution AB was added to each slide and left for 30 minutes at room temperature. Slides were washed again twice in PBS for 5 minutes each. Substrate solution (sigma fast-red as instruction manual) was prepared just before application to slides. Finally, slides were observed under LM to determine the end-point (when red stain appears). The reaction was eventually stopped with water, and counterstained with Mayer's Haematoxylin for 1 minute. Slides were rinsed in running tap water for 5 minutes and covered with a coverslip on permanent aqueous mounting medium.

6.4 Results

6.4.1 Presence of TRAIL, TRAIL-R1 and OPG protein in AAA samples

As is known, after an mRNA molecule is synthesised, many steps are required in order to produce a functional protein. Often, intracellular mechanisms conspire to alter or even destroy the mRNA or protein along the way. However, if mRNA is not expressed in the cell, the correlated protein cannot be transcribed. Thus, a further study of protein expression for TRAIL and its receptors was performed.

The investigation and analysis of mRNA expression among all three receptors were shown above (see chapter 5). It seems that TRAIL-R1 dominates in AAA formation between two death receptors. Osteoprotegerin was found to be significantly correlated with TRAIL and TRAIL-R1 and may play an important role in protection from AAA formation. However, antibodies for TRAIL-R3 and TRAIL-R4 were not available commercially when these experiments were carried out therefore only TRAIL, TRAIL-R1 and OPG protein were subjected to further study.

The reducing sample buffer worked well with pure control proteins but gave a high background when used with protein isolated from the AAA. It was considered that the reducing sample buffer might breakdown proteins too much and caused the high background, so a comparison of non-reducing sample buffer and reducing sample buffer was carried out. However, non-reducing sample buffer did not reduce the high background either. The reducing sample buffer was used since.

Recombinant soluble human TRAIL protein was diluted into 30μg/ml, 20μg/ml and 10μg/ml and then subjected to Western blotting. The picture following shows the standard curve of human TRAIL. The human TRAIL was successfully detected by the methods detailed in chapter 6 methods and the band density of TRAIL protein was changed while the protein concentration changed.

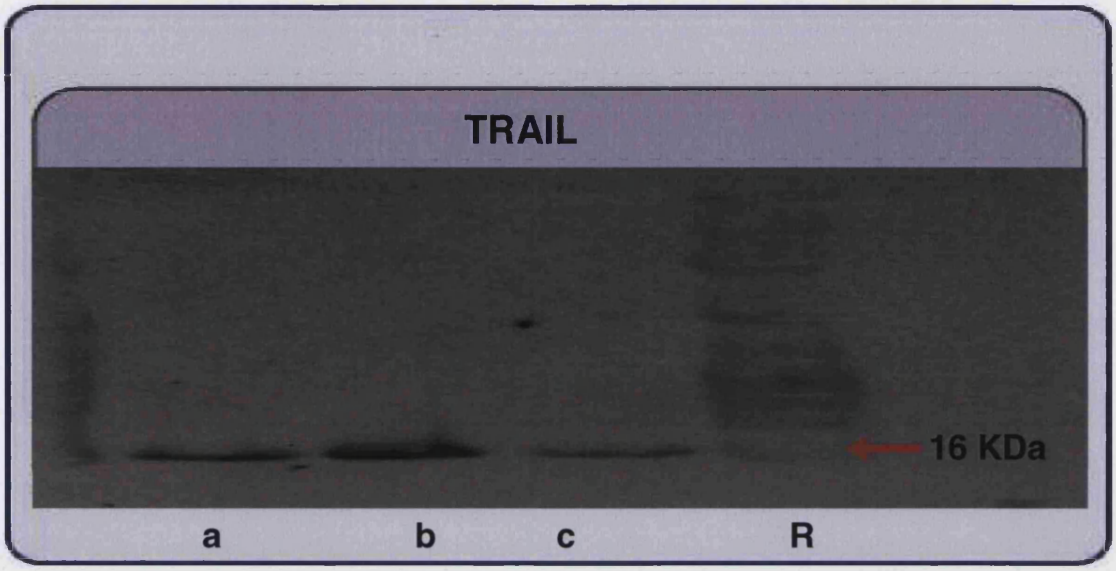

Figure 6.6 shows the standard curve for recombinant soluble human TRAIL examined by Western blot as detailed in methods. Dilution for TRAIL was a 20μg/ml, b 30μg/ml and c 10μg/ml respectively. R indicates the rainbow size marker. The protein for TRAIL is in the right place according to the rainbow marker developed on the same film (indicated by red arrow).

Recombinant human TRAIL-R1 proteins (dilution 30μg/ml, 20μg/ml and 10μg/ml) were detected by Western blot and developed on the film. They were shown on the following film though not very clear. The density of bands is still correlated with the concentration of the protein. TRAIL-R1 at 10μg/ml could not be detected on the film for two possible reasons. First, this might be because of a loading or dilution failure of this protein. Secondly, such a small amount of TRAIL-R1 protein was not detectable by Western blot under the conditions used (detailed in methods).

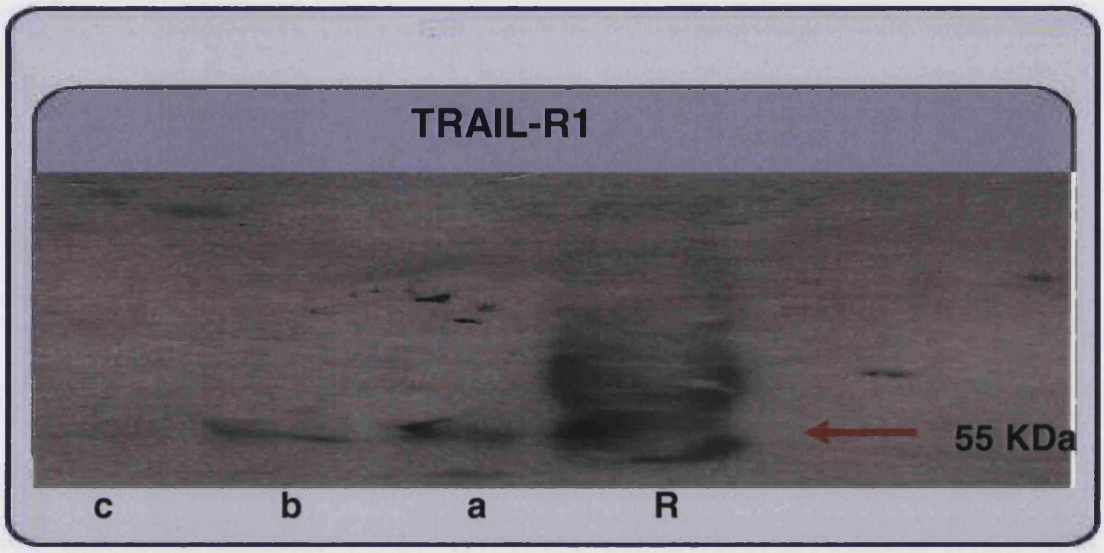

Figure 6.7 shows the standard curve for recombinant soluble human TRAIL-R1 examined by Western blot (detailed in methods). Dilution for TRAIL-R1 was a 30μg/ml, b 20μg/ml and c 10μg/ml respectively. The bands of protein are not very sharp. However, the tendency still can be observed that band density intensifies while the protein concentration increases. The TRAIL protein of 10μg/ml could not be detected. R indicates the rainbow marker loaded on the same gel with these proteins. The bands were detected at the 55kDa position according to the rainbow size marker.

Human purified OPG protein was detected by Western blot as shown in figure 6.50. The samples were diluted to 30µg/ml, 20µg/ml and 10µg/ml. The band of protein with dilution of 10µg/ml is not very clear. However, the standard curve tendency can be seen. The band density increases while protein dilution increases. The possible reasons for the poorly defined band at 10µg/ml protein may be, firstly, loading error and secondly, this small amount OPG protein can not be detected under the conditions of antibody dilution used.

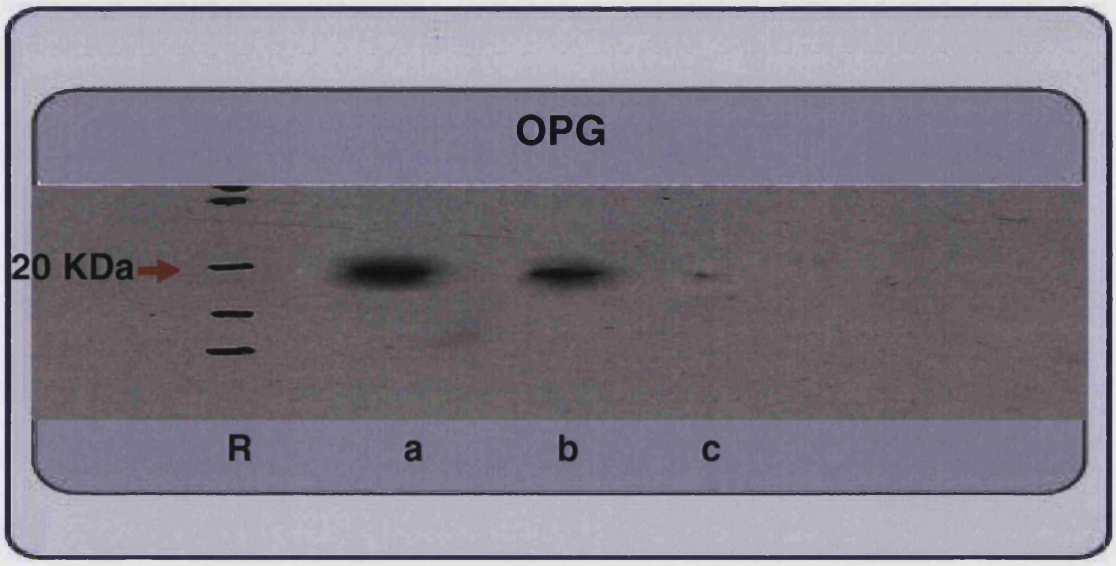

Figure 6.8 shows the standard curve for recombinant soluble human OPG. The dilution range for OPG was 30µg/ml (a), 20µg/ml (b) and 10µg/ml (c). Dilution for the primary antibody was 1:1000. The changes of band density follow the change of dilution for protein. R indicates the rainbow size marker on the film marked with pen from the positions on the original membrane. Red arrow indicates the position of the target protein.

The protein for TRAIL, TRAIL-R1 and OPG was determined by Western blot as shown in Figure 6.9. These samples were extracted from AAA (detailed in 6.3.1.1) and loaded with rainbow marker (R) on each gel. The protein obtained from AAA were observed and shown on the film without cross reaction, for this reason they were eligible for protein dot blotting.

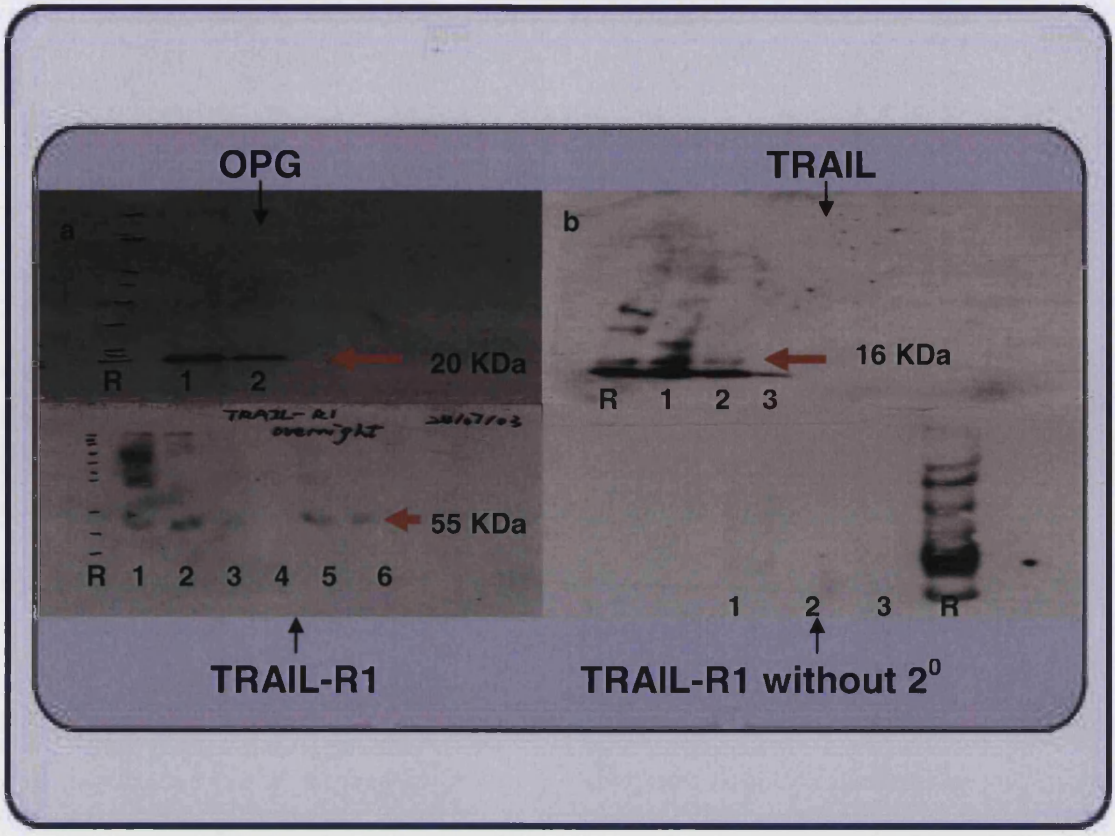

Figure 6.9 shows 4 Western blot analyses performed on AAA protein to detect OPG expression in 12% acrylamide gel, and TRAIL, TRAIL-R1 protein expression in 9% acrylamide gel. A rainbow marker was loaded on each gel for band size identification. Panel a shows a membrane loaded with two different AAA protein samples indicated as 1 and 2 probed with mouse anti-human OPG (dilution 1:1000). Panel b shows 3 AAA samples (1, 2 and 3) probed with polyclonal rabbit anti-human TRAIL antibody (dilution1:500). The continuous line underneath the protein bands here are the bottom of the gel. Panel c shows 6 different AAA protein samples labelled 1-6 probed with polyclonal rabbit anti-human TRAIL- R1 antibody (dilution 1:1000). Sample d here was not expressed TRAIL-R1 protein. The other band images are not clear, however there were no cross reactions. Panel d represents a Western blot of 3 AAA samples probed with anti-TRAIL-R1 but without a secondary antibody (2^0). It clearly shows that TRAIL-R1 primary antibody works well in AAAs. Red arrows indicate the molecular weight of each protein respectively. R indicates the rainbow marker on each film.

The samples from normal aortae and AAAs were subjected to Dot blot procedures described in the methodology section in chapter 6.

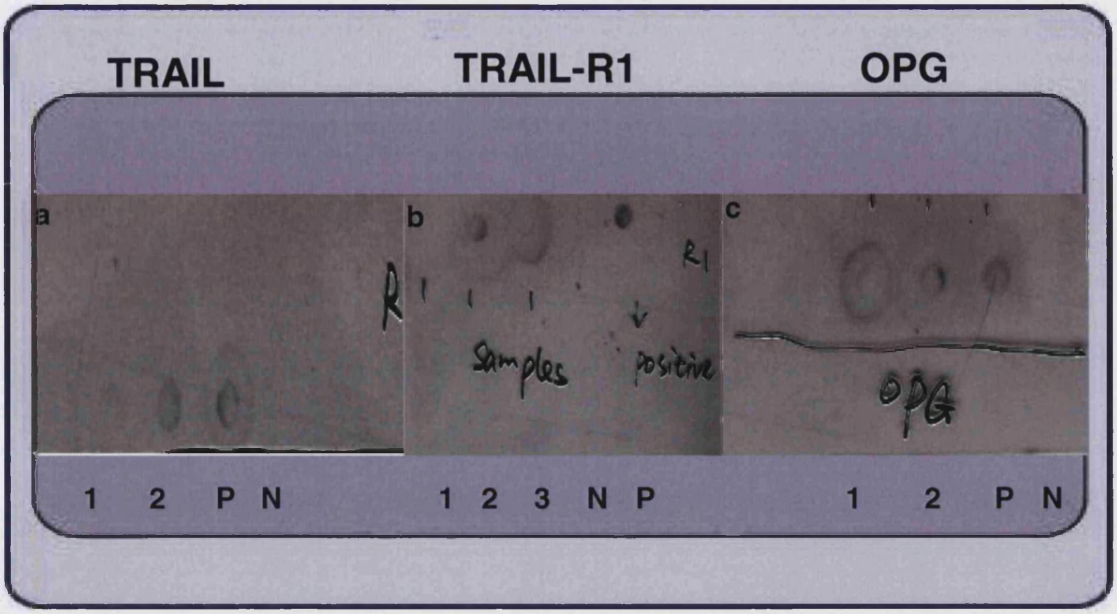

Figure 6.10 shows the representative films of TRAIL (panel a), TRAIL-R1 (panel b) and OPG (panel c) protein expression in AAA samples determined by protein Dot blots. P indicates positive control (purified protein) for antibody used on each film. N indicates negative control (purified water) on each film. Two AAA samples probed for TRAIL are shown on panel a indicated as a and b. Three AAA proteins samples probed for TRAIL-R1 are shown on panel b indicated as a, b and c. Sample 1 did not express TRAIL-R1 protein. Two AAA protein samples probed for OPG are shown here on panel c indicated as 1 and 2.

The presence of TRAIL protein in human AAA tissue was confirmed in fresh AAA tissue that was paraffin-embedded and prepared as described in section 6.3.2.4 for immunohistochemistry staining.

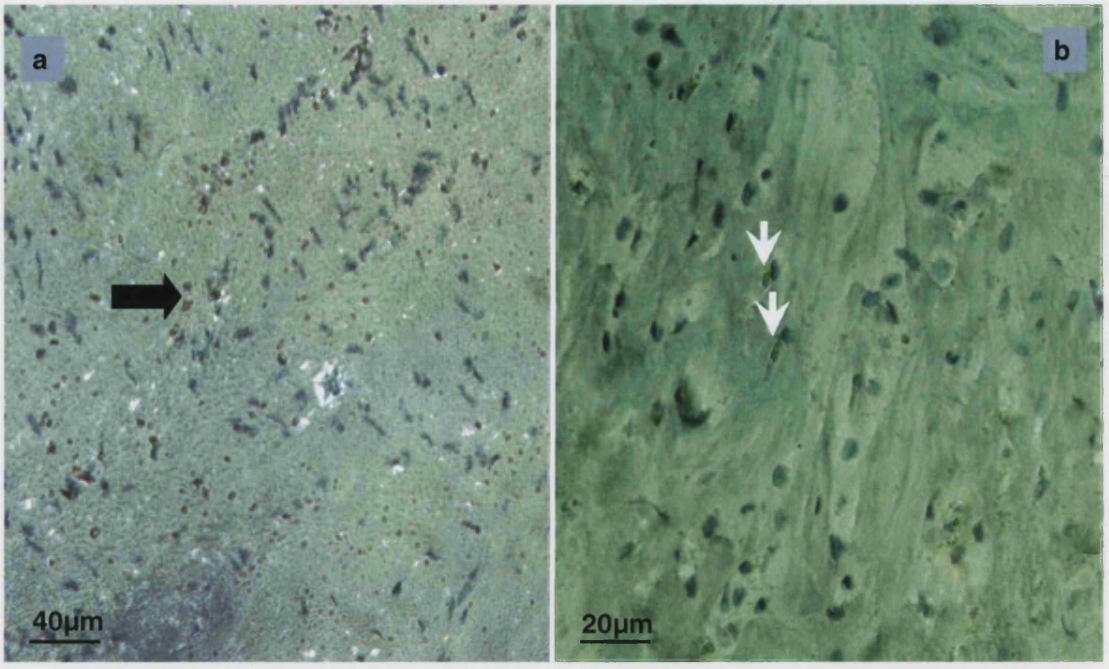

Figure 6.11 Immunohistochemical staining was performed for TRAIL (a and b). Arrows indicate positive staining. The micrograph in Panel b was taken using higher power microscopy than panel a originally.

The presence of TRAIL-R2 in human AAA tissue was visualised in fresh AAA that was also paraffin-embedded and stained as detailed in 6.3.2.4 shown in figure 6.12. The panel b of the figure shows obvious cholesterol deposition.

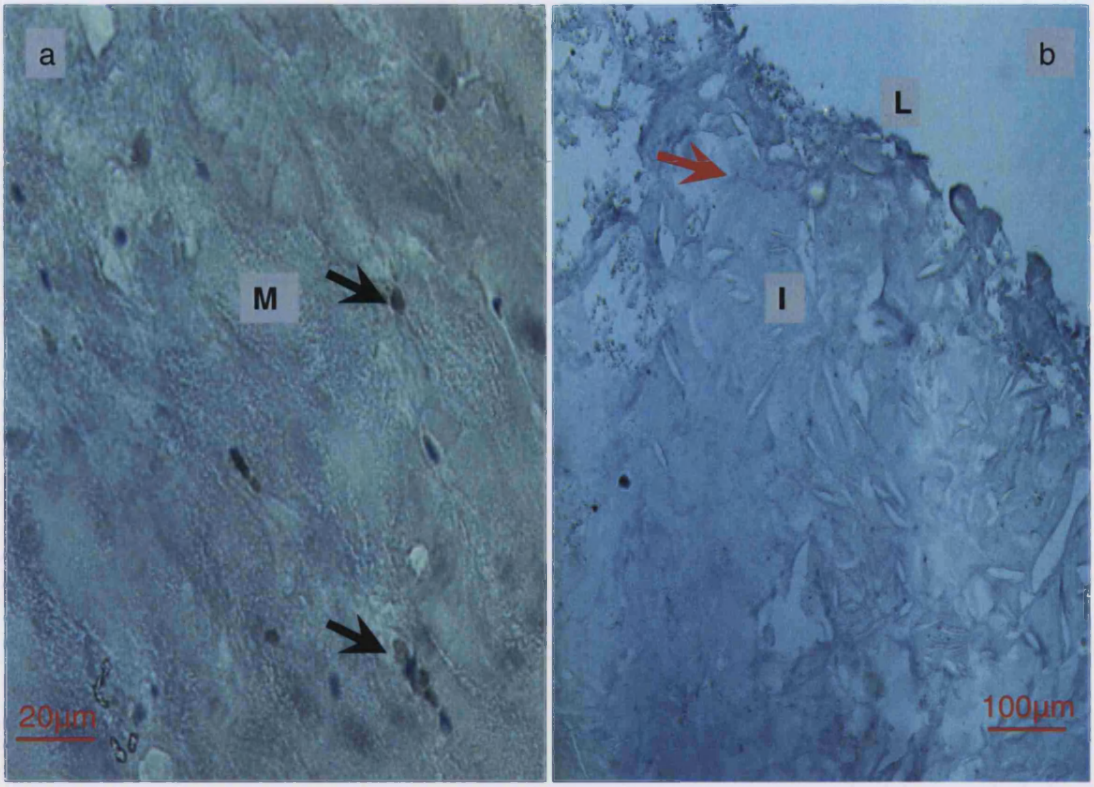

Figure 6.12 Immunohistochemical staining for TRAIL-R2 was performed. Black arrows in picture a indicate positive staining on the medial layer of AAA (M). The open, needle-like spaces (red arrows indicated) in the picture b are cholesterol clefts on the intimal layer (I). L= lumen

OPG existence in human AAA tissue was confirmed in fresh AAA tissue that was subjected to paraffin-embedding and immunohistochemistry staining. Figure 6.13 shows that more OPG is expressed in the medial layer of AAA than in the *tunica adventitia* layer of AAA.

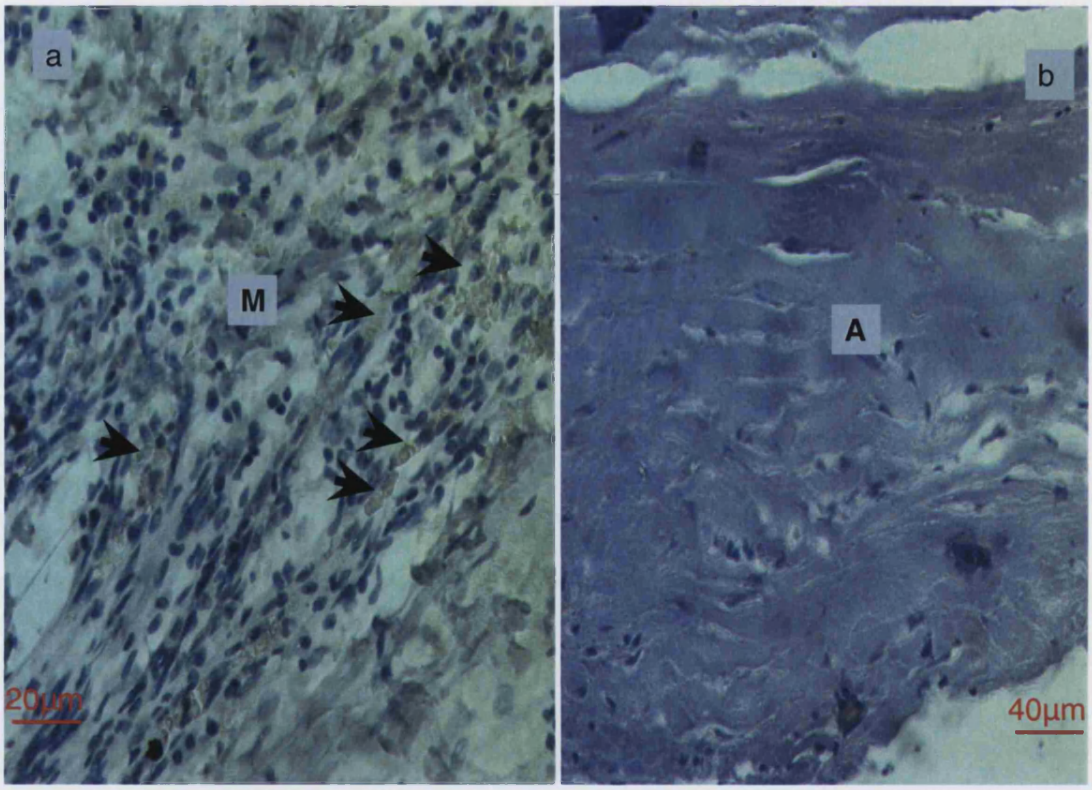

Figure 6.13 Immunohistochemical staining for OPG. Picture a shows *tunica media* (M) and picture b shows *tunica adventitia* (A) in cross section. Arrows indicate positive staining. Negative controls of staining were done but are not shown here.

6.4.2 Protein expression in normal aortae

Isolated protein from 12 normal aortae was subjected to dot blots. Most normal aortic vessel walls (90%) express TRAIL-R1, 64% express TRAIL and 54% express OPG. A normal aorta sample with atherosclerosis only expresses OPG. Both normal aortae whose ages are 15 and 24 year old respectively, express TRAIL and TRAIL-R1 but no OPG.

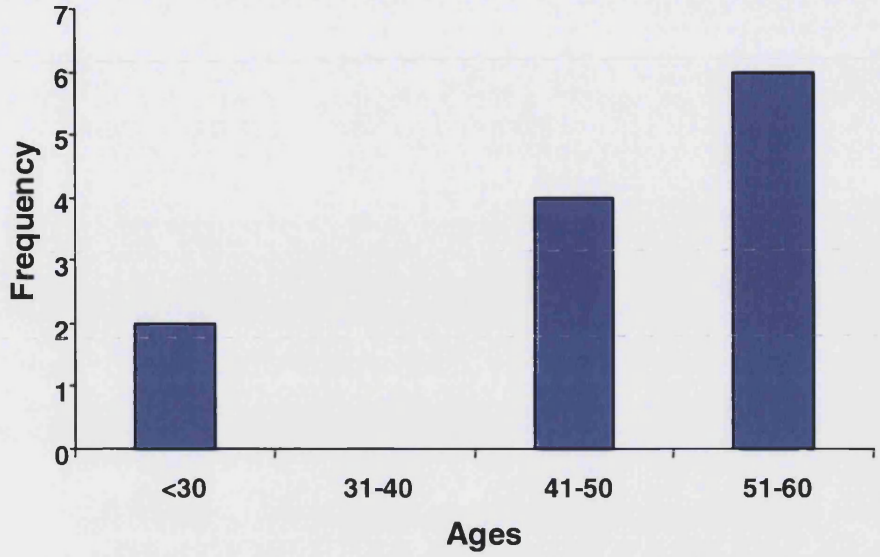

Figure 6.14 shows frequency distribution histogram of donor age of normal aortae examined. Most patients were aged from 50-60-year old including one with atherosclerosis. Two patients were aged younger than 30-year old.

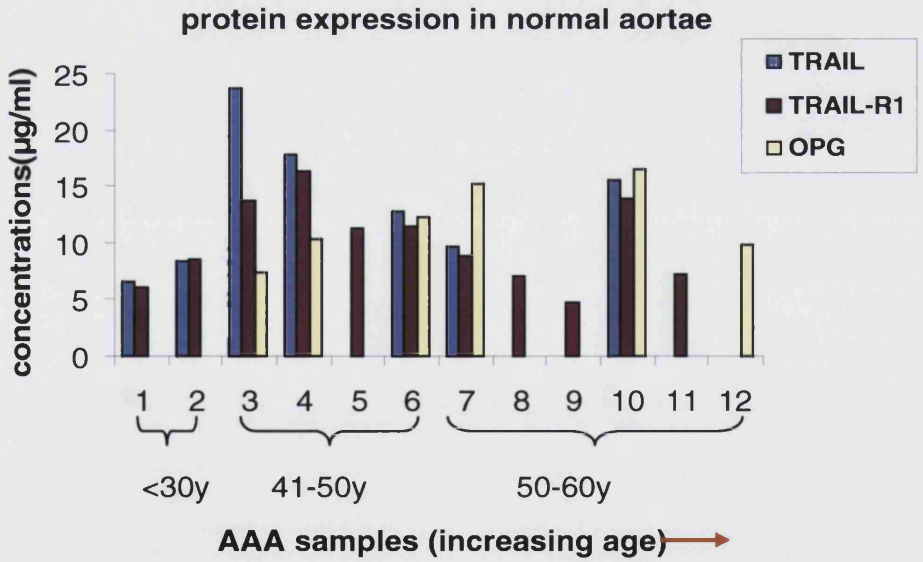

Figure 6.15 The summary graph of protein expression in normal aortae (n=12) in the order of donor ages (Figure 6.14). Every group of bar series represents a sample. TRAIL-R1 was expressed the most often and OPG was expressed half of the vessels. The last normal aorta (sample 12) was the one with atherosclerosis. There is no correlation was found between ages of AAA donor and concentration of protein expression.

Combining the age with protein expression in normal aortae, youngest age group only express TRAIL, TRAIL-R1 but no OPG. Oldest age group only express TRAIL-R1 or OPG excluding one expressing all three proteins. The middle age group express all three proteins and in relatively higher abundance compared to the other two groups. This was shown in Figure 6.15.

6.4.3 Protein expression in AAA

Following graph shows concentrations of protein expression in normal aortae and AAAs. No significant difference was found. More protein was expressed in normal aortic walls than in AAAs.

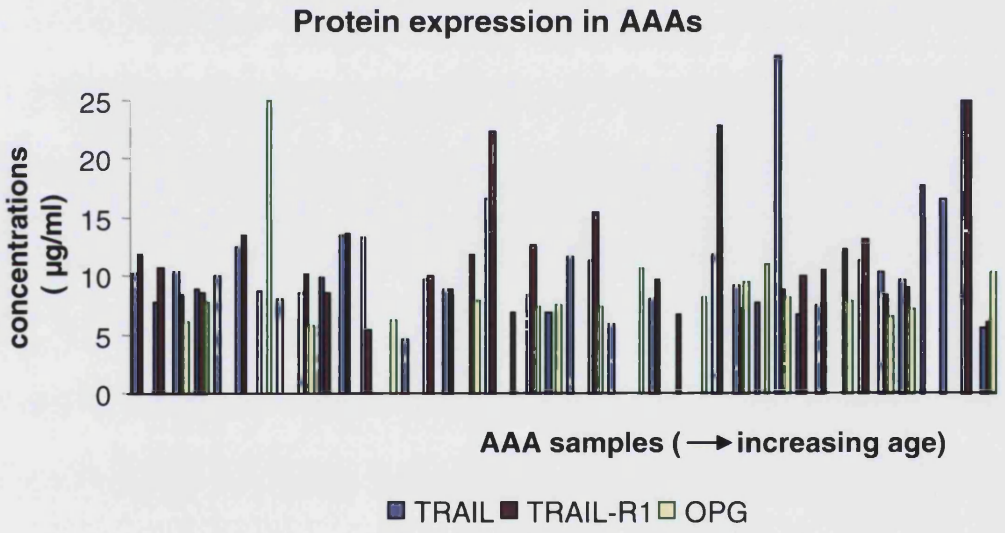

Figure 6.16 This diagram indicates the level of normalised total protein expression for TRAIL (blue), TRAIL-R1 (pink) and OPG (green) in 42 AAA samples. The sample was arranged according to the order of the age of donors for AAA. No certain pattern was found. However, the diagram shows clearly that significantly more TRAIL-R1 protein was expressed than OPG protein in AAAs (p<0.01, paired t test, confidence >95%). TRAIL was expressed at a similar level to TRAIL-R1. They were weakly correlated (r=0.35). In contrast, TRAIL was expressed at a significantly higher than OPG (***p<0.001, by two tailed t test).**

6.4.4 Protein expression correlated with the diameters of AAA size

Abdominal aortic aneurysms were subclassified into two categories according to their diameters. This classification is based on three stages of AAA progression: development, growth and rupture. These three stages correlate with the diameter of AAA (Maeda T, 1996). Since all the AAA specimens were obtained from elective surgeries, the diameter is above 50mm. The average AAA size of patients is 6.7 cm from 01/1990-06/2001 in Royal United Hospital, Bath. The diameters of sample AAAs were between 5cm and 8.3cm (mean diameter 6.5 ±1 cm). Thus, the samples are representative.

Accordingly, AAA diameters smaller than 69mm and greater than 50mm were considered as AAA at the growth stage. Aneurysm diameters greater than 69mm were considered as AAA at the final stage.

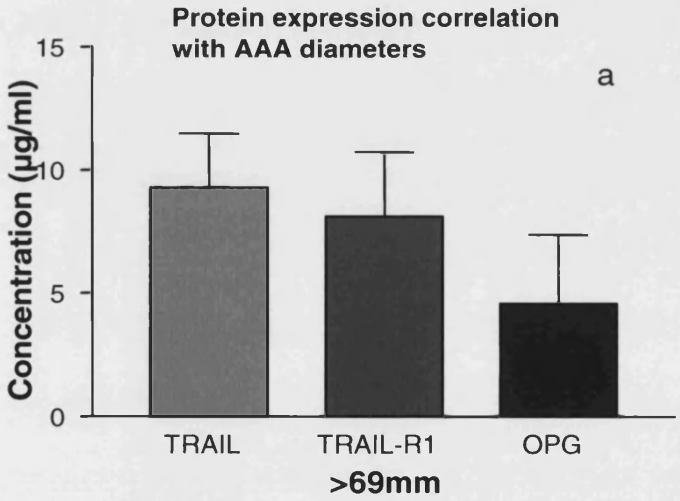

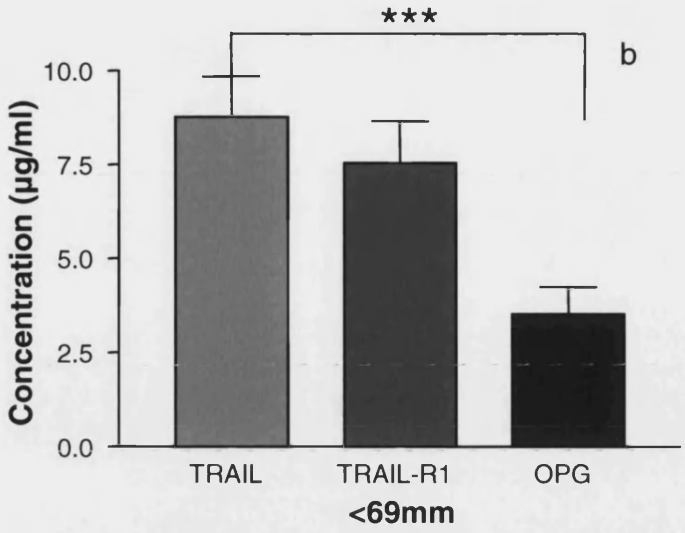

Figure 6.17 TRAIL, TRAIL-R1 and OPG protein expression in AAA. Panel a indicates their expression in the group whose diameter is greater than 69mm (n=7) and panel b indicates their expression in the group whose diameter is less than 69mm (n=19). The same trend was found in both groups that TRAIL was expressed the most and OPG was expressed the least. TRAIL was expressed significantly higher than OPG in the group with a diameter of less than 69mm. The top of the bar represents standard error.

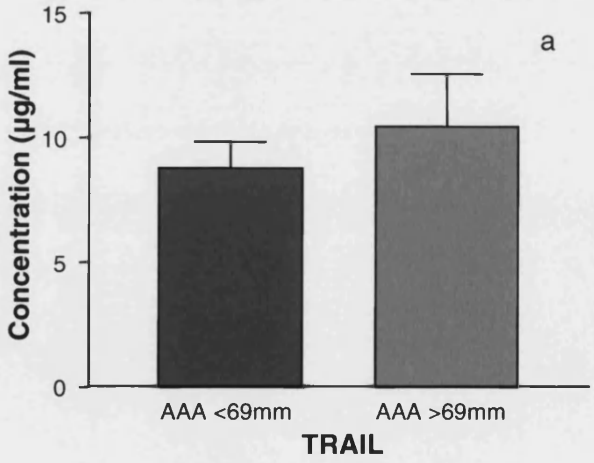

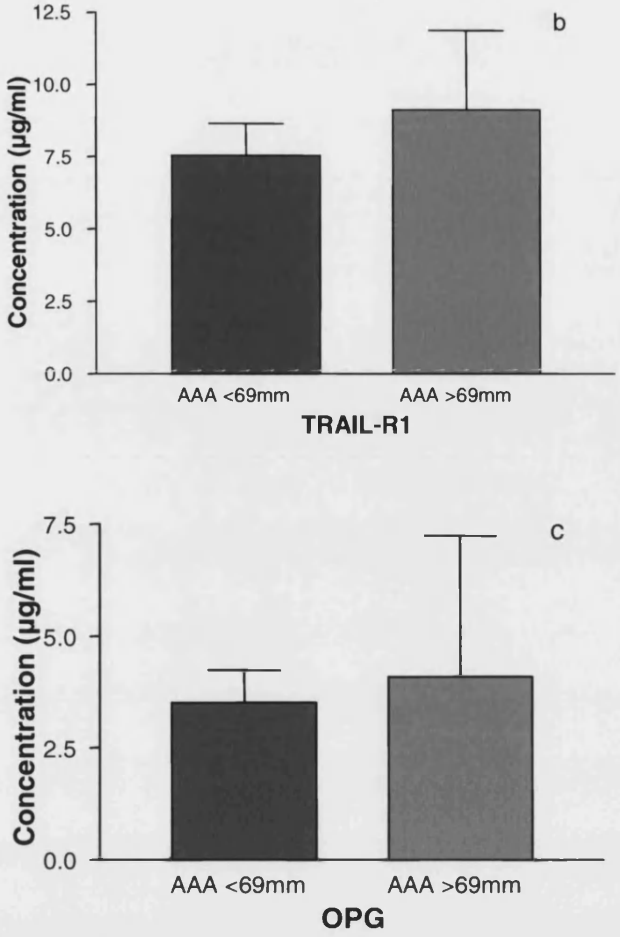

Figure 6.18 These graphs illustrate protein expression levels in AAA. Graph a shows the protein expression for TRAIL in both AAA groups. Graph b shows protein expression for TRAIL-R1 in both AAA groups. Graph c shows the protein expression for OPG in both AAA groups. No significant difference in expression of these 3 proteins in either AAA groups. There is a tendency that all three of them increase as the diameters increase. The top of the bar represents standard error.

6.4.5 Comparison of protein expression between normal aortae and AAA

6.4.5.1 Frequency of protein expression in normal aortae and AAAs

Comparing protein expression in normal aortae and AAA, more AAA vessels expressed TRAIL than normal aortic vessels. Fewer AAA vessels expressed TRAIL-R1 and OPG than normal aortic vessels.

Frequency of protein expression in normal aortae & AAA

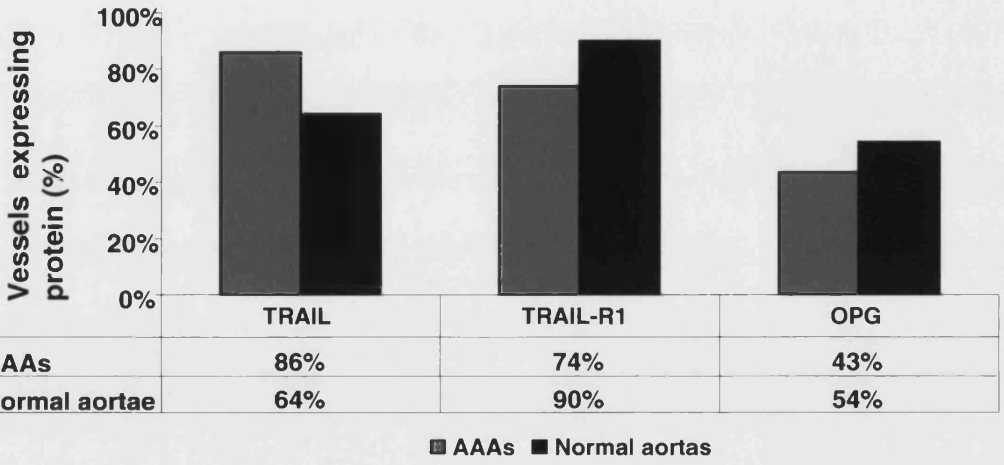

Figure 6.19 The graph illustrates the frequency of protein expression in 11 normal aortae and in 42 AAA vessel walls. TRAIL was expressed more often in AAAs than in normal aortae, and TRAIL-R1 and OPG were expressed in fewer AAA than normal aortae. There is, however, no significant difference between the frequencies of expression of protein.

Proteins for TRAIL and TRAIL-R1 were widely expressed in the AAAs and normal aortae while mRNA for both of them was only detected in approximately 50% of vessel walls.

As was suggested in the last chapter, TRAIL-R1 dominated initially in AAA formation and the mRNA expression for TRAIL and OPG is perfectly correlated. Hence, the concentration of proteins for OPG could represent the effect of apoptosis inhibition. Comparing proteins expression for TRAIL, TRAIL-R1 and

OPG in normal aortae (n=11) and AAAs (n=42), significant differences were found between normal and abnormal aortae (*p<0.05, using a one-way ANOVA test, confidence >95%). The normal aorta with atherosclerosis was not included as a normal control in this comparison.

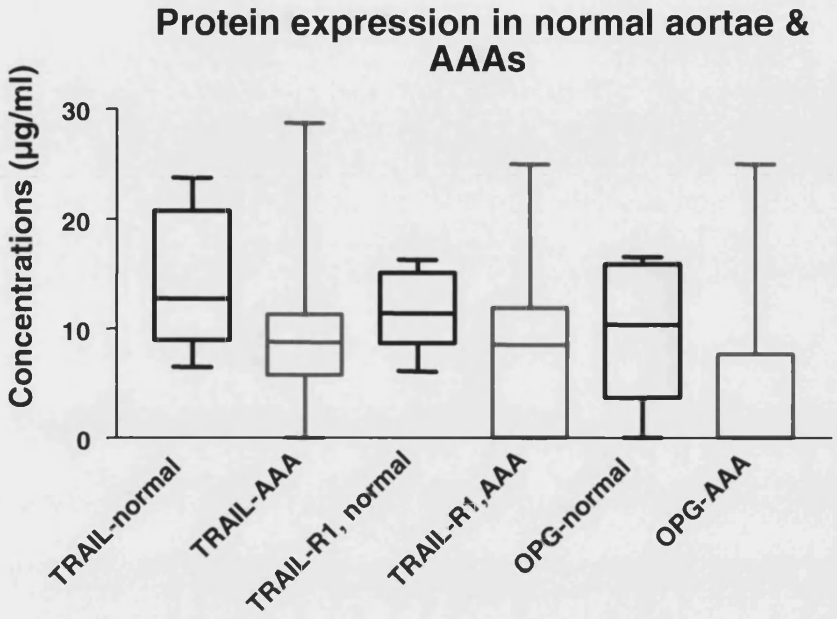

Figure 6.20 Summary box and whisk graphs of protein expression in normal aortae and aneurysm. More TRAIL, TRAIL-R1 and OPG were expressed in normal aortae than in AAAs.

6.4.5.2 Concentration of protein expression in normal aortae and AAA

The expression of TRAIL protein was greater in the AAA but less TRAIL-R1 and OPG were expressed in the AAA compared to normal aortae. This is compatible with the mRNA results that TRAIL is upregulated in the AAA tissue and its receptors are downregulated.

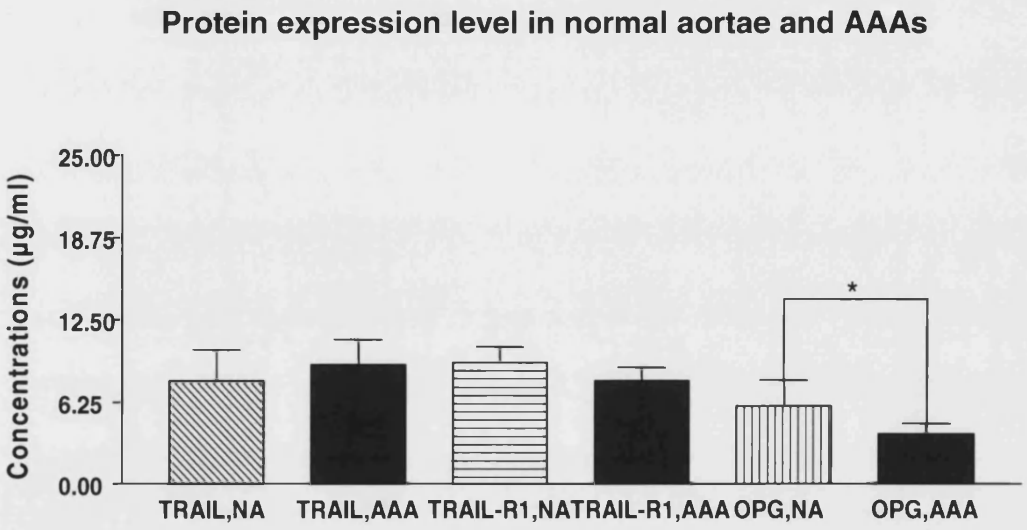

Figure 6.21 The graph shows that TRAIL, TRAIL-R1 and OPG were expressed in the normal aortae and AAAs. The same tendency was observed here as TRAIL was expressed the most and OPG was expressed the least in both normal aortae and AAA. More TRAIL was expressed in the AAA but TRAIL-R1 and OPG were expressed less in the AAA compare to in the normal aortae. Significant difference was found of OPG protein between normal aorta and AAA. OPG was found to be significantly expressed higher in the normal aortae. NA refers to normal aortae. (*P< 0.001, one-way ANOVA test, confidence> 95%). The top of the bar represents standard error.

6.4.6 The correlation between Calcification Score and protein

As shown in chapter 5, CT scans demonstrate that the proximal is the least calcified area and the distal is the most calcified area in AAA. Figure 6.22 demonstrates that this is irrespective of AAA diameter.

AC score correlation with different AAA locations

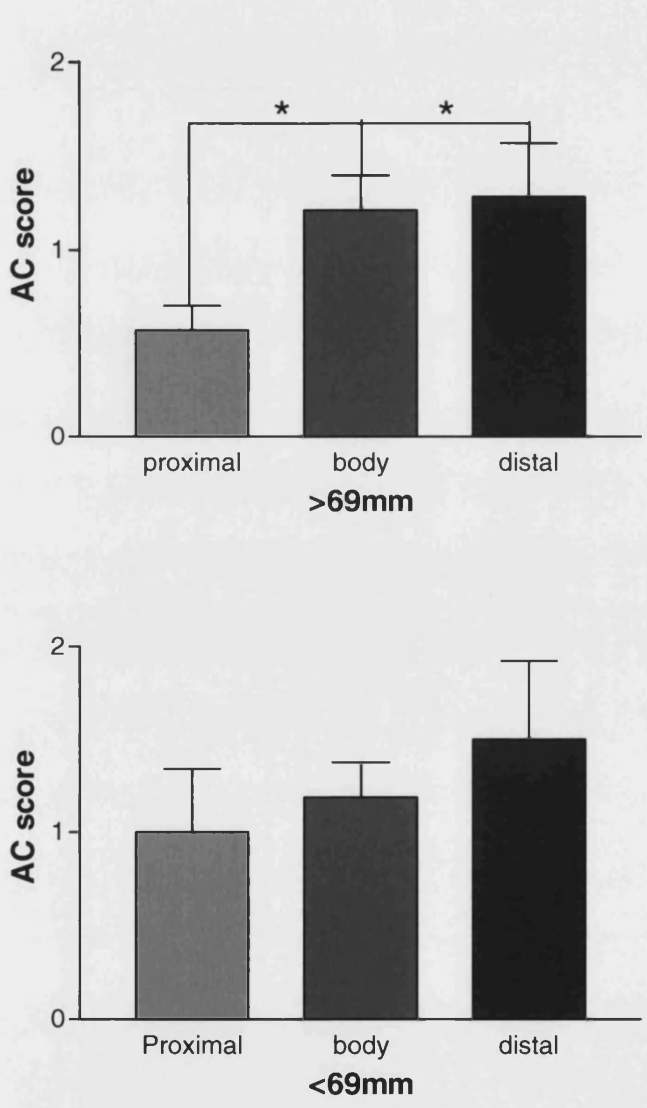

Figure 6.22 AC score correlation with proximal, body and distal AAA area in different AAA diameters' groups. Figure a shows AC score in AAA whose diameter is greater than 69mm (n=7) and figure b shows AC score in AAA whose diameter is smaller than 69mm (n=19). These graphs clearly show that distal is the most calcified area and proximal is the least calcified area irrespective of diameter. (*p<0.05) The top of the bar represents standard error.

Sufficient evidence exists showing that OPG is expressed in calcified vessel walls (Dhore *et al.*, 2001) but there is no study about TRAIL and TRAIL-R1 protein expression in the vessel wall. Thus it is worth exploring their expression in the three areas under examination (proximal, body and distal) to draw a better conclusion.

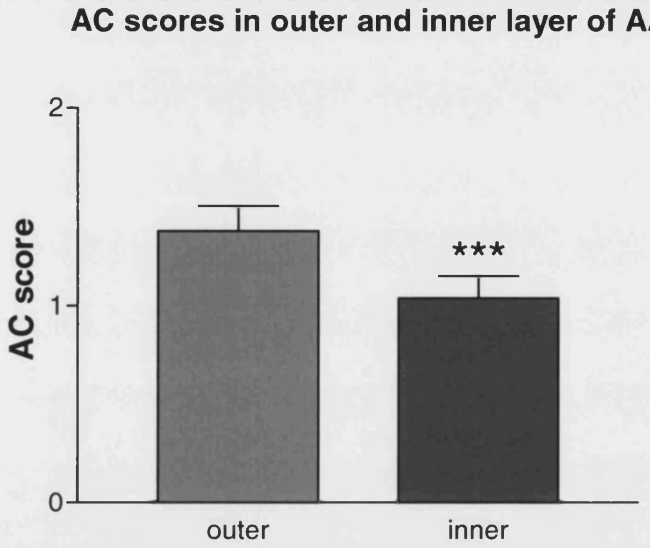

Figure 6.23 AC score of outer and inner layer of AAAs. Inner layer of AAA is significantly less calcified than outer layer of AAAs (*p<0.0001, paired t test, confidence >95%). The top of the bar represents standard error.**

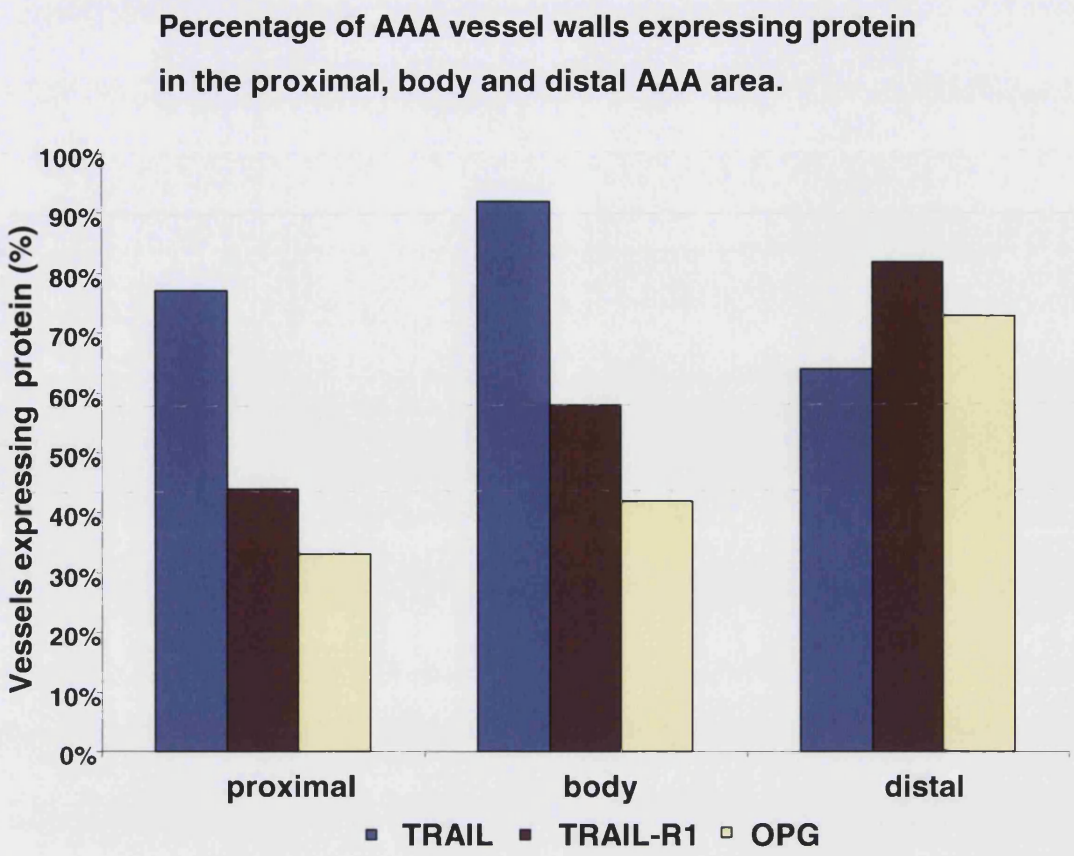

Figure 6.24 This graph shows the frequency of protein expression in proximal, body, distal AAAs (n=42). More vessels in the AAA express TRAIL-R1 and OPG protein as the area becomes more calcified (body and distal region), while the body area expresses the most TRAIL and the distal area expresses the least TRAIL. This is consistent with mRNA expression findings.

6.4.7 Concentration of protein expression in different areas of AAA walls

Protein concentration in proximal, body and distal AAA

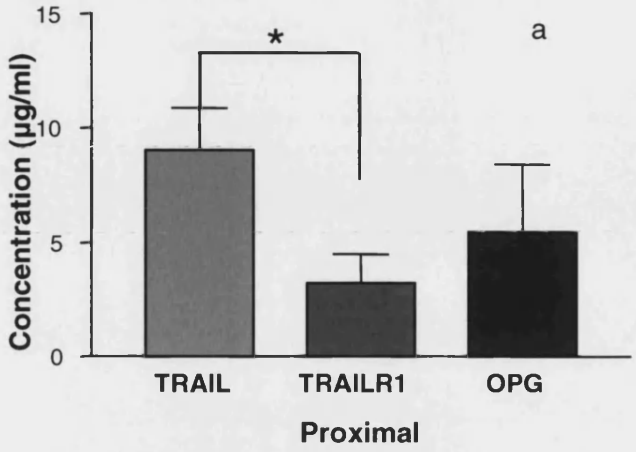

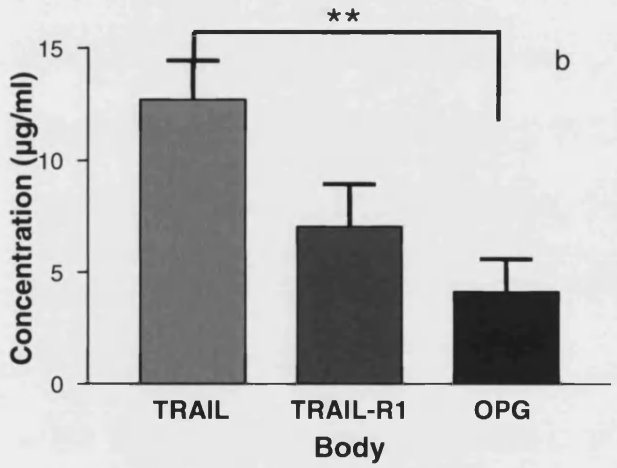

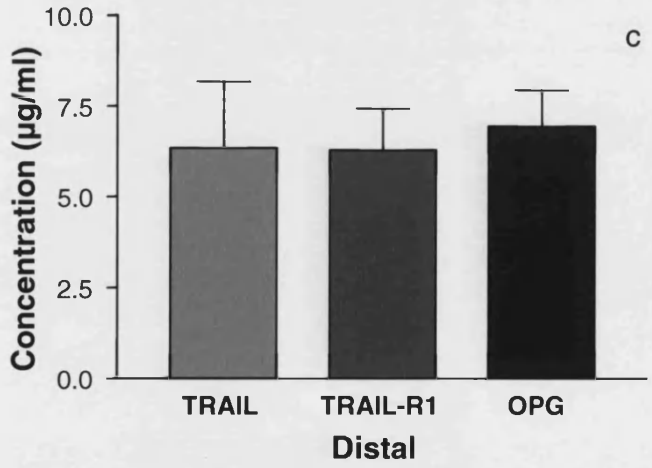

Figure 6.25 show TRAIL, TRAIL-R1 and OPG protein expression in proximal (n=9), body (n=11) and distal area (n=12) in AAA. Graph a shows their expression in proximal AAA. TRAIL was expressed the most and significantly higher than TRAIL-R1. TRAIL-R1 was expressed the least. Graph b shows their expression in body AAA. TRAIL was expressed the most and OPG was expressed the least. Graph c shows their expression in distal AAA. They were expressed very similarly. The top of the bar represents standard error.

The expression of proteins was compared in each AAA region individually. TRAIL, TRAIL-R1 and OPG were spread fairly equally in the distal region. Significant differences were found in proximal and body AAAs, which are considered as processes of ongoing calcification.

Protein levels in proximal, body and distal AAA

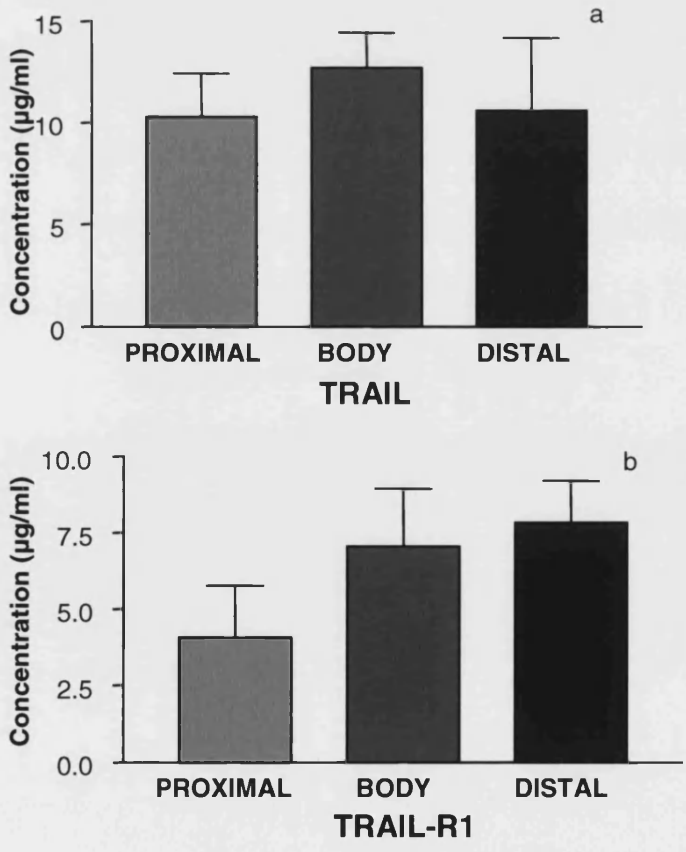

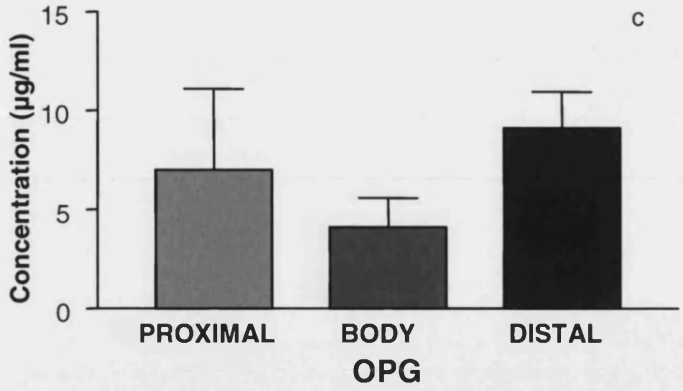

Figure 6.26 TRAIL, TRAIL-R1 and OPG protein expression in proximal, body and distal AAA. Panel a indicates TRAIL expression in these regions. TRAIL was expressed very similarly in all three regions. Panel b indicates TRAIL-R1 expression in these regions. TRAIL-R1 was expressed the most in the distal AAA and the least in the proximal AAA. Panel c indicates OPG expression in distal AAA. OPG was expressed the least in the body AAA and most in the distal AAA. The top of the bar represents standard error.

A similar protein expression for TRAIL was observed in these three regions. Thus, the capacity of the TRAIL-rTRAIL system to induce or inhibit apoptosis depends on TRAIL receptors. TRAIL death receptor (TRAIL-R1) was expressed the most abundantly in the most calcified area (distal AAA). This implies that the potential to induce apoptosis increases in the more calcified AAA. TRAIL decoy receptor (OPG) was expressed the least in the body AAA (enlargement of AAA) and the most profusely in the distal AAA. This entails that OPG was counter-regulated in the most calcified area. Also this suggests that OPG might be competing with death receptors of TRAIL in the body AAA to inhibit apoptosis induced by TRAIL.

The ratios of TRAIL to TRAIL-R1 and TRAIL to OPG were compared with AC score in figure 6.27. There is not any linear regression between the ratios and AC score. This indicates AAA formation is not simply related to the calcification level of vessel walls. It implies a more complex situation that is influenced by the position within the vessel wall.

Ratios (of TRAIL/TRAIL-R1 and TRAIL/OPG) correlations with AC score

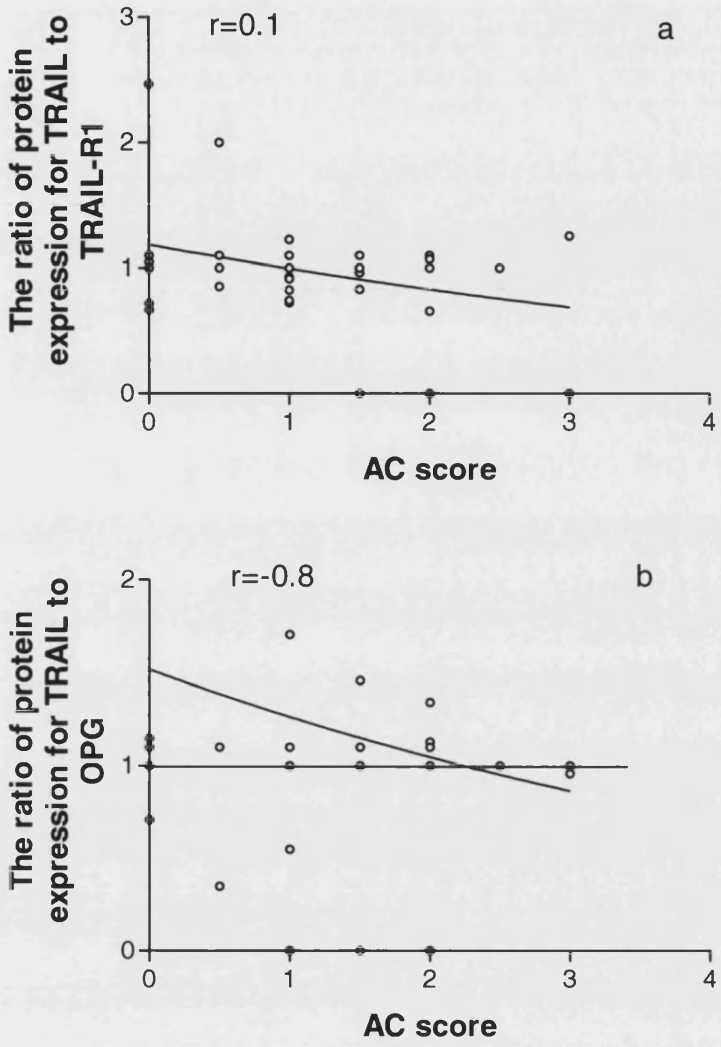

Figure 6.27 Non-linear regression between TRAIL to TRAIL-R1 and AC score; and TRAIL/ OPG and AC score. Panel a indicates non-linear regression between TRAIL to TRAIL-R1 and AC score; and graph b indicates non-linear regression between TRAIL/ OPG and AC score. TRAIL was expressed very similarly in all areas of AAA (see Figure 6.26**), thus TRAIL to TRAIL-R1 indicates the possibility of TRAIL to induce apoptosis. The ratio of TRAIL to OPG indicates the potential of TRAIL to inhibit apoptosis. This indicates that the possibility of intervention by inhibition or induction of apoptosis is reduced when the AC score elevated.**

6.5 Discussion

6.5.1 Protein expression for TRAIL, TRAIL-R1 and OPG in normal aortae

All normal aortae were obtained with informed consent from Bristol Southmead Hospital. Considering the age difference of the specimen donors, no OPG was expressed in younger age group (<25 year old) and in 70% vessel walls of older age group (>40 year old). This agrees with the finding of higher OPG expression in the old than in the young (Hak *et al.*, 2000; Jono *et al.*, 2002). Very imbalanced distribution of the three proteins was found in the age above 50. This might imply that more apoptosis occurs in the elderly.

6.5.2 Protein expression for TRAIL, TRAIL-R1 and OPG in AAA

Osteoprotegerin (OPG), a decoy receptor of TRAIL discovered in 1997, can inhibit osteoclast maturation to protect from osteoclast remodelling (Simonet *et al.*, 1997). Increasingly evidence suggests the involvement of OPG in vascular disease. It has been identified in human carotid stenosis (Golledge *et al.*, 2004), and serum levels of OPG have been found to be positively correlated with the onset and severity of atherosclerotic artery disease (Erdogan *et al.*, 2004b; Jono *et al.*, 2002; Nitta *et al.*, 2003). It was also found to be distributed around calcification areas associated with inflammatory cells and vascular SMC (Moran *et al.*, 2005).

When TRAIL, TRAIL-R1 and OPG expression was compared on AAA walls, TRAIL and TRAIL-R1 were expressed at very similar levels (weak positively correlated), but OPG is expressed significantly less than either (weak negatively correlated). A recent study suggests that OPG protein may be down-regulated in calcified arteries, whereas the expression of transcription factors that regulate mineralisation and osseous differentiation programs, and the up-regulation of osteogenic genes such as alkaline phosphatase, bone sialoprotein, or bone GLA protein in vascular smooth muscle cells in the course of medial calcification has

been demonstrated (Dhore *et al.*, 2001). This is compatible with the finding that OPG expression is less than TRAIL and TRAIL-R1 in the AAA.

The potential morbidity of an aneurysm increases with increasing size. Larger aneurysms are more prone to rupture and cause life-threatening complications. Serum OPG was found to be correlated weakly with aneurysm growth rate (Moran *et al.*, 2005). Aneurysms were analysed after sub-classification into two groups according to AAA diameter. TRAIL-R1 protein was expressed more often in the AAA group with bigger AAA than in the other group. This implies that TRAIL might influence the disorder of elastin metabolism and participate in both stages of AAA formation. Osteoprotegerin protein was expressed along with TRAIL-R1. Overall, TRAIL and its receptors show greatest expression in the larger aneurysm group (diameter greater than 69mm, see **Figure 6.17**). This suggests a possible correlation between TRAIL and its receptors with aneurysm size that warrants further investigation.

6.5.3 The comparison of protein expression between normal aortae and AAA

The reason for analysing the frequency of protein expression is to ascertain the difference between their absence and presence. More TRAIL was expressed than OPG in AAAs. Interestingly, TRAIL-R1 and OPG were expressed on fewer AAA vessel walls than normal aortae. This finding is consistent with mRNA expression. However, only 50% of AAA vessels expressed TRAIL-R1 mRNA but more AAA vessels expressed TRAIL-R1 protein. Firstly, this could be because protein dot blot used is more sensitive for detecting TRAIL-R1 protein than RT-PCR used for mRNA detection. Secondly, protein might last longer than mRNA post *mortem* even though the tissue was strictly snap-frozen after being transferred to the laboratory to minimise destruction by proteinase inhibitors. Finally, it could be because mRNA was already transcribed into protein at the analysis stage. Therefore, less mRNA was found than protein for TRAIL-R1 in AAA.

6.5.3.1 Concentrations of protein expression in normal aortae and AAAs

There are differences in TRAIL, TRAIL-R1 and OPG levels between normal aortae and AAAs. According to **Figure 6.21**, TRAIL was expressed higher in AAA and TRAIL was expressed less in AAA than normal aorta. OPG was significantly higher in the normal aorta compare to AAA. This is consistent with discoveries of mRNA detection and demonstrates that TRAIL, TRAIL-R1 and OPG contribute to AAA formation.

Osteoprotegerin was found to be expressed higher in the age-matched AAA tissue (n=5) than in aortic occlusive disease (n=10), thoracic aorta (n=10) undergoing coronary artery bypass graft (CABG) and normal aorta (n=5) (Moran *et al.*, 2005). The findings in this project do not agree with this. More OPG was expressed in normal aortae (n=11) than in AAA (n=42). Three factors could be responsible for this. Firstly, a much smaller number of AAA was examined in the Moran *et al.* studies than in this study. Secondly, thoracic aorta begins at the lower border of the fourth thoracic vertebra and ends in front of the lower border of the twelfth at the aortic hiatus. Abdominal aorta follows it and ends on the body of the fourth lumbar vertebra dividing into the two common iliac arteries (Gray H., 1918). Anatomically, the normal aorta sample used in this project is closer to AAA. Previous finding in chapter 5 between umbilical artery and normal aorta suggests that different vascular bed may express the TRAIL system differently. Finally, greater age difference of normal aorta samples and AAA in this project could be a reason of these opposite findings. The average age of normal aorta donors in this project was 46±13 and that of AAA was 76±7 while the age was matched in Moran *et al.* study (65±6). Taken together, these findings may imply that OPG is upregulated from the young to the older (around 60-year old) and downregulated after seven to eight decades of life. It may also imply that OPG is downregulated while the AAA diameter gets bigger and reaches the certain point (average 6.5±1 cm) since AAA is an increasing dilation of the abdominal aorta.

6.5.4 Protein expression in different AAA areas

The observations in comparison of three AAA regions as described in chapter 5 not only indicate that TRAIL, TRAIL-R1 and OPG proteins were expressed in the atherosclerotic lesion of human aorta but also, more importantly, show that the magnitude of TRAIL-R1 expression increases in proportion to the stage of atherosclerosis. TRAIL-R1 was expressed the most in distal AAA and the least in proximal AAA. TRAIL was expressed similarly in all areas. This confirms the hypothesis that as a death receptor, TRAIL-R1 induces apoptosis to initiate calcification in AAAs. As a decoy receptor, OPG was expressed the least in body AAA and the most in distal AAA, suggesting that OPG might protect cells from apoptosis in a protective manner in body AAA and reactive manner in distal AAA. In addition, the weak negative correlation between calcification level (determined by AC score) and the ratios of TRAIL to OPG and TRAIL to TRAIL-R1 indicated TRAIL-R1 and OPG increase when calcification level increases. This is partly consistent with serum OPG correlation with AAA growth rate.

7.

Chapter 7 Apoptosis in AAAs

7.1 Introduction

7.1.1 Apoptosis in aneurysm smooth muscle cells

Apoptosis has been observed in rat SMCs *in vitro* (Bennett *et al.*, 1994), cultured human SMCs (Bjorkerud *et al.*, 1994) and in remodelling of sheep arterial walls (Cho *et al.*, 1995). Smooth muscle cell disappearance and extensive apoptosis were also found to co-localise in the medial layer of advanced saccular cerebral aneurysms in rats. In addition, apoptosis-affected SMCs frequently appear in the medial layer of pre-aneurysms or early aneurysms in the rat model of saccular cerebral aneurysms (Kondo *et al.*, 1998). Particularly, these changes were at the distal site of the aorta where the aneurysmal changes started. More apoptotic cells were detected while apoptosis was at an early stage rather than at a later stage. The aneurysm body develops from the early stages of aneurysm formation often the late stages of aneurysm established the proximal area of the aneurysms. In another words, this indicates that apoptosis primarily occurs in the body of aneurysms before they enlarged.

Furthermore, since SMCs have been found going through all the stages of apoptosis, this demonstrates that they undergo apoptosis during the complete formation of aneurysm (Thompson *et al.*, 1997). The role of apoptosis in SMCs in *tunica media* of aneurysm has not been clearly elucidated but the above evidence provides support for apoptosis involvement in the formation of aneurysm in animal models.

7.1.2 Apoptosis within the human abdominal aortic aneurysms

Human aneurysm, similarly to animal aneurysm, is a progressive weakening of the aortic wall. Aorta dilates gradually to form AAA and normally it is asymptomatic until the aneurysm eventually ruptures. Important pathological features of AAA include calcification of the vessel wall (Halloran and Baxter, 1995), medial lamellae degeneration (Zatina *et al.*, 1984), accelerated collagen turnover (Satta *et al.*, 1995) and decreased medial SMC density (Zhang *et al.*, 2003; Lopez-Candales *et al.*, 1997).

As mentioned in chapter 3, elastic content and elastic fibre structure and production of elastin-degrading proteinases contribute to altered human aortic wall tone. The tensile strength, resiliency and completeness of the vessel wall normally depend on the elastin and collagen on the arterial wall and these two components' failure will cause aneurysm rupture (Thompson *et al.*, 1997). Therefore, aneurysm could be a consequence of endothelial cells in the aneurysm acting as a mechanosensor perceiving increased wall shear stress. Internal elastic lamina degeneration. Smooth muscle cells are reported to synthesise and secrete connective tissue matrix, including elastic tissues (Ross, 1971). Thus, a reduction in SMCs number would result in medial layer vessel wall thinning. Both changes could contribute to increasing aortic wall stress.

Apoptotic cells were also observed in the human AAA and display all stages of apoptosis characterisation. Especially these cells were SMCs in the medial layer of AAA. Therefore, apoptosis might participate to the degeneration of AAA.

Molecular apoptotic marker (P21) was also documented to be observed between AAA and normal aorta (Thompson *et al.*, 1997). Medial SMCs were found to express FAS in aneurysm tissue. This confirms apoptosis might alter SMC to precipitate the AAA formation. TRAIL, like FASL is a member of TNF family and capable of inducing apoptosis. Significant difference of TRAIL and its death receptors were discovered between normal aorta and AAA in the last chapter. It is highly likely that TRAIL and its death receptors might also participate in AAA formation. However, the question of co-localisation of TRAIL and apoptosis in the aneurysm wall has not been elucidated, further investigation is therefore needed.

7.1.3 Smooth muscle cells in AAA

The vascular SMC is the most abundant cell type in the medial layer of human aortae. The SMC layer confers the strength and elasticity of the aortic wall. They are important in controlling vascular tone and the disruption of their integrity is a factor in the formation of aneurysms. They also can synthesise proteins such as collagen, elastin and laminin, which compose the extracellular matrices of the *tunica media* (Cheuk and Cheng, 2005).

The vascular SMCs fail to protect and repair injury to critical load bearing matrix structures in the aortic wall. The elastic lamina is broken down and the SMC layer appears disorganised (Cheuk and Cheng, 2005) which might respond to the products of atherosclerosis (Cohen *et al.*, 1992). Ultimately these processes result in the instability of the aortic wall and subsequent formation of AAA.

It is well documented that SMC migrate from the *tunica media* to the *tunica intima* in the early AAA. This could be a key process of atherosclerosis. Also apoptosis occurring in the SMC could result in the weakness of atherosclerotic plaque (Chan *et al.*, 2005). In addition, those cells with osteoblastic characteristics, producing all the major components of osteoid, have been isolated from the vascular media (Bostrom, 2001).

Thus it is imperative to understand the characterisation of SMC in the AAA wall and interaction of TRAIL in the SMC.

7.1.4 Terminal deoxynucleotidyl transferase biotin-dUTP nick end labelling (TUNEL) assay introduction

Numerous histological methods are used to detect apoptosis of different stages. Typical assays include Annexin-V binding, caspase enzyme activity, TUNEL assay and DNA gel electrophoresis. Annexin-V binding assay can separate necrotic cells from those undergoing apoptosis. Caspase enzyme assay can determine which stage of apoptosis may be occurring in cells. As mentioned in chapter 3, DNA becomes fragmented in pieces of 200bp or less length in the process of apoptosis at final stage. These DNA fragmentations are very easy to be visualised by agarose gel or TUNEL assay.

TUNEL assay uses terminal deoxynucleotidyl transferase (TDT) to transfer biotin-dUTP to those strand breaks of cleaved DNA to detect apoptotic cells. It is one of the commonly used methods to detect the late stage cells undergoing apoptosis. Also it is the most popular method which can be used in tissue sections (Hawkins *et al.*, 1997). TRAIL induces apoptosis by caspase-dependent pathways, which involve late dissipation of the mitochondrial membrane potential

and cytochrome c release that follows activation of caspase-8 and caspase-3 and induction of DNA fragmentation (Thomas *et al.*, 2000). The AAA samples obtained from selective surgeries were considered to be at a mature stage. They were theorised to be at the late stage of apoptosis if there was any expression. In addition, they were preserved in the form of paraffin sections. According to the limitation of AAA samples and storage of specimens, TUNEL assay was used to identify apoptosis. In another words, the most reliable technique in detecting the extent of apoptosis in tissue sections would most likely be combining the two techniques based on apoptotic morphology and specific labelling of apoptotic DNA and TUNEL assay is the most appropriate assay for this study (Anna-Kaisa Eerola, 2000).

Large numbers of DNA fragments appearing in apoptotic cells results in a multitude of 3'-hydroxyl termini in the DNA. It can be used to identify apoptotic cells by labelling the 3'-hydroxyl ends with directly conjugated fluorescent-deoxyuridine triphosphate nucleotides (FITC-dUTP). TDT catalyses a template independent addition of deoxyribonucleoside triphosphates to the 3'-hydroxyl ends of double- or single-stranded DNA with either blunt, recessed or overhanging ends. Non-apoptotic cells do not incorporate significant amounts of the FITC-dUTP owing to the lack of exposed 3'-hydroxyl DNA ends. The apoptotic cells in tissue sections can be identified by the biotin-labelled cleavage sites which are detected by reaction with HRP conjugated streptavidin and visualised by DAB showing a brown colour under LM (Chemicon international., 2006).

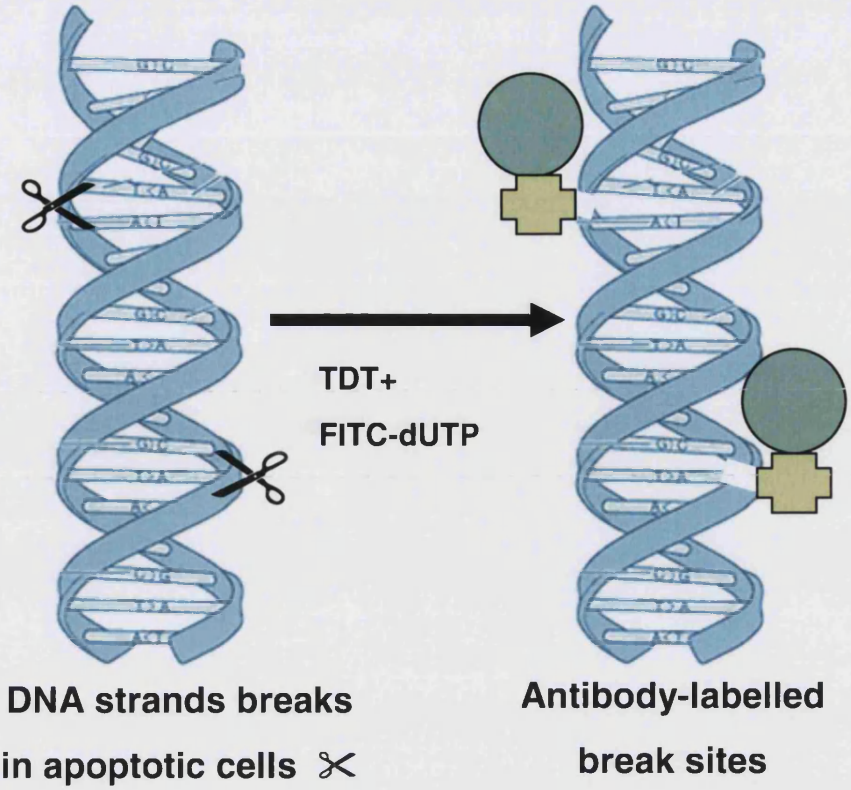

Figure 7.1 Diagrammatic representation of the addition of FITC-dUTP catalysed TDT to the 3'-OH sites of DNA breaks. The DNA strand breaks are detected by enzymatically labelling the free 3'-OH termini with modified nucleotides. The new DNA ends that are generated upon DNA fragmentation are typically localised in morphologically identifiable nuclei and apoptotic bodies.

7.1.5 Alternative apoptosis cellular marker introduction

Human FLIP, known as an inhibitor of caspase 8 (FLICE), caspase 10 or FADD, is an inhibitor of extrinsic apoptosis pathway. FLIP has four splice variants, α, μ, γ and κ. They contain two death effector domains and one caspase domain and compete with mediating apoptosis caspase to inhibit apoptosis (Hu *et al.*, 1997). Molecular weights of these four splices are variable from 28 kDa to 58 kDa. To confirm apoptosis is involved in AAA formation it would be interesting to investigate the presence of FLIP.

7.1.6 Indicator of smooth muscle cells and atherosclerosis

Smooth muscle actin, α-actin, is one of few gene which is strictly expressed in vascular smooth muscle cells. It is altered by cell proliferation, and pathological conditions such as atherosclerosis (Reddy *et al.*, 1990).

Smooth muscle heavy chain (SMHC) isoform has two types of clones, SMMS-1 and SMMS-2 which were first isolated by Nagai *et al.* (1989). It has been found that SMMS-1 was expressed more selectively in aorta than SMMS-2 during early normal vascular development and in experimental arteriosclerosis and atherosclerosis development (Kuro-o M *et al.*, 1989). Intimal smooth muscles diminished the expression of both isoforms of SMHC, whereas α-actin was well preserved during the progression of atherosclerosis. Hence, SMMS-1 and SMMS-2 are important molecular markers for studying human vascular smooth muscle cell differentiation as well as the cellular mechanisms of atherosclerosis. Furthermore SMMS-1 is an important cell marker for the study of development of atherosclerosis in aortae (Aikawa *et al.*, 1993).

7.2 Aims and objectives

- To determine whether apoptosis is in the AAA tissue
- To determine how much apoptosis occurs in AAA
- To determine whether the TRAIL-rTRAIL system expresses in the human cultured SMC
- To determine whether atherosclerosis is localised in the AAA tissue

7.3 Materials and methods

7.3.1 Terminal deoxynucleotidyl transferase biotin-dUTP nick end labelling (TUNEL) assay materials and methods

- Aqueous mounting medium for fluorescence with DAPI, Vector Laboratories Ltd, Orton Southgate, Peterborough, UK
- Protease K, Sigma-Aldrich Co Ltd, Poole, UK,
- Internal apoptosis positive control, ApopTag kits, CHEMICON Europe, Ltd., UK
- Zeiss fluorescence microscope, Carl Zeiss Inc., USA

Normal aorta and AAA tissue samples were stored in 10% formalin for 24 hours and then deparaffinised. The tissue sections were cut into 4-5 µm slides and pre-treated with Protease K for 15 minutes at room temperature. The slides were washed twice in PBS for 2 minutes each followed by applying 75µl/ $5cm^2$ equilibration buffers for at least 10 seconds at room temperature. Then 55µl/ $5cm^2$ working strength TDT enzyme was applied on each slide and incubated in a humid incubator at 37°C for 1 hour. These slides were then immersed into the working strength stop buffer to end the reaction. After agitation for 15 seconds, slides were incubated for 10 minutes at room temperature. They were washed three times in PBS for 1 minute each. Subsequently, 65µl/ $5cm^2$ warm working strength antidigoxigenin conjugate was applied to the slides. The slides again were incubated in a humid incubator for 30 minutes at room temperature. Final wash was carried out by rinsing with PBS four times for 2 minutes each. An aqueous mounting medium containing DAPI mount (2 drops) was used and slides were finally visualised under a microscope by DAPI (wavelength 350-400nm) (Chemicon international., 2006).

Internal positive control, AAA samples and internal negative controls (AAA slides without exposing to TDT enzyme) were performed according to the above protocol. Samples sizes were around $5mm^2$ since TUNEL was proved to be very

sensitive to small size sample fixation (Labat-Moleur *et al.*, 1998). Images were viewed using a FITC filter in Zeiss fluorescence microscope or LM. The desired area of analysis is located visually by using the camera on the Zeiss microscopy. Scan area are set and the scan initiated using 10X and 40X objective magnification. Negative control tissue was used to define the false-colour assignments. Ten contiguous fields per slide were chosen randomly and the number of apoptotic cells was manually counted because the background colour of slides made automated counting problematic. Apoptotic index (AI) was determined.

AI= (number of TUNEL-positive cell nuclei/ total number of cell nuclei) %

7.3.2 Calcification detection

Various techniques are used to characterise biological mineralisation in intact tissues and cell cultures including the von Kossa staining method, CT scan and fourier transformed infrared spectroscopes (FTIR). A study demonstrated that Von Kossa staining alone is not an appropriate way to identify and quantify bone-like mineral (Bonewald *et al.*, 2003), therefore, this was used to verify the presence and location of calcium deposition.

7.3.3 Von Kossa staining materials and methods

- Aqueous safranin O, Sigma-Aldrich Co Ltd, Poole, UK
- IMS, Sigma-Aldrich Co Ltd, Poole, UK
- Silver nitrate, Sigma-Aldrich Co Ltd, Poole, UK
- Sodium thiosulphate, Sigma-Aldrich Co Ltd, Poole, UK
- DePeX mounting medium (DPX), BDH laboratory supplies, Poole, UK

Paraffin-embedded sections were cut into 4-5µm thickness slices. These slides were soaked with water, and then treated with a 5% silver nitrate solution (25mg silver nitrate in 500ml distilled water). The slides were exposed to strong light for 45-60 minutes to let the silver deposit by replacing the calcium. Then they were washed with distilled water and treated with 3% sodium thiosulphate for 5

minutes followed by washing with water. Counterstain in 0.5% aqueous safranin O for 60 seconds. Finally dehydrate slides with 95% and 100% IMS in the order and amount slides in DPX. Slides were ready to be visualised as metallic silver under the LM. The calcium deposition was shown in black, cytoplasm was shown in pink and nuclei were shown in red.

Normal aorta tissue, negative control for each AAA slides (staining without sliver nitrate) and AAA sample were followed above protocol.

7.3.4 Haematoxylin and Eosin (H&E) staining

- Acid Alcohol 1%: 70% Alcohol 99ml + conc. Hydrochloric Acid 1ml
- Eosin powder: Sigma-Aldrich Co Ltd, Poole, UK
- Mayer's Haemotoxylin, Sigma-Aldrich Co Ltd, Poole, UK
- DePeX mounting medium, BDH laboratory supplies, Poole, UK

Deparaffinsed sections were placed in haematoxylin for 5 minutes followed by washing in running water for 5 minutes. Then slides were placed in 1% acid alcohol for 60 seconds. Slides were washed in running water again for 5 minutes and thereafter were immersed in eosin (eosin Y (Yellowish): 1.0g + Distilled Water 100ml) for 5 minutes. After washing in water for another 5 minutes, slides were dehydrated and mounted in DPX.

Slides were viewed under LM to identify blue nuclei, pink cytoplasm, dark pink fibres to distinguish the sections structure.

7.3.5 Smooth muscle cell culture materials and methods

- 6 well plate, Orange Scientific, Belgium
- Acutase, TCS CellWorks Ltd, Botolph Claydon, UK
- Cell dissociation solution, Sigma-Aldrich Co Ltd, Poole, UK
- Dulbecco's Modified Eagle Medium (DMEM), Gibco, Life Tech, Paisley, UK
- Foetal calf serum (FCS), Globepharm, UK

- Hank's Balanced Salt Solution (HBSS), Gibco, Life Tech, Paisley, UK
- L-Glutamine 200 mM, Gibco Life Tech, Paisley, UK
- Penicillin/Streptomycin 10,000 units ml^{-1} Penicillin and 10,000 µg ml^{-1} Streptomycin, Gibco Life Tech, Paisley, UK
- Trypsin EDTA x10 solution, Sigma-Aldrich Co Ltd, Poole, UK

As a consequence, SMCs have been cultured as an *in vitro* model of vascular calcification. They were cultured from abnormal tissue e.g. AAA and normal tissue e.g. umbilical artery and normal aortae as control samples.

It is relatively difficult to extract cells from the *tunica media* in the AAA than in the normal artery because the atherosclerosis plaque composed the majority of the tissue. However, by increasing the foetal calf serum (FCS) concentration to 20%, the cells grow much easier.

Fresh human artery vessel wall tissues were placed into sterile specimen pots containing Hank's Balanced Salt Solution (HBSS) at 4°C immediately for transport and short-term storage. Sterile forceps were used to strip the medial layer of the vessel wall from the intima and adventitia. This was then minced using crossed scalpels and placed in 6-well plates and covered with 1.0 ml of medium (DMEM with 10%-20% (FBS), 1% Penicillin and streptomycin, 1% glutamine). The plate was stored in the humidified 5%CO_2 incubator at 37°C. The medium was changed twice a week while the cells attached firmly to the wells. Cells migrated from tissue and were harvested when they had grown to semi-confluence.

The tissue pieces were removed carefully and cells were retrieved with 0.1% trypsin once growth was seen. The trypsinised cells were suspended, then centrifuged for 10 minutes at 1,200 rpm. The supernatant was removed carefully and the cell pellet plus remaining liquid was transferred to 250ml culture dishes with sufficient medium to cover the bottom of the flask. Flasks were incubated at 37°C about half an hour to allow cells to attach to the bottom firmly. Finally, flask were stored in the incubator at 37°C (Rebecca R.Pauly *et al.*, 1998).

7.3.6 Smooth muscle cells staining materials and methods

- Acetone, VWR International, Poole, UK
- Aquamount, VWR International, Poole, UK
- Fast Red, Sigma-Aldrich Co Ltd, Poole, UK
- PBS (10X), VWR International, Poole, UK
- Lab-tek chamber slide, 8 well on glass, Sigma-Aldrich Co Ltd, Poole, UK
  Mayer's Haemotoxylin, Sigma-Aldrich Co Ltd, Poole, UK
- Methanol, VWR International, Poole, UK
- Negative control Mouse IgG1, DakoCytomation Ltd, Ely, UK
- Smooth muscle cells primary antibody (Mouse Anti-human α-actin antobody), DakoCytomation Ltd, Ely, UK
- VECTA STAIN ABC Kit (Alkaline Phosphatase Mouse IgG), Vector Laboratories Ltd, Orton Southgate, Peterborough, UK

To confirm appropriate SMCs have been cultured, α-actin as a specific antibody for SMCs has been used (Jerareungrattan *et al.*, 2005).

The cells were passaged into chamber slices when cells became confluent. When the cells attached to the bottom of the chamber and became confluent again, staining was performed following the procedure below.

Slices were fixed in ice-cold acetone for 5 minutes then washed with washing buffer (PBS) 3x3minutes. Then they were incubated at room temperature with normal horse serum solution for 20 minutes to block non-specific binding of immunoglobulin. Primary antibody α-actin was incubated with cells at dilution of 1:200, 1:100 and 1:50 for 1.5 hours or overnight at room temperature in the wet box. Chamber slides were rinsed in PBS for 3x3 minutes. Then these slides were incubated with diluted secondary antibody buffer (1 drop in 50µl biotinylated in 10ml PBS) for 30 minutes at room temperature. At the same time, enzyme solution AB (100µl, (2 drops solution A in 10ml PBS, add 2 drops solution B, mix well)) was prepared and left for 30 minutes at the room temperature. The slides were then washed in PBS for 3x3minutes and enzyme solution AB was added to

each slide and incubated for 30 minutes at room temperature. Slides were then washed in PBS again 3x3 minutes. Substrate solution (Sigma fast-red prepared according to manufacturer's instruction manual) was prepared just before incubating slides. Finally, slides were observed under LM to determine end-point (when red stain appears). The reaction was stopped with water, and counterstained with Meyer's Haematoxylin for 2 minutes. Chamber slides were rinsed under running tap water for 10 minutes and covered by coverslip with permanent aqueous mounting medium.

7.3.7 Horseradish peroxidase (HRP) staining materials and methods

- DAB detection kit, Vector Laboratories Ltd, Orton Southgate, Peterborough, UK
- DePeX mounting medium, BDH laboratory supplies, Poole, UK
- Fast red, Sigma-Aldrich Co Ltd, Poole, UK
- Hydrogen peroxidase, Sigma-Aldrich Co Ltd, Poole, UK
- PBS (10X), VWR International, Poole, UK
- Mayer's Haematoxylin, Sigma-Aldrich Co Ltd, Poole, UK
- Negative control Mouse IgG1, DakoCytomation Ltd, Ely, UK
- VECTA Elite STAIN ABC Kit , Vector Laboratories Ltd, Orton Southgate, Peterborough, UK

Sample slides were deparaffinised and rehydrated according to this protocol aligned with negative control and positive control slides. Slides were firstly rehydrated twice in PBS 5 minutes each. They were then incubated with block solution (BSA) for 60 minutes to block non-specific binding of immunoglobulin. The blocking solution was then removed and slides were incubated in diluted primary antibody in the wet box overnight at room temperature. The slides were incubated with hydrogen peroxidase buffer (3% H_2O_2 in PBS) for half an hour at 4°C followed by rinsing twice in PBS for 5 minutes each. These slides were incubated in diluted secondary antibody buffer (1drop in 10ml PBS) after primary antibody for 30 minutes at room temperature. At the same time, enzyme solution AB (100µl, (2 drops solution A in 10ml PBS, add 2 drops solution B, mix well))

were prepared and remained for 30 minutes at the room temperature. Slides were washed twice in PBS for 5minutes each. Enzyme solution AB was added to each slide and left for 30 minutes at room temperature. Slides were washed again twice in PBS for 5 minutes each. Substrate solution (DAB detection kit as instruction manual) was prepared just before incubating on the slides. Finally, slides were observed under LM to determine end-point (when brown stain appears). The reaction was eventually stopped with water. Slides were rinsed with running water and mounted with coverslips with DPX mounting medium.

7.3.8 Apoptosis cellular markers detection

FLIP expression in AAAs

- Rabbit polyclonal anti-FLIP, Abcam plc., Cambridge, UK

FLIP detection was established by immunohistochemistry analysis. Parallel slides of each AAA samples were tested. Normal SMCs were used as a positive control. Rabbit anti-FLIP antibody was used at dilution of 1:50. HRP method was used and DAB was demonstrated as chromogen. These sections were lightly counterstained with haematoxylin and mounted with DPX mounting medium.

7.3.9 Indicator of smooth muscle cells and atherosclerosis (Smooth muscle actin (α-actin) and smooth muscle myosin heavy chain -1 (SMMS-1) expression in AAAs)

- Mouse anti-human smooth muscle myosin heavy chain (SMMS-1) DakoCytomation Ltd, Ely, UK
- Smooth muscle cells primary antibody (Mouse Anti-human α-actin antibody), DakoCytomation Ltd, Ely, UK

The combination of α-actin and SMMS is a good marker of calcification of AAA at the histological level. It is ideal to compare both of their expression in normal

aorta and AAA. However, the difficulty of obtaining fresh normal aortae made this comparison impossible.

The detection of SMC markers was also carried out by immunohistochemistry. Negative control, normal SMCs (a positive control) and parallel slides of each AAA sample were performed. Primary antibodies were diluted of 1:50. Slides were incubated overnight in the wet box. HRP method was used and DAB was demonstrated as chromogen. These sections were lightly counterstained with haematoxylin and mounted with DPX mounting medium.

7.4 Results

7.4.1 Normal and abnormal aorta structure

The H&E stained normal aorta paraffin section showed normal histological structure of vessel wall. As previous detailed in chapter 2, *tunica intima, tunica media* and *tunica adventitia* compose the artery wall. The *tunica intima* is mainly composed of a single layer of endothelial cells, forming the lining of the vessel. The *tunica media* is the middle layer of a blood vessel. It consists of smooth muscle cells and elastic tissue. A continuous layer of elastic tissue forms the boundary between *tunica media* and *tunica intima*, called elastic lamina. *Tunica adventitia* is mostly composed by fibrous connective tissue.

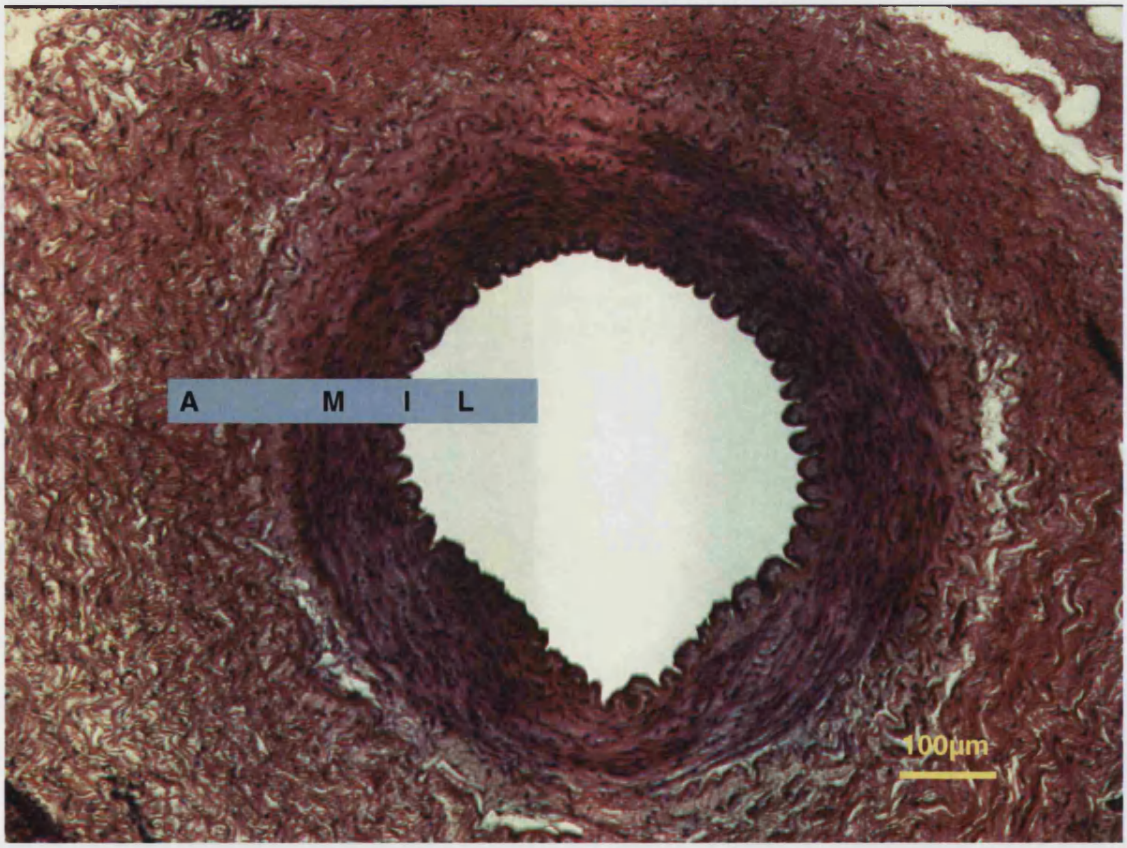

Figure 7.2 Human normal aorta stained by H&E. The slide depicts the typical appearance of normal aorta in cross-section. It has a thick wall and a narrower lumen. Because of the large amount of muscle in the wall, it appears round in cross-section. Note the uniformity of the SMCs in the

***tunica media* (M). L refers to lumen, I refers to *tunica intima* and A refers to *tunica adventitia*.**

Endothelial cytoplasm is inconspicuous even under high power microscopy, but the nuclei are visible at the boundary between the lumen and the wall of a vessel. Smooth muscle cells are well organised into layers.

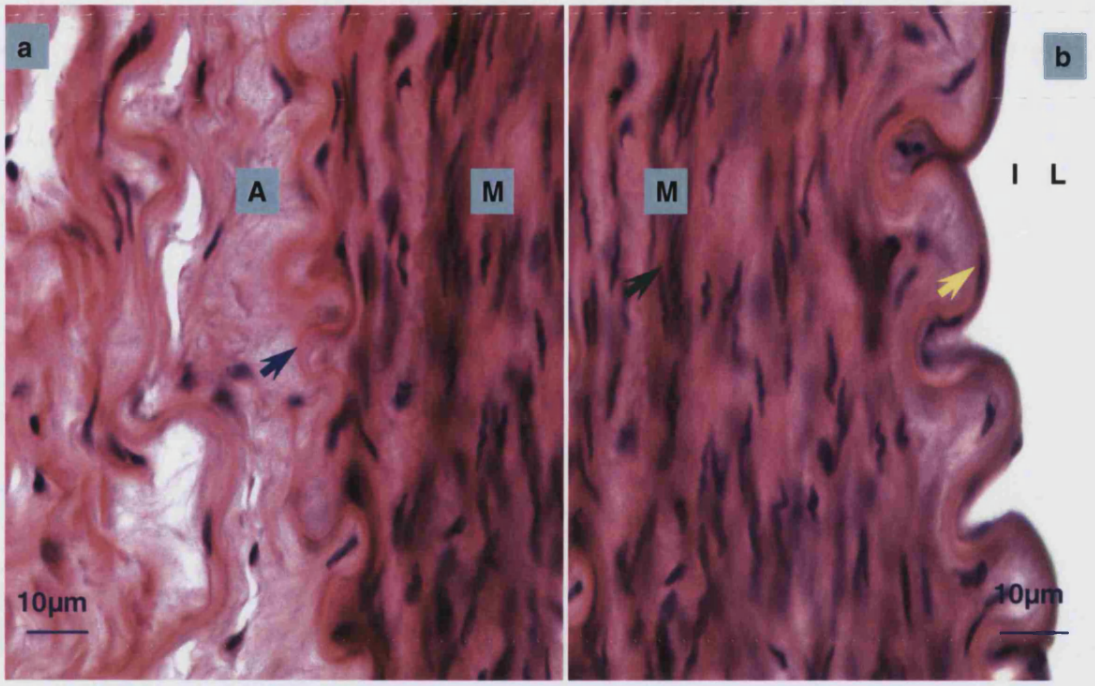

Figure 7.3 Light microscopic appearance of normal aorta by H&E staining under high power microscopy. Picture a shows *tunica adventitia* (A) and *tunica media* (M). Blue arrow indicates elastic fibre. Picture b shows *tunica media* (M) and *tunica intima* (I). Green arrow indicates SMC in the medial layer. Yellow arrow indicates elastic lamina. L refers to lumen

In contrast, cells in AAA sections are disordered as shown in Figure 7.4.

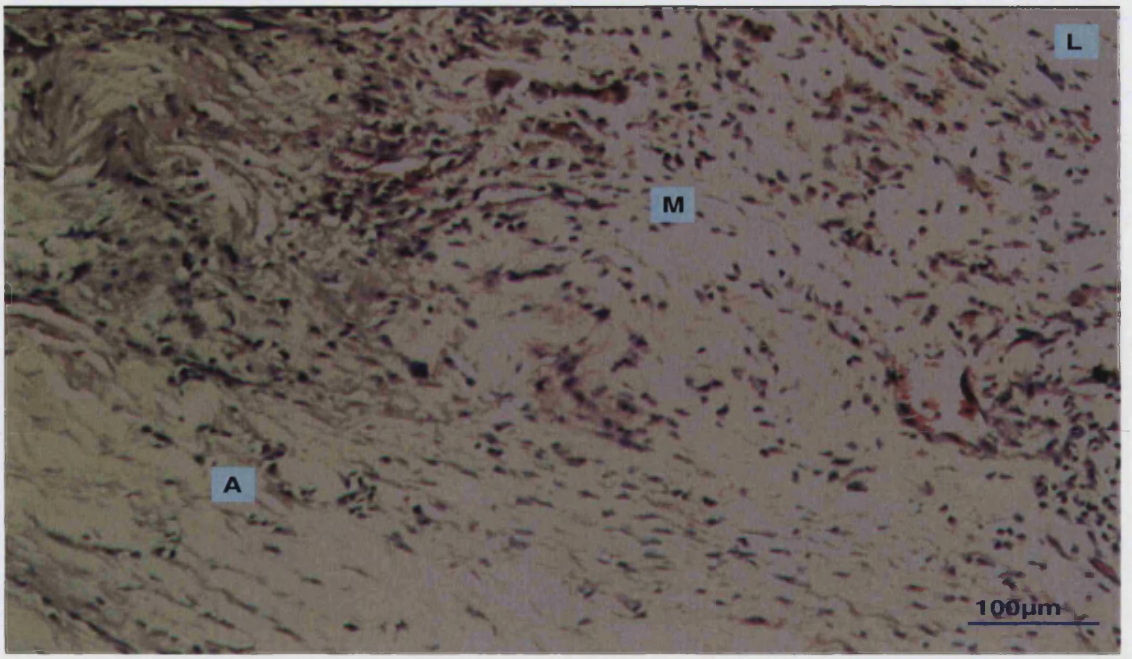

Figure 7.4 Representative photos of AAA paraffin section stained by H&E staining. Smooth muscle cells in *tunica media* (M) display irregular orientation.

High-power photomicrographs of AAA sections stained by H&E clearly demonstrate chaotic arrangement of cells in AAA as shown in Figure 7.5 and Figure 7.6.

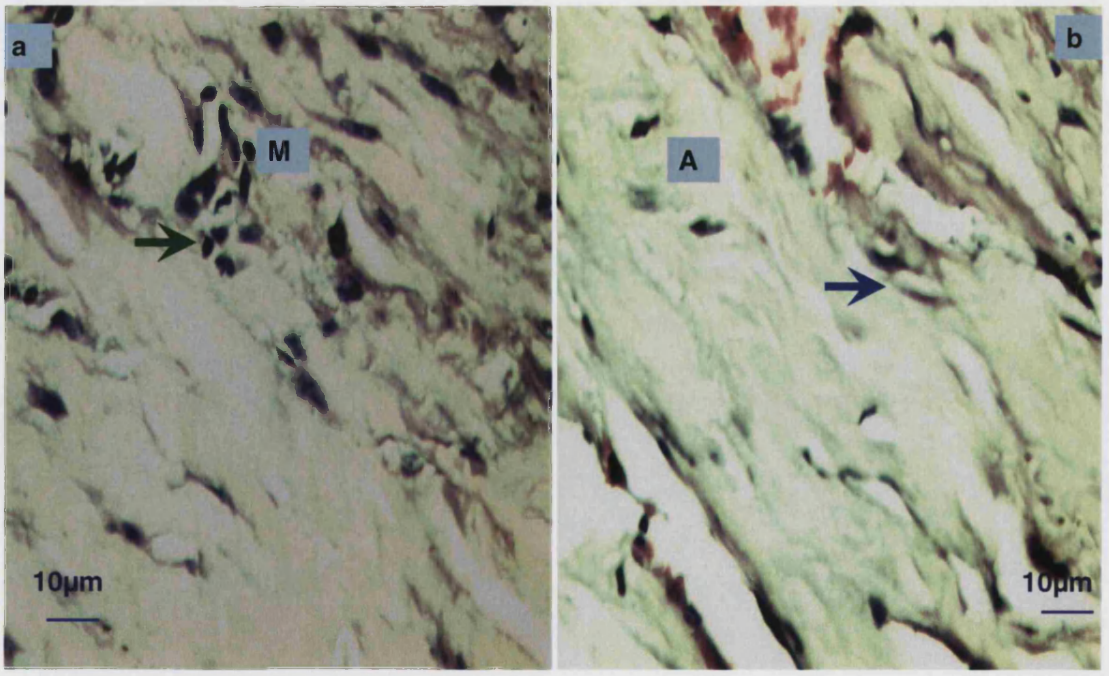

Figure 7.5 Light microscopic appearance of AAA by H&E staining under the high power microscopy. Panel a shows *tunica media* (M). Green arrow indicates SMC as patchy cells crowded together. Panel b shows *tunica adventitia*. Blue arrow indicates elastic fibres. L refers to lumen

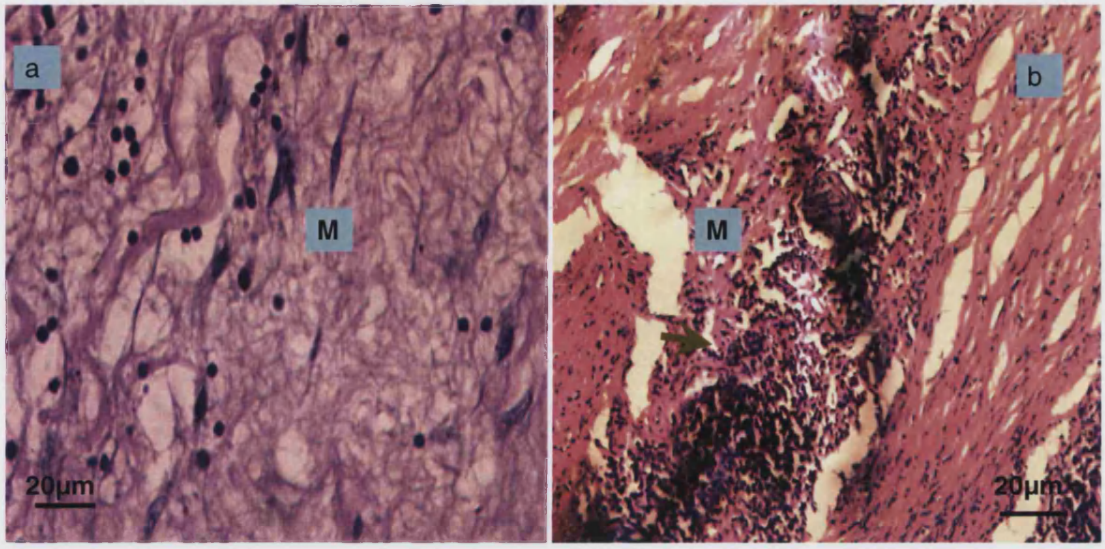

Figure 7.6 Inflammatory AAA sections stained by H&E. Panel a shows smooth muscle cells in the *tunica media* of AAA. Figure b shows dark blue inflammatory cells are scattered within the *tunica media* (M).

7.4.2 Apoptosis in the AAA

Apoptotic cells were confirmed by TUNEL assay shown in Figure 7.2. The unstained slide was purchased as normal control for TUNEL assay. The positive staining shows that apoptotic cells were capable of detection by TUNEL assay.

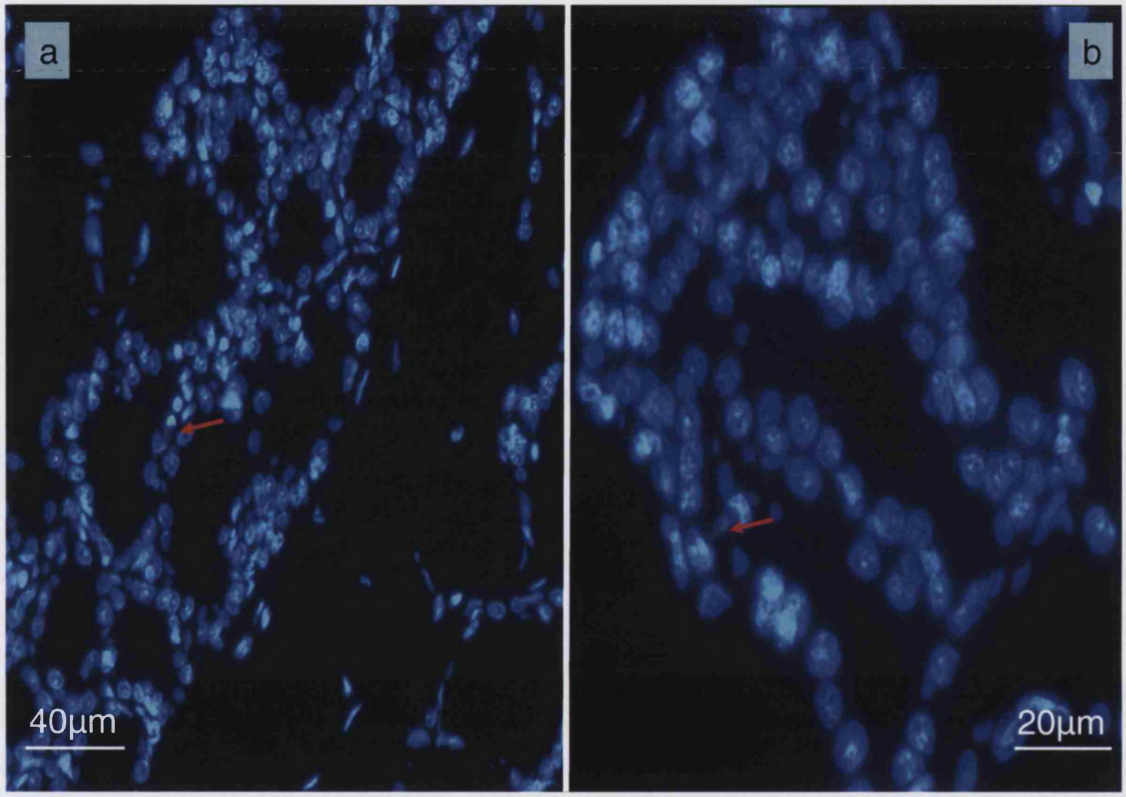

Figure 7.7 External normal control section for TUNEL assay. Five μm-thick section of normal control of TUNEL assay (female rodent mammary gland, purchased from Chemicon), is showing an apoptotic body (red arrows by TUNEL under fluorescence. Panel b depicts the identical field shown in A by higher microscopic power. Apoptotic body (red arrow) is positive stained. As detailed in the Chemicon Apop-tag protocol, 1-2% apoptosis appear in the normal control slides as indicated.

Human normal aortic slides were used as normal aortic control for apoptosis detection in human AAA tissue sections.

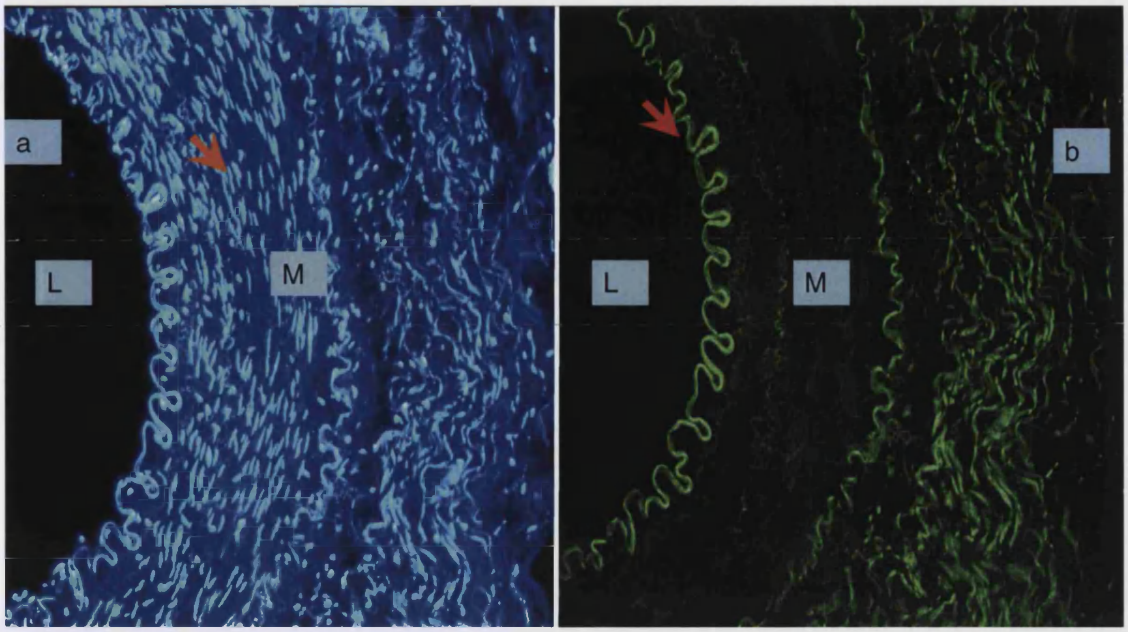

Figure 7.8 Normal aorta section stained by TUNEL assay. Fluorescence microscopic pictures showing normal aorta section stained by TUNEL assay. Picture a was taken under DAPI (wave range 350-400nm) and picture b taken under FITR (wave range 450-500nm). An arrow in picture a indicates smooth muscle cells in *tunica media* of AAA (M). An arrow in picture b indicates elastic lamina in intimal layer of AAA. L= lumen.

Human AAA sections were subjected to TUNEL assay. Figure 7.9 clearly shows thickened intimal wall and disorganised cells in the arterial wall of AAA.

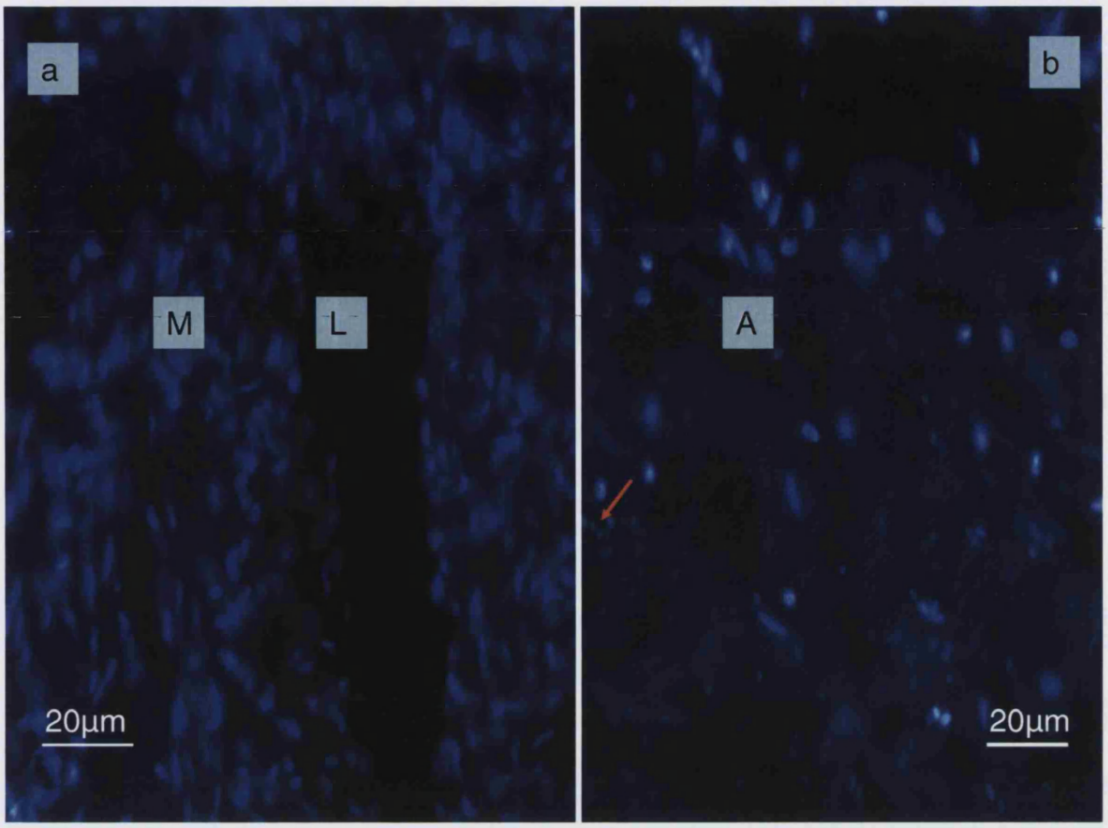

Figure 7.9 AAA section stained by TUNEL assay (low-power). Fluorescence microscopic pictures showing AAA section stained by TUNEL assay. Panel a shows the medial layer of AAA. Panel b shows the *tunica adventitia* layer of AAA. Note the intimal layer is thicker than that observed in normal aorta (Fig 7.3). The red arrow indicates red blood cells without nuclei and having the shape of a biconcave disc.

Positive staining for apoptotic bodies was observed in human AAA tissue section by TUNEL assay in Figure 7.10. More apoptotic cells were detected in the *tunica media* than in the *tunica adventitia.*

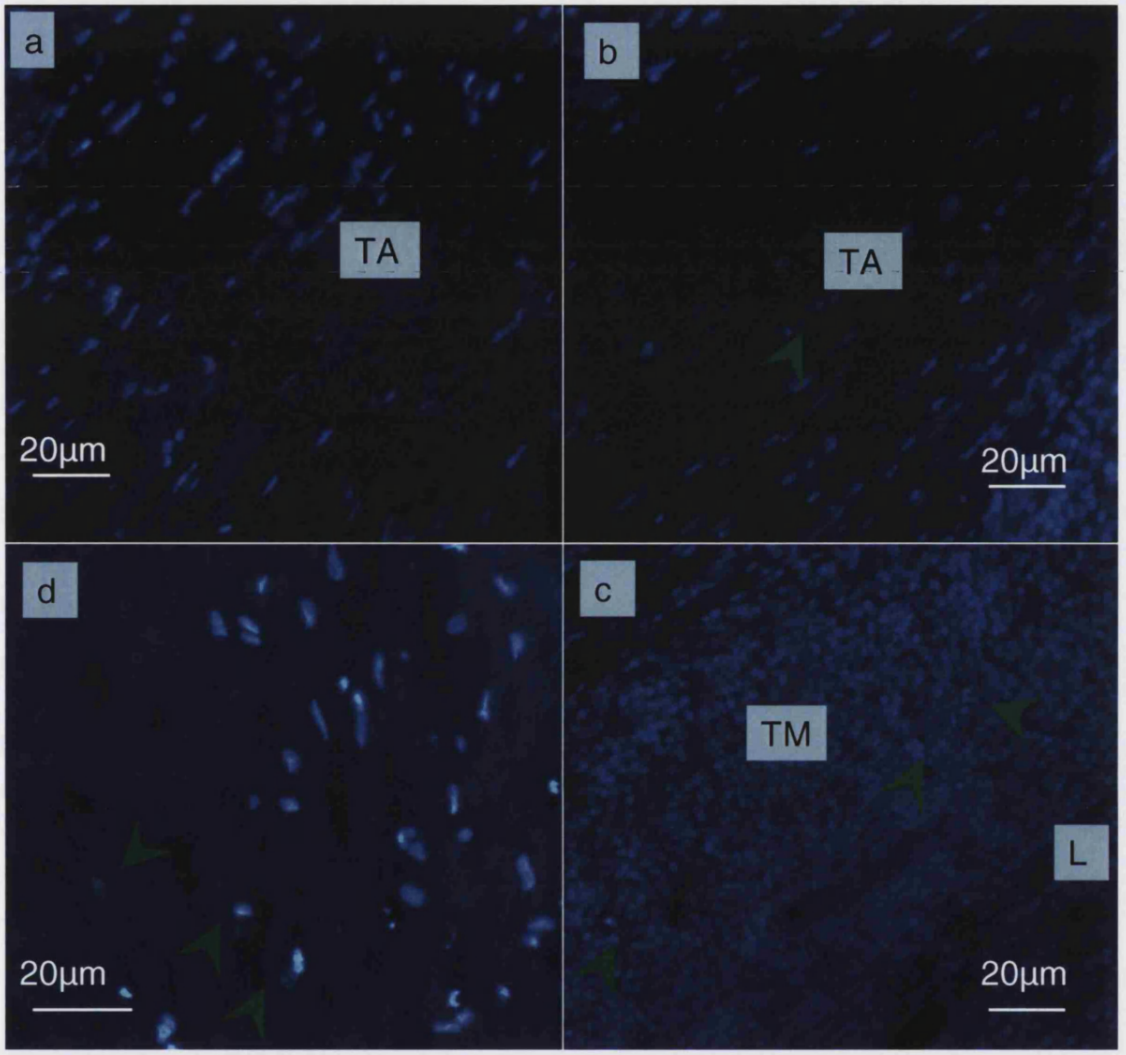

Figure 7.10 Aneurysm tissue stained by TUNEL assay (positive staining). Panel a shows a low-power magnification of *tunica adventitia* (TA). Panel b shows a low-power magnification of *tunica adventitia* (TA) displaying apoptosis (arrows indicate). Panel c shows a low-power magnification of *tunica media* of AAA (TM). Arrows indicate apoptosis. Overall impression from slides reading that more apoptosis is observed in TM than in TA (panel b). Panel d shows a high-power magnification of *tunica media* of AAA. Green arrows indicate apoptotic bodies, showing the greenish particles around the adjacent nucleus. L= lumen

Percentage of apoptotic cells in proximal, body and distal AAA area. More cells can be seen undergoing apoptosis in the body of AAA than in either the proximal or distal regions of AAA. The least number of apoptotic cells were found in the distal area (the most calcified AAA area according to CT scan AC score.

Areas of AAA	AI score (%)
Proximal (n=5)	27%±0.1%
Body (n=10)	37%±2.9%
Distal (n=7)	20%±2.2%

Table 7.1 Percentage of apoptotic cells by region. Twenty to forty percent cells were found going through apoptosis in these areas. The most affected area is the body AAA and the least affected is the distal AAA.

Figure 7.11 reveals the *vaso vasorum* of the AAA vessel walls. The cells in these micrographs are disorganised and their orientation is lost compared with the uniform alignment of cells in the normal aorta wall (Figure 7.8).

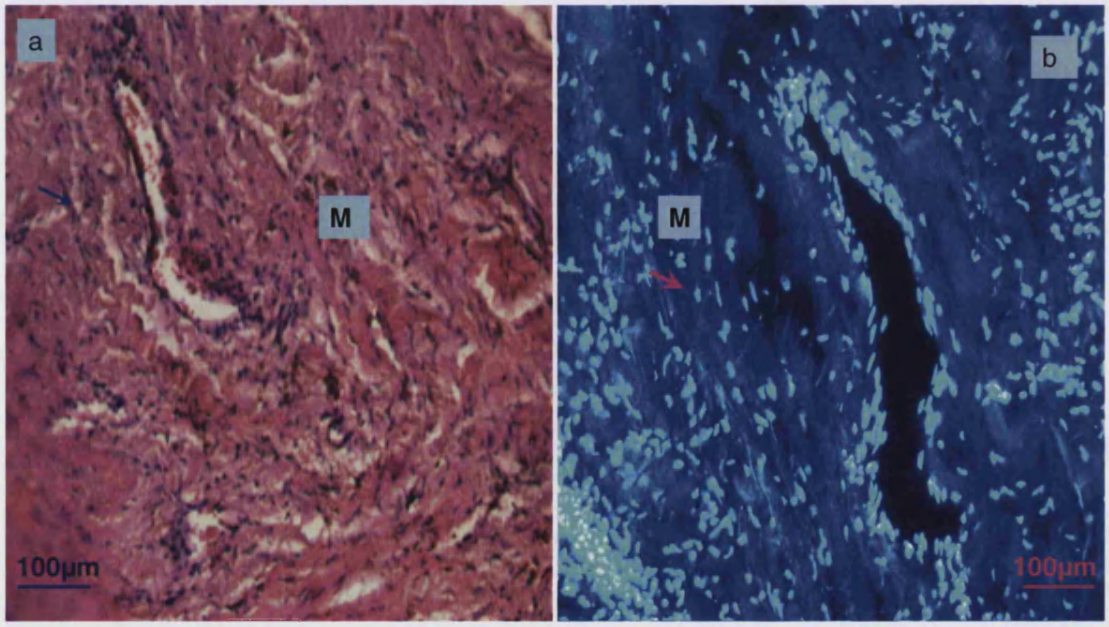

Figure 7.11 Vaso vasorum of aortic wall in AAA section. Consecutive sections of AAA were stained by H&E (a) and TUNEL (b) displaying part of the vaso vasorum inside the AAA wall. No apoptosis was observed. Arrows indicate disrupted structure of the *tunica media*.

Figure 7.12 shows extensive cell loss in the *tunica adventitia* in human AAA section.

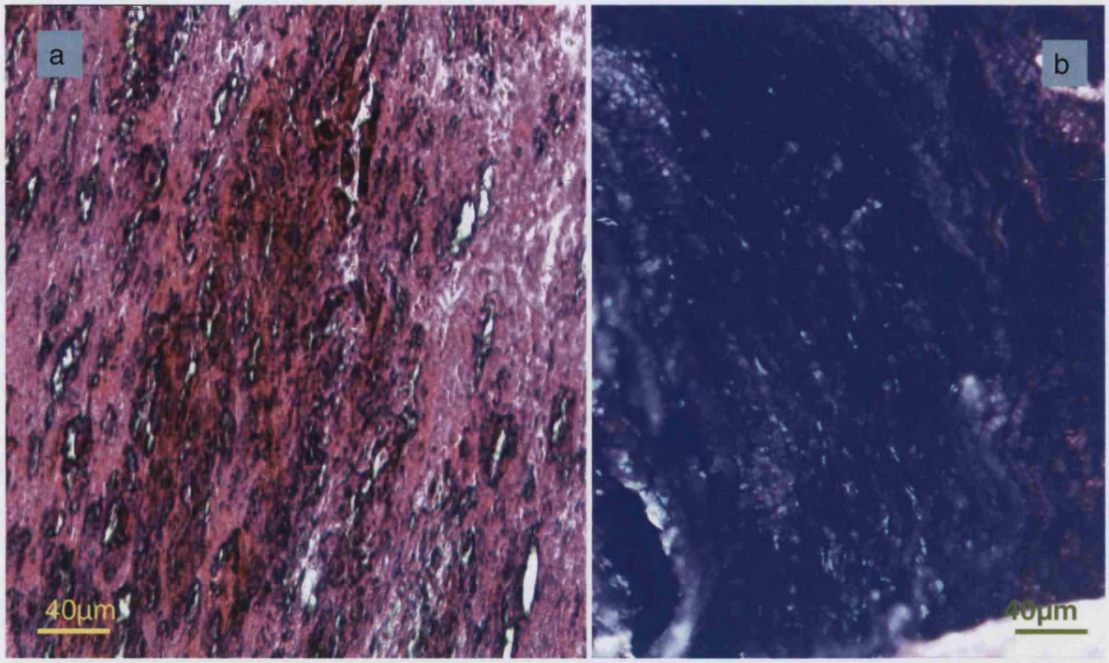

Figure 7.12 *Tunica adventitia* of AAA stained by H&E and TUNEL. Panel a shows H&E stained section demonstrating tissue destruction and cell loss. Panel b depicts a TUNEL stained section showing completely destroyed structure of AAA and very few nuclei.

The structure of AAA veseel wall was destroyed. The number of cells reduced dramatically comparing to normal aorta.

7.4.3 Apoptosis cellular marker

Human FLIP was found in AAA by Vries C. et al. (2000), and this backs up the evidence that apoptosis is localised in human AAA.

Human FLIP as another cellular marker of apoptosis was used to confirm the extent of apoptosis involvement in human AAA formation as shown in figure 7.8.

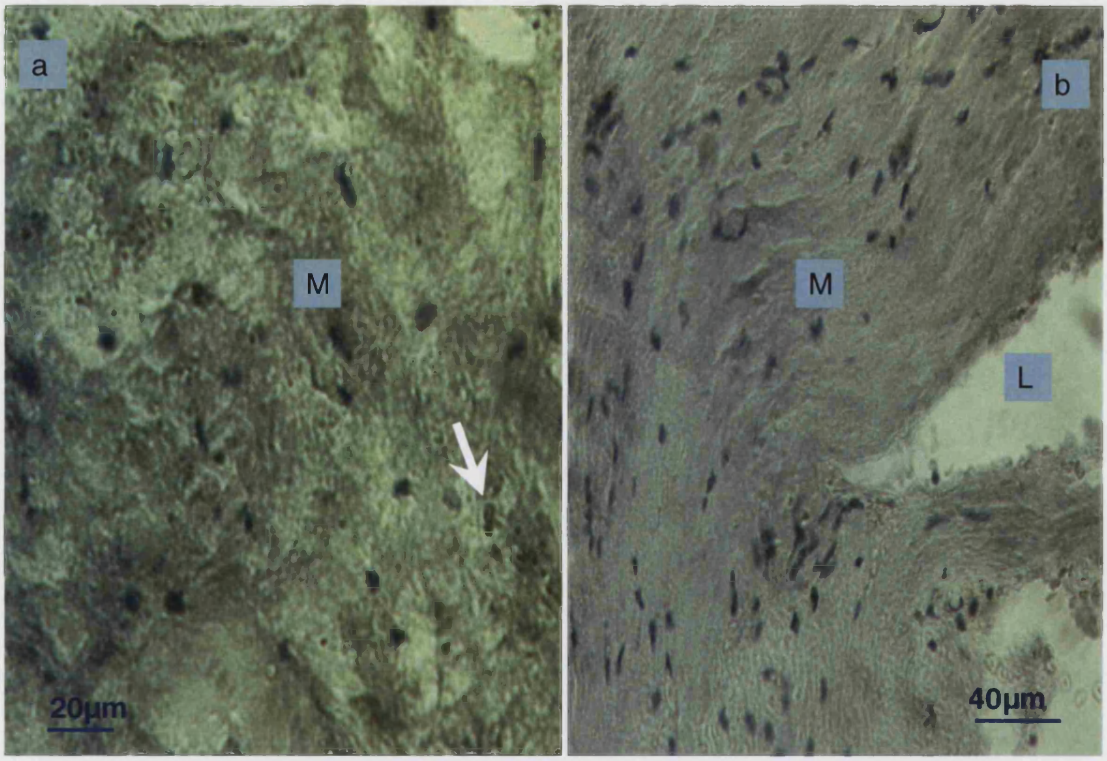

Figure 7.13 Human FLIP positive staining in AAA section. Brownish immunoperoxidase staining FLIP positive cells in AAA from formalin saline fixed tissue counterstained with haematoxylin. a. High-power magnification of medial layer of AAA. Note positive cells were indicated by a white arrow. b. Low-power magnification of media layer of AAA. Negative controls for staining were done but are not shown here.

7.4.4 Atheroclerosis cell marker

Smooth muscle actin and SMMS-1 was found in human AAA sections. Figure 7.9 demonstrates a loss of SMC. It also shows that atherosclerosis is localised within human AAA tissue. Normal aortic samples were not able to be obtained for the paraffin staining.

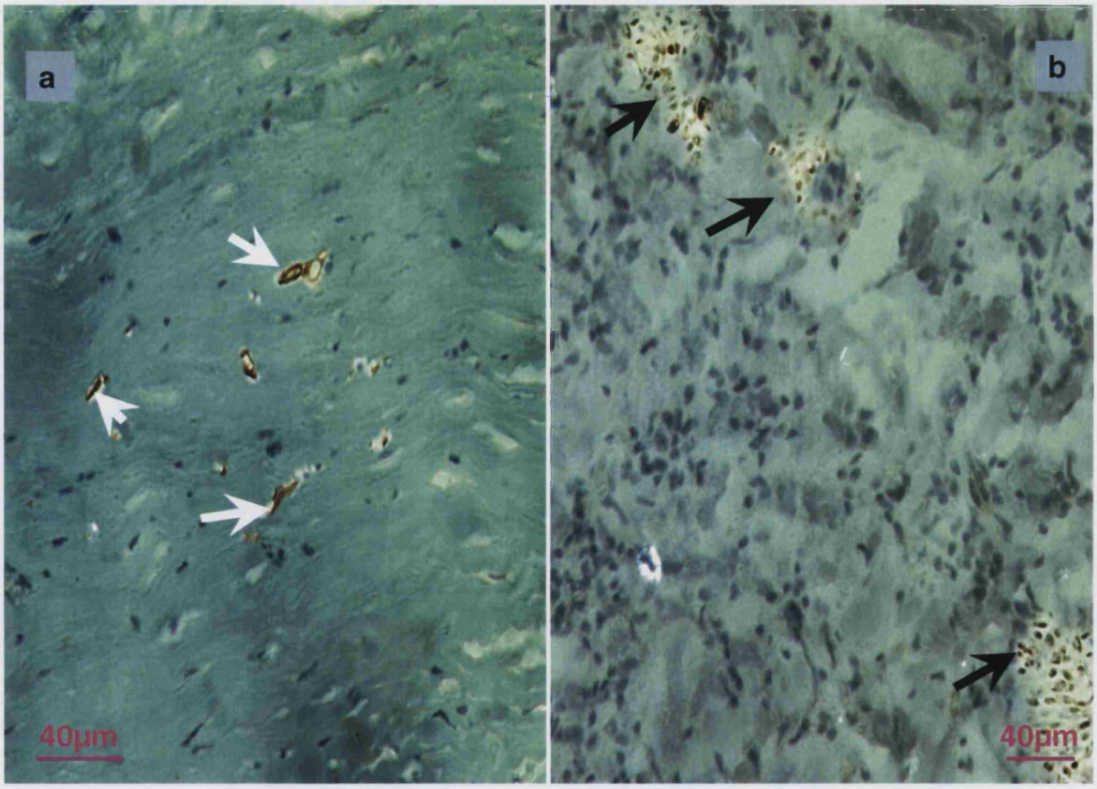

Figure 7.14 Actin and SMMS-1 staining of AAA tissue. Panel a is stained for actin, an indicator of smooth muscle cells (white arrows). Panel b depicts AAA tissue stained for SMMS-1 to differentiate areas of atherosclerosis as indicated by black arrows.

The number of SMCs was reduced in AAA comparing to that in normal aorta section. Atherosclerosis in AAA is not only be confirmed by pre-operative CT scan but also it was verified here by atherosclerosis marker SMMS-1.

7.4.5 The location of calcium deposition

Von Kossa staining revealed the location of calcification in AAA according to paralleled H&E staining. Not surprisingly, calcium deposited in the AAA vessel wall constantly and no calcification was detected in the normal aortae.

Calcium tends to be deposited in the neointimal part of atherosclerotic artery as it is verified by Schoppet *at al.* (Schoppet *et al.*, 2004). It is also proved by preoperative CT scan, calcium deposit in the outer side of AAA vessel wall.

Normal aorta was stained by Von Kossa methods as normal control for AAA sections. No calcium was found in figure 7.15.

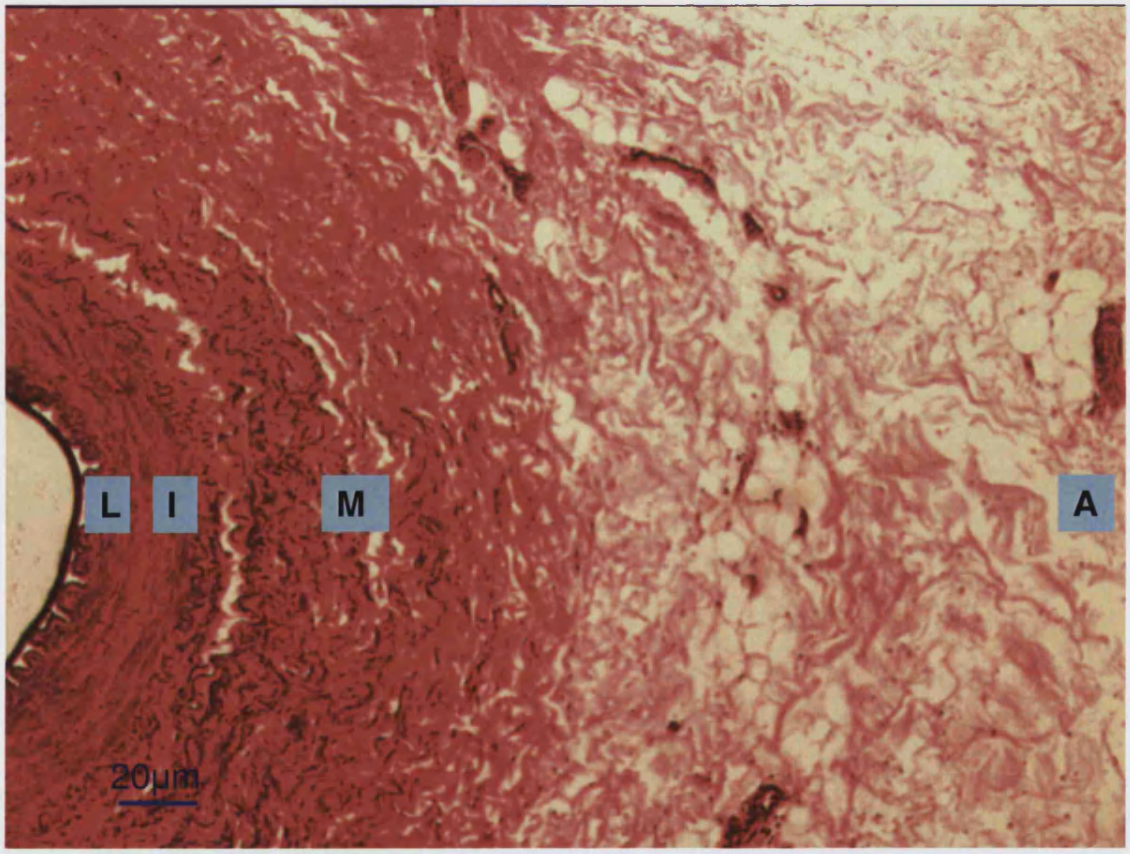

Figure 7.15 Normal aorta section stained by Von Kossa. L refers to lumen, I refers to *tunica intima*, M refers to *tunica media* and A refers to *tunica adventitia*. The tissue was counterstained with safranin O (in red). No calcium was detected by vonKossa.

Von Kossa staining was performed on human AAA sections as shown in figure 7.16. More calcification was found in medial layer than in *tunica adventitia.*

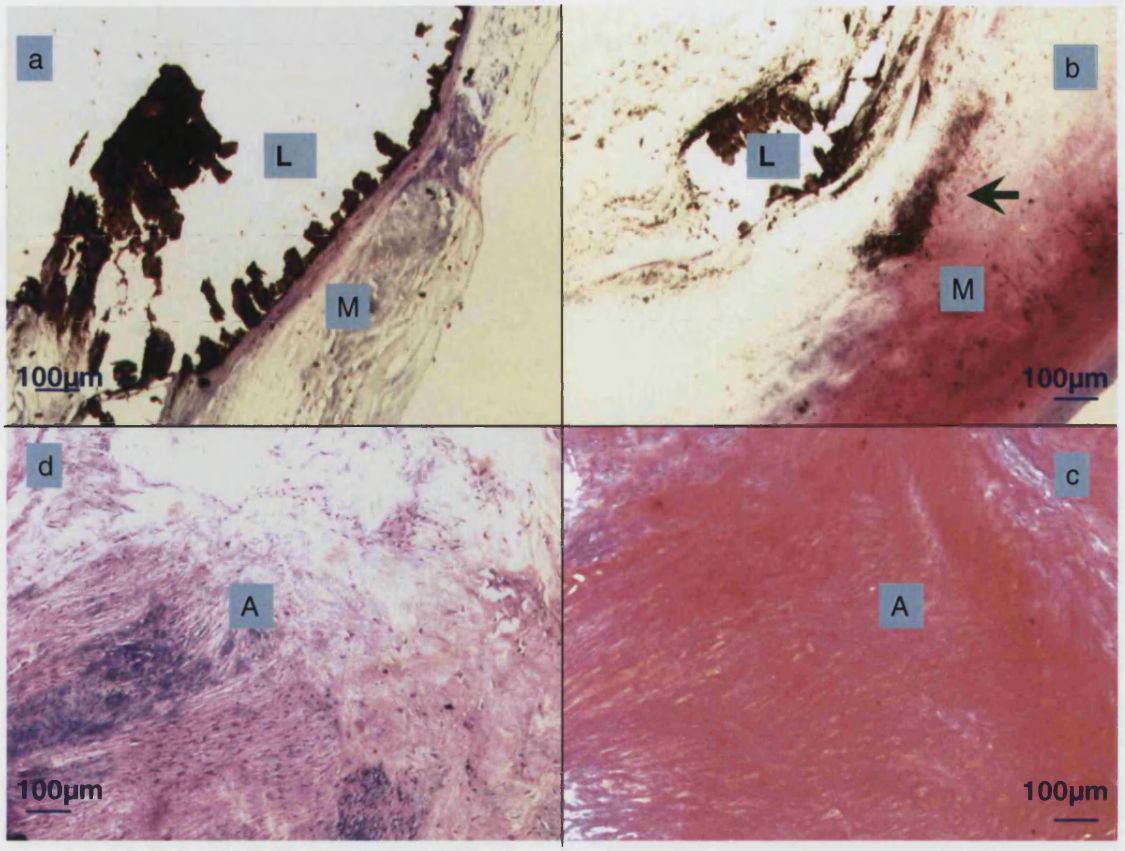

Figure 7.16 Aneurysm tissue stained with von Kossa and H&E (low-power). Light microscopic appearance of representative human AAA tissue: (a) Histological staining of AAA sections to demonstrate the distribution of disrupted architecture in the medial layer (M) of atherosclerotic aneurysm compare to normal aorta (see Figure 7.15). The haematoxylin-stained clusters of infiltrates are located on the edge of tissue facing lumen (L). (b) Von Kossa staining of consecutive section of AAA in panel a to demonstrate the calcium deposition which is found to be on the medial layer of AAA as green arrow indicates. (c) Von Kossa staining shows *tunica adventitia* (A) of AAA. No calcium was found in this AAA. (d) H&E staining section paralleled section of *tunica adventitia* in panel c.

Calcium deposits were more visible under high-power microscopy as shown in figure 7.17.

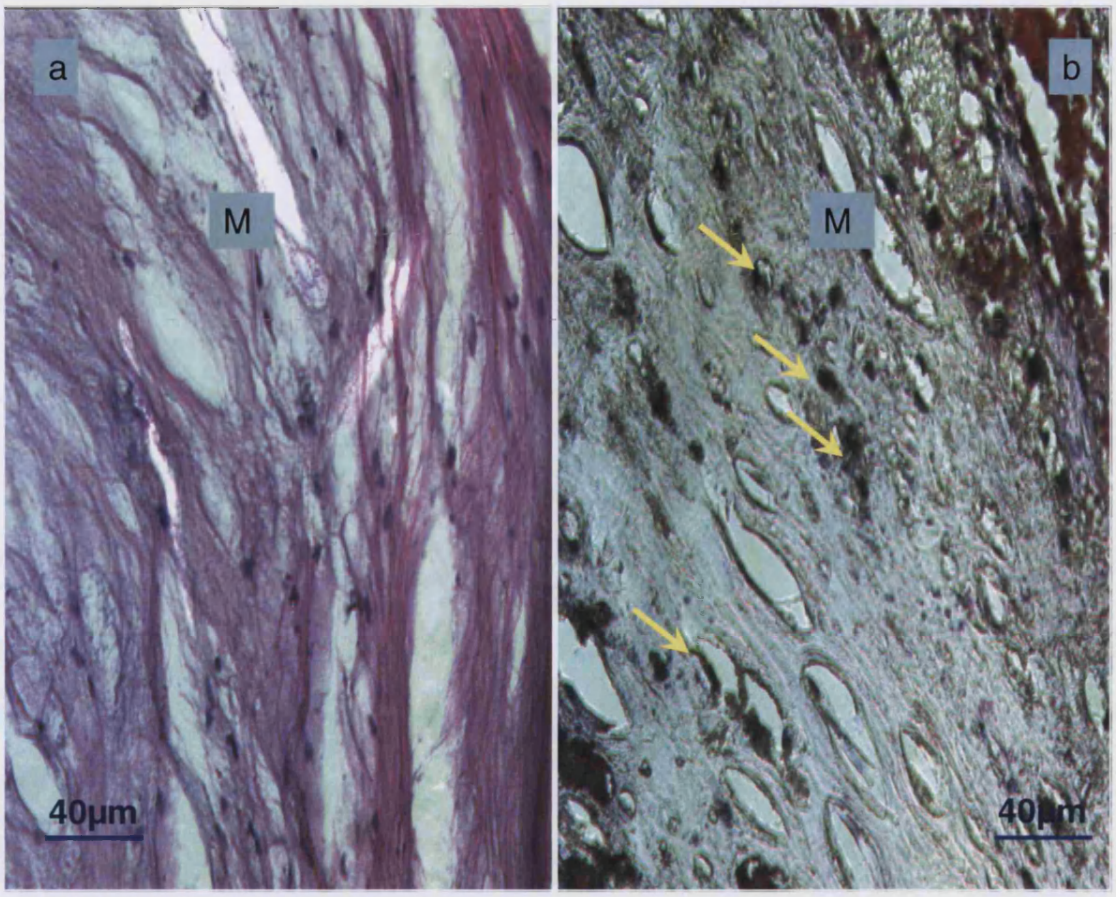

Figure 7.17 Aneurysm section stained by Von Kossa and H&E (hig-power). Panel a shows *tunica media* (M) of AAA. SMC cell number is reduced compared to normal aorta in Figure 7.16 and elastic fibres appear increased. The alignment of SMC is non-uniform. Panel b shows severe calcification of the *tunica media* (M) of AAA stained by Von Kossa. Yellow arrows indicate black lamellar deposits and black granular deposits.

7.4.6 Protein expression in the inner layer and outer layer of AAA

Since it is thought that aneurysms occur by the gradual thinning of the vessel wall through the degradation of its medial layer, the samples were dissected into two layers, outer and inner, to study TRAIL, TRAIL-R1 and OPG protein expression (figure 1c). Outer layer represents *tunica adventitia* and inner layer represents *tunica media* and tunic intimal. Protein expression for TRAIL and TRAIL-R1 is much higher in inner layer and OPG is absent. Previous finding by Von Kossa staining and H&E staining show that calcium mainly locates in the medial layer of AAA. The structure in AAA is disrupted. Smooth muscle cells are reduced compare to normal aorta and the orientation is not uniform. The elastic fibres in *tunica media* increased compare to normal aorta.

Protein expression in outer and inner layer of AAAs

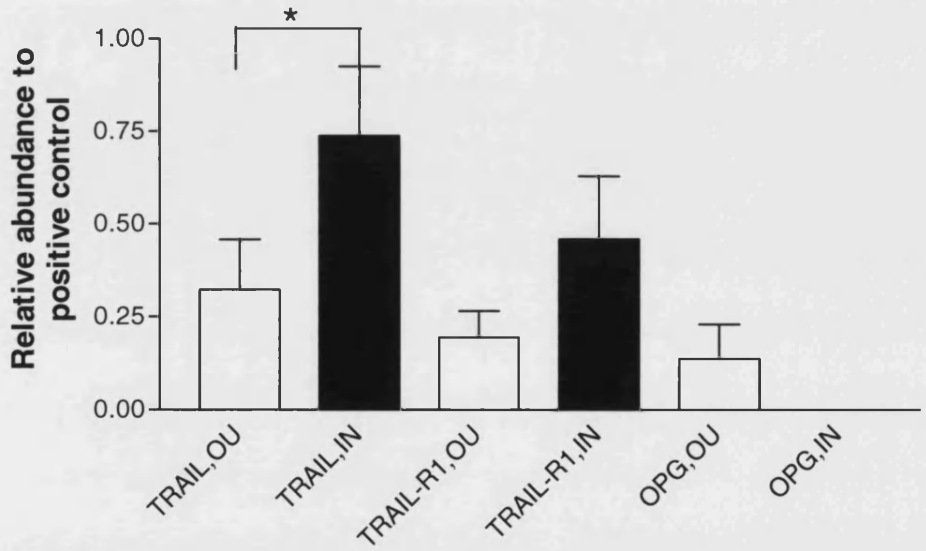

Figure 7.18 Protein expression in outer and inner layer of AAAs. Graph shows TRAIL, TRAIL-R1 and OPG protein expression in outer (OU) and inner (IN) layer of AAA vessel walls, examined by protein dot blots (n=6). TRAIL and its death receptor TRAIL-R1 were expressed more in the inner layer consisting of the *tunica media* and *tunica intima*, but the decoy receptor OPG was absent in the inner layer. TRAIL was significantly higher in the inner layers than the outer.

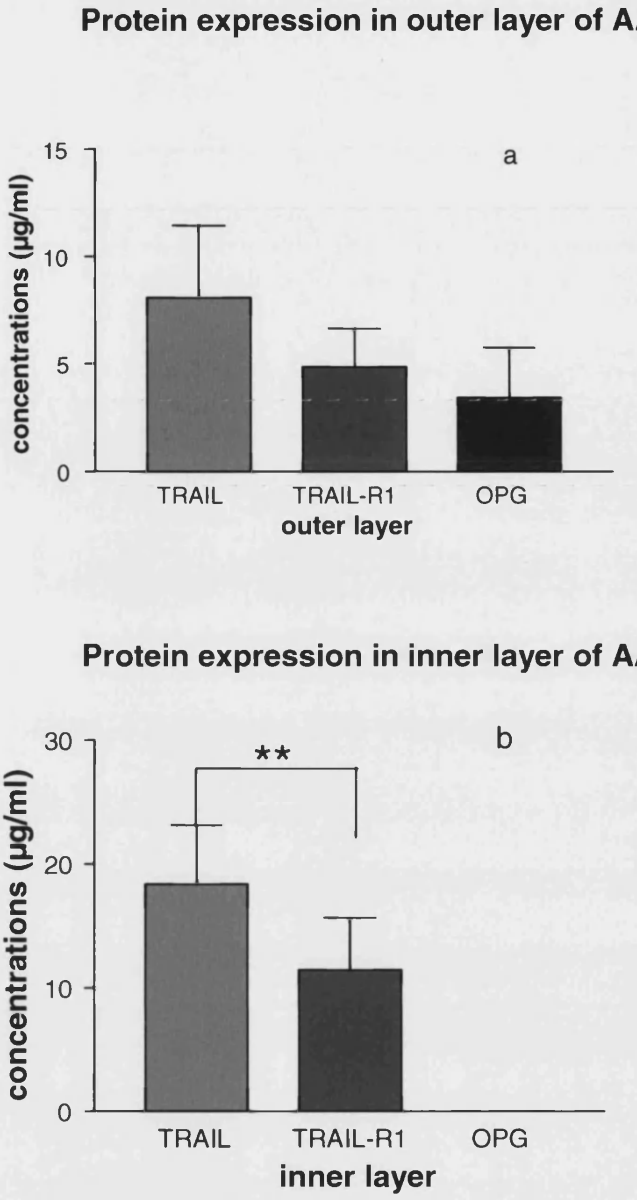

Figure 7.19 Protein expression in outer and inner layers of AAAs. The graph show protein expression in the outer (n=6) and inner (n=6) layers of AAA samples. Panel a indicates protein expression in the outer layer of AAAs and panel b indicates protein expression in the inner layer of AAAs. There is a significant difference between TRAIL, TRAIL-R1 and OPG in the inner layers of vessel walls (p<0.01, by one-way ANOVA). The top of the bar represents standard error.**

OPG was not present in the inner layer of AAA vessel walls among any of the AAA tested. TRAIL and TRAIL-R1 were expressed more often in the inner layer than in the outer layer. The Inner layer of AAA vessel walls contained much less calcification (even zero) than the outer layer, which was proved by CT scan and

morphology. The fact that OPG was increasingly expressed and TRAIL and TRAIL-R1 decreased in the more calcified areas is consistent with the finding of their mRNA expression.

7.4.7 Messenger RNA expression for TRAIL-rTRAIL system in cultured SMCs

Cells were cultured from an umbilical artery, the intimal and medial layers of normal aortae and AAA specimens. To detect mRNA expression for the TRAIL-rTRAIL system, PCR was carried out on cultured cells.

As mentioned in chapter 2, the SMCs failed to protect and repair injury to arterial wall and ultimately results in instability of the arterial wall in the AAA formation. Utilising *in vitro* VSMC tissue culture, the role of the VSMC in aneurysmal degeneration could be clarified.

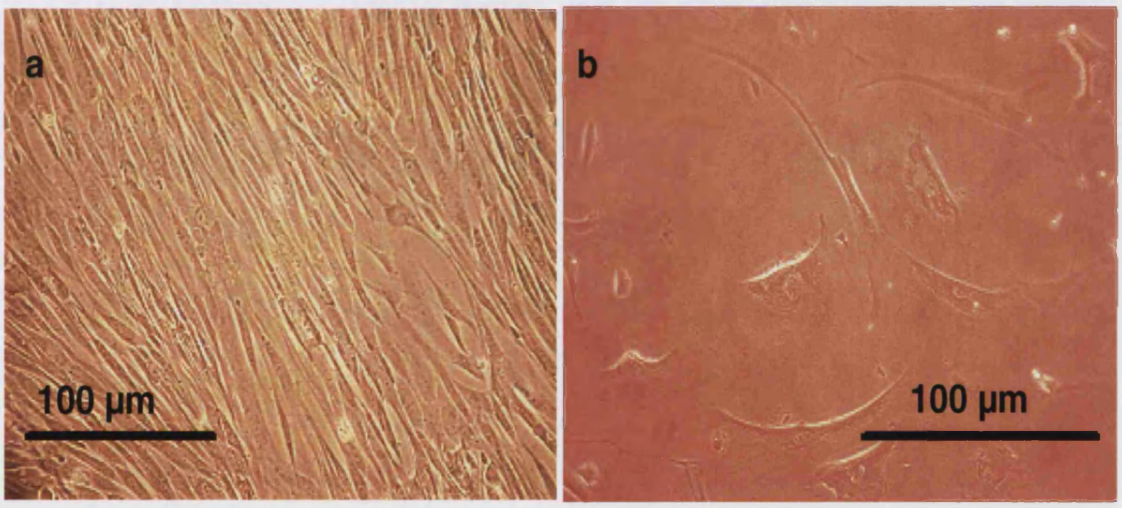

Figure 7.20 Smooth muscle cell culture. Panel a shows cultured SMCs from a normal umbilical artery. Panel b shows cultured SMCs from AAA. SMCs from AAA retained a narrow spindle-shape with a centrally located nucleus, similar to normal SMCs but grew more slowly.

The cultured cells were transferred to chamber slides for α-actin staining when they became confluent, to confirm that the majority of cultured cells were SMCs.

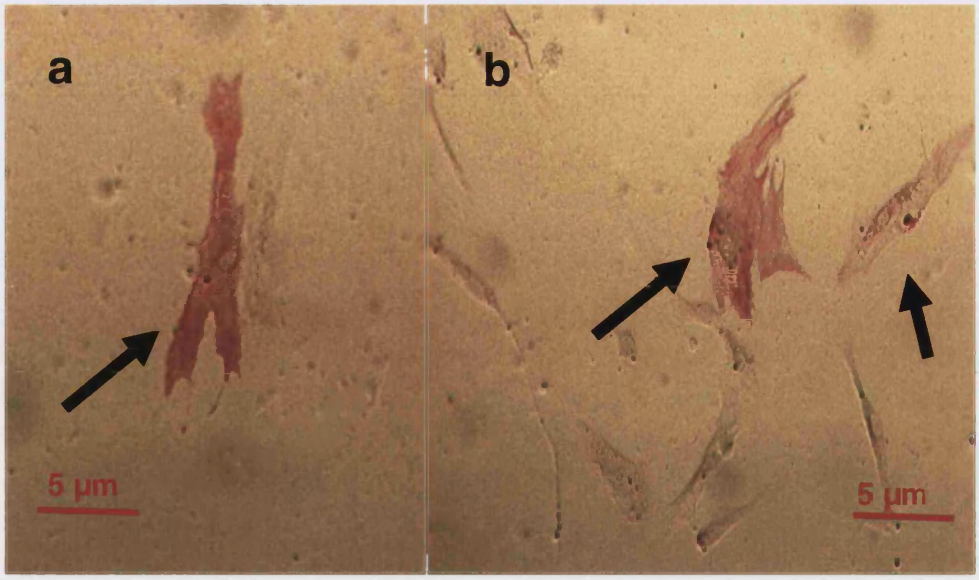

Figure 7.21 Both Panels a and b show cultured SMCs from AAA with α-actin staining under LM. Smooth muscle cells were observed in a rosy-pink colour, as indicated by the black arrows. They appear spindle-shaped with a single nucleus in the middle. This confirmed the existence of SMCs.

SMCs which were obtained from an umbilical artery and the media of normal aorta specimens were subjected to RT-PCR to study mRNA expression of TRAIL and its receptors. Firstly, a comparison of mRNA was carried out on SMCs from umbilical artery, cells from medial normal aortae and cells from intimal normal aortae. Then, normal aorta cells were arrested for 48 hours and followed by RT-PCR. Surprisingly, cells from the same normal aorta showed a very great difference after being arrested, as detailed below. No further study has been carried out in SMC cells from AAAs.

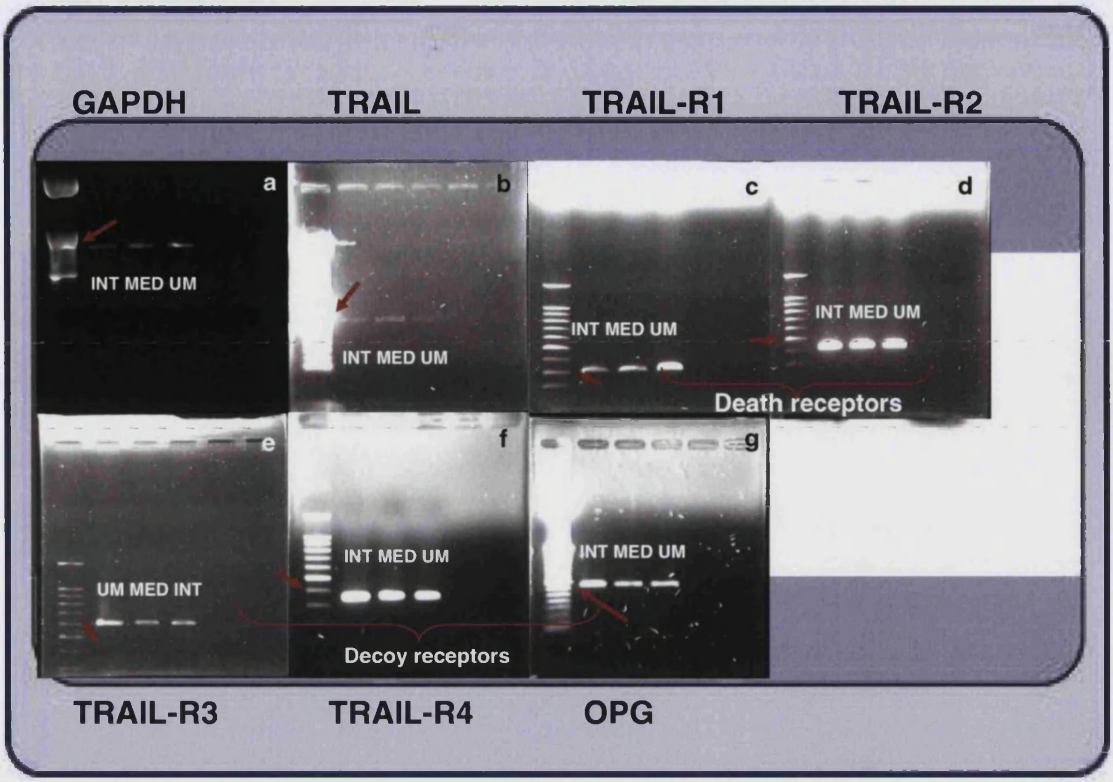

Figure 7.22 PCR gel images for cells isolated from normal artery. These gel images demonstrate the mRNA expression of SMCs from an umbilical artery and cells from intimal and medial layers of normal aortae. UM indicates SMCs from an umbilical artery; INT represents cells from intimal normal aortae and MED represents cells from medial normal aortae. PCR products from these cells were loaded and run on a 1.2% agarose/TBE analytical gel and stained with ethidium bromide. The PCR products were then compared with the standard loaded in the same gel, to identify their size. Red arrows indicate the size of the samples on the DNA ladder. Panel a indicates the PCR products of GAPDH, all three samples show very similar levels of GAPDH expression. Panel b indicates the PCR products of TRAIL; panel c indicates the PCR products of TRAIL-R1; panel d indicates the PCR products for TRAIL-R2; panel e indicates the PCR products for TRAIL-R3; panel f indicates the PCR products for TRAIL-R4; and panel g indicates the PCR products for OPG.

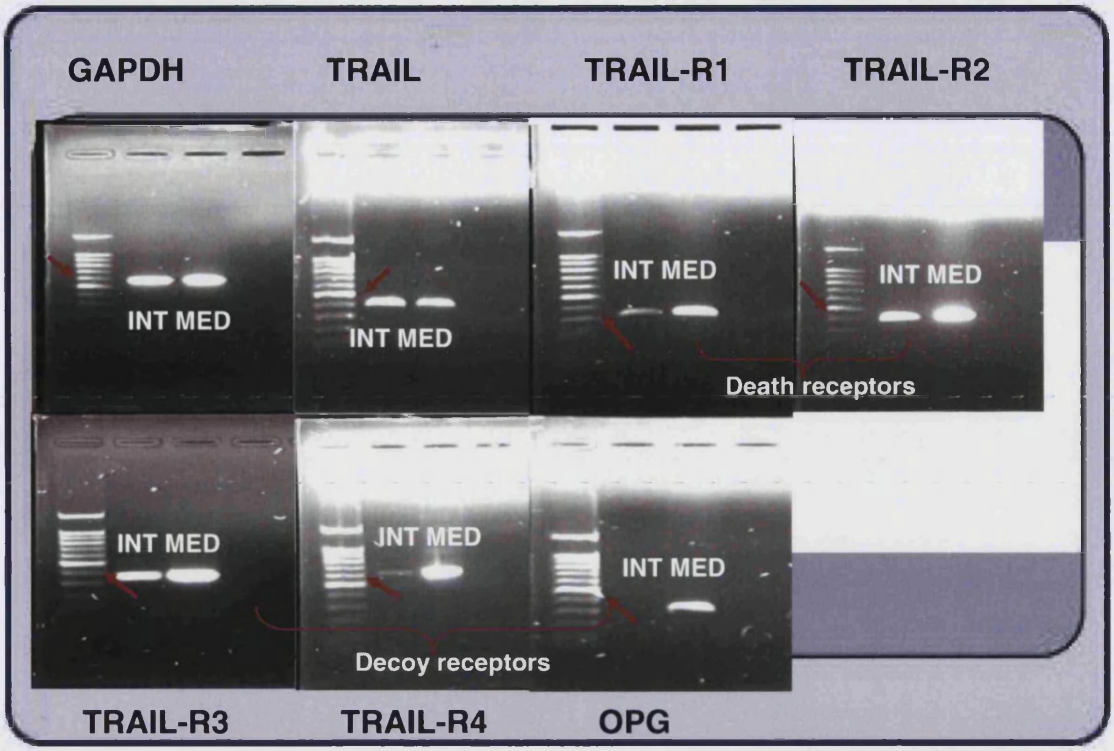

Figure 7.23 PCR gel image for cells isolated from normal aorta (arrested). These gel images show the mRNA expression of cells from intimal and medial layers of normal aortae after being arrested for 48 hours. INT represents cells from intimal normal aortae and MED represents cells from medial normal aortae. The PCR products from these cells were loaded and run in the 1.2% agarose/TBE analytical gel and stained with ethidium bromide. The PCR products were then compared with the DNA ladder, loaded in the same gel. Red arrows indicate the size of the samples on the DNA size ladder. Panel a indicates the PCR products for GAPDH, both samples show very similar levels of GAPDH expression. Panel b indicates the PCR products for TRAIL; panel c indicates the PCR products for TRAIL-R1; panel d indicates the PCR products for TRAIL-R2; panel e indicates the PCR products for TRAIL-R3; and panel f indicates the PCR products for TRAIL-R4. Panel g indicates PCR products for OPG and there was a missing band for intimal cells.

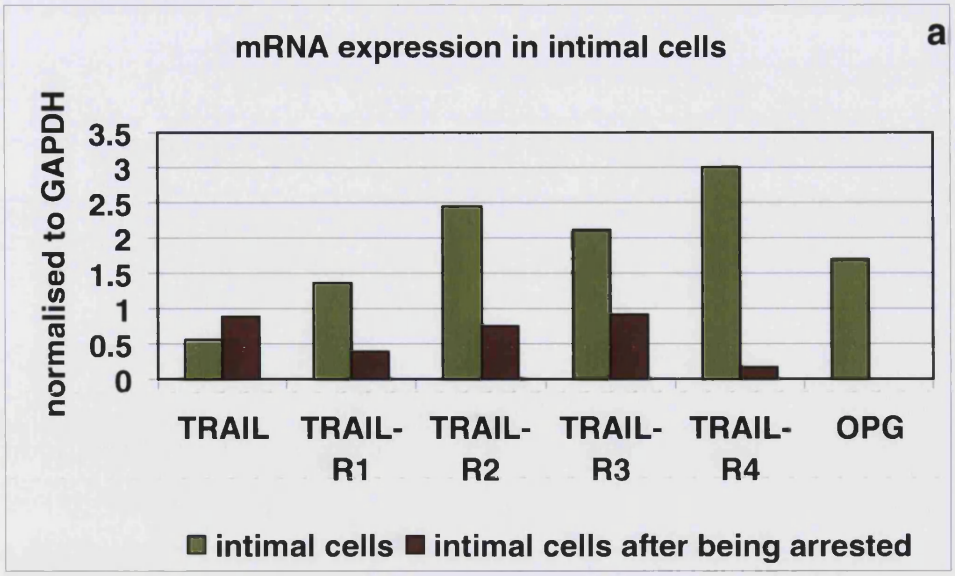

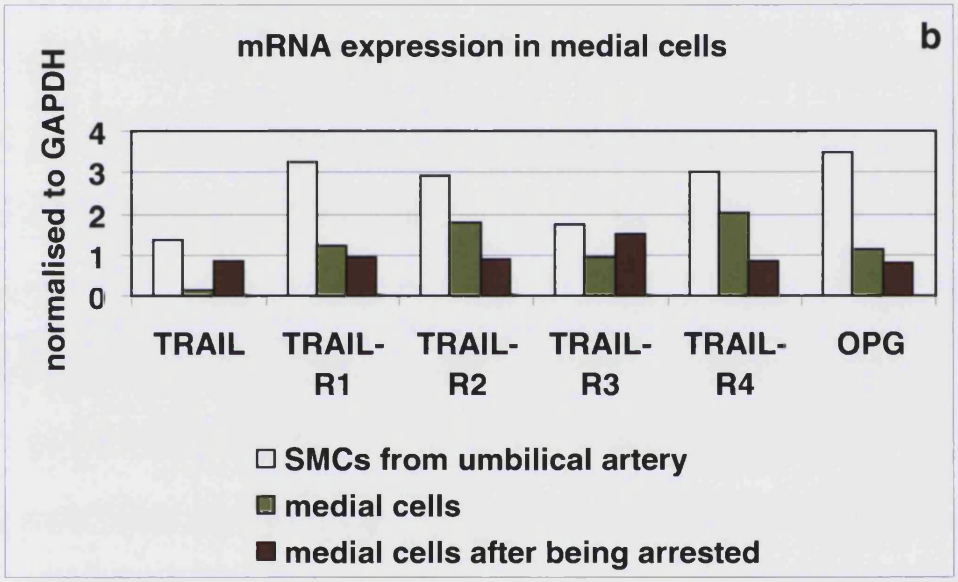

Figure 7.24 Comparsion graph of cells from normal aorta. These graphs compare the mRNA expression (normalised to GAPDH) of TRAIL and its receptors in cells from normal arteries. Panel a shows the expression of cells from intimal normal aortae. Panel b illustrates the expression of cells from medial normal aortae and SMCs from umbilical arteries. The graphs show the changes in the mRNA expression of TRAIL and its receptors in cells before and after being arrested.

Cells from medial normal aorta are mainly SMCs, which are cells thought to be involved in vascular calcification (Bostrom, 2001).They were confirmed by α-actin staining and showed a similar mRNA expression pattern to SMCs from umbilical arteries (shown in Figure 7.24b). Interestingly, when those cells were arrested for 48 hours, the mRNA levels for TRAIL and its receptors were observed to change considerably. TRAIL increased dramatically in medial cells after being arrested, while TRAIL-R2 decreased. Among decoy receptors, TRAIL-R4 also showed a considerable decrease. In the other three receptors, the mRNA expression remained similar to previous levels. When cells from intimal normal aortae were arrested for 48 hours, the mRNA expression of the TRAIL-rTRAIL system showed a similar trend to that in medial cells. TRAIL increased and both TRAIL-R1 and OPG reduced greatly, as did TRAIL-R4. It is also noteworthy that OPG was not found in the intimal cells after 48 hours arrest. However, this is a very preliminary result which has not been repeated. It indicates that further investigation should be made into the behaviour of cells, especially in the behaviour of SMCs from AAA.

Thus far, the results suggest that intimal and medial aortic cells secret TRAIL and all five receptors. TRAIL increased over the course of the cell culture in both cell types from normal aortae with variable expression for its receptors.

7.5 Discussion

7.5.1 Apoptosis in the aneurysm

Cells were found to be undergoing apoptosis in different areas of AAA vessel wall. However, only a very small proportion of apoptotic cells were visualised in the tissue sections. Relatively, the least apoptotic cells were found in the distal AAA (most calcified region). As mentioned in chapter 3 the apoptotic cells are available to be observed under LM for only a few minutes and apoptotic bodies only can be visualised for only a few hours before they undergo phagocytosis under ultrasound (Kerr, 1971). This could explain why a much smaller percentage of cells were found in apoptosis. It has been suggested that even the presence of a small detected percentage can still represent a considerable magnitude of cell loss (Arends *et al.*, 1994). Also comparatively less apoptosis detected in the distal area may imply that apoptosis occurred early and frequently in this area.

Combining the findings of highest calcification in the distal AAA, the theory of the blood flow dynamics (detailed in chapter 5) and the apoptotic index of the different areas, the following possibilities can be suggested. Apoptosis that occurs in the distal area (where aneurysm occurred firstly, early stage) might be involved in the arterial wall remodelling. Blood flow dynamics increases aortic wall stress causing injury of the arterial wall leading to atherosclerosis. In addition, the histological features of thinning of the *tunica media* and the disappearance in the elastic lamina are contributory to aneurismal changes. After formation of an aneurysm apoptosis continues to occur frequently in the neck of AAA (proximal area), which might explain why more apoptosis was found in the proximal than in the distal area in the AAA samples examined. The AAA samples used here were all under the established stage.

7.5.2 Smooth muscle cells atherosclerosis cell marker and difference of normal and abnormal aortic structure

The thinning of the *tunica media* is a feature specific to AAA in this study. The internal elastic lamina was clearly defined in normal aorta but fragmented or missing in aneurysm sections. In the medial wall, the number of medial SMCs is decreased with variable size displaying a disorderly fashion. Some SMCs showed distorted cell shape by α-actin. The normal characteristics of the *tunica media,* including well defined connective tissue and medial SMCs, were missing in AAA. This study identifies a reduction in SMC number in AAA. Sometimes, inflammatory cells accumulated in the AAA wall. This is consistent with the finding from the medical records that 10-15% of patients who underwent AAA repair developed inflammation.

7.5.3 The correlation of calcium deposition with TRAIL-rTRAIL system

It is interesting to note that OPG protein was not expressed on the inner layer of the AAA wall (*tunica intima* and inner *tunica media*), an area of less calcification compared to the outer layer (see**Figure 7.19**). TRAIL and TRAIL-R1 protein were also expressed more on the inner layer of AAA walls. As detailed in chapter 2, AAA are characterised by destruction of elastin and collagen in the media and adventitia (Crawford *et al.*, 2003; Ernst, 1993). It is often associated with atherosclerosis (Jorgensen *et al.*, 2004).Taken together, this indicates that TRAIL and TRAIL-R1 involvements in AAAs are associated more with the progression of AAA than the calcification level of the AAA wall. This suggests that TRAIL and TRAIL-R1 may interplay in the *tunica media* of AAA. These features of the inner layer of the AAA wall may result in the expansion and degradation of AAAs. In addition, the imbalance of OPG in the *tunica media* and intima may be a result of OPG post-binding relationships with TRAIL, protecting cells from apoptosis, or this may be one reason why apoptosis is found in AAA wall. Furthermore, OPG protein was co-expressed with TRAIL-R1 in AAA. This verifies again that OPG protection is a reaction of TRAIL-R1 initiation.

Another explanation for the results in **Figure 7.19** would be that TRAIL and TRAIL-R1 play a role in the AAA medial wall thickening and neointimal formation. As discussed in chapter 2, SMCs in the medial layer of the aorta vessel wall migrate from their original location toward the intimal layer. The higher level of TRAIL-R1 expression in the inner layer of AAA walls indicates that it is an influencing factor of SMCs.

7.5.4 Messenger RNA expression of TRAIL and its receptors in vascular cells

TRAIL has been found to be expressed in human and animal atherosclerotic plaques and in cultured human smooth muscle cells (Stocker and Keaney, Jr., 2004).The primary data from Figure 7.22 showed that TRAIL death receptors, TRAIL-R1 and TRAIL-R2 were both expressed by intimal cells and medial cells isolated from normal aortae. TRAIL selectively induces apoptosis in tumourgenic cells or transformed cells but not normal cells (Willey et. al, 1995). Thus, normal vascular cells are assumed to be cells which are susceptible to TRAIL-induced cell death; this might be due to the high expression of decoy receptors.

Of particular interest, TRAIL was reported as being induced in a P53-dependent manner or P53-independent manner by DNA damage (Meng and El-Deiry, 2001). This might suggest that TRAIL is expressed in a similar manner to the p53 gene in vascular cells. As mentioned in chapter 3, the tumour suppressor gene P53 is known to block the cell cycle at the S phase, eventually inducing apoptosis (Kulesz-Martin *et al.*, 2005). The P53 protein has been found to be over-expressed in 30 per cent of human angioplasty restenosis sites and only induces apoptosis of cells infected with dominant proto-oncogenes but not normal cells (Bennett *et al.*, 1995). The fact that expressions of TRAIL increase and TRAIL death receptors decrease in both intimal cells and medial cells after being arrested suggests that down-regulation of death receptors may be a response to an increase in TRAIL. This also confirms the above finding that there are negative correlations among TRAIL and its decoy receptors after being arrested.

The above results could not be repeated because of the difficulties of obtaining fresh normal aorta tissue and growing SMCs from end-stage AAAs. It would be

very interesting to test apoptosis induced by TRAIL and mRNA and protein change in itself and its receptors in normal and abnormal vascular cells if the fresh tissue storage and transport problems could be solved.

Section III

GENERAL DISCUSSION AND FUTURE WORKS

Chapter 8 General discussions

8.1 General Discussions

This project has evaluated the presence of the TRAIL-rTRAIL system and its possible effects in human AAA. The early part of the study confirmed that apoptosis and atherosclerosis (vascular calcification) was associated with human AAA. The study demonstrated for the first time that gene expression for TRAIL and its receptors and protein expression for TRAIL, TRAIL-R1 were present in the in human AAA and confirmed previous reports of their presence in normal aorta.

Human AAA has been documented to be associated with atherosclerosis (vascular calcification). Abdominal aortic aneurysm occurs in 7.5% of the male population over 65 years old but is rare under the age of 50 years old. It causes 2% of all deaths in men over 65 years old. There were 6800 AAA-related deaths in 2004 in England and Wales alone (Quick C., 2004). The prevalence is still increasing (Quick C., 2004) and small AAA increase in diameter by 0.26cm per year in a study of small AAA in England (Powell J., 2004). Only 10% of patients living with AAA are alive 8 years after being diagnosed compared with 65% survival rate in unaffected subjects in a similar population (Wilmink T., 2004). The only effective way to treat AAA is surgery (ref). The mean hospital costs over four years per patient undergoing endovascular abdominal aortic aneurysm repair (EVAR) was £13,632 compared to £4983 in the no intervention group, therefore the mean difference is £8649 in England (Greenhalgh et al., 2006). Thus far, there is no evidence to show that altered blood pressure, weight or serum lipid affects AAA growth (Powell J., 2004). Hence, it is necessary to find an effective way to slow AAA growth before the surgical intervention is necessary.

Recently, human calcification has been proved to be a regulated process with similarities to bone modelling and remodelling (Shanahan et al., 2000; Bostrom, 2000; Shanahan et al., 1994). Osteoprotegerin is an inhibitor of osteoclast formation which was found to be in bone cells and endothelial cells (Aubin and Bonnelye, 2000). Mice deficient in OPG often exhibit extensive bone fractures and medial calcification of the aorta and the renal arteries (Schinke and Karsenty, 2000). This is compatible with findings of coexisting bone fractures and vascular calcification in humans (Pennisi et al., 2004; Sattler et al., 2004; Schulz

et al., 2004). These studies indicated that OPG might play a role in osteoporosis and vascular calcification. Additionally, apoptosis and its cellular marker were found to be expressed in the human AAA. The TRAIL-rTRAIL system is capable of regulating apoptosis and OPG is a decoy receptor of TRAIL.

To confirm that apoptosis and vascular calcification is associated with human AAA, TUNEL assay, Von kossa staining and other immuno-chemical stains were used (chapter 8). Atherosclerosis cellular maker (SMMS) was performed to prove that human AAA is association with atherosclerosis. Human FLIP staining, as an apoptosis cellular marker, was also performed. On the molecular lever, mRNA and protein expressions were examined by RT-PCR and protein blot respectively. To explore these factors, comparisons were carried out between human normal aorta and AAA. TRAIL and its receptors mRNA and protein were found to be expressed which is in agreement with the ubiquitous expression of TRAIL-rTRAIL system in various human tissues. Because both normal aorta and AAA express TRAIL and its receptors, it implies a possible function of inducing or inhibiting apoptosis in the vessel wall. The significant difference of mRNA ($p< 0.05$) and protein ($p<0.01$) for TRAIL –rTRAIL system between normal aorta and AAA suggests that it may be involved in the initiation of vascular calcification. The fact that TRAIL death receptors were lower in the more calcified specimens than more calcified AAAs is consistent with this idea. However, the study had some unavoidable shortcomings. To compare the TRAIL-rTRAIL system expression in human normal and abnormal tissue more precisely, it would be ideal to choose age-matched normal and abnormal specimens. They both should have had a CT-scan on normal and abnormal specimens prior to experimentation. This would establish that the normal specimens were, in fact, healthy and free of calcification. However, normal aorta sample were obtained from kidney transplant donors and it could not be ruled out that some calcification may have been present on normal vessel wall. The samples obtained from open AAA repair mostly had pre-operative CT scan while there was no access of CT scan for normal aorta samples. Also, age-matched sampling was technically impossible because the criteria governing AAA open surgery and kidney transplant donors (normal aortae resource).

The limitations of human AAA specimens restrict the age and the AAA development level. Thus, AAA specimens were separated to three body parts according to location as well as calcification level: proximal, body and distal to imitate three AAA development stages. Also the blood flow systematic theory supports this separation. Apoptosis-inhibiting receptors; TRAIL-R3, TRAIL-R4 and OPG were expressed in all areas of AAA walls examined. This is consistent with bone-related inhibitors of calcification which were found to be exhibited at all stages of human atherosclerosis (Dhore et al., 2001). Correspondingly, apoptosis-inducing receptors; TRAIL-R1 and TRAIL-R2 were expressed mainly on the more calcified AAA walls than the less calcified ones. This is also consistent with the results of bone-related activators of calcification which were found restricted to lesions with advanced calcification. In a similar manner, Dhore et al. suggested that vascular calcification is the result of time and plaque-stage-restricted activation and continuous inhibition. The fact that TRAIL death receptors decreased in the more calcified specimens compared to the more calcified AAAs is also consistent with this idea. However, there are questions that remain to be addressed. There are two further ways of exploring these questions. Firstly serum levels of the TRAIL-rTRAIL system could be measured in patients who are diagnosed with small AAA on a regular basis (such as monthly) in addition CT scans or ultrasound scans could be performed about twice per year. This is a possibility for the future as it is reported that small AAA increases 0.26cm per year in a study of small AAA in England (Powell J., 2004). It is possible that AAA screening will be launched in the near future. This would provide a huge databank of information in a short time that may help in future research. The second possibility is to further develop AAA in animal models. Several researchers have already successfully generated AAA in rat (Kaito et al., 2003) and swine (Ruiz et al., 1997). A recent study successfully created AAA in pigs by performing a double-layered peritoneal patch. The aneurysm was proven to have a similar morphology to human aneurysms and also to have the potential for further growth leading to rupture (Maynar et al., 2003). However, it cannot completely represent human AAA because there no atherosclerosis occurs in AAA of animal models.

The pattern of expression for TRAIL in the AAA is remarkably similar to that in the normal aortae, where TRAIL was widespread in both vessel walls. This

indicated that the ratio of TRAIL to its receptors is crucial in determining the potential influence on apoptotic events. The affinities of TRAIL with its five receptors are still unclear making it difficult to determine which receptors are more important in the process of vascular calcification.

The very high positive correlation beyween TRAIL-R2 mRNA with TRAIL-R3, TRAIL-R4 and OPG mRNA and the negative correlation between TRAIL-R1 mRNA with TRAIL, TRAIL-R2, TRAIL-R4, OPG mRNA in AAA indicate that TRAIL-R1 may be the dominant force in vascular calcification out of the 2 death receptors.

Is it only coincidence that TRAIL-rTRAIL system shares similarity with inhibitors and activators of bone calcification in calcified arterial walls? Or are they correlated to a certain extent? OPG is a favourite link between TRAIL-rTRAIL system and bone-related proteins. OPG has been found in bone marrow stromal cells, osteoblast-like cells, and osteosarcoma cells (Dhore *et al.*, 2001) as well as being found in the vascular wall, endothelial cells and vascular smooth muscle cells (Schoppet *et al.*, 2004). This study reveals that TRAIL receptor protein is up-regulated in the more calcified regions compared with less calcified regions. Taken together, these factors suggest that decoy receptors continuously prevent calcification whereas death receptors are restricted to the active calcification area similar to the behaviour of bone calcification proteins (Dhore *et al.*, 2001).

Further protein study of OPG and TRAIL-R1 confirmed the involvement of the TRAIL-rTRAIL system in vascular calcification. TRAIL-R1 proteins were expressed more than OPG proteins in AAA and specifically in the most calcified areas of AAA. OPG protein was up-regulated in the less calcified area and down-regulated in severely calcified areas. This might indicate that a counter-regulatory mechanism exists for OPG that limits apoptosis in the less calcified area and thereby delaying the onset of calcification. OPG has been found to play a role in the process of vascular calcification in an animal model, this strongly implies that OPG may also play a role in human vascular calcification. Serum OPG levels significantly increased as the severity of coronary artery disease increased. Increased OPG level might be a compensatory self-defensive response to the progression of atherosclerosis (Jono *et al.*, 2002)

It has been reported using western blot analysis that OPG associated with endothelial cells is likely to be native dimeric OPG. Whereas the OPG predominantly found in the synovial lining is not a native dimer but possibly a breakdown product or monomer of OPG (Jono *et al.*, 2002).

8.2 Future works

To explore the possible function of the entire TRAIL-rTRAIL system in human AAA, more studies need to be carried out. Firstly, the protein expression for TRAIL-R3 and TRAIL-R4 in human AAA needs to be confirmed. The antibodies for these analyses were not commercially available at the time of this study. The antibodies, anti-TRAIL-R3 and anti-TRAIL-R4 are now both available from Biolegend, San Diego, USA for use as primary antibodies in Western blot analysis. If the presence and level of expression of TRAIL-R3 and TRAIL-R4 is in agreement with their mRNA expression in human normal and abnormal aortic tissue, a full characterisation of death receptors and decoy receptors in human aortic wall will be possible.

Secondly, further study can be carried out in testing TRAIL and OPG serum level in AAA patients. Recording OPG and TRAIL serum level in follow-up AAA patients with their CT scan AC score could be very useful. It is well known that AAA diameter increases as patient age increases. However, the question has not been addressed whether calcification level increases followed with the increasing of AAA size. It will be very interesting if there are correlations between OPG serum levels, TRAIL serum levels, AAA diameter and AAA calcification levels. As mentioned in chapter 7, OPG serum levels have been found to be weakly correlated with AAA growth rate (Moran et al., 2005). There does not appear to be any technical difficulties in carrying out this study.

Thirdly, further studies could be performed *in vitro* to investigate the biological activity of cells isolated from normal aorta and AAA. It would be interesting to expose normal aorta cells to TRAIL and its death receptors and then examine the change in the number of apoptotic cells. Cells have been successfully explanted from AAA and normal aortic tissue in this study. Careful arrangement of the collection, transport and storage conditions for specimens will ensure a good source of material for the isolation and culture of cells for such studies.

Fourthly, animal studies can be carried out to strengthen the evidences of the TRAIL-rTRAIL system function in human AAA. As mentioned in chapter 8, AAA animal models were effectively created on rats and swine. It might be possible to

test the potential therapeutic effect of the TRAIL-rTRAIL system by looking at the aneurysm development rate after subjecting animal models to decoy receptors and/or blocking TRAIL death receptors. It is also worth increasing TRAIL and TRAIL death receptor level in animals with AAA to observe the correlation of AAA growth rate and TRAIL and its death receptors serum concentrations.

Ultimately, because the human body and prevalent living conditions are very different from any likely animal model, a clinical trial of TRAIL and OPG could be useful to test the effectiveness and side effect of the TRAIL-rTRAIL intervention in AAA.

8.3 Summary

To recapitulate, this project investigates and demonstrates the presence of the TRAIL-rTRAIL system and possible biological interaction in human AAA. It demonstrates that significant difference of the TRAIL-rTRAIL system in human normal and abnormal aortic tissue and differences in all different areas of human AAA vessel walls. This is associated with vascular calcification levels examined by pre-operative CT scan and apoptosis areas determined by TUNEL assay. These suggest that the possible biological function of the TRAIL-rTRAIL system in human AAA that may participate in the AAA development. Interference of this system could influence human AAA development in its early stage. Optimistically, this also implies a possible medical treatment to be used to slow human AAA expansion, an alternative to surgical treatment.

A very recent study has suggested that OPG serum level can be a predictive biological marker for sub-clinical disease and near-term cardiovascular events in diabetic II patients (Xiang et al., 2006). In addition, 78% patients in this study have more than one cardiovascular disease. This may suggest that TRAIL-rTRAIL system could also have biological interference in the other vascular calcification diseases. Further investigation needs to be carried out to warrant fully explanation.

VII Appendix A

Buffer recipe for western blot

lysis buffer	
	0.15M NaCl
	5mM EDTA (pH=8).
	1% Triton X100
	10mM Tris-cl (pH=4).
	Protease inhibitors
2X sample buffer (reducing). pH=8	
	130mM Tris-Cl
	20%(v/v). Glycerol
	4.6%(w/v). SDS
	0.02% Bromophenol blue
	2% DTT
2X sample buffer (non-reducing). pH=8	
	130mM Tris-Cl
	20%(v/v). Glycerol
	4.6%(w/v). SDS
	0.02% Bromophenol blue
8X resolving gel buffer:100ml	
	0.8g SDS (add last).
	36.3g Trizma base(=3M).
	Adjust pH to 8.8 with concentrated HCl
4X stacking gel buffer:100ml	
	0.4g SDS (add last).
	6.05g Trizma Base(=0.5M).
	Adjust pH to 6.8

running buffer:1L	
	3.03g Trizma Base (=0.25M).
	14g Glycine(=1.92M).
	10g SDS(Add last).
Blotting buffer:1L	
	3.3g Trizma Base (=0.25M).
	14g Glycine(=1.92M).
	pH should be 8.3 ,
	200ml Methanol with 800ml blotting buffer
Stripping buffer 0.5L	
	0.2M Glycine,PH=2.5
	0.05% Tween 20
water-saturate-1-butanol	
	50% water
	50% saturate-butanol
9% Resolving gel	
	7.2ml 30 acrylamide
	3ml 8X Resovling gel buffer
	13.8ml water
	12µl TEMED (add last).
	60µl 20% ammonium persulfate
12% Resovling gel	
	9.6 ml 30% acrylamide
	3ml 8X Resovling gel buffer
	11.4ml water
	12µl TEMED (add last).
	60µl 20% AMPS
5% stacking gel	

	1.3ml 30% acrylamide
	2ml 4X stacking gel buffer
	4.7ml water
	8µl TEMED (add last).
	21.6µl 20% AMPS
5%blocking buffer	
	5%marvel milk /0.05%PBS tween
Stripping buffer 0.5L	
(sterile filter solution and keep at 4C).	0.2M Glycine pH=2.5
	0.05% Tween 20

Buffer recipe for RT-PCR

1X TBE buffer	
	10.8g Trizma base
	5.5g Boric acid
	2ml 0.5M EDTA
	making up to 1L

1.2% agarose gel

1.2% agarose in 50ml 0.5X TBE buffer is dissolved by heating in the microwave. Add 10µl ethdium bromide per 50 ml solution; cool the solution down with tap water. Pour the mixture into gel tank with combs. After gel set, loading appropriate volume sample into each well, running gel at 50V for about 40 minutes (when the dye reach the end of gel)..

DEPC treatments

Soak equipment in 10ml DEPC in 1L DDH for 2 hours at room temperature. Dry them on the oven followed by autoclave.

The Laemmli system

The most widely used system for electrophoresis of proteins is probably that described by Laemmli,1970. It is a discontinuous system for resolving proteins denatured with SDS. The leading ion in the Laemmli buffer system is chloride, and the trailing ion is glycine. Accordingly, the resolving gel and the stacking gel are made up in Tris-HCl buffers (of different concentration and pH), while the tank buffer is Tris-glycine. All buffers contain 0.1% SDS.

Membrane for western blot

Nitrocellulose and reinforced PVDF membranes are generally used in Western blotting. For larger molecular weight proteins both types of filters works well. However, if your protein is less than 10 kb nitrocellulose should be used because it has a much higher binding capacity. The PVDF membranes will not work well under these circumstances.

Automated Autorad Developer

Kodak X-OMAT AR auto rad film was cut into appropriate size and placed on the nitrocellulose membrane for 30 seconds, 1 minutes and 5 minutes or even overnight at 4°C. Then the film was developed in the Fuji RG II X-ray film processor.

Scion Imaging Software

http://www.scioncorp.com accessed. Scion Image is an image processing and analysis program which is based in NIH *Image* on the Macintosh platform. To analyse the mean density of protein bands after enhanced chemiluminescence dectection.

- Open the saved file (.TIFF format) of interest and select the rectangular selection tool and outline the area of interest.
- Select 'measure' from the 'Analyse' menu. This computes the area and mean gray value of the selection.
- Move the outline selection box to the next area of interest and repeat the measurement.
- Continue until all areas of interest have been analysed.

Enzyme solution A and B (from Alkaline Phospahtase kits, Vectastain. UK)

Enzyme solution A: AvidinDH

Enzyme solution B: Biotinylated Enzyme

PCR image gel for RANK and RANKL

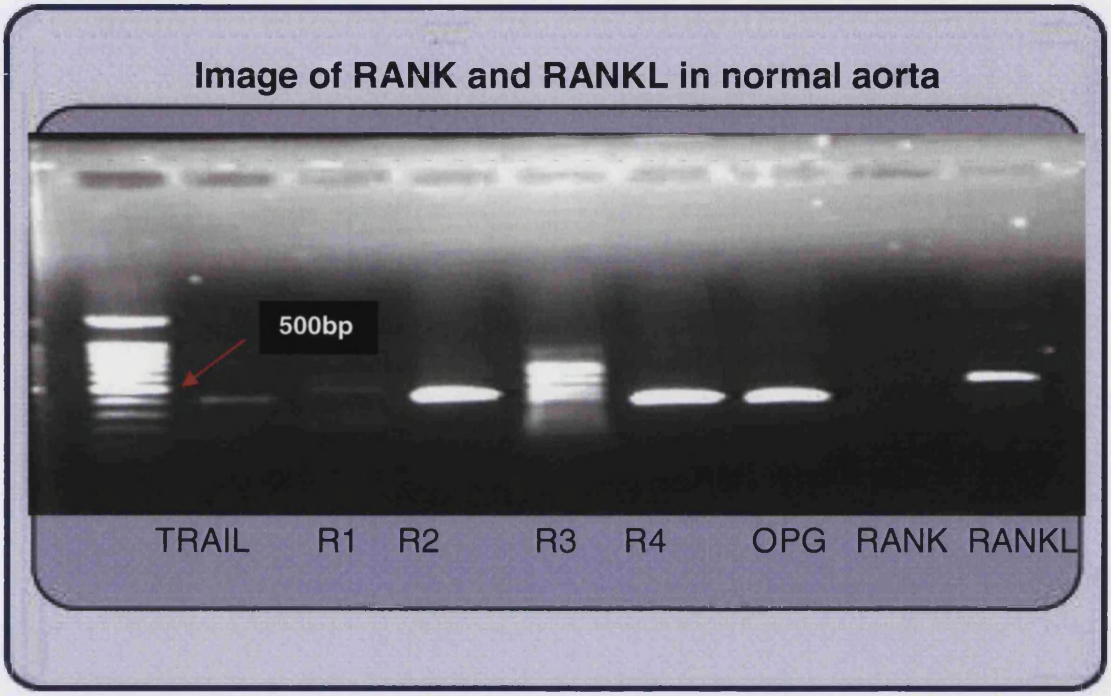

The representative gel image here shows eight PCR reactions that were set up on the isolated RNA for in normal aorta. The reactions amplified TRAIL, TRAIL-R1, TRAIL-R2, TRAIL-R3, TRAIL-R4, OPG , RANK and RANKL gene, as shown here. A 10µl aliquot of each product was loaded and run in the same 1.2% agarose/ TBE gel and stained with ethidium bromide. The PCR products were then compared with the standard, loaded in the same gel. The red arrows indicate the size of the samples on the DNA ladder.

VIII Appendix B

	Apoptosis	Necrosis
Patterns of death	Single cells	Groups of neighboring cells

Cell size	Shrinkage	Swelling
	Fragmentation	
Plasma membrane	Preserved continuity	Smoothing
	Blebbed	Early lysis
	Phosphatidylserine on surface	
Mitochondria	Increased membrane permeability	Swelling
	Contents released into cytoplasm	Disordered structure
	Cytochrome c; Apaf1	
	Structure relatively preserved	
Organelle shape	Contracted	Swelling
	"Apoptotic bodies"	Disruption
Nuclei	Chromatin:	Membrane disruption
	Clumps & Fragmented	
DNA degradation	Fragmented	Diffuse & Random
	Internucleosomal cleavage	
	Free 3' ends	
	Laddering on electrophoresis	
	DNA appears in cytoplasm	
Cell degradation	Phagocytosis	Inflammation
	No inflammation	Macrophage invasion
General stimuli	Developmental programs	Disease processes
	Endogenous signals	
	Intercellular signals	
	Disease processes	
Specific stimuli	Growth factor deprivation: NGF; IL-2	Toxic
	Death activators: Bind to surface receptors	Severe ischemia

	Cytokines: TNF-α; Lymphotoxin	Radiation
	FasL	
	TRAIL	
	Toxic: Hormones; Radiation; Mild ischemia	
	Oxidants in cell: Increased	
	DNA damage	
Cellular processes	Programmed cascade of reactions	No protein synthesis
	Caspase activation	No RNA transcription
	Internucleosomal endonucleases	Energy independent
	Transglutaminase activation	ATP depletion
	Requires	
	New RNA transcription	
	Protein synthesis	
	ATP	
Apoptosis inhibitors	Protease inhibitors IAP-1, 2 & 3, p35 etc.	
	Bcl-2 family (Some). Bcl-2, Bcl-xL, Bcl-w. Mcl-1	
Apoptosis promoters	Bcl-2 family (Some). Bax, Bcl-xS etc.	

Table 8.1 The diagram shows that the basic morphological changes happen when cells undergo apoptosis or necrosis.

This piece of work has been presented in the scientific conference of society of Vascular Medicine and Biology in California, USA in June 2004. It also has been nominated as one of 6 finalists for the Young Scientist of the Year Award.

This updated results of this work have been presented in the scientific session of South West Vascular Surgeons' conference in Oxford in March 2005.

This work is submitted to journals for publishing.

References

Aikawa, M., P.N.Sivam, Kuro-o M, K.Kimura, K.Nakahara, S.Takewaki, M.Ueda, H.Yamaguchi, Y.Yazaki, M.Periasamy, and . 1993. Human smooth muscle myosin heavy chain isoforms as molecular markers for vascular development and atherosclerosis. *Circ. Res.* 73:1000-1012.

Alcorn, H.G., S.K.Wolfson, Jr., K.Sutton-Tyrrell, L.H.Kuller, and D.O'Leary. 1996. Risk factors for abdominal aortic aneurysms in older adults enrolled in The Cardiovascular Health Study. *Arterioscler. Thromb. Vasc. Biol.* 16:963-970.

Allison, M.A., M.H.Criqui, and C.M.Wright. 2004. Patterns and risk factors for systemic calcified atherosclerosis. *Arterioscler. Thromb. Vasc. Biol.* 24:331-336.

Anna-Kaisa Eerola. Apoptosis and apoptosis regulating proteins and factors in small and large cell lung carcinoma. 2000. University of Oulu.

Aubin, J.E. and E.Bonnelye. 2000. Osteoprotegerin and its ligand: a new paradigm for regulation of osteoclastogenesis and bone resorption. *Osteoporos. Int.* 11:905-913.

Ballou, L.R., S.J.Laulederkind, E.F.Rosloniec, and R.Raghow. 1996. Ceramide signalling and the immune response. *Biochim. Biophys. Acta* 1301:273-287.

Bennett, M.R., G.I.Evan, and A.C.Newby. 1994. Deregulated expression of the c-myc oncogene abolishes inhibition of proliferation of rat vascular smooth muscle cells by serum reduction, interferon-gamma, heparin, and cyclic nucleotide analogues and induces apoptosis. *Circ. Res.* 74:525-536.

Bennett, M.R., G.I.Evan, and S.M.Schwartz. 1995. Apoptosis of rat vascular smooth muscle cells is regulated by p53-dependent and -independent pathways. *Circ. Res.* 77:266-273.

Berger, T. and M.Kretzler. 2002. TRAIL-induced apoptosis is independent of the mitochondrial apoptosis mediator DAP3. *Biochem. Biophys. Res. Commun.* 297:880-884.

Bjorkerud, S., B.Bjorkerud, and M.Joelsson. 1994. Structural organization of reconstituted human arterial smooth muscle tissue. *Arterioscler. Thromb.* 14:644-651.

Blacher, J., A.P.Guerin, B.Pannier, S.J.Marchais, and G.M.London. 2001. Arterial calcifications, arterial stiffness, and cardiovascular risk in end-stage renal disease. *Hypertension* 38:938-942.

Blair, J.M., H.Zhou, M.J.Seibel, and C.R.Dunstan. 2006. Mechanisms of disease: roles of OPG, RANKL and RANK in the pathophysiology of skeletal metastasis. *Nat. Clin. Pract. Oncol.* 3:41-49.

Blanchard, J.F. 1999. Epidemiology of abdominal aortic aneurysms. *Epidemiol. Rev.* 21:207-221.

Boatright, K.M., C.Deis, J.B.Denault, D.P.Sutherlin, and G.S.Salvesen. 2004. Activation of caspases-8 and -10 by FLIP(L). *Biochem. J.* 382:651-657.

Bollag, D.M., M.D.Rozycki, and S.J.Edelstein. 1996. protein methods.

Bonewald, L.F., S.E.Harris, J.Rosser, M.R.Dallas, S.L.Dallas, N.P.Camacho, B.Boyan, and A.Boskey. 2003. von Kossa staining alone is not sufficient to confirm that mineralization *in vitro* represents bone formation. *Calcif. Tissue Int.* 72:537-547.

Boom, R., C.J.Sol, M.M.Salimans, C.L.Jansen, P.M.Wertheim-van Dillen, and N.J.van der. 1990. Rapid and simple method for purification of nucleic acids. *J. Clin. Microbiol.* 28:495-503.

Bostrom, K. 2001. Insights into the mechanism of vascular calcification. *Am. J. Cardiol.* 88:20E-22E.

Bostrom, K.I. 2000. Cell differentiation in vascular calcification. *Z. Kardiol.* 89 Suppl 2:69-74.

Brandstrom, H., P.Gerdhem, F.Stiger, K.J.Obrant, H.Melhus, O.Ljunggren, A.Kindmark, and K.Akesson. 2004. Single nucleotide polymorphisms in the human gene for osteoprotegerin are not related to bone mineral density or fracture in elderly women. *Calcif. Tissue Int.* 74:18-24.

Brandstrom, H., F.Stiger, L.Lind, T.Kahan, H.Melhus, and A.Kindmark. 2002. A single nucleotide polymorphism in the promoter region of the human gene for osteoprotegerin is related to vascular morphology and function. *Biochem. Biophys. Res. Commun.* 293:13-17.

Bucay, N., I.Sarosi, C.R.Dunstan, S.Morony, J.Tarpley, C.Capparelli, S.Scully, H.L.Tan, W.Xu, D.L.Lacey, W.J.Boyle, and W.S.Simonet. 1998. osteoprotegerin-deficient mice develop early onset osteoporosis and arterial calcification. *Genes Dev.* 12:1260-1268.

Cates, J.R. 1997. Abdominal aortic aneurysms: clinical diagnosis and management. *J. Manipulative Physiol Ther.* 20:557-561.

Chai, J., E.Shiozaki, S.M.Srinivasula, Q.Wu, P.Datta, E.S.Alnemri, and Y.Shi. 2001. Structural basis of caspase-7 inhibition by XIAP. *Cell* 104:769-780.

Chan, W.L., N.Pejnovic, H.Hamilton, T.V.Liew, D.Popadic, A.Poggi, and S.M.Khan. 2005. Atherosclerotic abdominal aortic aneurysm and the interaction between autologous human plaque-derived vascular smooth muscle cells, type 1 NKT, and helper T cells. *Circ. Res.* 96:675-683.

Chapman, H.A., R.J.Riese, and G.P.Shi. 1997. Emerging roles for cysteine proteases in human biology. *Annu. Rev. Physiol* 59:63-88.

Chawla-Sarkar, M., D.W.Leaman, B.S.Jacobs, and E.C.Borden. 2002. IFN-beta pretreatment sensitizes human melanoma cells to TRAIL/Apo2 ligand-induced apoptosis. *J. Immunol.* 169:847-855.

Chemicon international. ApopTag plus fluorescein in situ apoptosis detection kit manual. 2006.

Chen, N.X. and S.M.Moe. 2003. Arterial calcification in diabetes. *Curr. Diab. Rep.* 3:28-32.

Cheuk, B.L. and S.W.Cheng. 2005. Expression of integrin alpha5beta1 and the relationship to collagen and elastin content in human suprarenal and infrarenal aortas. *Vasc. Endovascular. Surg.* 39:245-251.

Chirgwin, J.M., A.E.Przybyla, R.J.MacDonald, and W.J.Rutter. 1979. Isolation of biologically active ribonucleic acid from sources enriched in ribonuclease. *Biochemistry* 18:5294-5299.

Cho, A., D.W.Courtman, and B.L.Langille. 1995. Apoptosis (programmed cell death) in arteries of the neonatal lamb. *Circ. Res.* 76:168-175.

Choi, C. and E.N.Benveniste. 2004. Fas ligand/Fas system in the brain: regulator of immune and apoptotic responses. *Brain Res. Brain Res. Rev.* 44:65-81.

Chomczynski, P. and N.Sacchi. 1987. Single-step method of RNA isolation by acid guanidinium thiocyanate-phenol-chloroform extraction. *Anal. Biochem.* 162:156-159.

Chou, A.H., H.F.Tsai, L.L.Lin, S.L.Hsieh, P.I.Hsu, and P.N.Hsu. 2001. Enhanced proliferation and increased IFN-gamma production in T cells by signal transduced through TNF-related apoptosis-inducing ligand. *J. Immunol.* 167:1347-1352.

Cohen, G.M. 1997. Caspases: the executioners of apoptosis. *Biochem. J.* 326 (Pt 1):1-16.

Cohen, J.R., I.Sarfati, D.Danna, and L.Wise. 1992. Smooth muscle cell elastase, atherosclerosis, and abdominal aortic aneurysms. *Ann. Surg.* 216:327-330.

Collin-Osdoby, P. 2004. Regulation of vascular calcification by osteoclast regulatory factors RANKL and osteoprotegerin. *Circ. Res.* 95:1046-1057.

Crawford, C.M., K.Hurtgen-Grace, E.Talarico, and J.Marley. 2003. Abdominal aortic aneurysm: an illustrated narrative review. *J. Manipulative Physiol Ther.* 26:184-195.

Cregan, S.P., V.L.Dawson, and R.S.Slack. 2004. Role of AIF in caspase-dependent and caspase-independent cell death. *Oncogene* 23:2785-2796.

Crist, S.A., B.D.Elzey, A.T.Ludwig, T.S.Griffith, J.B.Staack, S.R.Lentz, and T.L.Ratliff. 2004. Expression of TNF-related apoptosis-inducing ligand (TRAIL) in megakaryocytes and platelets. *Exp. Hematol.* 32:1073-1081.

da Silva, M.A. and M.A.Arruda. 2006. Mechanization of the Bradford reaction for the spectrophotometric determination of total proteins. *Anal. Biochem.* 351:155-157.

Dawson, J., E.Choke, S.Sayed, G.Cockerill, I.Loftus, and M.M.Thompson. 2006. Pharmacotherapy of abdominal aortic aneurysms. *Curr. Vasc. Pharmacol.* 4:129-149.

Dellegrottaglie, S., J.Sanz, and S.Rajagopalan. 2006. Molecular determinants of vascular calcification: a bench to bedside view. *Curr. Mol. Med.* 6:515-524.

Demer, L.L. 2002. Vascular calcification and osteoporosis: inflammatory responses to oxidized lipids. *Int. J. Epidemiol.* 31:737-741.

Demer, L.L. and Y.Tintut. 2003. Mineral exploration: search for the mechanism of vascular calcification and beyond: the 2003 Jeffrey M. Hoeg Award lecture. *Arterioscler. Thromb. Vasc. Biol.* 23:1739-1743.

Dhore, C.R., J.P.Cleutjens, E.Lutgens, K.B.Cleutjens, P.P.Geusens, P.J.Kitslaar, J.H.Tordoir, H.M.Spronk, C.Vermeer, and M.J.Daemen. 2001. Differential expression of bone matrix regulatory proteins in human atherosclerotic plaques. *Arterioscler. Thromb. Vasc. Biol.* 21:1998-2003.

Dixon.K.J., Vince D.G., Cothren R.M., and Cornhill J.F. Characterization of coronary plaque in intravascular ultrasound using histological correlation. internatinal conference-IEEE/EMBS. 1997. Chicago, IL, USA. 30-10-1997. Ref Type: Conference Proceeding

Doherty, T.M., L.A.Fitzpatrick, A.Shaheen, T.B.Rajavashisth, and R.C.Detrano. 2004. Genetic determinants of arterial calcification associated with atherosclerosis. *Mayo Clin. Proc.* 79:197-210.

Du, C., M.Fang, Y.Li, L.Li, and X.Wang. 2000. Smac, a mitochondrial protein that promotes cytochrome c-dependent caspase activation by eliminating IAP inhibition. *Cell* 102:33-42.

Ellis, H.M. and H.R.Horvitz. 1986. Genetic control of programmed cell death in the nematode C. elegans. *Cell* 44:817-829.

Erdogan, B., E.Aslan, T.Bagis, A.Gokcel, S.Erkanli, M.Bavbek, and N.Altinors. 2004. Intima-media thickness of the carotid arteries is related to serum osteoprotegerin levels in healthy postmenopausal women. *Neurol. Res.* 26:658-661.

Ernst, C.B. 1993. Abdominal aortic aneurysm. *N. Engl. J. Med.* 328:1167-1172.

Fadeel, B. and S.Orrenius. 2005. Apoptosis: a basic biological phenomenon with wide-ranging implications in human disease. *J. Intern. Med.* 258:479-517.

Fanger, N.A., C.R.Maliszewski, K.Schooley, and T.S.Griffith. 1999. Human dendritic cells mediate cellular apoptosis via tumor necrosis factor-related apoptosis-inducing ligand (TRAIL). *J. Exp. Med.* 190:1155-1164.

Finley, R.S. 2003. Overview of targeted therapies for cancer. *Am. J. Health Syst. Pharm.* 60:S4-10.

Fitzpatrick, L.A., R.T.Turner, and E.R.Ritman. 2003. Endochondral bone formation in the heart: a possible mechanism of coronary calcification. *Endocrinology* 144:2214-2219.

Frederic H.Martini. 2005. Fundamentals of anatomy & physiology. Benjamin Cummings.

Ganten, T.M., T.L.Haas, J.Sykora, H.Stahl, M.R.Sprick, S.C.Fas, A.Krueger, M.A.Weigand, A.Grosse-Wilde, W.Stremmel, P.H.Krammer, and H.Walczak. 2004. Enhanced caspase-8 recruitment to and activation at the DISC is critical for sensitisation of human hepatocellular carcinoma cells to TRAIL-induced apoptosis by chemotherapeutic drugs. *Cell Death. Differ.* 11 Suppl 1:S86-S96.

Garcia-Touchard, A., T.D.Henry, G.Sangiorgi, L.G.Spagnoli, A.Mauriello, C.Conover, and R.S.Schwartz. 2005. Extracellular proteases in atherosclerosis and restenosis. *Arterioscler. Thromb. Vasc. Biol.* 25:1119-1127.

Geng, Y.J., Q.Wu, M.Muszynski, G.K.Hansson, and P.Libby. 1996. Apoptosis of vascular smooth muscle cells induced by *in vitro* stimulation with interferon-gamma, tumor necrosis factor-alpha, and interleukin-1 beta. *Arterioscler. Thromb. Vasc. Biol.* 16:19-27.

Giachelli, C.M., M.Y.Speer, X.Li, R.M.Rajachar, and H.Yang. 2005. Regulation of vascular calcification: roles of phosphate and osteopontin. *Circ. Res.* 96:717-722.

gli-Esposti, M.A., W.C.Dougall, P.J.Smolak, J.Y.Waugh, C.A.Smith, and R.G.Goodwin. 1997. The novel receptor TRAIL-R4 induces NF-kappaB and protects against TRAIL-mediated apoptosis, yet retains an incomplete death domain. *Immunity.* 7:813-820.

Gochuico, B.R., J.Zhang, B.Y.Ma, A.Marshak-Rothstein, and A.Fine. 2000. TRAIL expression in vascular smooth muscle. *Am. J. Physiol Lung Cell Mol. Physiol* 278:L1045-L1050.

Gohel, A., M.B.McCarthy, and G.Gronowicz. 1999. Estrogen prevents glucocorticoid-induced apoptosis in osteoblasts *in vivo* and *in vitro*. *Endocrinology* 140:5339-5347.

Golledge, J., M.McCann, S.Mangan, A.Lam, and M.Karan. 2004. Osteoprotegerin and osteopontin are expressed at high concentrations within symptomatic carotid atherosclerosis. *Stroke* 35:1636-1641.

Grataroli, R., D.Vindrieux, J.Selva, C.Felsenheld, A.Ruffion, M.Decaussin, and M.Benahmed. 2004. Characterization of tumour necrosis factor-alpha-related apoptosis-inducing ligand and its receptors in the adult human testis. *Mol. Hum. Reprod.* 10:123-128.

Gray H. 1918. Anatomy of human body. PHILADELPHIA: LEA & FEBIGER.

Greenhalgh, R.M., L.C.Brown, J.T.Powell, and S.G.Thompson. 2006. - Current interpretation of the UK EVAR Trials. - *Acta Chir Belg.*-8.

Griffith, T.S. and D.H.Lynch. 1998. TRAIL: a molecule with multiple receptors and control mechanisms. *Curr. Opin. Immunol.* 10:559-563.

Gronholdt, M.L. 1999. Ultrasound and lipoproteins as predictors of lipid-rich, rupture-prone plaques in the carotid artery. *Arterioscler. Thromb. Vasc. Biol.* 19:2-13.

Gruss, H.J. 1996. Molecular, structural, and biological characteristics of the tumor necrosis factor ligand superfamily. *Int. J. Clin. Lab Res.* 26:143-159.

Hak, A.E., H.A.Pols, A.M.van Hemert, A.Hofman, and J.C.Witteman. 2000. Progression of aortic calcification is associated with metacarpal bone loss during menopause: a population-based longitudinal study. *Arterioscler. Thromb. Vasc. Biol.* 20:1926-1931.

Hakansson, A., B.Zhivotovsky, S.Orrenius, H.Sabharwal, and C.Svanborg. 1995. Apoptosis induced by a human milk protein. *Proc. Natl. Acad. Sci. U. S. A* 92:8064-8068.

Halloran, B.G. and B.T.Baxter. 1995. Pathogenesis of aneurysms. *Semin. Vasc. Surg.* 8:85-92.

Hashimoto, S., R.L.Ochs, F.Rosen, J.Quach, G.McCabe, J.Solan, J.E.Seegmiller, R.Terkeltaub, and M.Lotz. 1998. Chondrocyte-derived apoptotic bodies and calcification of articular cartilage. *Proc. Natl. Acad. Sci. U. S. A* 95:3094-3099.

Hawkins, N.J., J.Lees, and R.L.Ward. 1997. Detection of apoptosis in colorectal carcinoma by light microscopy and in situ end labelling. *Anal. Quant. Cytol. Histol.* 19:227-232.

Hay, S. and G.Kannourakis. 2002. A time to kill: viral manipulation of the cell death program. *J. Gen. Virol.* 83:1547-1564.

He, C.M. and M.R.Roach. 1994. The composition and mechanical properties of abdominal aortic aneurysms. *J. Vasc. Surg.* 20:6-13.

Hiatt, W.R., L.Cox, M.Greenwalt, A.Griffin, and C.Schechter. 2005. Quality of the assessment of primary and secondary endpoints in claudication and critical leg ischemia trials. *Vasc. Med.* 10:207-213.

Higuchi, H., S.F.Bronk, M.Taniai, A.Canbay, and G.J.Gores. 2002. Cholestasis increases tumor necrosis factor-related apoptotis-inducing ligand (TRAIL)-R2/DR5 expression and sensitizes the liver to TRAIL-mediated cytotoxicity. *J. Pharmacol. Exp. Ther.* 303:461-467.

Hofbauer, L.C. and A.E.Heufelder. 2001. Role of receptor activator of nuclear factor-kappaB ligand and osteoprotegerin in bone cell biology. *J. Mol. Med.* 79:243-253.

Hofbauer, L.C., C.Shui, B.L.Riggs, C.R.Dunstan, T.C.Spelsberg, T.O'Brien, and S.Khosla. 2001. Effects of immunosuppressants on receptor activator of NF-kappaB ligand and osteoprotegerin production by human osteoblastic and coronary artery smooth muscle cells. *Biochem. Biophys. Res. Commun.* 280:334-339.

Hu, S., C.Vincenz, J.Ni, R.Gentz, and V.M.Dixit. 1997. I-FLICE, a novel inhibitor of tumor necrosis factor receptor-1- and CD-95-induced apoptosis. *J. Biol. Chem.* 272:17255-17257.

Huang, Y., Y.C.Park, R.L.Rich, D.Segal, D.G.Myszka, and H.Wu. 2001. Structural basis of caspase inhibition by XIAP: differential roles of the linker versus the BIR domain. *Cell* 104:781-790.

Hymowitz, S.G., M.P.O'Connell, M.H.Ultsch, A.Hurst, K.Totpal, A.Ashkenazi, A.M.de Vos, and R.F.Kelley. 2000. A unique zinc-binding site revealed by a high-resolution X-ray structure of homotrimeric Apo2L/TRAIL. *Biochemistry* 39:633-640.

Israels, L.G. and E.D.Israels. 1999. Apoptosis. *Stem Cells* 17:306-313.

Jackson, C.E. and J.M.Puck. 1999. Autoimmune lymphoproliferative syndrome, a disorder of apoptosis. *Curr. Opin. Pediatr.* 11:521-527.

Janssen, H.L., H.Higuchi, A.Abdulkarim, and G.J.Gores. 2003. Hepatitis B virus enhances tumor necrosis factor-related apoptosis-inducing ligand (TRAIL)

cytotoxicity by increasing TRAIL-R1/death receptor 4 expression. *J. Hepatol.* 39:414-420.

Jerareungrattan, A., M.Sila-asna, and A.Bunyaratvej. 2005. Increased smooth muscle actin expression from bone marrow stromal cells under retinoic acid treatment: an attempt for autologous blood vessel tissue engineering. *Asian Pac. J. Allergy Immunol.* 23:107-113.

Jian, B., N.Narula, Q.Y.Li, E.R.Mohler, III, and R.J.Levy. 2003. Progression of aortic valve stenosis: TGF-beta1 is present in calcified aortic valve cusps and promotes aortic valve interstitial cell calcification via apoptosis. *Ann. Thorac. Surg.* 75:457-465.

Jin, T.G., A.Kurakin, N.Benhaga, K.Abe, M.Mohseni, F.Sandra, K.Song, B.K.Kay, and R.Khosravi-Far. 2004. Fas-associated protein with death domain (FADD)-independent recruitment of c-FLIPL to death receptor 5. *J. Biol. Chem.* 279:55594-55601.

Jono, S., Y.Ikari, A.Shioi, K.Mori, T.Miki, K.Hara, and Y.Nishizawa. 2002. Serum osteoprotegerin levels are associated with the presence and severity of coronary artery disease. *Circulation* 106:1192-1194.

Jorgensen, L., K.Singh, G.K.Berntsen, and B.K.Jacobsen. 2004. A population-based study of the prevalence of abdominal aortic aneurysms in relation to bone mineral density: the Tromso study. *Am. J. Epidemiol.* 159:945-949.

Kang, J., R.R.Kisenge, H.Toyoda, S.Tanaka, J.Bu, E.Azuma, and Y.Komada. 2003. Chemical sensitization and regulation of TRAIL-induced apoptosis in a panel of B-lymphocytic leukaemia cell lines. *Br. J. Haematol.* 123:921-932.

Kaito, K., H.Urayama, and G.Watanabe. 2003. - Doxycycline treatment in a model of early abdominal aortic aneurysm. - *Surg Today.*-33.

Kayagaki, N., N.Yamaguchi, M.Nakayama, H.Eto, K.Okumura, and H.Yagita. 1999a. Type I interferons (IFNs) regulate tumor necrosis factor-related apoptosis-inducing ligand (TRAIL) expression on human T cells: A novel mechanism for the antitumor effects of type I IFNs. *J. Exp. Med.* 189:1451-1460.

Kayagaki, N., N.Yamaguchi, M.Nakayama, A.Kawasaki, H.Akiba, K.Okumura, and H.Yagita. 1999b. Involvement of TNF-related apoptosis-inducing ligand in human CD4+ T cell-mediated cytotoxicity. *J. Immunol.* 162:2639-2647.

Kerr, J.F., A.H.Wyllie, and A.R.Currie. 1972. Apoptosis: a basic biological phenomenon with wide-ranging implications in tissue kinetics. *Br. J. Cancer* 26:239-257.

Kiernan, J.A. 2001. Histological and Histochemical Methods: Theory and Practice. A Hodder Arnold Publication.

Kim, Y.S., K.H.Kim, J.A.Choi, J.H.Lee, H.K.Kim, N.H.Won, and I.Kim. 2000. Fas (APO-1/CD95) ligand and Fas expression in renal cell carcinomas: correlation with the prognostic factors. *Arch. Pathol. Lab Med.* 124:687-693.

Kondo, S., N.Hashimoto, H.Kikuchi, F.Hazama, I.Nagata, and H.Kataoka. 1998. Apoptosis of medial smooth muscle cells in the development of saccular cerebral aneurysms in rats. *Stroke* 29:181-188.

Krieg, A., T.Krieg, M.Wenzel, M.Schmitt, U.Ramp, B.Fang, H.E.Gabbert, C.D.Gerharz, and C.Mahotka. 2003. TRAIL-beta and TRAIL-gamma: two novel splice variants of the human TNF-related apoptosis-inducing ligand (TRAIL) without apoptotic potential. *Br. J. Cancer* 88:918-927.

Kulesz-Martin, M., J.Lagowski, S.Fei, C.Pelz, R.Sears, M.B.Powell, R.Halaban, and J.Johnson. 2005. Melanocyte and keratinocyte carcinogenesis: p53 family protein activities and intersecting mRNA expression profiles. *J. Investig. Dermatol. Symp. Proc.* 10:142-152.

Kuro-o M, R.Nagai, H.Tsuchimochi, H.Katoh, Y.Yazaki, A.Ohkubo, and F.Takaku. 1989. Developmentally regulated expression of vascular smooth muscle myosin heavy chain isoforms. *J. Biol. Chem.* 264:18272-18275.

Labat-Moleur, F., C.Guillermet, P.Lorimier, C.Robert, S.Lantuejoul, E.Brambilla, and A.Negoescu. 1998. TUNEL apoptotic cell detection in tissue sections: critical evaluation and improvement critical evaluation and improvement. *J. Histochem. Cytochem.* 46:327-334.

Laemmli, U.K. 1970. Cleavage of structural proteins during the assembly of the head of bacteriophage T4. *Nature* 227:680-685.

LeBlanc, H.N. and A.Ashkenazi. 2003. Apo2L/TRAIL and its death and decoy receptors. *Cell Death. Differ.* 10:66-75.

Lee, H.O., J.M.Herndon, R.Barreiro, T.S.Griffith, and T.A.Ferguson. 2002. TRAIL: a mechanism of tumor surveillance in an immune privileged site. *J. Immunol.* 169:4739-4744.

Lesauskaite, V., L.Ivanoviene, and A.Valanciute. 2003. [Programmed cellular death and atherogenesis: from molecular mechanisms to clinical aspects]. *Medicina (Kaunas.)* 39:529-534.

Lettre, G. and M.O.Hengartner. 2006. Developmental apoptosis in C. elegans: a complex CEDnario. *Nat. Rev. Mol. Cell Biol.* 7:97-108.

Leverkus, M., M.Neumann, T.Mengling, C.T.Rauch, E.B.Brocker, P.H.Krammer, and H.Walczak. 2000. Regulation of tumor necrosis factor-related apoptosis-inducing ligand sensitivity in primary and transformed human keratinocytes. *Cancer Res.* 60:553-559.

Leverkus, M., M.R.Sprick, T.Wachter, T.Mengling, B.Baumann, E.Serfling, E.B.Brocker, M.Goebeler, M.Neumann, and H.Walczak. 2003. Proteasome inhibition results in TRAIL sensitization of primary keratinocytes by removing the resistance-mediating block of effector caspase maturation. *Mol. Cell Biol.* 23:777-790.

Li, P., D.Nijhawan, I.Budihardjo, S.M.Srinivasula, M.Ahmad, E.S.Alnemri, and X.Wang. 1997. Cytochrome c and dATP-dependent formation of Apaf-1/caspase-9 complex initiates an apoptotic protease cascade. *Cell* 91:479-489.

Libby Peter. 2002. The Vascular Biology of Atherosclerosis.

Lieberman, J. 2003. The ABCs of granule-mediated cytotoxicity: new weapons in the arsenal. *Nat. Rev. Immunol.* 3:361-370.

Lopez-Candales, A., D.R.Holmes, S.Liao, M.J.Scott, S.A.Wickline, and R.W.Thompson. 1997b. Decreased vascular smooth muscle cell density in medial degeneration of human abdominal aortic aneurysms. *Am. J. Pathol.* 150:993-1007.

Lopez-Candales, A., D.R.Holmes, S.Liao, M.J.Scott, S.A.Wickline, and R.W.Thompson. 1997a. Decreased vascular smooth muscle cell density in medial degeneration of human abdominal aortic aneurysms. *Am. J. Pathol.* 150:993-1007.

Luiz Carlos Junqueira, Jose Carneiro, and Robert O Kelley. 1998. Basic histology. McGraw-Hill Publishing Co.

Lynch,M.M., B.H.Thorp, and C.C.Withe head. Avian tibial dyschondroplasia as a cause of bone deformity. Avian Pathol. 21, 275-285. 1992.

MacFarlane, M. 2003. TRAIL-induced signalling and apoptosis. *Toxicol. Lett.* 139:89-97.

Maeda T. 1996. clinical study on the growing process of abdominal aortic aneurysms. *Yonago Igaku Zasshi* 47:150-159.

Malyankar, U.M., M.Scatena, K.L.Suchland, T.J.Yun, E.A.Clark, and C.M.Giachelli. 2000. Osteoprotegerin is an alpha vbeta 3-induced, NF-kappa B-dependent survival factor for endothelial cells. *J. Biol. Chem.* 275:20959-20962.

Mariani, S.M. and P.H.Krammer. 1998. Differential regulation of TRAIL and CD95 ligand in transformed cells of the T and B lymphocyte lineage. *Eur. J. Immunol.* 28:973-982.

Marini, P., V.Jendrossek, E.Durand, C.Gruber, W.Budach, and C.Belka. 2003. Molecular requirements for the combined effects of TRAIL and ionising radiation. *Radiother. Oncol.* 68:189-198.

Marsters, S.A., J.P.Sheridan, R.M.Pitti, A.Huang, M.Skubatch, D.Baldwin, J.Yuan, A.Gurney, A.D.Goddard, P.Godowski, and A.Ashkenazi. 1997. A novel receptor for Apo2L/TRAIL contains a truncated death domain. *Curr. Biol.* 7:1003-1006.

Matsuda, T., A.Almasan, M.Tomita, J.N.Uchihara, M.Masuda, K.Ohshiro, N.Takasu, H.Yagita, T.Ohta, and N.Mori. 2005. Resistance to Apo2 ligand (Apo2L)/tumor necrosis factor-related apoptosis-inducing ligand (TRAIL)-mediated apoptosis and constitutive expression of Apo2L/TRAIL in human T-cell leukemia virus type 1-infected T-cell lines. *J. Virol.* 79:1367-1378.

Matsushita, M., N.Nishikimi, T.Sakurai, and Y.Nimura. 2000. Relationship between aortic calcification and atherosclerotic disease in patients with abdominal aortic aneurysm. *Int. Angiol.* 19:276-279.

Maynar, M., Z.Qian, J.Hernandez, F.Sun, C.DeMiguel, V.Crisostomo, J.Uson, L.F.Pineda, C.G.Espinoza, and W.R.Castaneda. 2003. - An animal model of abdominal aortic aneurysm created with peritoneal patch: technique and initial results. - *Cardiovasc Intervent Radiol.*-76.

Melloni, E., P.Secchiero, C.Celeghini, D.Campioni, V.Grill, L.Guidotti, and G.Zauli. 2005. Functional expression of TRAIL and TRAIL-R2 during human megakaryocytic development. *J. Cell Physiol* 204:975-982.

Michael Quinion. 1996. World Wide Word.

Min, H., S.Morony, I.Sarosi, C.R.Dunstan, C.Capparelli, S.Scully, G.Van, S.Kaufman, P.J.Kostenuik, D.L.Lacey, W.J.Boyle, and W.S.Simonet. 2000. Osteoprotegerin reverses osteoporosis by inhibiting endosteal osteoclasts and prevents vascular calcification by blocking a process resembling osteoclastogenesis. *J. Exp. Med.* 192:463-474.

Mitsiades, N., C.S.Mitsiades, V.Poulaki, D.Chauhan, P.G.Richardson, T.Hideshima, N.C.Munshi, S.P.Treon, and K.C.Anderson. 2002. Apoptotic signaling induced by immunomodulatory thalidomide analogs in human multiple myeloma cells: therapeutic implications. *Blood* 99:4525-4530.

Miyashita, T., A.Kawakami, T.Nakashima, S.Yamasaki, M.Tamai, F.Tanaka, M.Kamachi, H.Ida, K.Migita, T.Origuchi, K.Nakao, and K.Eguchi. 2004. Osteoprotegerin (OPG) acts as an endogenous decoy receptor in tumour necrosis factor-related apoptosis-inducing ligand (TRAIL)-mediated apoptosis of fibroblast-like synovial cells. *Clin. Exp. Immunol.* 137:430-436.

Moran, C.S., M.McCann, M.Karan, P.Norman, N.Ketheesan, and J.Golledge. 2005a. Association of osteoprotegerin with human abdominal aortic aneurysm progression. *Circulation* 111:3119-3125.

Muzio, M. 1998. Signalling by proteolysis: death receptors induce apoptosis. *Int. J. Clin. Lab Res.* 28:141-147.

Nakayama, M., N.Kayagaki, N.Yamaguchi, K.Okumura, and H.Yagita. 2000. Involvement of TWEAK in interferon gamma-stimulated monocyte cytotoxicity. *J. Exp. Med.* 192:1373-1380.

Nitta, K., T.Akiba, K.Uchida, A.Kawashima, W.Yumura, T.Kabaya, and H.Nihei. 2003. The progression of vascular calcification and serum osteoprotegerin levels in patients on long-term hemodialysis. *Am. J. Kidney Dis.* 42:303-309.

Ochi, M., H.Ohdan, H.Mitsuta, T.Onoe, D.Tokita, H.Hara, K.Ishiyama, W.Zhou, Y.Tanaka, and T.Asahara. 2004. Liver NK cells expressing TRAIL are toxic against self hepatocytes in mice. *Hepatology* 39:1321-1331.

Otto, C.M., R.A.Nishimura, K.B.Davis, K.B.Kisslo, and T.M.Bashore. 1991. Doppler echocardiographic findings in adults with severe symptomatic valvular aortic stenosis. Balloon Valvuloplasty Registry Echocardiographers. *Am. J. Cardiol.* 68:1477-1484.

Ou, D., X.Wang, D.L.Metzger, M.Robbins, J.Huang, C.Jobin, J.K.Chantler, R.F.James, P.Pozzilli, and A.J.Tingle. 2005. Regulation of TNF-related apoptosis-inducing ligand-mediated death-signal pathway in human beta cells by Fas-associated death domain and nuclear factor kappaB. *Hum. Immunol.* 66:799-809.

Parone, P.A., D.James, and J.C.Martinou. 2002. Mitochondria: regulating the inevitable. *Biochimie* 84:105-111.

Paul, S. and L.Smith. 2005. The metabolic syndrome in women: a growing problem for cardiac risk. *J. Cardiovasc. Nurs.* 20:427-432.

Pennisi, P., S.S.Signorelli, S.Riccobene, G.Celotta, P.L.Di, M.T.La, and C.E.Fiore. 2004. Low bone density and abnormal bone turnover in patients with atherosclerosis of peripheral vessels. *Osteoporos. Int.* 15:389-395.

Peter, M.E. 2004. The flip side of FLIP. *Biochem. J.* 382:e1-e3.

Pitti, R.M., S.A.Marsters, S.Ruppert, C.J.Donahue, A.Moore, and A.Ashkenazi. 1996. Induction of apoptosis by Apo-2 ligand, a new member of the tumor necrosis factor cytokine family. *J. Biol. Chem.* 271:12687-12690.

Plutzky, J. 2003. The vascular biology of atherosclerosis. *Am. J. Med.* 115 Suppl 8A:55S-61S.

Powell J. Medial therapy to slow AAA growth. Vascular Surgical Society of Great Britain and Ireland. 2004.
Ref Type: Conference Proceeding

Prisant, L.M. and J.S.Mondy, III. 2004. Abdominal aortic aneurysm. *J. Clin. Hypertens. (Greenwich.)* 6:85-89.

Pritzker, L.B., M.Scatena, and C.M.Giachelli. 2004. The role of osteoprotegerin and tumor necrosis factor-related apoptosis-inducing ligand in human microvascular endothelial cell survival. *Mol. Biol. Cell* 15:2834-2841.

Proudfoot, D. and C.M.Shanahan. 2001. Biology of calcification in vascular cells: intima versus media. *Herz* 26:245-251.

Proudfoot, D., J.N.Skepper, L.Hegyi, M.R.Bennett, C.M.Shanahan, and P.L.Weissberg. 2000. Apoptosis regulates human vascular calcification *in vitro*: evidence for initiation of vascular calcification by apoptotic bodies. *Circ. Res.* 87:1055-1062.

Proudfoot, D., J.N.Skepper, L.Hegyi, A.Farzaneh-Far, C.M.Shanahan, and P.L.Weissberg. 2001. The role of apoptosis in the initiation of vascular calcification. *Z. Kardiol.* 90 Suppl 3:43-46.

Qian, J. and Z.X.Chen. 2002. [TNF-related apoptosis-inducing ligand signaling pathway and hematopoietic malignancies]. *Zhongguo Shi Yan. Xue. Ye. Xue. Za Zhi.* 10:472-477.

Quick C. the epidemology of aneurysm. Vascular Surgical Society of Great Britain and Ireland. 2004.
Ref Type: Conference Proceeding

Raggi, P. 2005. Cardiovascular calcification in end stage renal disease. *Contrib. Nephrol.* 149:272-278.

Rebecca R.Pauly, Claudio Bilato, Robert Monticone, and Michael T.Crow. 1998. Vascular smooth muscle cells cultures. *Methods in cell biology* 52:133-154.

Reddy, S., K.Ozgur, M.Lu, W.Chang, S.R.Mohan, C.C.Kumar, and H.E.Ruley. 1990. Structure of the human smooth muscle alpha-actin gene. Analysis of a cDNA and 5' upstream region. *J. Biol. Chem.* 265:1683-1687.

Reginald Magee. 1998. Arterial disease in antiquity. *The Medical Journal of Australia* 169:663-666.

Religa, P., K.Bojakowski, Z.Gaciong, J.Thyberg, and U.Hedin. 2003. Arteriosclerosis in rat aortic allografts: dynamics of cell growth, apoptosis and expression of extracellular matrix proteins. *Mol. Cell Biochem.* 249:75-83.

Riederer, B.M. and S.R.Goodman. 1987. Immunological detection of high molecular weight proteins by gel and blot overlay. *Brain Res. Bull.* 19:715-722.

Riedl, S.J., M.Renatus, R.Schwarzenbacher, Q.Zhou, C.Sun, S.W.Fesik, R.C.Liddington, and G.S.Salvesen. 2001. Structural basis for the inhibition of caspase-3 by XIAP. *Cell* 104:791-800.

Ross, R. 1971. The smooth muscle cell. II. Growth of smooth muscle in culture and formation of elastic fibers. *J. Cell Biol.* 50:172-186.

Ruiz, C.E., H.P.Zhang, A.I.Butt, and P.Whittaker. 1997. - Percutaneous treatment of abdominal aortic aneurysm in a swine model: understanding the behavior of aortic aneurysm closure through a serial histopathological analysis. - *Circulation.*-48.

Russo, A., M.Terrasi, V.Agnese, D.Santini,. and V.Bazan. 2006. Apoptosis: a relevant tool for anticancer therapy. *Ann. Oncol.* 17 Suppl 7:vii115-vii123.

Sakata, N., K.Takeuchi, K.Noda, K.Saku, Y.Tachikawa, T.Tashiro, R.Nagai, and S.Horiuchi. 2003. Calcification of the medial layer of the internal thoracic artery in diabetic patients: relevance of glycoxidation. *J. Vasc. Res.* 40:567-574.

Salo, J.A., S.Soisalon-Soininen, S.Bondestam, and P.S.Mattila. 1999. Familial occurrence of abdominal aortic aneurysm. *Ann. Intern. Med.* 130:637-642.

Sambrook, J. and R.F.Fritsch. 1989. Molecular cloning. cold Spring Harbor, N.Y..

Satta, J., T.Juvonen, K.Haukipuro, M.Juvonen, and M.I.Kairaluoma. 1995. Increased turnover of collagen in abdominal aortic aneurysms, demonstrated by measuring the concentration of the aminoterminal propeptide of type III procollagen in peripheral and aortal blood samples. *J. Vasc. Surg.* 22:155-160.

Sattler, A.M., M.Schoppet, J.R.Schaefer, and L.C.Hofbauer. 2004. Novel aspects on RANK ligand and osteoprotegerin in osteoporosis and vascular disease. *Calcif. Tissue Int.* 74:103-106.

Sayers, T.J. and W.J.Murphy. 2006. Combining proteasome inhibition with TNF-related apoptosis-inducing ligand (Apo2L/TRAIL) for cancer therapy. *Cancer Immunol. Immunother.* 55:76-84.

Scatena, M. and C.Giachelli. 2002. The alpha(v)beta3 integrin, NF-kappaB, osteoprotegerin endothelial cell survival pathway. Potential role in angiogenesis. *Trends Cardiovasc. Med.* 12:83-88.

Schinke, T. and G.Karsenty. 2000. Vascular calcification--a passive process in need of inhibitors. *Nephrol. Dial. Transplant.* 15:1272-1274.

Schneider, P., J.L.Bodmer, M.Thome, K.Hofmann, N.Holler, and J.Tschopp. 1997a. Characterization of two receptors for TRAIL. *FEBS Lett.* 416:329-334.

Schneider, P., M.Thome, K.Burns, J.L.Bodmer, K.Hofmann, T.Kataoka, N.Holler, and J.Tschopp. 1997b. TRAIL receptors 1 (DR4) and 2 (DR5) signal FADD-dependent apoptosis and activate NF-kappaB. *Immunity.* 7:831-836.

Schneider, P. and J.Tschopp. 2000. Apoptosis induced by death receptors. *Pharm. Acta Helv.* 74:281-286.

Schoppet, M., N.Al-Fakhri, F.E.Franke, N.Katz, P.J.Barth, B.Maisch, K.T.Preissner, and L.C.Hofbauer. 2004. Localization of osteoprotegerin, tumor necrosis factor-related apoptosis-inducing ligand, and receptor activator of nuclear factor-kappaB ligand in Monckeberg's sclerosis and atherosclerosis. *J. Clin. Endocrinol. Metab* 89:4104-4112.

Schreurs O., Halstensen T.S., Dembic Z., Bogen B., and Schenck K. Fixation of tissue sections for TUNEL combined with staining for thymic epithelial cell marker. Biochemica. 4, 19-21. 1997.

Schulz, E., K.Arfai, X.Liu, J.Sayre, and V.Gilsanz. 2004. Aortic calcification and the risk of osteoporosis and fractures. *J. Clin. Endocrinol. Metab* 89:4246-4253.

Secchiero, P., A.Gonelli, E.Carnevale, D.Milani, A.Pandolfi, D.Zella, and G.Zauli. 2003. TRAIL promotes the survival and proliferation of primary human vascular endothelial cells by activating the Akt and ERK pathways. *Circulation* 107:2250-2256.

Sedghizadeh, P.P., C.M.Allen, K.E.Anderson, D.H.Kim, J.R.Kalmar, and J.C.Lang. 2004. Oral graft-versus-host disease and programmed cell death: pathogenetic and clinical correlates. *Oral Surg. Oral Med. Oral Pathol. Oral Radiol. Endod.* 97:491-498.

Semenza, G.L. 2006. VHL and p53: tumor suppressors team up to prevent cancer. *Mol. Cell* 22:437-439.

Shanahan, C.M., N.R.Cary, J.C.Metcalfe, and P.L.Weissberg. 1994. High expression of genes for calcification-regulating proteins in human atherosclerotic plaques. *J. Clin. Invest* 93:2393-2402.

Shanahan, C.M., D.Proudfoot, K.L.Tyson, N.R.Cary, M.Edmonds, and P.L.Weissberg. 2000. Expression of mineralisation-regulating proteins in association with human vascular calcification. *Z. Kardiol.* 89 Suppl 2:63-68.

Shi, Y. 2004. Caspase activation, inhibition, and reactivation: a mechanistic view. *Protein Sci.* 13:1979-1987.

SHIN, V., ZEBBOUDJ, A., BOSTRÖM, K., 2004. Endothelial cells modulate osteogenesis in calcifying vascular cells. *J. vasc. res.* 41: 193-201

Shire D., Bultler J., and Lewis R. 2003. Hole's essential of human anatomy and physiology. McGraw-Hill Companies.

Simonet, W.S., D.L.Lacey, C.R.Dunstan, M.Kelley, M.S.Chang, R.Luthy, H.Q.Nguyen, S.Wooden, L.Bennett, T.Boone, G.Shimamoto, M.DeRose, R.Elliott, A.Colombero, H.L.Tan, G.Trail, J.Sullivan, E.Davy, N.Bucay, L.Renshaw-Gegg, T.M.Hughes, D.Hill, W.Pattison, P.Campbell, S.Sander, G.Van, J.Tarpley,

P.Derby, R.Lee, and W.J.Boyle. 1997. Osteoprotegerin: a novel secreted protein involved in the regulation of bone density. *Cell* 89:309-319.

Singh, K., K.H.Bonaa, B.K.Jacobsen, L.Bjork, and S.Solberg. 2001. Prevalence of and risk factors for abdominal aortic aneurysms in a population-based study : The Tromso Study. *Am. J. Epidemiol.* 154:236-244.

Sinicrope, F.A. and R.C.Penington. 2005. Sulindac sulfide-induced apoptosis is enhanced by a small-molecule Bcl-2 inhibitor and by TRAIL in human colon cancer cells overexpressing Bcl-2. *Mol. Cancer Ther.* 4:1475-1483.

Song, K., Y.Chen, R.Goke, A.Wilmen, C.Seidel, A.Goke, B.Hilliard, and Y.Chen. 2000. Tumor necrosis factor-related apoptosis-inducing ligand (TRAIL) is an inhibitor of autoimmune inflammation and cell cycle progression. *J. Exp. Med.* 191:1095-1104.

Speer, M.Y., M.D.McKee, R.E.Guldberg, L.Liaw, H.Y.Yang, E.Tung, G.Karsenty, and C.M.Giachelli. 2002. Inactivation of the osteopontin gene enhances vascular calcification of matrix Gla protein-deficient mice: evidence for osteopontin as an inducible inhibitor of vascular calcification *in vivo. J. Exp. Med.* 196:1047-1055.

Spierings, D.C., E.G.de Vries, E.Vellenga, F.A.van den Heuvel, J.J.Koornstra, J.Wesseling, H.Hollema, and J.S.de. 2004. Tissue distribution of the death ligand TRAIL and its receptors. *J. Histochem. Cytochem.* 52:821-831.

Stanford, W. and B.H.Thompson. 1999. Imaging of coronary artery calcification. Its importance in assessing atherosclerotic disease. *Radiol. Clin. North Am.* 37:257-72, v.

Stocker, R. and J.F.Keaney, Jr. 2004. Role of oxidative modifications in atherosclerosis. *Physiol Rev.* 84:1381-1478.

Swank, M.W., V.Kumar, J.Zhao, and G.Y.Wu. 2006. A novel method of loading samples onto mini-gels for SDS-PAGE: Increased sensitivity and Western blots using sub-microgram quantities of protein. *J. Neurosci. Methods.*

Tanko, L.B., Y.Z.Bagger, and C.Christiansen. 2003. Low bone mineral density in the hip as a marker of advanced atherosclerosis in elderly women. *Calcif. Tissue Int.* 73:15-20.

Taylor, T.W. and T.Yamaguchi. 1994. Three-dimensional simulation of blood flow in an abdominal aortic aneurysm--steady and unsteady flow cases. *J. Biomech. Eng* 116:89-97.

Thomas, W.D., X.D.Zhang, A.V.Franco, T.Nguyen, and P.Hersey. 2000. TNF-related apoptosis-inducing ligand-induced apoptosis of melanoma is associated with changes in mitochondrial membrane potential and perinuclear clustering of mitochondria. *J. Immunol.* 165:5612-5620.

Thompson, R.W., S.Liao, and J.A.Curci. 1997. Vascular smooth muscle cell apoptosis in abdominal aortic aneurysms. *Coron. Artery Dis.* 8:623-631.

Thorne, S.A., S.E.Abbot, C.R.Stevens, P.G.Winyard, P.G.Mills, and D.R.Blake. 1996. Modified low density lipoprotein and cytokines mediate monocyte adhesion to smooth muscle cells. *Atherosclerosis* 127:167-176.

Tintut Y, Demer L. 2006. Role of osteoprotegerin and its ligands and competing receptors in atherosclerotic calcification. *J. inversti. med.* 54 (7): 395-401

Toloza, E.M., M.A.Morse, and H.K.Lyerly. 2006. Gene therapy for lung cancer. *J. Cell Biochem.*

Tyson, K.L., J.L.Reynolds, R.McNair, Q.Zhang, P.L.Weissberg, and C.M.Shanahan. 2003. Osteo/chondrocytic transcription factors and their target genes exhibit distinct patterns of expression in human arterial calcification. *Arterioscler. Thromb. Vasc. Biol.* 23:489-494.

Upchurch, G.R., Jr. and T.A.Schaub. 2006. Abdominal aortic aneurysm. *Am. Fam. Physician* 73:1198-1204.

Van, P.C., S.S.Cross, M.Saggese, C.Hudis, K.S.Panageas, L.Norton, R.E.Coleman, and I.Holen. 2006. Expression of osteoprotegerin (OPG), TNF related apoptosis inducing ligand (TRAIL), and receptor activator of nuclear factor kappaB ligand (RANKL) in human breast tumours. *J. Clin. Pathol.* 59:56-63.

Villahermosa, M.L., M.Thomson, P.E.Vazquez de, M.T.Cuevas, G.Contreras, L.Perez-Alvarez, E.Delgado, N.Manjon, L.Medrano, and R.Najera. 2000. Improved conditions for extraction and amplification of human immunodeficiency virus type 1 RNA from plasma samples with low viral load. *J. Hum. Virol.* 3:27-34.

Vidal K., van den Broek P, Lorget F, Donnet-Hughes A. 2004. Osteoprotegerin in human milk: a potential role in the regulation of bone metabolism and immune development. *Pediatr Res.* 55 (6): 1001-1008

Voelkel-Johnson, C. 2003. An antibody against DR4 (TRAIL-R1) in combination with doxorubicin selectively kills malignant but not normal prostate cells. *Cancer Biol. Ther.* 2:283-290.

Wajant, H. 2006. CD95L/FasL and TRAIL in tumour surveillance and cancer therapy. *Cancer Treat. Res.* 130:141-165.

Wang, A.Y., M.Wang, J.Woo, C.W.Lam, P.K.Li, S.F.Lui, and J.E.Sanderson. 2003. Cardiac valve calcification as an important predictor for all-cause mortality and cardiovascular mortality in long-term peritoneal dialysis patients: a prospective study. *J. Am. Soc. Nephrol.* 14:159-168.

Wang, J., L.Zheng, A.Lobito, F.K.Chan, J.Dale, M.Sneller, X.Yao, J.M.Puck, S.E.Straus, and M.J.Lenardo. 1999. Inherited human Caspase 10 mutations underlie defective lymphocyte and dendritic cell apoptosis in autoimmune lymphoproliferative syndrome type II. *Cell* 98:47-58.

Wang, S. and W.S.El-Deiry. 2003. TRAIL and apoptosis induction by TNF-family death receptors. *Oncogene* 22:8628-8633.

Watson, R.W. and J.M.Fitzpatrick. 2005. Targeting apoptosis in prostate cancer: focus on caspases and inhibitors of apoptosis proteins. *BJU. Int.* 96 Suppl 2:30-34.

Whitehall, J., M.Smith, and L.Altamirano. 2003. Idiopathic infantile arterial calcification: sonographic findings. *J. Clin. Ultrasound* 31:497-501.

Wiley, S.R., K.Schooley, P.J.Smolak, W.S.Din, C.P.Huang, J.K.Nicholl, G.R.Sutherland, T.D.Smith, C.Rauch, C.A.Smith, and . 1995. Identification and characterization of a new member of the TNF family that induces apoptosis. *Immunity.* 3:673-682.

Wilfinger, W.W., K.Mackey, and P.Chomczynski. 1997. Effect of pH and ionic strength on the spectrophotometric assessment of nucleic acid purity. *Biotechniques* 22:474-481.

Wilmink T. the nature history of aneurysm. Vascular Surgical Society of Great Britain and Ireland. 2004.

Wu, X.X., O.Ogawa, and Y.Kakehi. 2004. TRAIL and chemotherapeutic drugs in cancer therapy. *Vitam. Horm.* 67:365-383.

www.surgical-tutor.org.uk. Abdominal aortic aneurysms. internet . 2006. Ref Type: Electronic Citation

www.vascularweb.org. Abdominal Aortic Aneurysm. internet . 2006. Ref Type: Electronic Citation

Xiang, G.D., L.Xu, L.S.Zhao, L.Yue, and J.Hou. 2006. - The relationship between plasma osteoprotegerin and endothelium-dependent arterial dilation in type 2 diabetes. - *Diabetes.*-31.

De Vries C., van Achterberg T., Horrevoets A, ten Cate A, and Hans. 2000. PannekoekDifferential Display Identification of 40 Genes with Altered Expression in Activated Human Smooth Muscle Cells. J. Biol. Chem., 275 (31): 23939-23947

Yeh Wen-Chen, José Luis de la Pompa, and Mila E.McCurrach. 1998. FADD: Essential for Embryo Development and Signaling from Some, But Not All, Inducers of Apoptosis. *Science* 279:1954-1958.

Yoshimura, K., H.Aoki, Y.Ikeda, K.Fujii, N.Akiyama, A.Furutani, Y.Hoshii, N.Tanaka, R.Ricci, T.Ishihara, K.Esato, K.Hamano, and M.Matsuzaki. 2005. Regression of abdominal aortic aneurysm by inhibition of c-Jun N-terminal kinase. *Nat. Med.* 11:1330-1338.

Zatina, M.A., C.K.Zarins, B.L.Gewertz, and S.Glagov. 1984. Role of medial lamellar architecture in the pathogenesis of aortic aneurysms. *J. Vasc. Surg.* 1:442-448.

Zhang, J., J.Schmidt, E.Ryschich, H.Schumacher, and J.R.Allenberg. 2003. Increased apoptosis and decreased density of medial smooth muscle cells in human abdominal aortic aneurysms. *Chin Med. J. (Engl.)* 116:1549-1552.

Zhang, X.D., T.Nguyen, W.D.Thomas, J.E.Sanders, and P.Hersey. 2000. Mechanisms of resistance of normal cells to TRAIL induced apoptosis vary between different cell types. *FEBS Lett.* 482:193-199.

Zhong, H. and J.W.Simons. 1999. Direct comparison of GAPDH, beta-actin, cyclophilin, and 28S rRNA as internal standards for quantifying RNA levels under hypoxia. *Biochem. Biophys. Res. Commun.* 259:523-526.